N° d'ordre 77

Année 2012 - 2013

جامعة عبد المالك السعدي
Université Abdelmalek Essaadi

UNIVERSITE ABDELMALEK ESSAADI
FACULTE DES SCIENCES et TECHNIQUES
TANGER

Centre d'Etudes Doctorales : « Sciences et Techniques de l'Ingénieur »
Formation Doctorale : « Sciences et Techniques de l'Ingénieur »

THESE DE DOCTORAT

Présentée

Pour l'obtention du

DOCTORAT EN SCIENCES ET TECHNIQUES DE L'INGENIEUR

Par :
BAKKALI Abderrahmane

Discipline : Science Physique de l'Ingénieur

Spécialité : Mécanique des matériaux

Modélisation micromécanique des matériaux composites multifonctionnels

Soutenue le 14 Septembre 2013 devant le Jury

Pr. CHARIF D'OUAZZANE Saâd	**Université Hassan II Mohammedia - Casablanca**	**Président**
Pr. ALJINAIDI Abdulmalik Ali	**Université Roi Abdulaziz, Jeddah, Arabie Saoudite**	**Rapporteur**
Pr. EL OMRI Abderrahim	**Faculté des Sciences et Techniques - Tanger**	**Rapporteur**
Pr. ERCHIQUI Fouad	**Ecole de Génie, Université du Québec, Canada**	**Rapporteur**
Pr. FAKRI Nadia	**Faculté des Sciences et Techniques - Tanger**	**Examinateur**
Pr. CHERKAOUI Mohammed	**Université Georgia Tech - Lorraine, Atlanta - USA**	**Examinateur**
Pr. AJDOUR Mounia	**Faculté des Sciences et Techniques - Tanger**	**Invité**
Pr. AZRAR Lahcen	**Faculté des Sciences et Techniques - Tanger**	**Directeur de thèse**

Structure de recherche accréditée d'accueil :
Références : UAE/E05/FST, Equipe Modélisation Mathématique et Contrôle de la FST de Tanger

To my mother and father

Acknowledgments

I am deeply grateful to my advisor, Professor Lahcen AZRAR, for his guidance, support and encouragement during the years of the thesis. Without his help this work would not be done. Besides introducing me the subject of micromechanics he shows how to be an effective researcher.

I would like to thank Professor Nadia FAKRI for her help in introducing to me micromechanics and also to overcome the problems I faced.

The financial support of King Abdulaziz University is greatly appreciated. This work was supported under grant No. (7 - 4 - 1432/HiCi) and by the DSR research project at King Abdulaziz University in Jeddah, Saudi Arabia.

A part of this work is the results of the collaboration between the mathematical modeling and control team at the Faculty of Sciences and Techniques of Tangier and the Aerospace Engineering department at Texas A&M University, Texas, USA through the project of IIMEC (International Institute for Multifunctional Materials for Energy Conversion). Special thanks to Professor Lagoudas for welcoming me as an intern student at his team and leading all the work accomplished there. Also I would like to thank doctor Yves for co-advising during my internship at Aerospace Engineering department.

I would like to thank Professors Fouad ERCHIQUI, Abderrahim EL OMRI and Abdulmalik Ali ALJINAIDI for accepting to be rapporteurs of my thesis and taking the charges of my thesis report.

I would like also to thank Professors Saâd CHARIF d'OUAZZANE, Mounia AJDOUR and Mohammed CHERKAOUI for accepting to be comity members of the jury and judging my thesis work.

Finally, I would like to thank my family, specially my mother and father, for their love and unlimited support.

Acknowledgments

Abstract

The issue of accurately predicting the effective behavior of composite materials has taken the attention of many researchers in the last few decades and continues to be in the forefront of material research. Micromechanics have proven to be very powerful in analyzing and predicting the effective behavior of composite materials. In the frame of this thesis, various micromechanical models have been elaborated in order to investigate the effective behavior of different kinds of smart composites such as: piezoelectric, piezomagnetic, magnetoelectroelastic, viscoelectroelastic, viscomagnetoelectroelastic as well as shape memory alloys.

The effective properties of multi-phase magnetoelectroelastic composites have been investigated using different micromechanical models. An N-phase Incremental Self Consistent model is developed to circumvent the limitation of the Self Consistent predictions. The Self Consistent shows limitation for the prediction of some coupling coefficients. Also, the prediction of the Self Consistent model is very limited when the void inclusions are considered. The modeling is based on the solution of integral equations. The effective N-phase magnetoelectroelastic moduli are expressed as a function of magnetoelectroelastic concentration tensors based on the considered micromechanical models. The effective properties are obtained for various types, shapes and volume fractions of inclusions and compared with the existing results. Note that the effective properties of magnetoelectroelastic composites might be greatly affected by the presence of an interphase between the matrix and inclusions. To take this effect into account, accurately, a micromechanical modeling is developed to investigate the effective properties of magnetoelectroelastic composite with multi-coated inclusions and functionally graded interphases. The modeling is based on the solution of the integral equations that take into account the multi-coated and functionally graded effects and on the magnetoelectroelastic interfacial operators that allow expressing the generalized strain jump through the interphase. Taking into account the multi-coated and functionally graded effects in the modeling help in the design of new smart composites with higher coupling coefficients.

Piezoelectric and magnetoelectroelastic composites that contain a polymer phase show a significant time dependent behavior and particularly at elevated temperature. A micromechanical modeling is developed to investigate the viscoelectroelastic and viscomagnetoelectroelastic behaviors of heterogeneous piezoelectric and magnetoelectroelastic composite materials. The

modeling is based on generalizing the correspondence principle of linear viscoelasticity to the case of viscoelectroelasticity and viscomagnetoelectroelasticity. The viscoelastic correspondence principle is combined with Mori-Tanaka micromechanical model. The effective properties are predicted in the frequency and time domains based on Carson and Laplace transforms.

To investigate the nonlinear behavior of smart composites, the shape memory alloys are considered. The effective transformation behavior of this kind of composites is investigated based on the Mori-Tanaka model that takes the coating effects around the inclusions combined with the constitutive equations describing the transformation behavior of shape memory alloy materials. The obtained results are compared with one predicted based on the classical Mori-Tanaka model that does not consider the effect of the coating layer around the inclusion and also with the obtained ones based on the finite element method. It is shown that the developed model captures the effective transformation behavior better than the one that is based on the classical Mori-Tanaka model. As the obtained results do not agree well with the ones predicted based on the finite element method the developed methodological approaches need more refinement for this kind of nonlinear materials

Keywords: Smart composites, visco-piezoelectric, visco-magnetoelectroelastic, Shape memory alloy, micromechanics. Coating, interfacial operators, functionally graded, Mori-Tanaka, Self Consistent,

Table of contents

Table of contents

List of tables

List of tables

List of figures

Chapter 1

1. General introduction

Smart Composite materials such as piezoelectric, piezomagnetic, magnetoelectroelastic, magnetostrictif and shape memory alloy composites etc. have attracted the attention of several researchers due to their application in many industrial fields such automotive, aerospace, biomedical and civil engineering. Their appealing factor is represented by the possibility to obtain tailored properties for specific applications and to overcome classical limitations of the natural existing ones in term of flexibility, durability and reliability etc. For example, the adoption of light and flexible non-piezoelectric polymers in combination with piezoelectric ceramics in a multiphase construction leads to a more robust device, capable of conforming to complex surface shapes. These smart composites take the advantages of each phase and have better physical properties.

The development that has been doing in smart composite materials that exhibits coupling effects aims to reach smart composite with optimized coupling coefficients for sensing, actuation, electrical energy harvesting, conversion and storage etc. Figure 1.1 presents the possible coupling between the mechanical, electrical, magnetic and thermal fields.

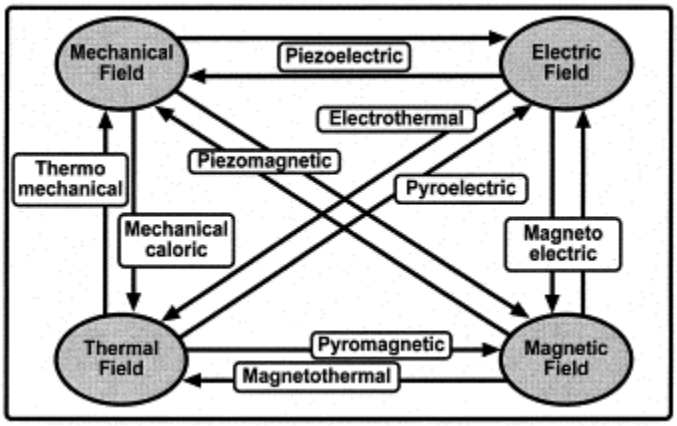

Figure 1.1: Diagram of different coupling effects that a smart composite might exhibit.

The complexity of composites (figure 1.2) at the micro level greatly complicates the analysis of the behavior of these composites, which is indispensable to design them. Composite materials

are examined as heterogeneous materials and the developments done in this area are due to the development of the used methods.

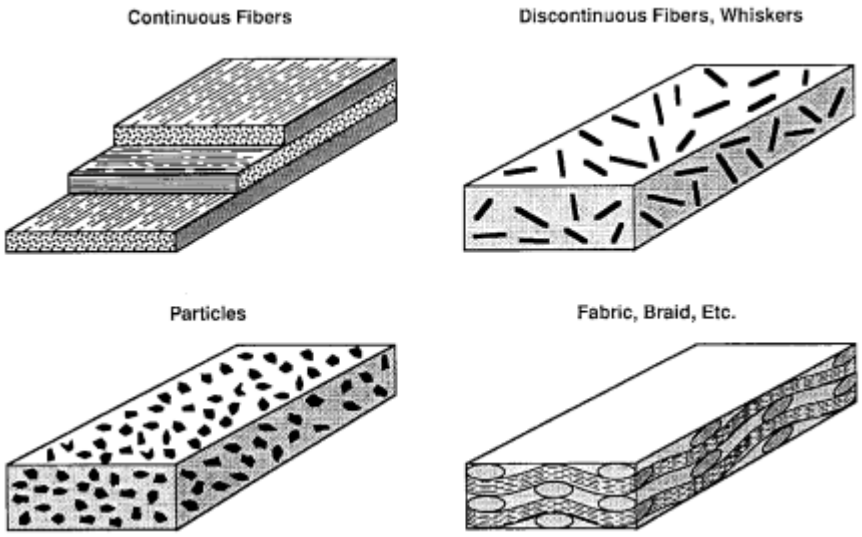

Figure 1.2: Composite materials.

Composite materials with coated reinforcements have taken the attention of many researchers. The effective properties of a composite are highly affected by the characteristics and the geometry of the interphase between the constituents. Consequently, studying the influence of a coating layer on composites may be valuable to better understand the transmission of mechanical, electrical and magnetic fields throughout the inclusion toward the matrix for the sake of the improvement of the strength and/or magnetoelectric (ME) effect. The increase of the strength may be obtained for example via the introduction of a stiff interphase of defined thickness as demonstrated by [1] for elastic composites. The ME enhancement is more tricky as it implies coupled mechanical, electrical and magnetic properties. The introduction of an active interphase allows comprehending the transmission of the different fields from the core towards the matrix. Micromechanical studies of composites with coating layers.

Analyzing and describing the behavior of composite materials could be done through different approaches. Phenomenological approach [2] is one way of characterizing composite materials which is based on experimental test. In many cases, it is not possible to realize experimental test

for all kinds of reinforcement shapes and types due to the volume and the cost of the required tests.

Another approach which is developed since many decades is the micromechanical approach. It describes the composites from its microstructure and local behavior. First simple models were developed by Voigt [3], Reuss [4] and Hill [5]. Then based on Eshelby [6] inclusion problem which allows showing the importance of the concentration stress phenomena, many micromechanical models were developed. Micromechanical models based on the Eshelby's inclusion problem take into account much more details about the microstructure which leads to accurate prediction of the effective behavior of composite materials. Micromechanical studies of composites with coating layers have aroused great interest among many researchers in recent years. Different models have been developed to predict the effect of the interphase layer on the effective properties of composites materials. Based on the integral equation and on the interfacial operators cherkaoui et al. [7, 8, 9] developed a coated inclusion problem to predict the effective properties of elastic and thermoelastic composites consisting of ellipsoidal coated inclusion embedded in matrix. [10, 11] extended the modeling to investigate the piezoelectric and thermopiezoelectric behavior of piezoelectric heterogeneous materials.

Micromechanical models predict the behavior of composite materials in terms of volume fraction, shape, orientation of reinforcements. Also, the effect between the matrix and reinforcements cloud be taken into account in the modeling. Another benefit of the micromechanical modeling includes the ability of taking into account the failure that might exist in composites in micro level such as matrix cracking, fiber matrix debonding and damage. All that makes micromechanical modeling as a powerful tool in analyzing and predicting the effective behavior of composite materials.

1.1 Considered smart composites

In the frame of this thesis a wide multifunctional heterogeneous materials are considered. The main aim is to develop mathematical models that allow predicting new composite materials with improved coupling effects. An overview of the considered multifunctional materials is presented here.

1.1.1 Piezoelectric composites

Piezoelectric composites present an electroelastic (piezoelectric) coupled effect. Piezoelectric materials have the property of converting mechanical energy into electrical energy (direct piezoelectric effect) and vice versa (converse piezoelectric effect). Piezoelectric composites were originally developed for underwater hydrophone applications in the low-frequency range, but have also been extended to such other applications as ultrasonic transducers for acoustic imaging and medical applications [12]. Piezoelectric ceramics are being investigated for use as sensor or actuator elements in smart structures.

1.1.2 Piezomagnetic composites

Piezomagnetic composites have magnetoelastic (piezomagnetic) coupled effect. They have the property of converting mechanical energy into magnetic energy (direct piezomagnetic effect) and vice versa (converse piezomagnetic effect). These materials have a wide range of applications such as magneto-mechanical transducers, magnetic sensors and ultrasonic generator [13].

1.1.3 Magnetoelectroelastic composites

Composite materials consisting of piezoelectric phase and piezomagnetic phase are called magnetoelectroelastic composites. These kinds of composites present electroelastic, magnetoelastic (piezomagnetic) and magnetoelectric coupled effects. The magnetoelectric coupled effect is the most important effect exhibited by these composites and it may be absent in all the phases and created only by the interaction between the piezoelectric and piezomagnetic phase. The magnetoelectric effect gives to these composites the ability to convert an electrical energy to magnetic one and vice versa. One example of applications of such materials is magnetoelectric sensors in optoelectronics and microwave electronics.

1.1.4 Viscopiezoelectric composites

Viscoelectroelastic composites [14] are composites consisting of piezoelectric and viscoelastic phases. At elevated temperature heterogeneous piezoelectric composites consisting of piezoelectric inclusions and polymer matrix show a time dependent behavior. At normal temperature polymers materials have an elastic behavior but at elevated temperature they show a significant viscoelastic behavior. The physical and mechanical properties of viscoelastic materials change with time and temperature. The addition of a polymer or any viscoelastic phase

to piezoelectric composites affects their behavior. Viscoelectroelastic composites show a dissipative behavior which could be used to eliminate vibration and noise.

1.1.5 Viscomagnetoelectroelastic composites

Viscomagnetoelectroelastic composites are composites consisting with piezoelectric, piezomagnetic and viscoelastic phases. Piezoelectric and piezomagnetic ceramics are brittle materials. The addition of a polymer matrix to composites containing piezoelectric and piezomagnetic inclusions provides them ductility and protect them from damage. But at elevated temperature the polymer matrix shows a significant viscoelastic behavior that affects the whole behavior of the composites. The electromagnetic, electroelastic and magnetoelastic coupling behaviors of viscoelectroelastic composites change with time and temperature. Viscoelectroelastic composites have a dissipative behavior which could be in industrial applications such as the elimination of noise and vibration and structures.

1.1.6 Shape memory alloy composites

Among the smart composite materials, the shape memory alloy (SMA) composites. They represent one of the most interesting materials, more and more adopted in structural engineering. SMAs composites are capable to recover their original shape (or to develop large reaction forces when they have their recovery restricted) through the imposition of a temperature and/or a stress field, due to phase transformations that the material undergoes. SMAs present several particular thermomechanical behaviors. The main phenomena related to these alloys are pseudoelasticity, shape memory effect, which may be one-way (SME) or two-way (TWSME), and phase transformation due to temperature variation. Due to their unique properties, SMAs have attracted great interest in various fields of applications ranging from aerospace [15] and naval [16] to surgical instruments [17].

1.2 Piezoelectricity

The phenomenon of piezoelectricity was discovered by Jacques and Pierre Curie brothers in 1880 [18]. They discovered that some crystals when compressed in certain directions show positive and negative charges on some portions of the surface. These charges are proportional to the pressure and disappear when it ceases. Materials that exhibit piezoelectricity have the ability

to develop an electric charge when a mechanical stress is applied which is the direct effect. They have a converse effect by developing a strain when an electrical field is applied. Thus, Piezoelectricity is the linear interaction between mechanical and electrical system. Figure 1.3 shows the use of piezoelectric sensors and actuators to control the vibration of a laminated beam.

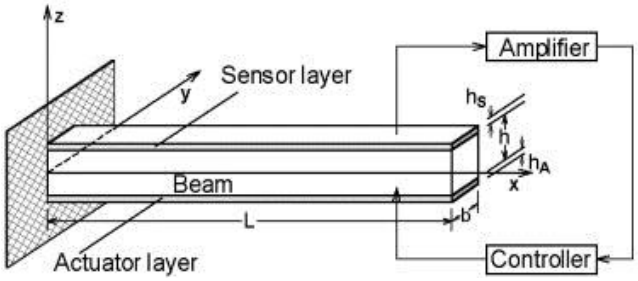

Figure 1.3: Laminated beam with piezoelectric sensors and actuators

The direct piezoelectric effect, the development of an electric charge by the application of a mechanical stress, was described as (Nye, 1957)[19].

$$P_i = d_{ijk}\sigma_{jk} \tag{1.1}$$

where P_i is the electric polarization (charge per unit area), d_{ijk} is the piezoelectric coupling tensor, and σ_{jk} is the applied mechanical stress tensor. The converse effect, the development of a mechanical strain by the application of an electric field to the piezoelectric, is described by

$$\varepsilon_{ij} = d_{ijk}E_k \tag{1.2}$$

where ε_{ij} is the produced strain and by applying the electric field E_k. In both cases, the piezoelectric coefficients d_{ijk} are numerically identical.

It should be noted that the piezoelectric effect is strongly linked to the crystal symmetry. A crystal having sufficiently low symmetry produces electric polarization under the influence of external mechanical force. Polycrystalline materials in which the crystal axes of the grains are randomly oriented exhibit no piezoelectric effect. Piezoelectric polycrystalline ceramics were discovered in the 1940s, soon followed by the development of the poling process in which the randomly oriented crystal axes are suitably aligned by the application of a strong electric field at elevated temperatures. After that discovery, researchers continued to develop better and more stable materials. Lead zirconate titanate (PZT) was first introduced in 1954 and has become the

most widely used piezoceramic. Today piezoelectric ceramics, or piezoceramics, are used more widely than piezoelectric crystals.

Mechanical stress σ_{kl} and electric field E_l are coupled within a piezoelectric solid medium. Constitutive equations for a piezoelectric material can be written as [20]

$$\begin{aligned} \varepsilon_{ij} &= s_{ijkl}\sigma_{kl} - d_{lij}E_l \\ D_i &= d_{ikl}\sigma_{kl} + \kappa_{il}E_l \end{aligned} \tag{1.3}$$

where σ, ε, E, and D are the stress tensor, strain tensor, electric filed and the electric displacement vector, respectively. s, d and κ are the elastic compliance tensor, piezoelectric tensor and the dielectric tensor, respectively.

An alternate expression of the constitutive behavior could be given, such as

$$\begin{aligned} \sigma_{ij} &= c_{ijkl}\varepsilon_{kl} - e_{lij}E_l \\ D_i &= e_{ikl}\varepsilon_{kl} + \kappa_{il}E_l \end{aligned} \tag{1.4}$$

where the piezoelectric tensor e_{lij} is related to the piezoelectric tensor d through the elastic tensor c by the following relationship

$$e_{ijk} = d_{imn}c_{mnjk} \tag{1.5}$$

1.3 Ferroelectricity

Ferroelectricity was discovered in 1920 in Rochelle salt by Valasek [21]. Ferroelectric materials are materials that exhibit, over some range of temperature, a spontaneous electric polarization that can be reversed or reoriented by application of an electric field. Ferroelectric materials undergo a structural phase transition from a paraelectric phase to a ferroelectric phase upon cooling through the Curie temperature, T_c. Above T_c temperature, the crystal has a centrosymmetric structure and has no spontaneous polarization. Bellow T_c, the crystal exhibits ferroelectricity and has a structure resulting from the change in the symmetry of the unit cell. When an external field is applied in a direction opposite to the polarization, the polarization can be reoriented in the direction of the electric field. This process is reversible and is called polarization switching. When the polarization is parallel to an applied electric field, the switching is done. However, it is not necessary that the polarization is exactly reoriented along the electric field direction.

The polarization-electric field hysteresis loop obtained in this way is an important characteristic of a ferroelectric. Figure 1.4 shows a typical hysteresis loop [22] from which the values of the remnant polarization and coercive electric field can be determined.

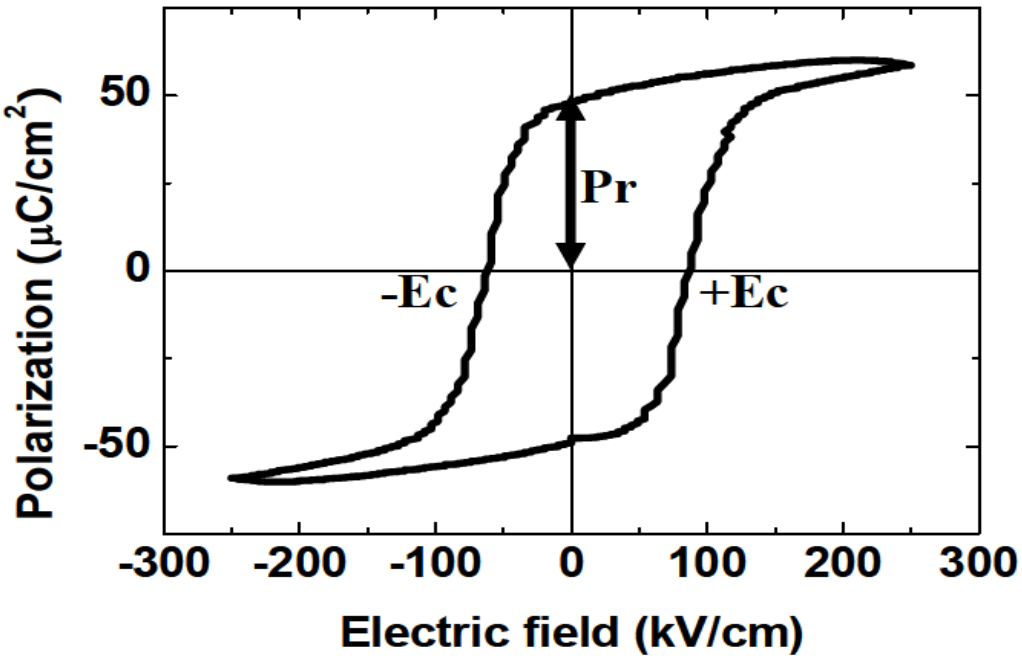

Figure 1.4: Polarization-electric field hysteresis loop measured in a ferroelectric material. P_r is the remnant polarization and E_c is the coercive electric field.

The net polarization of an initially unpolarized ferroelectric material is small. When an electric field is applied, there is a linear relationship between switchable polarization and the applied electric field. In this case, there is no polarization switching. As the electric field increases, however, domains in which the direction of spontaneous polarization is opposite to electric field begin to switch to a more energetically favorable direction. The switching process continues until all of the domains are aligned in the electric field direction. When the field returns to zero, the polarization does not return back to the initial value. The amount of switchable polarization after removal of an electric field is called the remnant polarization, Pr. The strength of the electric field to switch the opposite polarization domain is called the coercive electric field, E_c. This process can be repeated. Ferroelectric materials behave strongly nonlinear when they are under high electromechanical loads. The nonlinearity is mainly coming from domain switching which is the change of direction of the spontaneous polarization at the microstructure level.

1.4 Piezomagnetism

Piezomagnetism is the linear magnetomechanical effect analogous to the linear electromechanical effect. The first experimental observation of piezomagnetism was made in 1960, in the fluorides of cobalt and manganese [23]. Materials that exhibit a piezomagnetic effect have the ability to develop a magnetic field by applying physical stress or strain (direct effect), or a physical deformation by applying a magnetic field (converse effect). Thus, piezomagnetism is an interaction between the magnetic and mechanical system.

The direct piezomagnetic effect is described by [19].

$$H_i = -\Lambda_{ijk}\varepsilon_{jk} \tag{1.6}$$

where Λ_{ijk} is a third range piezomagnetic tensor.

The piezomagnetism phenomenon is related to the crystal symmetry and it is shown only by the absence of certain symmetry in a crystal structure. Mechanical stress σ and magnetic field H are coupled within a piezomagnetic solid medium. Constitutive equations for a piezomagnetic material can be written as [24]

$$\begin{aligned} \sigma_{ij} &= c_{ijkl}\varepsilon_{kl} - h_{lij}H_l \\ B_i &= h_{ikl}\varepsilon_{kl} + \mu_{il}H_l \end{aligned} \tag{1.7}$$

where σ, ε, H, and B are the stress tensor, strain tensor, magnetic field and the magnetic induction, respectively. c, h and μ are the elastic stiffness tensor, piezomagnetic tensor and the permeability magnetic tensor, respectively.

1.5 Magnetoelectric effects

The magnetoelectric (ME) effect is the generalization of electric polarization by a magnetic field and vice versa. This fascinating phenomenon was experimentally observed in 1960 by Astrov [25] and predicted by Landau and Lifshitz [26]. It is discovered that a sample of Cr_2O_3 shows a magnetoelectric effect. Magnetoelectric materials have the ability to convert an electrical energy into a magnetic one and vice versa. These properties make them very useful for sensors transducers, storage devices and medical imaging etc.

Figure 1.5: Application of magnetoelectric materials for sensors, transducers, storage devices and medical imaging.

The effects can be linear or/and non-linear with respect to the external fields. In general, this effect depends on temperature. The effect can be expressed in the following form [26]

$$\begin{aligned} P_i &= \chi_{ij}^{e} E_j + \alpha_{ij} H_j \\ M_i &= \chi_{ij}^{m} H_j + \alpha_{ij} E_j \end{aligned} \tag{1.8}$$

where P is the electric polarization, M the magnetization; E and H are the electric and magnetic field; α, χ^m and χ^m are the linear magnetoelectric moduli, dielectric and magnetic susceptibility moduli. Materials exhibiting the ME effect can be classified into two classes: single phase and composites. The ME effect exhibited by single phase materials is too weak to be practicable however magnetoelectroelastic composites consisting of a piezoelectric phase and a piezomagnetic phase show significant ME output qualified for potential applications.

Generally speaking the ME effect presented by composite materials is the results of the interaction between the piezoelectric phase and the piezomagnetic phase. Within a magnetoelectroelastic materials mechanic stress, electric field and magnetic field are coupled. The constitutive equation of a linear magnetoelectroelastic material is given by [27]

$$\begin{aligned} \sigma_{ij} &= c_{ijkl}\varepsilon_{kl} - e_{lij}E_l - h_{lij}H_l \\ D_i &= e_{ikl}\varepsilon_{kl} + \kappa_{il}E_l + \alpha_{il}H_l \\ B_i &= h_{ikl}\varepsilon_{kl} + \alpha_{il}E_l + \mu_{il}H_l \end{aligned} \tag{1.9}$$

where the elastic strain ε_{kl}, electric fields E_l, and magnetic fields H_l are independent variables related to stresses σ_{ij}, electric displacements D_i and magnetic inductions B_i. The tensors c_{ijkl}, e_{lij}, h_{lij}, α_{il}, κ_{il} and μ_{il} are the elastic, piezoelectric, piezomagnetic, magnetoelectric, dielectric and magnetic permeability constants respectively.

1.6 Ferromagnetism

Historically, the term ferromagnet was used for any material that could exhibit spontaneous magnetization: a net magnetic moment in the absence of an external magnetic field. Magnetic materials respond differently at applied magnetic field. Many properties of ferromagnetic materials are analogous to ferroelectric but with corresponding magnetic parameters. A ferromagnetic material undergoes phase transition from a high-temperature phase above T_c that does not have a macroscopic magnetic moment (paramagnetic phase) to a low-temperature phase below T_c that has spontaneous magnetization even when external magnetic field is switched off. Ferromagnets tend to concentrate magnetic flux density, they have spontaneous magnetization, which leads to their widespread usage in applications such as, transformer cores, permanent magnets, and electromagnets. The magnetization of ferromagnetic materials is a nonlinear process. Ferromagnetics are thus known as nonlinear media. A typical hysteresis loop is shown in Figure 1.6.

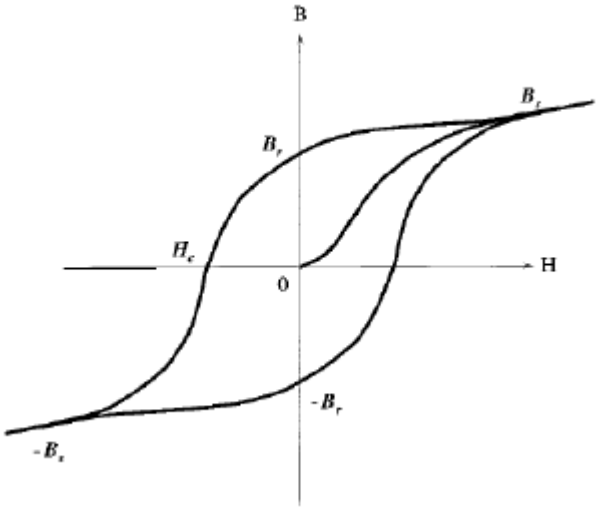

Figure 1.6: Hysteresis loop for ferromagnets [28].

The ferromagnet starts in an unmagnetized state and upon increased magnetic field magnetic induction rises to the saturation induction, B_s. When the field is reduced to zero, the induction decreases to B_r, known as remnant field. The reverse field, H_c, required to reduce the induction to zero is called the coercivity.

The characteristic of hysteresis loop determines the suitability of ferromagnetic materials for particular application. For example, more square-shaped hysteresis loop, with two stable magnetization states, is suitable for magnetic data storage, while a small hysteresis loop that is easily cycled between states is suitable for transformer core.

1.7 Shape memory alloys

The key characteristic of all SMAs is the occurrence of a martensitic phase transformation. The martensitic transformation is a shear dominant diffusionless solid-state phase transformation occurring by nucleation and growth of the martensitic phase from a parent austenitic phase (Olson and Cohen, 1982)[29]. When an SMA undergoes a martensitic phase transformation, it transforms from its high-symmetry, usually cubic, austenitic phase to a low-symmetry martensitic phase, such as the monoclinic variants of the martensitic phase in a NiTi SMA. The martensitic transformation possesses well-defined characteristics that distinguish it among other solid state transformations.

SMAs exhibit the following macroscopic phenomena not present in traditional materials.

Shape memory effect (SME) (figure 1.7) [30]**:** SMAs is loaded below austenitic start temperature, A^{0s}, while still in the austenitic phase to full transformation to the detwinned martensitic state and then unloaded fully retaining the transformation strain.

Pseudoelasticity (figure 1.8) [30]**:** SMAs is loaded above austenitic finish temperature, A^{0f}, to full transformation to the detwinned martensitic state and then unloaded fully transforming back to the austenitic state, while recovering all the transformation strain exhibiting hysteresis.

The shape memory effect is used for actuation while the pseudoelasticity is used for applications such as vibration isolation and damping.

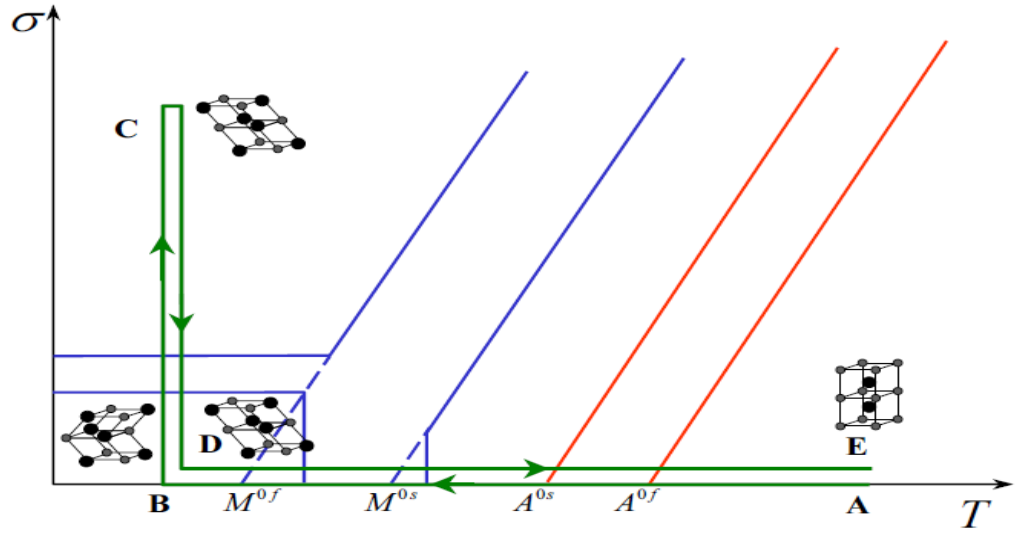

Figure1.7: Schematic representation of the thermodynamical loading path demonstrating the shape memory effect in SMAs.

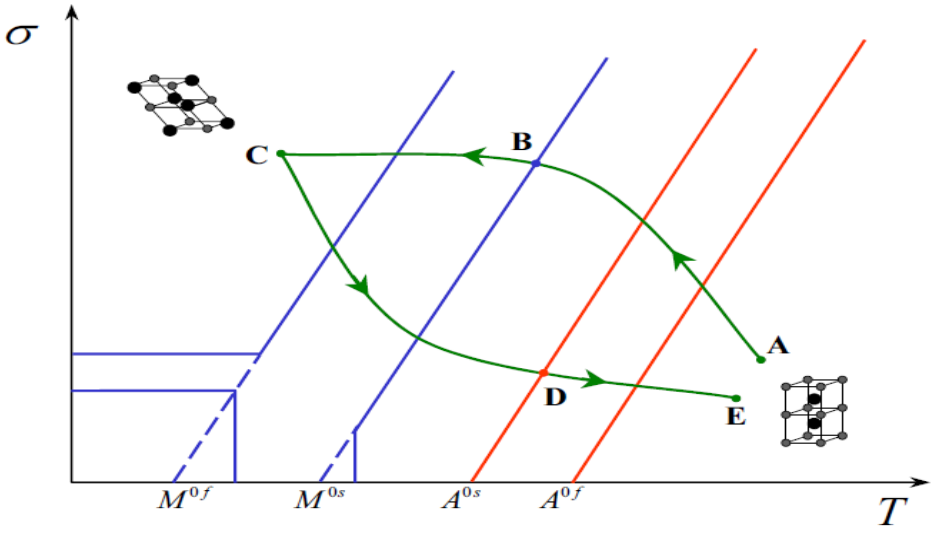

Figure1.8: Schematic of a thermomechanical loading path demonstrating pseudoelastic behavior of SMAs.

The medical applications of SMAs are shown in figure 1.9 [31].

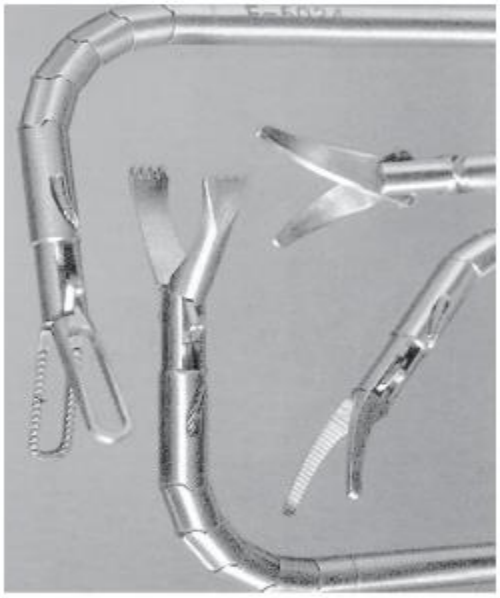

Figure 1.9: Laparoscopy tools. The actions of grippers, scissors, tongs and other mechanisms are performed by SMA.

1.8 Viscoelastic behaviors

As the viscoelastic behavior effect will be coupled to multifunctional effects of piezo and magneto composites, the viscoelastic behaviors will be reviewed here.

Some properties of viscoelastic materials are creep, relaxation, absorb energy etc. These properties make of them very used in different industrial applications. Among the applications is the use for passive control. Also the addition of viscoelastic materials to piezoelectric and magnetoelectroelastic materials will provide them beside of their actuation and sensing effect with a damping effect.

Responses of viscoelastic materials depend not only of the current loading, but also histories of loadings. Creep and relaxation are examples of viscoelastic responses. Creep is the increase in the deformation of materials under a constant stress. Relaxation is when a material is subject to a constant strain, the stress continuously decreases with time.

This section presents the concept of linear viscoelastic materials. There are many common models to describe the behavior of linear viscoelastic materials such as the Maxwell, Kelvin-

Voigt (KV) and Standard Linear Solid (SLS) models etc. The spring-dashpot mechanical analogs are commonly used to describe behaviors of the above viscoelastic models.

Maxwell model

The mechanical analogy of Maxwell model is shows in figure 1.10. It is a spring and a dashpot arranged in series. E_0 is the spring constant and η is dashpot constant.

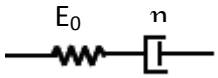

Maxwell

Figure 1.10: Maxwell model.

The differential equation that describe the behavior of this model is given by [32]

$$\frac{d\varepsilon(t)}{dt} = \frac{1}{E_0}\frac{d\sigma(t)}{dt} + \frac{1}{\eta}\sigma(t) \tag{1.10}$$

When a constant strain is applied, the solution to (1.10) leads the expression of the relaxation modulus $E(t)$, one can write

$$E(t) = E_0 e^{-(\frac{E_0}{\eta})t} = E_0 e^{-(\frac{t}{\tau_r})} \tag{1.11}$$

where τ_r is the relaxation time defined as $\tau_r = \frac{\eta}{E_0}$

When a constant stress is applied, the solution to (1.10) leads to the expression of the creep compliance $J(t)$, one can write

$$J(t) = \frac{1}{E_0}(1 + \frac{t}{\eta}) \tag{1.12}$$

Kelvin Voigt model

The mechanical analogy of the (KV) model is shown in figure 1.11. It has a spring and a dashpot arranged in parallel.

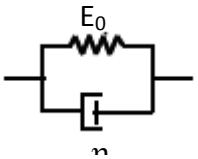

Kelvin-Voigt

Figure 1.11: Kelvin Voigt model.

The governing equation of Kelvin Voigt model is given by [26]

$$\sigma(t) = E_0 \varepsilon(t) + \eta \frac{d\varepsilon(t)}{dt} \tag{1.13}$$

Applying a constant strain, the relaxation modulus $E(t)$ is obtained

$$E(t) = \eta\delta(t) + E_0 \tag{1.14}$$

where $\delta(t)$ is Dirac function.

Applying a constant stress, the creep compliance $J(t)$ is obtained

$$J(t) = \frac{1}{E_0}(1 - e^{-(\frac{E_0}{\eta})t}) \tag{1.15}$$

Standard Linear Solid

The mechanical analogy of (SLS) is shown in figure 1.12. It combines a spring and a Maxwell model in parallel or a spring and (KV) model and series.

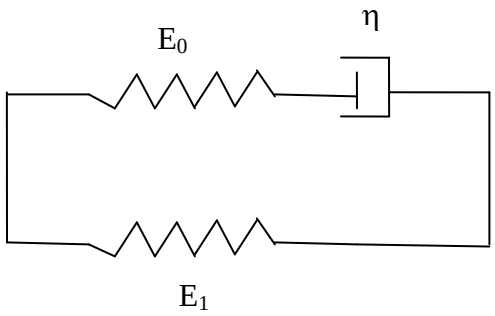

Figure 1.12: Standard Linear Solid model.

The governing equation of the Standard Linear model is given by [32]

$$\frac{\sigma(t)}{\eta} + \frac{1}{E_0}\frac{d\sigma(t)}{dt} = \frac{E_1}{\eta}\varepsilon(t) + (1 + \frac{E_1}{E_0})\frac{d\varepsilon(t)}{dt} \tag{1.16}$$

Applying a constant strain leads to the expression of the relaxation modulus $E(t)$, one can write

$$E(t) = E_0 e^{-(\frac{t}{\tau_r})} + E_1 \tag{1.17}$$

Applying a constant stress leads to the expression of the creep compliance $J(t)$, one can write

$$J(t) = \frac{1}{E_1}(1 - \frac{E_0}{E_0 + E_1} e^{-(\frac{t}{\tau_c})}) \tag{1.18}$$

where $\tau_c = \frac{E_0}{E_0 + E_1}$ is the creep time.

The Boltzman superposition integral [33]

The above expressions of the creep and relaxation modulus are valid under a constant stress and a constant strain. For general loading condition, the constitutive equations for linear viscoelastic materials can be derived based on the Boltzman superposition theory.

For an arbitrary stress input as illustrated in figure 1.13, the superposition principle is used by considering the arbitrary input as multiple step inputs applied at different times.

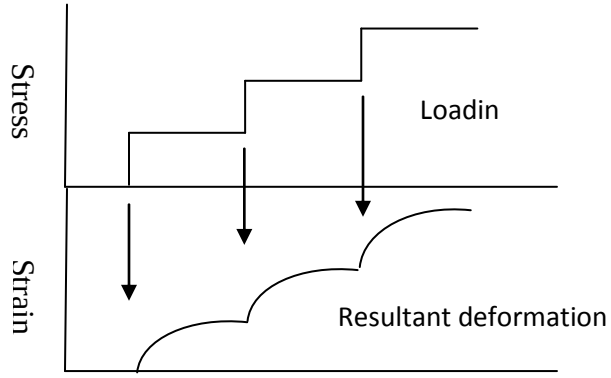

Figure 1.13: Creep behavior of an ideal viscoelastic solid.

The total strain at time t is given by

$$\varepsilon(t) = \Delta\sigma_1 J(t - t_1) + \Delta\sigma_2 J(t - t_2) + ... + \Delta\sigma_n J(t - t_n) = \sum_{k=1}^{n} \Delta\sigma_k J(t - t_k) \tag{1.19}$$

where $J(t - \tau_1)$ is the creep compliance function and $\Delta\sigma$ is the instantaneous stress jump.

Dividing and multiplying (1.19) by $\Delta t_k = t_{k+1} - t_k$, one can write

$$\varepsilon(t)=\sum_{k=1}^{n}J(t-\tau_k)\frac{\Delta\sigma_k}{\Delta t_k}\Delta t_k \tag{1.20}$$

When Δt_k approaches zero then (1.20) could be rewritten as follow

$$\varepsilon(t)=\int_0^t J(t-\tau)\frac{d\sigma}{d\tau}d\tau \tag{1.21}$$

Using similar procedure, the expression of $\sigma(t)$ is obtained. One can write

$$\sigma(t)=\int_0^t E(t-\tau)\frac{d\varepsilon}{d\tau}d\tau \tag{1.22}$$

where $E(t-\tau)$ is the relaxation function.

The constitutive equation of linear viscoelastic materials is determined by equation (1.21) and (1.22). Equations (1.21) and (1.22) seen simple but they are difficult to be used. To simplify their utilization they are expressed in the frequency domain by using the Laplace transform.

Using the Laplace transform to (1.22) leads to the following expression

$$\sigma(\omega)=E(\omega)\varepsilon(\omega) \tag{1.23}$$

where $E(\omega)=E^{'}(\omega)+iE^{''}(\omega)$ is the complex modulus. $E^{'}(\omega)$ and $E^{''}(\omega)$ are respectively the real part and imaginary parts of the complex moduli and $i=\sqrt{-1}$.

Using (1.23), one can solve the viscoelastic problem as a special case of the elastic one where the elastic moduli are complex and frequency dependent.

1.9 Extended time dependent constitutive equations

In this section, the Boltzman integral equation (1.22) is extended to the case of linear piezoelectric and magnetoelectroelastic materials.

The time dependent constitutive equations for viscoelectroelastic materials are given as follow [14].

$$\begin{aligned}\sigma_{ij}(t)&=\int_0^t c_{ijkl}(t-\tau)\frac{d\varepsilon_{kl}(\tau)}{d\tau}d\tau+\int_0^t e_{lij}(t-\tau)\frac{dE_l(\tau)}{d\tau}d\tau\\ D_i(t)&=\int_0^t e_{ikl}(t-\tau)\frac{d\varepsilon_{kl}(\tau)}{d\tau}d\tau+\int_0^t \kappa_{il}(t-\tau)\frac{dE_l(\tau)}{d\tau}d\tau\end{aligned} \tag{1.24}$$

Using the condensed notation (Fakri et al. (2003)), equations (1.24) could be written in a condensed form where

$$\Sigma_{iJ}(t)=\int_0^t E_{iJKl}(t-\tau)\frac{dZ_{Kl}(\tau)}{d\tau}d\tau \tag{1.25}$$

where $E_{iJKl}(t)=\begin{cases} c_{ijkl}(t) & (J,K=1,2,3) \\ e_{lij}(t) & (J=1,2,3;K=4) \\ e_{ikl}(t) & (J=4;K=1,2,3) \\ -\kappa_{il}(t) & (J=4;K=4) \end{cases}$ is the time dependent viscoelectroelastic relaxation tensor and

$$Z_{Mn}=\begin{cases} \varepsilon_{mn} & (M=1,2,3) \\ -E_n & (M=4) \end{cases} \qquad \Sigma_{iJ}=\begin{cases} \sigma_{ij} & (J=1,2,3) \\ D_i & (J=4) \end{cases}$$

are the generalized strain and stress.

Using the Laplace transform to (1.25) leads to the following expression in the frequency domain

$$\Sigma_{iJ}(\omega)=E_{iJKl}(\omega)Z_{Kl}(\omega) \tag{1.26}$$

where

$E_{iJKl}(\omega)=E'_{iJKl}(\omega)+iE''_{iJKl}(\omega)$ is the complex viscoelectroelastic moduli. $E'_{iJKl}(\omega)$ and $E''_{iJKl}(\omega)$ are respectively the real part and imaginary part of the complex viscoelectroelastic moduli and $i=\sqrt{-1}$.

For viscomagnetoelectroelastic materials, the time constitutive equation is given as follow:

$$\begin{aligned} \sigma_{ij}(t)&=\int_0^t c_{ijkl}(t-\tau)\frac{d\varepsilon_{kl}(\tau)}{d\tau}d\tau+\int_0^t e_{lij}(t-\tau)\frac{dE_l(\tau)}{d\tau}d\tau+\int_0^t h_{lij}(t-\tau)\frac{dH_l(\tau)}{d\tau}d\tau \\ D_i(t)&=\int_0^t e_{ikl}(t-\tau)\frac{d\varepsilon_{kl}(\tau)}{d\tau}d\tau+\int_0^t \kappa_{il}(t-\tau)\frac{dE_l(\tau)}{d\tau}d\tau+\int_0^t \alpha_{il}(t-\tau)\frac{dH_l(\tau)}{d\tau}d\tau \\ B_i(t)&=\int_0^t h_{ikl}(t-\tau)\frac{d\varepsilon_{kl}(\tau)}{d\tau}d\tau+\int_0^t \alpha_{il}(t-\tau)\frac{dE_l(\tau)}{d\tau}d\tau+\int_0^t \mu_{il}(t-\tau)\frac{dH_l(\tau)}{d\tau}d\tau \end{aligned} \tag{1.27}$$

The time dependent constitutive equations (1.24) and (1.27) will be used to predict the effective properties of heterogeneous viscoelectroelastic and viscomagnetoelectroelastic composites based on various micromechanical modelings.

1.10 Review of some micromechanical modelings

The prediction of mechanical behavior of composite materials requires sophisticated modeling tools. Micromechanical modeling offers the opportunity to model materials on a microstructural level. Micromechanical models provide the overall behavior of the composite materials from known properties of the individual constituents. Some basic features are common to any micromechanical modeling approach:

A. The geometric definition of a representative volume element (RVE) which possesses the essential characteristics of the microstructure.
B. The constitutive description of the mechanical behavior of each phase and the interaction between them.
C. A homogenization procedure based on the RVE to derive the macroscopic material behavior.

The study of micromechanics has been an active research area for many decades and continues to be the forefront of analysis of composite materials. Excellent reviews of micromechanics could be found in the open literature in Hashin [34], Nemat-Nasser and Hori [35], Milton [36], Christensen [37], and Mura [38]. A small review of some micromechanical models is presented in the following subsections.

1.10.1 Analytical models

1.10.1.1 Simple models

1.10.1.1.1 Voigt approximation

The first model and the simplest one was introduced by Voigt. According to Voigt the effective stiffness of the composite is obtained based on the assumption that the strain is uniform throughout the composite. Based on this assumption, the effective stiffness is derived in terms of volume fractions and stiffnesses of its constituents.

$$C_{ijkl}^{eff} = f_I C_{ijkl}^{(I)} + f_M C_{ijkl}^{(M)} \tag{1.28}$$

where f_I and f_M are the volume fraction of the inclusion and matrix, respectively; $C_{ijkl}^{(I)}$ and $C_{ijkl}^{(M)}$ are the elastic stiffness constants of the inclusion and matrix, respectively.

1.10.1.1.2 Reuss approximation

Another very simplistic model is the one proposed by Reuss. According to Reuss the effective compliance of the composite is derived based on the assumption that the stress is uniform throughout out the composite. Based on this assumption the effective compliance is obtained in terms of volume fractions and compliances of its constituents, One can write.

$$S_{ijkl}^{eff} = f_I S_{ijkl}^{(I)} + f_M S_{ijkl}{}^{(M)} \tag{1.29}$$

where f_I and f_M are the volume fraction of the inclusion and matrix, respectively; $S_{ijkl}^{(I)}$ and $S_{ijkl}^{(M)}$ are the elastic compliance constants of the inclusion and matrix, respectively.

It was shown by Hill that Reuss and Voigt approximation bound the actual effective moduli. The Voigt approximation provides the upper bound and the Reuss approximation provides the lower.

1.10.1.2 Micromechanical models based on the solution of integral equations

The micromechanical models presented here are based on the solution of the integral equation which is first derived by [39].

1.10.1.2.1 Local equations of elasticity and the integral equation

The constitutive equations of elastic materials is given by

$$\sigma_{ij} = C_{ijkl}\varepsilon_{kl} \tag{1.30}$$

where σ is the stress, ε is the strain and c is the elastic stiffness tensor.

The following gradient equation is used.

$$\varepsilon_{kl} = \frac{1}{2}(u_{k,l} + u_{l,k}) \tag{1.31}$$

The equilibrium equation in the absence of the body force is written as follow

$$\sigma_{ij,i} = 0 \tag{1.32}$$

Using the compatibility equation and the symmetry of the elastic stiffness tensor one can write

$$\sigma_{ij} = C_{ijkl}u_{k,l} \tag{1.33}$$

Replacing (1.33) into (1.32) the following partial differential equation is obtained

$$(C_{ijkl}u_{k,l})_{,j} = 0 \tag{1.34}$$

A homogeneous fictitious media, called “reference media” which has the elastic moduli C_{iJkl}^{0}, is considered. The expression of the local elastic moduli is given by:

$$C_{ijkl}(r) = C^0_{ijkl} + \delta C_{ijkl}(r) \tag{1.35}$$

where ‘’r’’ is the position vector in the media considered and δC is the deviation part. Introducing (1.35) into (1.34) leads to partial differential system

$$C^0_{ijkl} u_{k,lj}(r) + (\delta C_{ijkl}(r) u_{k,l}(r))_{,j} = 0 \tag{1.36}$$

Now, the elastic Green tensor denoted by $G(r - r')$, of the reference medium corresponding to the response at the position r due to unit force applied at r’. This tensor verifies the following partial differential equation.

$$C^0_{ijkl} G_{km,lj}(r) + \delta_{im}\delta(r - r') = 0 \tag{1.37}$$

The displacement could be expressed as follow

$$u_m(r) = \int_V u_k(r')\delta_{km}\delta(r - r')dV' \tag{1.38}$$

From equation (1.37) and using the fact that $G_{im,l} = -G_{im,l'}$ lead to the following integral equation

$$u_m(r) = -\int_V C^0_{ijkl} G_{im,j'l'}(r - r')u_k(r')dV' \tag{1.39}$$

One can see that

$$G_{im,j'l'}u_k = (G_{im,j'}u_k)_{,l'} - G_{im,j'}u_{k,l'} \tag{1.40}$$

Using (1.40) and the Stock’s theorem, (1.39) becomes

$$\begin{aligned} u_m(r) = &-\int_S C^0_{ijkl} G_{im,j'}(r - r')u_k(r')n'_l\, dS' + \int_S C^0_{ijkl} G_{im}(r - r')u_{k.l'}(r')n'_j\, dS' \\ &- \int_V C^0_{ijkl} G_{im}(r - r')u_{k.l'j'}(r')dV' \end{aligned} \tag{1.41}$$

The first integral represents the elastic displacement field in a homogeneous solid with geometry and boundary condition similar to the considered solid. This elastic displacement field is denoted by $u^0(r)$.

The second integral represents the static boundary condition and could be written as follow

$$u_m(r) = \int_S C^0_{ijkl} G_{im}(r - r')u_{k.l'}(r')n'_j\, dS' = \int_S G_{im}(r - r')\sigma_{ij}n'_j\, dS' = \int_S G_{im}(r - r')T^d_i dS' \tag{1.42}$$

Only the displacement boundary conditions are considered, so the second integral equals zero. Finally, using (1.36), (1.41) becomes

$$u_m(r) = u^0_m + \int_V G_{im}(r - r')(\delta C_{ijkl'}(r')u_{k.l'}(r'))_{,j'}dV' \tag{1.43}$$

Or:

$$u_m(r) = u_m^0 + \int_V G_{im}(r-r')(\delta C_{ijkl'}(r')\varepsilon_{kl'}(r'))_{,j'}dV' \quad (1.44)$$

Substituting (1.44) into (1.31) leads to the following integral equation

$$\varepsilon_{mn}(r) = \varepsilon_{mn}^0 + \int_V \frac{1}{2}(G_{im,n}(r-r') + G_{ni,m}(r-r'))(\delta C_{ijkl'}(r')\varepsilon_{kl'}(r'))_{,j'}dV' \quad (1.45)$$

As before, we can decompose the integral, and moreover, if we assume that it vanishes at the boundary, one can find

$$\varepsilon_{mn}(r) = \varepsilon_{mn}^0 - \int_V \frac{1}{2}(G_{im,nj'}(r-r') + G_{ni,mj'}(r-r'))\delta C_{ijkl'}(r')\varepsilon_{kl'}(r')dV' \quad (1.46)$$

Taking into account the fact that $G_{im,l} = -G_{im,l'}$ and considering

$$\Gamma_{mnij} = -\frac{1}{2}(G_{im,nj}(r-r') + G_{ni,mj}(r-r')) \quad (1.47)$$

One can get the following integral equation

$$\varepsilon_{mn}(r) = \varepsilon_{mn}^0 - \int_V \Gamma_{mnij}\delta C_{ijkl}(r')\varepsilon_{kl}(r')dV' \quad (1.48)$$

1.10.1.2.2 Solution of the integral equation

The integral equation is solved based on the work of Eshelby [6]. Consider an infinite media with elastic moduli C_{ijkl}^0 which contains a single inclusion "I" of volume V^I and elastic moduli V^I assumed to be constant inside the volume V^I. The inhomogeneity can be simulated by an "equivalent inclusion". Based on these assumption one can write

$$\delta C_{ijkl} = (C_{ijkl}^I - C_{ijkl}^0)\theta^I(r) = \Delta C_{ijkl}^I \theta^I(r) \quad (1.49)$$

where $\theta^I(r)$ is the characteristic function of V^I ($\theta^I(r)$ equals 1 inside the volume V^I and 0 outside of V^I). The introduction of (1.49) into (1.48) and averaging (1.48) over the volume V^I lead to

$$\varepsilon_{mn}^I = \varepsilon_{mn}^0 - \frac{1}{V^I}\int_{V^I}\int_V \Gamma_{mnij}(r-r')\Delta C_{ijkl}^I \theta^I(r')\varepsilon_{kl}(r')dV'dV \quad (1.50)$$

The exact solution of this equation is difficult to be obtained, an approximation is made by replacing $\varepsilon_{kl}(r')$ by its average value ε_{kl}^{I} as follows:

$$\varepsilon_{mn}^{I} = \varepsilon_{mn}^{0} - \frac{1}{V^{I}} \int_{V^{I}} \int_{V^{I}} \Gamma_{mnij}(r - r') \Delta C_{ijkl}^{I} \varepsilon_{kl}^{I} dV' dV \tag{1.51}$$

(1.51) could be reformulated in the following form

$$\varepsilon_{mn}^{I} = \varepsilon_{mn}^{0} - \frac{1}{V^{I}} T_{mnij}^{II} \Delta C_{ijkl}^{I} \varepsilon_{kl}^{I} \tag{1.52}$$

where $T_{mnij}^{II} = \int_{V^{I}} \int_{V^{I}} \Gamma_{mnij}(r - r') dV' dV$ represents the interaction tensor which depends on the properties of the infinite medium and the shape of the inclusion that the infinite medium contains.

1.10.1.2.3 The extended approach

The above developed equations could be extended to other kinds of materials such piezoelectric materials, magnetoelectroelastic materials etc. [40, 41] extended the modeling to the case of piezoelectric and thermopiezoelectric materials by using extended fields. The localization equation [41] that gives the relationship between the average generalized strain field Z_{Kl}^{I} in the inclusion with the generalized strain field in the infinite medium Z^{0} is given as follow

$$Z_{Kl}^{I} = Z_{Kl}^{0} - \frac{1}{V^{I}} T_{iJKl}^{II} \Delta E_{iJMn}^{I} Z_{Mn}^{I} \tag{1.53}$$

Z is the generalized strain field given by

$$Z_{Mn} = \begin{cases} \varepsilon_{mn} & (M = 1,2,3) \\ -E_{n} & (M = 4) \end{cases} \tag{1.54}$$

in which ε is the elastic strain tensor and E is the electric field.

E is the electroelastic moduli given by

$$E_{iJMn} = \begin{bmatrix} c_{ijmn} & e^{t}{}_{nij} \\ e_{imn} & -\kappa_{in} \end{bmatrix} \tag{1.55}$$

in which c is the elastic tensor, e the piezoelectric tensor and the dielectric tensor.

Finally T^{II} is the condensed notation of the four electroelastic tensors given by

$$T_{iJKl}^{II} = \int_{V^I} \int_{V^I} \Gamma_{iJKl}(r - r')dV'dV \tag{1.56}$$

where $\Gamma_{iJKl}(r - r') = -G_{JK,li}$ *with* $i,l = 1,2,3$ *and* $J,K = 1,2,3,4$

The explicit expression of $G_{JK,li}$ is given by Fakri et al. (2003) [40]

$$\begin{aligned}
&-\frac{1}{2}(G_{jk,li}(r - r') + G_{jl,ki}(r - r')) && for J \text{ and } K = 1,2,3 \\
&-\frac{1}{2}(G_{4k,li}(r - r') + G_{4l,ki}(r - r')) && for J = 4 \text{ and } K = 1,2,3 \\
&-G_{j4,li}(r - r') && for J = 1,2,3 \text{ and } K = 4 \\
&-G_{44,li}(r - r') && for J = 4 \text{ and } K = 4
\end{aligned}$$

The tensor T^{II} will be used to derive some models for effective properties of the composite.

1.10.1.2.4 Dilute Model

Dilute approximation is the next simplistic micromechanics approximation after Voigt and Reuss approximations. The key assumption made in dilute approximation model is based on the idea that a single inclusion embedded in infinite medium in one RVE. The particles are supposed to be very far apart from each other so the interaction between particles could be ignored. For an ellipsoidal particle, this solution has been obtained by [42, 43]. The effective elastic moduli for two-phase elastic composites with ellipsoidal inclusion are given by

$$C_{ijkl}^{eff} = C_{ijkl}^{M} + f_I(C_{ijmn}^{I} - C_{ijmn}^{M}) : A_{mnkl}^{Dil}(C^M) \tag{1.57}$$

where A^{Dil} is the concentration tensor that relates the local strain tensor in the inclusion with the applied strain on the composite. The Dilute concentration tensor is derived from (1.52) by replacing C^0 by the elastic moduli of the matrix C^M and ε^0 by the applied strain on the composite $\bar{\varepsilon}$. One can write the relationship that relates the average strain in the inclusions with the applied strain on the composite through the Dilute concentration tensor as follow

$$\varepsilon_{ij}^{I} = A_{ijkl}^{Dil}\bar{\varepsilon}_{kl} \tag{1.58}$$

Where $A^{Dil}_{mnkl} = (I_{klmn} + \frac{1}{V^I} T^{II}{}_{ijkl} \Delta C^I{}_{ijmn})^{-1}$, $\Delta C^I{}_{ijmn} = C^I{}_{ijmn} - C^M{}_{ijmn}$ and T^{II} is the interaction tensor.

1.10.1.2.5 Self Consistent model

The Self Consistent method is based on the work of Eshelby [6]. It was originally put forward in [44] in the study of the conductivity of composite materials. The application of the method to the mechanical behavior of polycrystalline and matrix based composites followed [45, 46, 47]. It was extended to the case of multi-site in [48]. [49] generalized the Self Consistent method to study the elastoplastic behavior of composite materials. The essential assumption employed is the consideration of a single inclusion embedded within an effective matrix having the effective elastic moduli of the composites, and thus the interactions of the inclusions are accounted for. It should be noted that the Self Consistent method gives an implicit expression of the effective moduli which is computed iteratively. The Self Consistent method has its limitation for composites with high volume fraction of inclusion and high modulus contrast between the constituents [50]. Also it fails to give correct estimation of composites with void inclusions [51]. The effective elastic moduli for two-phase elastic composites with ellipsoidal inclusion are given by

$$C^{eff}_{ijkl} = C^M_{ijkl} + f_I (C^I_{ijmn} - C^M_{ijmn}) : A^{Sc}_{mnkl} (C^{eff}) \tag{1.59}$$

where A^{Sc} is the concentration tensor that relates the local strain tensor in the inclusion with the applied strain on the composite. The Self Consistent concentration tensor is derived from (1.52) by replacing C^0 by the effective elastic moduli C^{eff} and ε^0 by the applied strain on the composite $\bar{\varepsilon}$. One can write the relationship that relates the average strain in the inclusions with the applied strain on the composite through the Self Consistent concentration tensor as follow

$$\varepsilon^I_{ij} = A^{Sc}_{ijkl} \bar{\varepsilon}_{kl} \tag{1.60}$$

where $A^{Sc}_{mnkl} = (I_{klmn} + \frac{1}{V^I} T^{II}{}_{ijkl} \Delta C^I{}_{ijmn})^{-1}$ and $\Delta C^I{}_{ijmn} = C^I{}_{ijmn} - C^{eff}{}_{ijmn}$

The Self Consistent model gives an implicit equation of the effective moduli that comes from the fact that A^{Sc} depends on the effective moduli C^{eff}. The effective moduli are predicted iteratively. To initialize the iterative process the initial value of the effective moduli is obtained from the Voigt model by

$$C_{ijkl}^{eff} = f_I C_{ijkl}^{I} + f_M C_{ijkl}^{M} \quad (1.61)$$

The concentration tensor is initialized by the identity tensor

$$A^{Sc} = I \quad (1.62)$$

If these conditions are respected, the iterative algorithm will converge to the effective moduli C^{eff}. In the numerical applications one sees that there are some cases where there is no convergence. To stop the process, a stopping criterion is defined as follow

$$\frac{\left\| \left\| C_{ijkl}^{n+1} \right\| - \left\| C_{ijkl}^{n} \right\| \right\|}{\left\| C_{ijkl}^{n+1} \right\|} \leq \delta \quad (1.63)$$

where C^n represents the approximation of the effective moduli at the nth step and δ the maximum admitted deviation.

1.10.1.2.6 Mori-Tanaka model

The Mori-Tanaka model was originally developed by [52]. Since then, the method has been successfully applied to many problems in the mechanics and physics of composite materials. The method was initially linked with Eshelby's [6] equivalent inclusion method and a review of many applications in this context is given in [53]. [54] re-examined the underlying assumptions of the method and reformulated it in a direct approach**.** The method has also received considerable attention from a theoretical standpoint by [55, 56, 57, 58] and has been shown to be on strong theoretical footing for the elastic behavior of two-phase composite media.

The main assumption of this method is the consideration of a single inclusion embedded in an infinite matrix subjected to the uniform average matrix strain. This method provides an explicit formulation for the calculation of effective properties of composites. Also, it allows one to perform homogenization analysis at minimum computational cost. The effective elastic moduli for two-phase elastic composites with ellipsoidal inclusion is given by

$$C_{ijkl}^{eff} = C_{ijkl}^{M} + f_I (C_{ijmn}^{I} - C_{ijmn}^{M}) : A_{mnkl}^{MT} (C^{M}) \quad (1.64)$$

where A^{MT} is the concentration tensor that relates the local strain tensor in the inclusion with the applied strain on the composite. The Self Consistent concentration tensor is derived from (1.50) by replacing C^0 by the elastic moduli of the matrix C^M and ε^0 by the average strain in the matrix ε^M. Then using the flowing relationship

$$\bar{\varepsilon} = f^M \varepsilon^M + f^I \varepsilon^I \quad (1.65)$$

One can write the relationship that relates the average strain in the inclusion ε^I with the applied strain on the composite $\bar{\varepsilon}$ through the Mori-Tanaka concentration tensor as follow

$$\varepsilon_{ij}^I = A_{ijkl}^{MT}\bar{\varepsilon}_{kl} \tag{1.66}$$

where $A_{mnkl}^{MT} = (I_{klmn} + \frac{f_M}{V^I} T^{II}{}_{ijkl}\Delta C^I{}_{ijmn})^{-1}$ and $\Delta C^I{}_{ijmn} = C^I{}_{ijmn} - C^M{}_{ijmn}$

1.10.1.3 Hashin-Shtrikman type variational bounds

Paul was the first to use the variational bounding techniques of linear elasticity to examine the bounds on the moduli of the multiphase materials. Paul [59] obtained the bounds for alloyed materials based on the principle of minimum potential and complementary energy.

Hashin [60] and Hashin Shtrikman [61] attempted to tighten the Paul's bounds to obtain more useful estimates of moduli for isotropic heterogeneous materials.

According to Hashin [60], the bounds for the effective elastic moduli are derived by assuming that the particles are spherical and that the action of whole heterogeneous material on any one inclusion is transmitted through a spherical shell, which lies wholly in the matrix. Hashin and Shtrikman [61] further extended their work by involving the elastic polarization tensor, to the derivation of upper and lower bounds for the effective elastic moduli of quasi-isotropic and quasi-homogeneous multiphase materials of arbitrary phase geometry. When the ratios between the different phase moduli are not too large the bounds derived are close enough to provide a good estimate for the elastic moduli. For the particulate two phase isotropic materials these bounds, lower (K_1^*) and upper (K_2^*) can be written as

$$K_1^* = K_1 + \frac{f_2}{\frac{1}{K_2 - K_1} + \frac{3f_1}{3K_1 + 4G_1}} \tag{1.67}$$

$$G_1^* = G_1 + \frac{f_2}{\frac{1}{G_2 - G_1} + \frac{6(K_1 + 2G_1)f_1}{5G_1(3K_1 + 4G_1)}} \tag{1.68}$$

$$K_2^* = K_2 + \frac{f_1}{\frac{1}{K_1 - K_2} + \frac{3f_2}{3K_2 + 4G_2}} \tag{1.69}$$

$$G_2^* = G_2 + \frac{f_1}{\frac{1}{G_1 - G_2} + \frac{6(K_2 + 2G_2) f_1}{5G_2(3K_2 + 4G_2)}} \tag{1.70}$$

where $K_2^* > K_1^*$; $G_2^* > G_1^*$; $f_1 + f_2 = 1$, K and G are the bulk and shear moduli.

The shear and bulk modulus are related the Young modulus (E) and to Poisson's ratio (ν) by the following relationship

$$K = \frac{E}{3(1-2\nu)} \;;\; G = \frac{E}{2(1+\nu)}$$

and they are related to Lame's parameter (λ) by

$$K = \frac{\lambda(1+\nu)}{3\nu} \;;\; G = \frac{\lambda(1-2\nu)}{2\nu}$$

1.10.2 Numerical methods

The effective properties of composites can be approximately obtained by numerically solving the governing equations over RVE associated with appropriate boundary conditions. Numerous numerical methods have been employed for resolving the micro fields, such as early finite difference methods, boundary element methods, and finite element methods (FEM). There are many micromechanics models that deal actually with the composites with the assumption of periodic microstructures. The reinforcements are arranged in rectangular, square, hexagonal array, or some other pattern of array. The smallest element is taken as RVE with periodic boundary conditions. Different RVE undergoes identical deformation when the composite medium is subjected to uniform far field loading. These approaches include fast Fourier transforms [62], discrete Fourier transforms [63], the transformation field analysis [64], method of cells (MOC) developed by Aboudi [65, 66, 67, 68], and RVE-based finite element methods [69]. Bellow, assumptions and geometry of the method of cells are presented.

1.10.2.1 The method of cells

The method of the unit cell is based upon the approximation that a composite could can by approximated by a periodic array. In using this periodicity, it is possible to analyze a single representative volume element of the continuum rather than the whole continuum. The representative volume element is then used as the building block from which the continuum is

constructed, as shown in figure 1.14 a. The representative volume element must meet two criteria. First, the element must include enough information to correctly represent the continuum. Secondly, the element must be structurally to the composite. These conditions are met by the cell structure in figure 1.14 b [67]. The microstructure of the composite is modeled by within each representative volume element, attempting to better represent the interaction between the matrix and fiber. The matrix is represented by a number of elements inside of each volume cell while the reinforcing material is allotted a single element. For the continuous fiber case pursued here, the matrix is assigned three elements in the cell. The coordinate system is set up so that the fibers are assumed to extend into the global x1 direction.

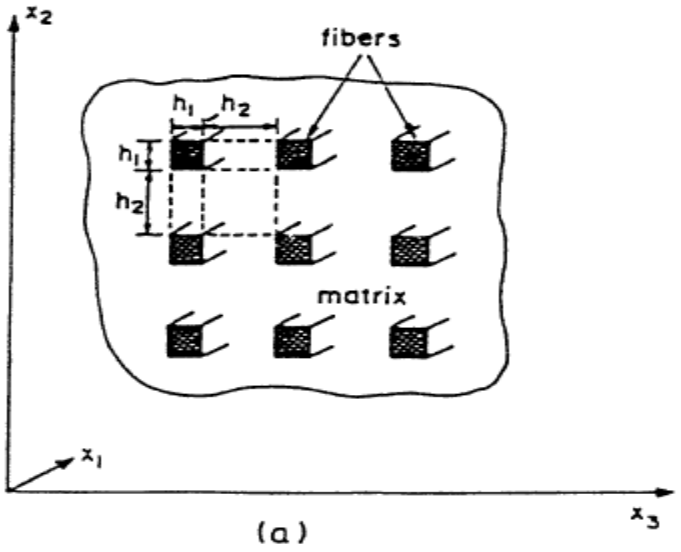

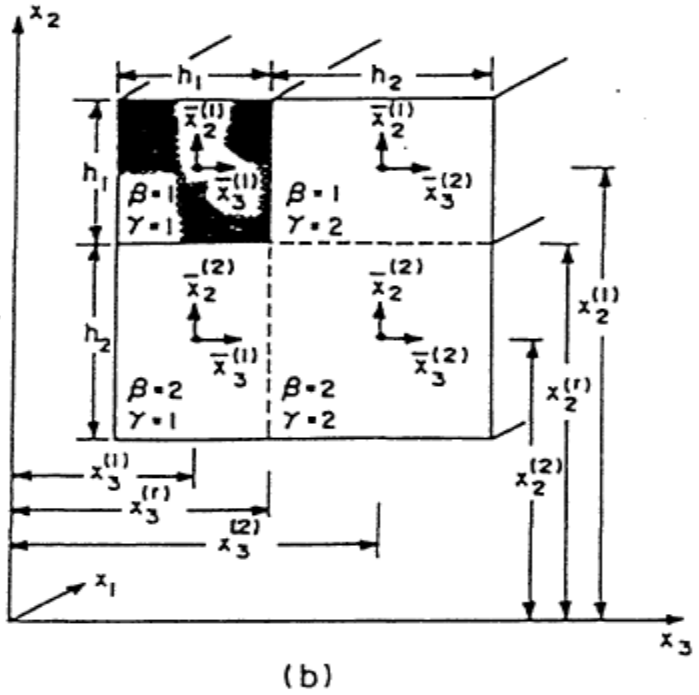

Figure 1.14: Geometry and unit cell for the method of cells (a) Composite arranged as a periodic array of fibers (b) Unit cell for the method of cells.

The periodic array can then be seen in the x_2, x_3 plan with a cross sectional view of the element shown in figure 1.14 b. Following the Aboudi's notation for numbering the element, the fiber element is designated by β=1 and γ=1. The reaming element (β, γ) = (1, 2), (2, 1) and (2, 2) are matrix elements. The length of one side of the element is assumed to be h_1+h_2 where h_1 is the width of the fiber. Since the fiber is transversely isotropic (isotropic in h_2, h_3 plane), the cross sectional area of the fiber is then h_1^2. The remaining length can be calculated based on the fiber volume fraction of the composite. As show in figure 1.14 b local coordinate systems are defined for each element, the origin of each centered in the element. These local coordinates are designated by $\bar{x}_2^{\beta}$ and $\bar{x}_3^{\gamma}$.

Using the local coordinate system, the displacements within each element are interpolated linearly from the center. It is possible to use a linear displacement since it is the average properties of the composite that are being calculated. Following Aboudi's notation, the displacement interpolations inside each element is written:

$$u_i^{(\beta\gamma)} = w_i^{(\beta\gamma)} + \bar{x}_2^{\beta}\phi_i^{(\beta\gamma)} + \bar{x}_3^{\gamma}\psi_i^{(\beta\gamma)} \tag{1.71}$$

where $i = 1,2,3$ and $w_i^{(\beta\gamma)}$ is the displacement of the center of the element. As the displacement interpolation is linear, $\phi_i^{(\beta\gamma)}$ and $\psi_i^{(\beta\gamma)}$ represent the constants coefficients of the linear dependence on the subcell coordinates.

Based on this displacement interpolation, the strain are then calculated as

$$\left\{\varepsilon_{ij}^{(\beta\gamma)}\right\} = \frac{1}{2}\left[\partial_i u_j^{(\beta\gamma)} + \partial_j u_i^{(\beta\gamma)}\right] \tag{1.72}$$

where ∂ represents partial differentiation with respect to the coordinate noted in the subscript and $i, j = 1,2,3$. The strain tensor is ordered here as

$$\left\{\varepsilon_{ij}^{(\beta\gamma)}\right\} = \left[\varepsilon_{11}^{(\beta\gamma)}\ \varepsilon_{22}^{(\beta\gamma)}\ \varepsilon_{33}^{(\beta\gamma)}\ 2\varepsilon_{12}^{(\beta\gamma)}\ 2\varepsilon_{13}^{(\beta\gamma)}\ 2\varepsilon_{23}^{(\beta\gamma)}\right] \tag{1.73}$$

The stress could be calculated as follow

$$\left\{\sigma_{ij}^{(\beta\gamma)}\right\} = \left[C_{ijkl}^{(\beta\gamma)}\right]\left\{\varepsilon_{kl}^{(\beta\gamma)}\right\} \tag{174}$$

where $\left[C_{ijkl}^{(\beta\gamma)}\right]$ is the stiffness matrix.

1.11 Overview of the dissertation

This dissertation focuses on investigating the effective behaviors and the effects of multifunctional materials such as magnetoelectroelastic composites, piezoelectroelastic composites as well as the non-linear transformation behavior of SMA composite materials. Different micromechanical models are developed and adapted in order to predict the effective behavior of these multifunctional composites.

In chapter 2, the effective behavior of two-phase and three-phase magnetoelectroelastic composites has been investigated by using different micromechanical models such as Incremental Self Consistent, Self Consistent, Mori-Tanaka and Dilute. The Self Consistent model underestimate the prediction of the effective properties of composite materials at high volume fraction of inclusion and for composites with void inclusions the prediction is limited for very low void concentrations. The aim of this chapter is to develop an N-phase Incremental Self Consistent model for magnetoelectroelastic materials to correct the anomalies showed by the Classical Self Consistent model. The Incremental Self Consistent model showed its efficiency for the prediction of the effective behavior at high volume fraction of inclusion as well as for composites with void inclusions. N-phase Mori-Tanaka and Dilute models have been developed and a comparison between the predictions of different micromechanical models has been done. The mathematical modeling is based on the magnetoelectroelastic Green's tensors that lead to the integral equation. The solution of the integral equation, obtained based on the Eshelby assumptions, leads to localization equation. Using the localization equation and based on different micromechanical approximation the concentration tenors for each micromechanical model are derived. Then using the homogenization process the expression of the effective behavior of magnetoelectroelastic composites is obtained. Numerical results have been presented for two-phase composites and three-phase composites with and without void by emphasizing the effect of shape and concentration inclusions [70, 71, 72].

This chapter is journal article entitled "Modeling of effective properties of multi-phase magnetoelectroelastic heterogeneous materials", published in the international journal Computers, Materials & Continua, (2011).

In chapter 3, the effective properties of magnetoelectroelastic composites with multicoated inclusions and functionally graded interphase are investigated based on different micromechanical models. The modeling is developed in the general case of anisotropic composites with non homothetic multi-coated ellipsoidal inclusions and functionally graded interphases. The integral equation taking into account the continuously varying interphase properties as well as the multi-functional coating effects is introduced based on the Green's tensors and interfacial operators. Magnetoelectroelastic composites with functionally graded interphases are analyzed and the effective properties are derived. Based on the Mori-Tanaka, Self Consistent and Incremental Self Consistent models the numerically predicted effective properties of magnetoelectroelastic composites are presented with respect to the volume fractions, shapes of the multi-coated inclusions and the thickness of the coatings [73, 74, 75, 76, 77, 78].

This chapter is a journal article entitled "Micromechanical modeling of magnetoelectroelastic composite materials with multi-coated inclusions and functionally graded interphases", published in the International Journal Intelligent Materials Systems and Structures, (2013).

In chapter 4, a micromechanical modeling is developed to predict the time dependent effective properties of viscoelectroelastic composites. The convolution model is adopted and various relaxation tensors can be considered. Time dependent and frequency dependent constitutive electroelastic equations are used. Two kinds of composites were considered: Two-phase viscoelectroelastic composites and multi-coated viscoelectroelastic composites. Using the correspondence principle of linear viscoelectroelasticity, the Mori-Tanaka micromechanical mean field approach is extended to the Carson domain. Based on the integral equation and on viscoelectroelastic interfacial operators the concentration tensors for viscoelectroelastic composites are derived. Various viscoelectroelastic models can be used. The effective properties are derived in the Carson domain and then are inverted numerically to the time domain by using the inverse of Laplace transform. The effective properties are then obtained in frequency and time domains. The effect of shape and volume fraction of reinforcements as well as the thickness of the coating is shown on the effective.

This chapter is a journal article entitled "Viscoelectroelastic effective properties of heterogeneous and multi-coated piezoelectric materials", submitted to the International Journal Solid and Structures, (2013).

In chapter 5, the methodological approach developed in chapter 4 is generalized to predict the effective viscomagnetoelectroelastic behavior of magnetoelectroelastic composites. Two kinds of composites were considered: Three-phase viscomagnetoelectroelastic composites consisting of a polymer matrix and piezoelectric and piezomagnetic inclusions and a three-phase composites consisting of piezoelectric inclusions surrounded by piezomagnetic inclusion embedded in a polymer matrix. Generalizing the correspondence principle of linear viscoelectroelasticity to the case of magnetoelectroelastic composites, the Mori-Tanaka micromechanical model is extended to Carson domain. Based on the integral equation and on viscoelectroelastic interfacial operators the concentration tensors for viscomagnetoelectroelastic composites are resulted. The effective properties are derived in the Carson domain and then inverted numerically to the time domain by using the inverse of the Laplace transform. The effective properties are presented in frequency and time domain [79].

Chapter 5 is a journal article entitled "Viscomagnetoelectroelastic effective properties of heterogeneous and multi-coated magnetoelectroelastic materials", will be submitted to an international journal.

Chapter 6 aims to develop a micromechanical modeling to investigate the nonlinear effective properties of shape memory alloy (SMA) composite materials. The SMA composite considered here is consisting of elastic inclusions embedded in an SMA matrix. The difficulty of modeling these kinds of composites is that SMA matrix undergoes a phase transformation after loading. The SMA matrix in the beginning is austenite and then after loading this matrix undergoes a phase transformation which leads to the apparition of the martensitic phase. After sufficient loading the matrix becomes fully martensitic. To take into account the effect of the apparition of the austenitic phase on the inclusion and then on the composites behavior the Mori-Tanaka multi-coated micromechanical model is used. The effective transformation behavior of the SMA composites is predicted by combining the Mori-Tanaka multi-coated micromechanical model with the constitutive equations of SMA materials [80].

Finally, Chapter 7 summarizes the important findings of the thesis. Concluding remarks and recommendations for future work are presented.

In the scope of the thesis the following articles are published:

- Bakkali, A.; Azrar, L.; Fakri, N. (2011): Modeling of effective properties of multiphase magnetoelectroelastic heterogeneous materials" Journal Computers, Materials & Continua, Vol. 23, N°3, pp 201-231.
- Bakkali, A.; Azrar, L.; Aljinaidi, A. A. (2012): Multi-coated magnetoelectroelastic composites with functionally graded interphases. MATEC Web of Conferences, Vol. 1, 09001.
- Bakkali, A.; Azrar, L.; Aljinaidi, A. A. (2013): Micromechanical modeling of magnetoelectroelastic composite materials with multi-coated inclusions and functionally graded interphases. Journal of Intelligent Materials Systems and Structures, Vol. 24, pp 1754-1769.
- Bakkali, A.; Azrar, L.; Aljinaidi, A. (2013): Effective properties of heterogeneous magnetoelectroelastic materials with multi-Coated inclusions. Key Engineering Materials, Vol. 550, pp 25-32.
- Azrar, L.; Bakkali, A.; Aljinaidi, A. A. (2013): Viscoelectroelastic effective properties of heterogeneous and multi-coated piezoelectric materials. Submitted to the International Journal of Solids and Structures.

References

[1]Kari, S., Berger, H., Gabbert, U., Guinovart-Diaz, R., Bravo-Castillero, J., Roriguez-Ramos, R., 2008. Evaluation of influence of interphase material parameters on effective material properties of three phase composites. Compos. Sci. Technol. 68, 684–691.

[2] Lemaitre, J. (1975): ModèIes rhéologique et lois d'écoulement. Ecole d'été de Métallurgie Physique de Villars-sur-ollon, édition du CNRS septembre.

[3] Voigt, W. (1889): Uber die beziehung zurischen den beiden elastizitats konstanten isotroper korper. Wied, Ann, Vol. 38.

[4] Reuss, A. (1929): Berechnung der fliessgrenze von mischkristallen auf grund der plastizitatsbedingun f'r einkristall. Z .Ang. Math. Mech.,Vol. 9.

[5] Hill, R. (1965): Continuum micro-mechanism of elastoplastic polycrystals. J. Mech. Phys. Solids, Vol. 1, pp. 89-101.

[6] Eshelby, J. (1957): The determination of the elastic field of an ellipsoidal inclusion, and related problems. Proceedings of the Royal Society of London, Series A, Vol. 241, pp. 376-396.

[7]Cherkaoui, M.; Sabar, H. and Berveiller, M. (1994): Micromechanical approach of the coated inclusion problem and applications to composites materials. J. Eng. Mater. Technol., 116: 247-278.

[8]Cherkaoui, M.; Sabar, H. and Berveiller, M. (1995): Elastic composites with coated reinforcement: A micromechanical approach for nonhomothetic topology. Int. J. Engng Sci., 33: 829-843, No. 6.

[9]Cherkaoui, M.; Sabar, H. and Berveiller, M. (1996): Elastic behavior of composites with coated inclusions: micromechanical approach and applications," Compos. Sci. Technol., 56: 877-882.

[10] Dinzart, F. and Sabar, H. (2009): Electroelastic behavior of piezoelectric composites with coated reinforcements: Micromechanical approach and applications. International Journal of Solids and Structures, 46: 3556–3564.

[11] Koutsawa, Y.; Biscani, F.; Belouettar, S.; Belouettar, H. and Carrera, E. (2010): Multi-coating inhomogeneities approach for the effective thermo-electro-elastic properties of piezoelectric composite materials. Composite structures, 92: 964–972.

[12] Gururaja, T. R.; Safari, A., Newnham, R. E.; Cross, L. E. (1987): Piezoelectric ceramic-polymer composites transducers application. Electronics Ceramics, ed. L. M. Livenson, pp. 92-128, Marcel Dekker, New York.

[13] Dapino, M. (2002): On magnetostrictive materials and their use in smart material transducer**.** Structural Engineering and Mechanics Journal, USA , pp. 1-28.

[14]Muliana, A.; Li, K. (2010): Time-dependent response of active composites with thermal, electrical, and mechanical coupling effect. International Journal of Engineering Science, Vol. 48, pp. 1481–1497.

[15] Jardine, A. P.; Kudva, J. M.; Martin, C.; Appa, K. (1996): Shape memory alloyTi-Ni actuators for twist control of smart wing designs. In: SPIE Proceedings of Mathematics and Controls in Smart Structures. Vol. 2717. SPIE.

[16] Garner, L. J.; Wilson, L. N.; Lagoudas, D. C.; Rediniotis, O. K. (2000): Development of a shape memory alloy actuated biomimetic vehicle. Smart Mater. Struct. 9 (5), 673–683.

[17] Ilyin, A.; Dudin, M.; Makarova, I. (1995): NiTi instruments for TMJ surgeries. In: Conf. Proc. Superelastic Shape Memory Implants in Medicine. Tomsk, Russia.

[18]Curie, J. ; Curie, P. (1880) : Développement, par pression, de l'électricité polaire dans les cristaux hémièdres à faces inclinées. Comptes Rendus de l'Académie des Sciences 91:294; 383; Bulletin de la Société minéralogique 3:90.

[19]Nye, J. F. (1957): Physical properties of crystals. Oxford University Press.

[20] Lkeda, T. (1990): Fundamentals of Piezoelectricity: Oxford University Press.

[21] Valasek See J. (1920). "Piezoelectric and allied phenomena in Rochelle salt". Physical Review 15: 537.

[22] Xu, Y. (1991): Ferroelectric Materials and Their Applications. North-Holland, New York.

[23] Borovik-Romanov, A. S. (1960): Piezomagnetism in the antiferromagnetic fluorides of cobalt and manganese. Soviet Phys. JETP 11, 786.

[24] Lee, J.; Boyd, J. G.; Lagoudas, D C. (2005): Effective properties of three-phase electro-magneto-elastic composites. Int. J. Engineering Science, Vol. 43, pp. 790-825.

[25] Astrov, D. N. (1960): The magnetoelectric effects in antiferromagnetics, Sov. Phys. JETP, 11, 708-709.

[26] Landau, L. D.; Lifshitz, E. M. (1960): Electrodynamics of continuous media. Pergamon, Oxford.

[27]Li, J.Y.; Dunn, M. L. (1998): Micromechanics of magnetoelectroelastic composite materials: average fields and effective behavior. Journal of Intelligent Material and Structures, Vol. 9, pp.404-416.

[28] Hill, N. A. (2000): Why are there so few magnetoelectric materials, J. Phys. Chem. B 104, 6697-6709.

[29] Olson, G. B.; Cohen, M. (1982): Stress assisted isothermal martensitic transformation: Application to TRIP steels. Metall. Trans. A 13A, 1907–1914.

[30] Pavlin, B. E. (2002): Micromechanical modeling of porous shape memory allows. Ph. D dissertation, Texas A&M University.

[31] Machado, L. G; Sav, M. A. (2003): Medical applications of Shape memory allows. Brazilian Journal of Medical and Biological Research, Vol. 36, pp. 683-691.

[32] Roylance, D. (2001): Engineering Viscoelasticity. Cambridge, MA 02139: Massachusetts Institute of Technology.

[33] Harvey, T. B.; Shuhua, H. and Zackary, R. K. (2011): A brief review of elasticity and viscoelasticity for solids. Advanced in Applied Mathematics and Mechanics, Vol. 3, pp. 1-51

[34] Hashin, Z. (1983): Analysis of composite materials-a survey. Journal of Applied Mechanics, Vol. 50, pp. 481-505.

[35] Nemat-Nasser, S; Hori, M. (1993): Micromechanics: Overall Properties of Heterogeneous Materials, 2nd ed., North-Holland, Amsterdam.

[36] Milton, G.W. (2001): Theory of Composites, Cambridge University Press.

[37] Christensen, R.M. (1979): Mechanics of Composite Materials, Dover Publication, Inc., New York.

[38] Mura, T. (1987): Micromechanics of Defects in Solids, Martinus Nijhoff, Dordrecht, 1987.

[39] Dederich, P .H.; Zeller, R. (1973), Z. Phys. 259, pp.103-113.

[40]Fakri, N.; Azrar, L.; El Bakkali, L. (2003): Electoelastic behavior modeling of piezoelectric composite materials containing spatially oriented reinforcements. International Journal of Solids and Structures, Vol. 40, Issue 2, pp. 361-384.

[41]Fakri, N.; Azrar, L. (2010): Thermal and electro-elastic behavior of piezo-composites and inhomogeneous piezoelectric materials with voids. Journal of Intelligent Materials Systems and Structures, Vol. 21, N°2, pp. 161-174.

[42] Deee. W. F. (1980): The analvsis of dislocation, crack, and inclusion problems in piezoelectric solids. Ph.D Dissertation; Stanford University.

[43] Wang, B. (1992): Three-dimensional analysis of an ellipsoidal inclusion in a piezoelectric material. Int. J. Solids Structures 29,293-308.

[44] Hershev, A. V. (1954): The elasticity of an isotropic aggregate of anisotropic cubic crystals. J. Appl. Mech. 21, 236-241

[45] Kroner. E. (1958): Berechnung der elastischen konstanten des vielkristalls aus den konstanten des einkristalls. Z. Phys: lSi, 5041518.

[46] Budiansky, B. (1965): On the elastic moduli of some heterogeneous materials. J. Mech. Phys. Solids, 13, 223-227.

[47] Hill, R. (1965): A self-consistent mechanics of composite materials. J. Mech. Phys. Solids, 13,213-222.

[48]Fassi Fehri, O. (1985): le problème de la paire d'inclusion plastiques et hétérogènes dans une matrice anisotrope application à l'étude du comportement des matériaux composites et de la plasticite. Thèse de doctorat d'état (Metz).

[49]Lipenski, P.; Berveiller, M (1989): Elastoplasticity of micorinohomogeneous metals et large strains. int. J. plasticity, 5, 149-172.

[50] Banerjee, B. (2002): Micromechanics-based prediction of thermoelastic properties of high energy materials. University of Utah, Ph.D dissertation.

[51] Christensen, R.M. (1979): Mechanics of Composite Materials, Dover Publication, Inc., New York.

[52] Mori, T.;Tanaka, K. (1973): Average stress in matrix and average elastic energy of materials with misfitting inclusions. Acta Metall. 21,571-574.

[53] Taya, M.; Arsenault, R. J. (1989): Metal Matrix Composites, Thermomechanical Behavior. Pergamon Press, Oxford.

[54] Benveniste, Y. (1987): A new approach to the application of Mori-Tanaka's theory in composite materials. Mech. Mater. 6, 147-157..

[55] Weng, G. (1990): The theoretical connection between Mori-Tanaka's theory and the Hashin-Shtrikman-Walpole bounds. lnt. J. Engng Sci. 28, 1111-1120.

[56] Weng, G. J. (1992): Explicit evaluation of Willis' bounds with ellipsoidal inclusions. Int. J. Engng Sci. 30, 83-92.

[57] Benveniste, Y.; Dvorak, G. J.; Chen, T. (1991): On diagonal symmetry of the approximate effective stiffness tensor of heterogeneous media. J. Mech. Phys. Solids 39, 927-946.

[58] Ferrari, M. (1991): Asymmetry and the high concentration limit of the Mori-Tanaka effective medium theory. Mech. Mater. 11, 251-256.

[59] B. Paul, Feb. (1960): Prediction of elastic constants of multiphase materials. Transactions of the Metallurgical Society of AIME, pp. 36-41.

[60] Hashin Z. (1962): The elastic moduli of heterogeneous materials. J Appl. Mech. Vol. 29, pp. 143-150.

[61] Hashin Z.; Shtrikman, S. (1963): A Variational Approach to the Theory of Elastic Behavior of Multiphase Materials, J. Mech. Phys. Solids, Vol. 211, pp. 127-140.

[62] Moulinec, H.; Suquet, P. (1994): A fast numerical method for computing the linear and nonlinear mechanical properties of composites. Comptes Rendus de l'Acadmie des sciences, Serie II, 318,1417-1423.

[63] Muller, W.H. (1996). Mathematical versus experimental stress analysis of inhomogeneities in solids. Journal of Physics IV, 6, 1-139-C1-148.

[64] Dvorak, G.J. (1992): Transformation field analysis of inelastic composite materials. Proceedings of the Royal Society of London A, 437, 311-327.

[65] Aboudi, J. (1982): A continuum theory for fiber-reinforced elastic-viscoplastic composites. International Journal of Engineering Science, 20, 605-621.

[66] Aboudi, J. (1987): Closed form constitutive equations for metal matrix composites. International Journal of Engineering Science, 25, 1229-1240.

[67] Aboudi, J. (1989): Micromechanical analysis of composites by method of cells. Applied Mechancis Review, 42, 193-221.

[68] Aboudi, J. (1996): Micromechanical analysis of composites by method of cells-update. Applied Mechancis Review, 49, S83-S91.

[69] Sun, C.T.; Vaidya, R.S. (1996): Prediction of composite properties from a representative volume element. Composites Science and Technology, 56, 171-179.

[70] Bakkali, A; Azrar, L.; Fakri, N. (2010): Modélisation mathématique du comportement effectif des matériaux multifonctions. Workshop, Modélisation, analyse et contrôle des systemes, 16-17 Avril 2010, Meknes, Maroc.

[71] Bakkali, A; Azrar, L.; Fakri, N. (2010): Micromechanics modeling of the effective moduli of magnetoelectroelastic composite materials. international Symposium on Aircraft Materials ACMA-2010, 19-12-Mai 2010, Marrakech,-Morocco.

[72]Bakkali, A.; Azrar, L.; Fakri, N. (2011): Modeling of effective properties of multiphase magnetoelectroelastic heterogeneous materials" Journal Computers, Materials & Continua, Vol. 23, N°3, pp 201-231.

[73]Bakkali, A.; Azrar, L. ; Aljunaidi, A.; Fakri, N. (2011): Modélisation micromécanique des matériaux composites magnétoéléctroélastiques avec des renforcements enrobes. In proceedings of the 10th Conference of Mechanics, Oujda, April 19-22, 2011.

[74] Bakkali, A.; Azrar, L.; Aljunaidi, A. A. (2012): Multi-coated magnetoelectroelastic composites with functionally graded interphases. Conference on Structural Nonlinear Dynamics and Diagnosis, 29 Avril 02 Mai, 2012, Marrakech, Maroc.

[75] Bakkali, A.; Azrar, L.; Aljunaidi, A. A. (2012): Micromechanical modeling of magneto-electro-elastic composites materials with multi-coated reinforcements. Symposium on Aircraft Materials ACMA-201é, 9-12 Mai, 2012, Fès, Maroc.

[76]Bakkali, A.; Azrar, L.; Aljinaidi, A. A. (2012): Multi-coated magnetoelectroelastic composites with functionally graded interphases. MATEC Web of Conferences, Vol. 1, 09001.

- [77]Bakkali, A.; Azrar, L.; Aljinaidi, A. A. (2013): Micromechanical modeling of magnetoelectroelastic composite materials with multi-coated inclusions and functionally graded interphases. Journal of Intelligent Materials Systems and Structures, , Vol. 24, pp 1754-1769.

[78]Bakkali, A.; Azrar, L.; Aljinaidi, A. (2013): Effective properties of heterogeneous magnetoelectroelastic materials with multi-Coated inclusions. Key Engineering Materials, Vol. 550, pp 25-32.

[79]Bakkali, A.; Azrar, L.; Aljinaidi, A. A. (2013): electroviscoelastic effective properties of heterogeneous piezoelectric materials. In proceedings, le 11eme congrès de mécanique, du 23 au 26 Avril, 2013, Agadir, Maroc.

[80]IIMEC intership report (2011): Micromechanical modeling of SMA composite materials. Aerospace Engineering department, Texas A&M University, Texas, USA.

Chapter 2

2. Modeling of effective properties of multi-phase magnetoelectroelastic heterogeneous materials

Abstract

In this paper an N-phase Incremental Self Consistent model is developed for magnetoelectroelastic composites as well as the N-phase Mori-Tanaka and classical Self Consistent. Our aim here is to circumvent the limitation of the Self Consistent predictions for some coupling effective properties at certain inclusion volume fractions. The anomalies of the SC estimates are more drastic when the void inclusions are considered. The mathematical modeling is based on the heterogeneous inclusion problem of Eshelby which leads to an expression for the strain-electric-magnetic field related by integral equations. The effective N-phase magnetoelectroelastic moduli are expressed as a function of magnetoelectroelastic concentration tensors based on the considered micromechanical models. The effective properties are obtained for various types, shapes and volume fractions of inclusions and compared with the existing results.

2.1 Introduction

The concept of new multifunctional materials constitutes now a scientific challenge especially for smart composites which include magnetoelectroelastic composites. Efforts are currently under way to develop materials that have superior properties to those currently existing. This has resulted in the development of composite materials that exhibit remarkable properties, which are created by the interaction between the constituent phases. There are many advantages to using composite materials more than traditional materials, such as the possibility of weight or volume reduction in a structure while maintaining a comparable or improved performance level.

Composite materials consisting of a piezoelectric phase and a piezomagnetic phase show a remarkably large magnetoelectric coefficients and large coupling coefficients between elastic, electric and magnetic fields, which do not exist in either constituent. The magnetoelectric coupling in the composite is created through the interaction between the piezoelectric and the piezomagnetic phases. The product property of composites offers great opportunities to design new materials that are capable of responding in a desired way to the internal or environment changes, which may not be achieved by traditional materials. The coupling effects in magnetoelectroelastic composites materials have many uses in many engineering fields such aeronautics, automotives and medical imagery. The double coupling effects in piezoelectric materials and the triple ones in magnetoelectroelastic are very useful for sensors and actuators.

The effective properties of piezoelectric composites materials have been investigated by many researchers. Dunn and Wienecke (1996, 1997) have given the closed-form expressions for the infinite-body Green's functions for a transversally isotropic piezoelectric medium and the four Eshelby tensors for spheroid inclusions in transversally isotropic solids. Dunn and Taya (1993) predicted the effective properties using the Dilute, Self Consistent, Mori-Tanaka, and Differential micromechanical models. Fakri, Azrar and El Bakkali (2003) predicted the behavior of piezoelectric composite materials and presented the numerical results for the effective electroelastic properties in term of phase properties, orientation angles, volume fraction and shapes of inclusions. Odegard (2004) proposed a new modeling approach to predict the bulk electromechanical properties of piezoelectric composites and compared the obtained results with those obtained by the Mori-Tanaka approach and the finite element method. Li (2004) applied the Self Consistent approach to predict the effective pyroelectric and thermal expansion

coefficients of ferroelectric ceramics taking into account the texture change due to domain switching during poling.

For magnetoelectroelastic composites, Li and Dunn (1998) investigated the magnetoelectroelastic coupling effects using the mean field Mori-Tanaka method and presented numerical results for fibrous and laminated composites. Wu and Huang (2000) investigated the magnetoelectric coupling effect in a fibrous composites with piezoelectric and piezomagnetic phases. Based on the eigenstrain formulation and Mori-Tanaka approach, the magnetoelectroelastic Eshelby tensors and the effective material properties of the composite are obtained explicitly. Li (2000) studied the average magnetoelectroelastic field in a multi-inclusion or inhomogeneities embedded in an infinite matrix. Feng, Fang and Hwang (2004) investigated the effective properties of composite consisting of piezomagnetic inhomogeneities embedded in a non-piezomagnetic matrix by using a unified energy method and the Mori-Tanaka and Dilute approaches. Zhang and Soh (2005) extended the micromechanical Self Consistent, Mori-Tanaka and Dilute to study the coupled magnetoelectroelastic composite materials. Srinivas and Li (2005) developed a Self Consistent approach to calculate the macroscopic magnetoelectric coefficients by emphasizing the effects of shape, volume fraction and orientation distribution of particles of both phases. Lee, Boyd and Lagoudas (2005) developed a finite element analysis and micromechanics based averaging of a representative volume element to determine the effective dielectric, magnetic, mechanical, and coupled-field properties of an elastic matrix reinforced with piezoelectric and piezomagnetic fibers. A special emphasis on the poling directions of the piezoelectric and piezomagnetic fibers is done. Srinivas, Li, Zhou and Soh, (2006) developed a mean field Mori-Tanaka model to calculate the effective magnetoelectroelastic moduli of matrix-based multiferroic composites by emphasizing the effects of shape and orientation distribution of second phase particles composites. More recently, Fakri and Azrar (2010) developed the Incremental Self Consistent method to thermoelectroelastic materials to predict the electro elastic and thermal response of piezocomposites with and without voids.

The classical Self Consistent model, which is widely used, overestimates the predictions of some magnetoelectroelastic composites effective properties for moderate and high concentrations of reinforcements and diverges for some coefficients. For magnetoelectroelastic composites with void inclusions the predictions are limited for very low void concentrations and are erroneous for

volume fraction greater than 10%. The aim of this paper is on one hand to develop an N-phase Incremental Self Consistent model for magnetoelectroelastic materials. On the other hand to present an accurate model based on the Self Consistent procedure for N-phases coupled materials In this work, a micromechanical modeling is used to predict the behavior of multi-phase magnetoelectroelastic composites. The nine interaction tensors which are used to predict the effective moduli of multi-phase magnetoelectroelastic composites based on various micro mechanical approaches such Self Consistent, Mori-Tanaka, Dilute and Incremental Self Consistent schemes are derived. Numerical results are obtained for various shapes of inclusions and compared with the existing ones. A mathematical modeling based on the Incremental Self Consistent model is developed for multi-phase magnetoelectroelastic composites. It is clearly demonstrate in this work that the Incremental Self Consistent model gives more accurate results than the classical Self Consistent model.

2.2 Basic equations

Let us consider the linear magnetoelectroelastic effect, where the magnetic, electric and elastic fields are coupled through the following constitutive equations:

$$\begin{aligned} \sigma_{ij} &= c_{ijkl}\varepsilon_{kl} - e_{lij}E_l - h_{lij}H_l \\ D_i &= e_{ikl}\varepsilon_{kl} + \kappa_{il}E_l + \alpha_{il}H_l \\ B_i &= h_{ikl}\varepsilon_{kl} + \alpha_{il}E_l + \mu_{il}H_l \end{aligned} \tag{2.1}$$

where the elastic strain ε_{kl}, electric fields E_l, and magnetic fields H_l are independent variables related to stresses σ_{ij}, electric displacements D_i and magnetic inductions B_i. The tensors c_{ijkl}, e_{lij}, h_{lij}, α_{il}, κ_{il} and μ_{il} are the elastic, piezoelectric, piezomagnetic, magnetoelectric, dielectric and magnetic permeability constants respectively. Let us note that $c_{ijkl} = c_{jikl} = c_{ijlk} = c_{jilk}$, $e_{lij} = e_{lji}$ and $h_{lij} = h_{lji}$. In the constitutive equations we use $-E_l$ and $-H_l$ rather than E_l and H_l as they will permit the construction of a symmetric matrix of constitutive moduli. The following gradient expressions are used:

$$\varepsilon_{kl} = \frac{1}{2}(u_{k,l} + u_{l,k}) \qquad E_l = -\varphi^e_{,l} \qquad H_l = -\varphi^m_{,l} \tag{2.2}$$

where u_k, φ^e, φ^m are the elastic displacements, electric and magnetic potentials, respectively.

The equilibrium equations, in the absence of body forces, electric charge and electric current densities, are as follows:

$$\sigma_{ij,i} = 0 \qquad D_{i,i} = 0 \qquad B_{i,i} = 0 \tag{2.3}$$

In order to make easy the manipulation of these equations, the condensed notations are used. These notations are identical to those using the conventional subscripts except that the lower case subscripts assume the range of 1-3, while the capital subscripts take the range of 1-5, and the repeated capital subscripts are summed over 1-5. With these notations, the generalized strain field denoted by Z_{Mn} can be expressed as

$$Z_{Mn} = \begin{cases} \varepsilon_{mn} & (M = 1,2,3) \\ -E_n & (M = 4) \\ -H_n & (M = 5) \end{cases} \tag{2.4}$$

Note that Z_{Mn} can be derived from the generalized potential field U_M given by

$$U_M = \begin{cases} u_m & (M = 1,2,3) \\ \varphi^e & (M = 4) \\ \varphi^m & (M = 5) \end{cases} \tag{2.5}$$

Similarly, the generalized stress field $\sum_{iJ}$ is given by

$$\sum_{iJ} = \begin{cases} \sigma_{ij} & (J = 1,2,3) \\ D_i & (J = 4) \\ B_i & (J = 5) \end{cases} \tag{2.6}$$

The magnetoelectroelastic constants can then be represented as follows:

$$E_{iJMn} = \begin{cases} c_{ijmn} & (J, M = 1,2,3) \\ e_{nij} & (J = 1,2,3; M = 4) \\ h_{nij} & (J = 1,2,3; M = 5) \\ e_{imn} & (J = 4; M = 1,2,3) \\ h_{imn} & (J = 5; M = 1,2,3) \\ -\kappa_{in} & (J = 4; M = 4) \\ -\alpha_{in} & (J = 4; M = 5 or J = 5; M = 4) \\ -\mu_{in} & (J = 5; M = 5) \end{cases} \tag{2.7}$$

The symmetry of E_{iJMn} can be obtained from those of c_{ijmn}, e_{nij} , h_{nij} , κ_{in} , α_{in} and μ_{in} . By using these shorthand notations, eqs. (2.1) can be rewritten as a single equation as follows:

$$\Sigma_{iJ} = E_{iJMn} Z_{Mn} \tag{2.8-a}$$

Note that Z_{Mn}, U_M, $\sum_{iJ}$ and E_{iJMn} are not tensors, and they can be conveniently expressed in matrix form as follows :

$$E_{iJMn} = \begin{bmatrix} c_{ijmn} & e^t{}_{nij} & h^t{}_{nij} \\ e_{imn} & -\kappa_{in} & -\alpha_{in} \\ h_{imn} & -\alpha_{in} & -\mu_{in} \end{bmatrix} \tag{2.8-b}$$

$$Z_{Mn} = U_{M,n} \tag{2.8-c}$$

The magnetoelectroelastic coefficients can then be represented by the (12×12) matrix E. Similarly, Z is a (12×1) vector. Thus, in order to express the equilibrium equations, each individual tensor must be transformed by the well known law of tensor transformations. The resulting tensors can then be reunified into the form of Eqs.(2.4) to (2.7). Substituting Eqs. (2.2) into Eqs.(2.1) and considering matrix symmetry, one obtains:

$$\sum_{iJ} = E_{iJMn} U_{M,n} \tag{2.9}$$

Introducing Equation (2.9) in the equilibrium equation (2.3), the following partial differential equation is obtained:

$$(E_{iJMn} U_{M,n})_{,i} = 0 \tag{2.10}$$

2.3 Integral equation formulation

Let us consider a homogeneous fictitious media called "reference media" which has the magnetoelectroelastic moduli E^0_{iJMn}. The expression of the local magnetoelectroelastic moduli is given as follow:

$$E_{iJMn}(r) = E^0_{iJMn} + \delta E_{iJMn}(r) \tag{2.11}$$

where "r'' is the position vector in the media considered and δE is the deviation part. The introduction of this expression into (2.10) leads to

$$E^0_{iJMn} U_{M,ni}(r) + (\delta E_{iJMn}(r) U_{M,n}(r))_{,i} = 0 \tag{2.12}$$

Now, let us introduce the magnetoelectroelastic Green's tensors, denoted by $G_{MJ}(r - r')$, of the reference media corresponding to the response at the position r due to a unit point force or charge at r'. These tensors satisfy the following partial differential equation:

$$E^0_{iJMn} G_{MK,in}(r-r') + \delta_{JK}\delta(r-r') = 0 \tag{2.13}$$

This partial differential equation, satisfied by the magnetoelectroelastic Green's tensors, condensed nine partial differential equations. Based on (2.13), and after some mathematical manipulations and the consideration of the boundary condition, the expression of the local generalized field $U_M(r)$ is derived:

$$U_K(r) = U^0_K(r) + \int_V G_{JK}(r-r')(\delta E_{iJMn}(r') U_{M,n}(r'))_{,i'} dV' \tag{2.14}$$

Using the fact that $Z_{Kl} = U_{K,l}$ and considering the condition that the local generalized strain field vanishes at the boundaries the expression of the local generalized strain field can be written as:

$$Z_{Kl}(r) = Z^0_{Kl}(r) - \int_V \Gamma_{iJKl}(r-r')(\delta E_{iJMn}(r') Z_{Mn}(r'))dV' \tag{2.15}$$

where $\Gamma_{iJKl}(r-r') = -G_{JK,li}(r-r')$ is a condensed notation of nine tensors.

This equation is an integral formulation of the generalized strain field $Z_{Kl}(r)$. To solve this equation the equivalent inclusion approach will be used.

2.4 Averaged field

Consider an infinite media with magnetoelectroelastic moduli E^0_{iJMn} which contains a single inclusion ''I" of volume V^I and magnetoelectroelastic moduli E^I_{iJMn} assumed to be constant inside the volume V^I. The inhomogeneity can be simulated by an "equivalent inclusion". Based on these assumptions, as done by Eshelby (1957) in the elastic case and by Deeg (1980) in the electroelastic case, one obtains

$$\delta E_{iJMn} = (E^I_{iJMn} - E^0_{iJMn})\theta^I(r)$$

Or $$\delta E_{iJMn} = \Delta E^I_{iJMn}\theta^I(r) \tag{2.16}$$

where $\theta^I(r)$ is the characteristic function of V^I ($\theta^I(r)$ equals 1 inside the volume V^I and 0 outside of V^I). Based on Eq. (2.15), the average generalized strain field Z^I_{Kl} in the considered inclusion is given by the following expression:

$$Z^I_{Kl} = Z^0_{Kl} - \frac{1}{V^I}\int_{V^I}\int_V \Gamma_{iJKl}(r-r')\Delta E^I_{iJMn}\theta^I(r')Z_{Mn}(r')dV'dV \tag{2.17}$$

The exact solution of the above integral equation is difficult to be obtained. An approximation is then made by replacing $Z_{Mn}(r')$ by its average value Z_{Kl}^{I} in the considered inclusion as follows:

$$Z_{Kl}^{I} = Z_{Kl}^{0} - \frac{1}{V^{I}} \int_{V^{I}} \int_{V^{I}} \Gamma_{iJKl}(r - r') \Delta E_{iJMn}^{I} Z_{Mn}^{I} dV' dV \tag{2.18}$$

This equation can be reformulated in the following form:

$$Z_{Kl}^{I} = Z_{Kl}^{0} - \frac{1}{V^{I}} T_{iJKl}^{II} \Delta E_{iJMn}^{I} Z_{Mn}^{I} \tag{2.19}$$

where $T_{iJKl}^{II} = \int_{V^{I}} \int_{V^{I}} \Gamma_{iJKl}(r - r') dV' dV$ represents the condensed notation of the nine interaction tensors. These tensors are computed numerically for various shapes of inclusions using the Gaussian quadrature integration for the considered inclusion shape.

2.4.1 Spherical inclusion

A spherical inclusion with radius "q" is considered. In spherical system attached at the inclusion, the vector $\vec{q}$ becomes

$$q_p = q\chi_p \qquad p = 1, 2, 3 \tag{2.20}$$

where $\vec{\chi} = \begin{cases} \sin\theta cos\varphi \\ \sin\theta \sin\varphi \\ \cos\theta \end{cases}$

q, θ and φ are the spherical coordinates of the vector $\vec{q}$ defined in the following domains: q∈[0, +∞[, θ ∈[0, π] and φ ∈[0, 2π].

Application of the Fourier transform to Eq. (2.13) leads to the following expression

$$E_{iJMn}^{0} \tilde{G}_{JK}(q) q_n q_i = \delta_{MK} \tag{2.21}$$

The introduction of the equation (2.20) into (2.21) leads to the algebraic problem

$$E_{iJMn}^{0} \chi_n \chi_i (q^2 \tilde{G}_{JK}(q)) = \delta_{MK} \tag{2.22}$$

Let us introduce a matrix M defined by

$$M_{JM} = E_{iJMn}^{0} \chi_n \chi_i \tag{2.23-a}$$

The inverse of M is given by

$$M_{JK}^{-1} = q^2 \tilde{G}_{JK}(q) \tag{2.23-b}$$

The explicit expression of the matrix M is given by

$$M = \begin{bmatrix} A & B \\ B^t & C \end{bmatrix} \tag{2.23-c}$$

Expressions of matrices A, B and C are derived for piezoelectric and piezomagnetic media which belong to crystallographic classes of tetragonal symmetry. With spherical coordinate, these matrices are expressed as:

$$A = \begin{bmatrix} c_{11}x_1^2 + c_{22}x_2^2 + c_{55}x_3^2 & (c_{12}+c_{66})x_1x_2 & (c_{13}+c_{55})x_1x_3 \\ (c_{12}+c_{66})x_1x_2 & c_{66}x_1^2 + c_{22}x_2^2 + c_{44}x_3^2 & (c_{23}+c_{44})x_2x_3 \\ (c_{13}+c_{55})x_1x_3 & (c_{23}+c_{44})x_2x_3 & c_{55}x_1^2 + c_{44}x_2^2 + c_{33}x_3^2 \end{bmatrix} \quad B = \begin{bmatrix} (e_{31}+e_{15})x_3x_1 & (h_{31}+h_{15})x_3x_1 \\ (e_{32}+e_{15})x_2x_3 & (h_{32}+h_{15})x_2x_3 \\ e_{15}x_1^2 + e_{25}x_2^2 + e_{33}x_3^2 & h_{15}x_1^2 + h_{25}x_2^2 + h_{33}x_3^2 \end{bmatrix}$$

$$C = \begin{bmatrix} \kappa_{11}x_1^2 + \kappa_{22}x_2^2 + \kappa_{33}x_3^2 & \alpha_{11}x_1^2 + \alpha_{22}x_2^2 + \alpha_{33}x_3^2 \\ \alpha_{11}x_1^2 + \alpha_{22}x_2^2 + \alpha_{33}x_3^2 & \mu_{11}x_1^2 + \mu_{22}x_2^2 + \mu_{33}x_3^2 \end{bmatrix}$$

where $x_1 = \sin\theta cos\varphi$, $x_2 = \sin\theta\sin\varphi$, and $x_3 = cos\theta$

The expression of T_{iJKl}^{II} in spherical coordinates system is then given by:

$$\begin{aligned} T_{iJKl}^{II} &= \frac{a^3}{6}\int_0^{\pi}\sin\theta\Big[\int_0^{2\pi}(\chi_i\chi_l q^2\tilde{G}_{JK}d\varphi + \int_0^{2\pi}\chi_i\chi_K q^2\tilde{G}_{Jl})d\varphi\ \Big]d\theta \quad K = 1,2,3 \\ T_{iJ4l}^{II} &= \frac{a^3}{3}\int_0^{\pi}\sin\theta d\theta\int_0^{2\pi}(\chi_i\chi_l q^2\tilde{G}_{J4})d\varphi \\ T_{iJ5l}^{II} &= \frac{a^3}{3}\int_0^{\pi}\sin\theta d\theta\int_0^{2\pi}(\chi_i\chi_l q^2\tilde{G}_{J5})d\varphi \end{aligned} \tag{2.24}$$

2.4.2 Ellipsoidal inclusion

An ellipsoidal inclusion with a, b, and c as half axes is considered. The used ellipsoidal coordinates are expressed in the principal system of the inclusion:

$$\vec{R} = \begin{cases} R_1 = r_1 \\ R_2 = \dfrac{a}{b}r_2 \\ R_3 = \dfrac{a}{c}r_3 \end{cases} \quad \text{and} \quad \vec{Q} = \begin{cases} Q_1 = q_1 \\ Q_2 = \dfrac{b}{a}q_2 \\ Q_3 = \dfrac{c}{a}q_3 \end{cases}$$

The matrix relationship between $\vec{Q}$ and $\vec{q}$ is as follows:

$$q_i = \phi_{it} Q_t \tag{2.25}$$

With $$\boldsymbol{\phi} = \begin{bmatrix} 1 & 0 & 0 \\ 0 & \frac{a}{b} & 0 \\ 0 & 0 & \frac{a}{c} \end{bmatrix}$$

The expression of $\vec{Q}$ in this coordinate system is then

$$Q_t = Q\chi_t \qquad t = 1,2,3$$

The final expressions of T^{II}_{iJKl} are similarly given by:

$$\begin{aligned} T^{II}_{iJKl} &= \frac{abc}{6}\int_0^{\pi} \sin\theta \left[\int_0^{2\pi} \phi_{lt}\chi_t\phi_{iu}\chi_u Q^2 \tilde{G}_{JK} d\varphi + \int_0^{2\pi} \phi_{Kt}\chi_t\phi_{iu}\chi_u Q^2 \tilde{G}_{Jl} d\varphi \right] d\theta \quad K = 1,2,3 \\ T^{II}_{iJ4l} &= \frac{abc}{3}\int_0^{\pi} \sin\theta d\theta \int_0^{2\pi} (\phi_{lt}\chi_t\phi_{iu}\chi_u Q^2 \tilde{G}_{J4}) d\varphi \\ T^{II}_{iJ5l} &= \frac{abc}{3}\int_0^{\pi} \sin\theta d\theta \int_0^{2\pi} (\phi_{lt}\chi_t\phi_{iu}\chi_u Q^2 \tilde{G}_{J5}) d\varphi \end{aligned} \tag{2.26}$$

In this case the matrix M is given by

$$M_{JK} = E^0_{iJKl}\phi_{it}\chi_t\phi_{lu}\chi_u \quad \text{and} \quad M^{-1}_{JK} = Q^2\tilde{G}_{JK}(q)$$

The explicit expression of the matrix M in ellipsoidal coordinates can be directly obtained by replacing x_1, x_2 and x_3 in (2.23-c) by:

$$x_1 = \sin\theta\cos\varphi\,,\; x_2 = \frac{a}{b}\sin\theta\sin\varphi\,,\; x_3 = \frac{a}{c}\cos\theta$$

2.5 Micromechanical models

2.5.1 N-phase Self Consistent approach

The Self Consistent model has been originally developed for estimating macroscopic moduli of polycrystalline metals (Hershey 1954 [9], Kroner 1958 [10]). The Self Consistent model continues to be used by a great number of researchers for estimating homogenized moduli of heterogeneous materials including elastic, elastoplastic, viscoplasitic, piezoelectric materials, etc. In the one site Self Consistent approach the composite is considered as an inclusion embedded in a matrix which takes the properties of the whole composites E^{eff}. Based on the equivalent inclusion problem of Eshelby, the expression of the concentration tensor A^{SC} is given by Dunn et al [2, 3] and Fakri et al [6] for piezoelectric composites.

$$A^{SC}_{MnKl} = (I_{KlMn} + \frac{1}{V^I} T^{II}{}_{iJKl} \Delta E^I{}_{iJMn})^{-1} \tag{2.27}$$

where $\Delta E^I{}_{iJMn} = E^I{}_{iJMn} - E^{eff}{}_{iJMn}$

For magnetoelectroelastic composite materials $A^{SC}{}_{MnKl}$ is the shorthand notation of nine concentration tensors defined as functions of the tensor T^{II} . This tensor has to be computed first and the numerical procedure can be found in [6].

For an N-phase medium, the effective magnetoelectroelastic moduli E^{eff} , predicted by the Self Consistent model, is expressed as:

$$E^{eff}{}_{iJKl} = \sum_{I=1}^{N} f^I E^I{}_{iJMn} A^{SC}{}_{MnKl} \tag{2.28}$$

where $f^I = \frac{V^I}{V}$ is the concentration of the inclusions I. If the first phase (N=1) is taken as the matrix (symbol 'm'), the last expression becomes

$$E^{eff}{}_{iJKl} = E^m{}_{iJKl} + \sum_{I=2}^{N} f^I (E^I{}_{iJMn} - E^m{}_{iJMn}) A^{SC}{}_{MnKl} \tag{2.29}$$

Let us recall that $\sum_{I=1}^{n} f^I A^{SC}{}_{MnKl} = I_{MnKl}$, where I_{MnKl} is the shorthand notation of the four identity tensors, $E^m{}_{iJMn}$ corresponds to the magnetoelectroelastic matrix moduli and $E^I{}_{iJMn}$ corresponds to the magnetoelectroelastic inclusions moduli. These formulations permit one to predict the effective magnetoelectroelastic moduli for the N-phase composites. For a two phase composites, the expression of $E^{eff}{}_{iJKl}$ becomes

$$E^{eff}{}_{iJKl} = E^m{}_{iJKl} + f^I (E^I{}_{iJMn} - E^m{}_{iJMn}) A^{SC}{}_{MnKl} \tag{2.30}$$

Note that equations (2.28) and (2.30) give coupled and implicit expression of the effective magnetoelectroelastic moduli of the magnetoelectroelastic material. The concentration tensors A^{SC} are functions of E^{eff} . This kind of equations is generally solved by iterative methods. A detailed algorithm for numerical computation is given in [6].

2.5.2 N-phase Incremental Self Consistent approach

The development of the N-phase Incremental Self Consistent approach for the magnetoelectroelastic heterogeneous materials is one the main theoretical and numerical results of this paper. This is due to the fact that the Self Consistent method gives erroneous predictions of effective coefficients of composites materials at high concentration of reinforcements. An improvement of SCM, by an incremental way has been developed for piezo composite materials by Fakri and Azrar [7] for two phases. In this paper, an extension of the ISC scheme to magneto-electro-elastic effective properties and its development for N-phase magnetoelectroelastic composites are done.

For N-phase materials, the resulting composite must be characterized by concentrations " f^J " of phases (reinforcements) $0< f^J < 1;\ J=1, N$.

$\Delta f_J = \dfrac{f^J}{S}$ is considered as partial concentration of the phase J and S is the number of steps. At the ith step, the volume fraction of the phase J is $f_i^J = i\Delta f_J$. The concept of the volume preservation must be used for computing the finite increment of the total volume fraction of reinforcements which will be added at the ith step. This volume preservation can be expressed by means of magnetoelectroelastic behaviors of each phase in the following manner:

After (i-1) steps, the magnetoelectroelastic coefficients of composite can be expressed by means of magnetoelectroelastic coefficients of each phase as

$$\sum_{J=1}^{N}(i-1)\Delta f_J E^J + \left[1-\sum_{J=1}^{N}(i-1)\Delta f_J\right]E^M = E^C{}_{i-1} \tag{2.31}$$

where E^J and E^M are the magnetoelectroelastic coefficients of the phase J and the matrix respectively. $E^C{}_{i-1}$ represents the composite magnetoelectroelastic coefficients for the step (i-1).

At the i-th step in the Self Consistent scheme, the next increment of phase J is Δf_i^J. It must be introduced in an equivalent matrix which has the behavior of the built composite in the last steps. So, one can write:

$$\sum_{J=1}^{N}\Delta f_i^J E^J + \left[1-\sum_{J=1}^{N}\Delta f_i^J\right]E^C{}_{i-1} = \sum_{J=1}^{N} i\Delta f_J E^J + \left[1-\sum_{J=1}^{N} i\Delta f_J\right]E^M \tag{2.32}$$

where Δf_i^J is the increment that must be added at the ith step into the equivalent matrix.

The substitution of (2.31) into (2.32) leads to the following equation:

$$\sum_{J=1}^{N}\left[\Delta f_i^J+\left[1-\sum_{J=1}^{N}\Delta f_i^J\right](i-1)\Delta f_J\right]E^J+\left[1-\sum_{J=1}^{N}\Delta f_i^J\right]\left[1-\sum_{J=1}^{N}(i-1)\Delta f_J\right]E^M=\sum_{J=1}^{N}i\Delta f_J E^J+\left[1-\sum_{J=1}^{N}i\Delta f_J\right]E^M \quad (2.33)$$

From this equation, the following formulations are derived:

$$\Delta f_i^J+\left[1-\sum_{J=1}^{N}\Delta f_i^J\right](i-1)\Delta f_J=i\Delta f_J \quad (2.34)$$

$$\left[1-\sum_{J=1}^{N}\Delta f_i^J\right]\left[1-\sum_{J=1}^{N}(i-1)\Delta f_J\right]=1-\sum_{J=1}^{N}i\Delta f_J \quad (2.35)$$

From (2.34) and (2.35) the general expression of the volume fraction Δf_i^J to be injected at the step 'i' into the phase *J* is given by:

$$\Delta f_i^J=\frac{\Delta f_J}{1-\sum_{J=1}^{N}(i-1)\Delta f_J} \quad (2.36)$$

Expression (2.36) shows that the incremental volume fraction of reinforcements Δf_i^J continuously increases as a function of the step number 'i'. It is important to point out that the overall properties of the equivalent homogeneous material obtained by this procedure depends on the number of steps S.

$$E^{eff\,(i)}{}_{iJKl}=E^{eff\,(i-1)}{}_{iJKl}+\sum_{J=1}^{N}\Delta f_i^J\,(E^I{}_{iJMn}-E^{eff\,(i-1)}{}_{iJMn})A^{SC}{}_{MnKl} \quad (2.37)$$

with $E^{eff\,(0)}=E^M$

Note that the Incremental Self Consistent scheme does not affect the expression of the concentration tensors A on which the method is based. So, the formulations used in this study and in the traditional Self Consistent method are the same. The two methods differ only in the manner of introducing the reinforcements' concentration. In order to compare the effectiveness of the presented approach the Mori Tanaka as well as the dilute approach is presented for N-phase composites.

2.5.3 N-phase Mori-Tanaka Approach

The Mori-Tanaka model has been and continues to be the most widely used approach in the micro mechanics dilute heterogeneous materials with ellipsoidal inclusions. The Mori-Tanaka mean field approach takes into account the effect of other inhomogeneities by considering a

finite concentration of inclusions embedded in an infinite matrix of magnetoelectroelastic moduli E^I_{iJKl} and E^m_{iJKl}, and gives a straightforward explicit expression of the effective moduli. The corresponding concentration tensor A^{MT} is then given by the solution for a single inclusion embedded in an infinite matrix in the same manner as the heterogeneous inclusion problem of Eshelby.

For N phases, the Mori-Tanaka concentration tensor A^{MT} is given as follows:

$$A^{MT}_{iJKl} = A^{Dil}_{iJMn}(f^m I_{KlMn} + \sum_{i=1}^{N} f^i A^{Dil}_{KlMn})^{-1} \tag{2.38}$$

To apply this to N phase composites, it is necessary to find A^{Dil} and A^{MT} for each phase [2]. Similarly to the Self Consistent approach, the effective behavior of N phase composites can be obtained by

$$E^{eff}_{iJKl} = E^m_{iJKl} + \sum_{I=2}^{N} f^I (E^I{}_{iJMn} - E^m{}_{iJMn}) A^{MT}_{MnKl} \tag{2.39}$$

Note that the matrix phase is explicitly taken into account but only in an average sense.

2.5.4 N-phase Dilute Approach

This approach has an equivalent scheme than the above approaches but does not consider any interaction between the inhomogeneities. The expression of strain-electro-magnetic fields $Z^I{}_{Kl}$ of inclusion can be then derived from that obtained in the Self Consistent approach with the difference that in this case, the infinite matrix has magnetoelectroelastic moduli E^m as equivalent behavior. The concentration tensor A^{Dil} is given [2]

$$A^{Dil}{}_{MnKl} = (I_{KlMn} + \frac{1}{V^I} T^{II}{}_{iJKl} \Delta E^I{}_{iJMn})^{-1} \tag{2.40}$$

where, $\Delta E^I{}_{iJMn} = E^I{}_{iJMn} - E^m{}_{iJMn}$ The effective behavior prediction of N phase composites, in this case, is expressed as

$$E^{eff}{}_{iJKl} = E^m{}_{iJKl} + \sum_{I=2}^{N} f^I (E^I{}_{iJMn} - E^m{}_{iJMn}) A^{Dil}{}_{MnKl} \tag{2.41}$$

The effective magnetoelectroelastic formulations (2.29, 2.37, 2.39 and 2.41) are applicable to a wide range of inclusion types, shapes and volume fractions. The coupling elastic-electric-magnetic effective behaviors can be investigated and optimized with respect to the volume

fraction, shape and type of inclusions which may be elastic, piezoelectric or magnetoelectroelastic.

2.6 Numerical results

2. 6.1 Two phase composites

The Micromechanical models presented in this paper are used to predict the effective magnetoelectroelastic coefficients. These models permit to take into account the effect of phase number and concentrations, shape inclusions, as well as its polling orientation. Before investigating the three phase composites effective behaviors, the numerical results of the two phase composites is first considered.

Consider a magnetoelectroelastic composite in which the matrix is piezomagnetic ($CoFe_2O_4$) and the elliptic inclusions are piezoelectric ($BaTiO_3$) having half axes a, b and c. The global coordinate system for the matrix is (x_1, x_2, x_3) and the third half axis c is on the polling direction x_3. The material properties of both phases are transversely isotropic with x_3 the axis of symmetry. The magnetoelectroelastic characteristics of the two materials, used in this paper, are both listed in table 2.1 which are obtained from [20].

Note that in the two considered phases the magnetoelectric effect does not exist neither in the matrix nor in the inclusion. This coupling effect will be induced in magnetoelectroelastic composite through the interaction between phases.

Numerical results of effective properties for different inclusions shapes based on the Mori-Tanaka, Dilute, Self Consistent and Incremental Self Consistent approaches are obtained using the presented concentration tensors and the obtained numerical results are well compared with available numerical ones [11, 12, 20].

Figure 2.1 shows the magnetoelectric coefficient α_{33} for fibrous composite (c/a=1000, b=a) with respect to the volume fraction predicted by the Mori-Tanaka and Self consistent models. The two models predict the same results and α_{33} is maximized at 45% of inclusion concentration. The same results are already obtained by Zhang and Soh [20].

Table 2.1: Material properties of $BaTiO_3/CoFe_2O_4$

	C_{11}	C_{12}	C_{13}	C_{33}	C_{44}
$BaTiO_3$	166	77	78	162	43
$CoFe_2O_4$	286	173	170	269.5	45.3
	e_{15}	e_{31}	e_{33}	κ_{11}	κ_{33}
$BaTiO_3$	11.5	-4.4	18.6	11.2×10^{-9}	12.6×10^{-9}
$CoFe_2O_4$	0	0	0	0.08×10^{-9}	0.093×10^{-9}
	h_{15}	h_{31}	h_{33}	μ_{11}	μ_{33}
$BaTiO_3$	0	0	0	5×10^{-6}	10×10^{-6}
$CoFe_2O_4$	550	580.3	699.7	-590×10^{-6}	157×10^{-6}

Units: elastic constant GPa; dielectric constants C^2/Nm^2; magnetic constants Ns^2/C^2, piezoelectric constants C/m^2; piezomagnetic constants N/Am; magnetoelectric coefficients Ns/VC.

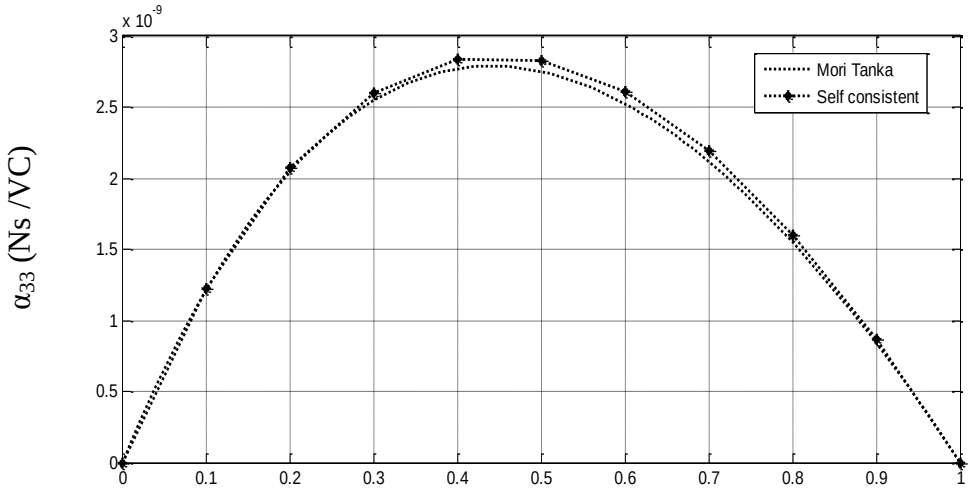

Figure 2.1: Effective electromagnetic modulus α_{33} for fibrous composite $BaTiO_3/ CoFe_2O_4$ predicted by Mori-Tanaka and Self Consistent models.

The prediction based on the Incremental Self Consistent method is presented in figure 2.2 at different steps (2 to 100). The convergence of the procedure is demonstrated for e_{33} with respect to inclusion volume fraction. It is shown that the Incremental Self Consistent Model improves the prediction of the Self Consistent model which is usually criticized for its deficiency at high concentrations of inclusions. It is demonstrated that with 10 steps of increments, this method gives nearly the same results as with 20, 30, 50, and 100 steps until the concentration 50% of spherical $BaTiO_3$. For large concentrations, a good convergence is clearly seen with 50 steps, but

20 steps give very close results. For the numerical predictions in this paper, the Incremental Self Consistent model with 20 steps of the increment is used.

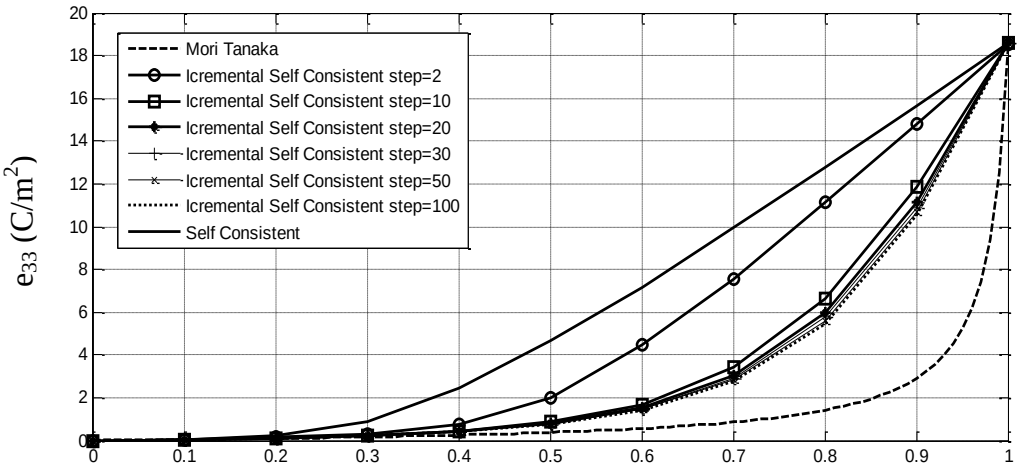

Figure 2.2: Effective piezoelectric modulus e_{33} for spherical composite $BaTiO_3$/ $CoFe_2O_4$ predicted by Mori-Tanaka, Self Consistent and Incremental Self Consistent models.

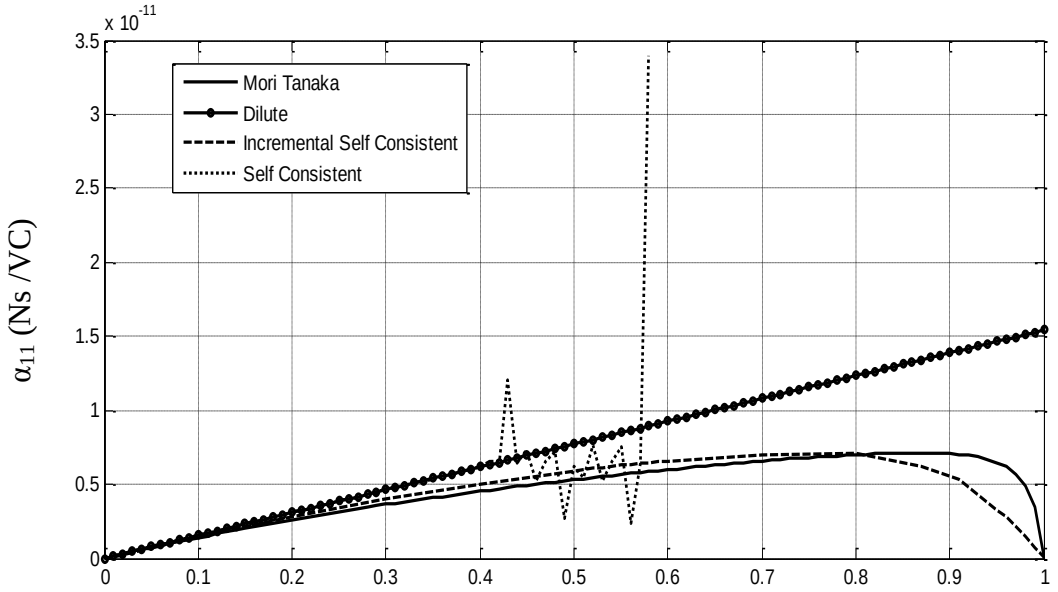

Figure 2.3: Effective electromagnetic modulus α_{11} for fibrous composite $BaTiO_3$/ $CoFe_2O_4$ predicted by Mori-Tanaka, Dilute, Self Consistent and Incremental Self Consistent models.

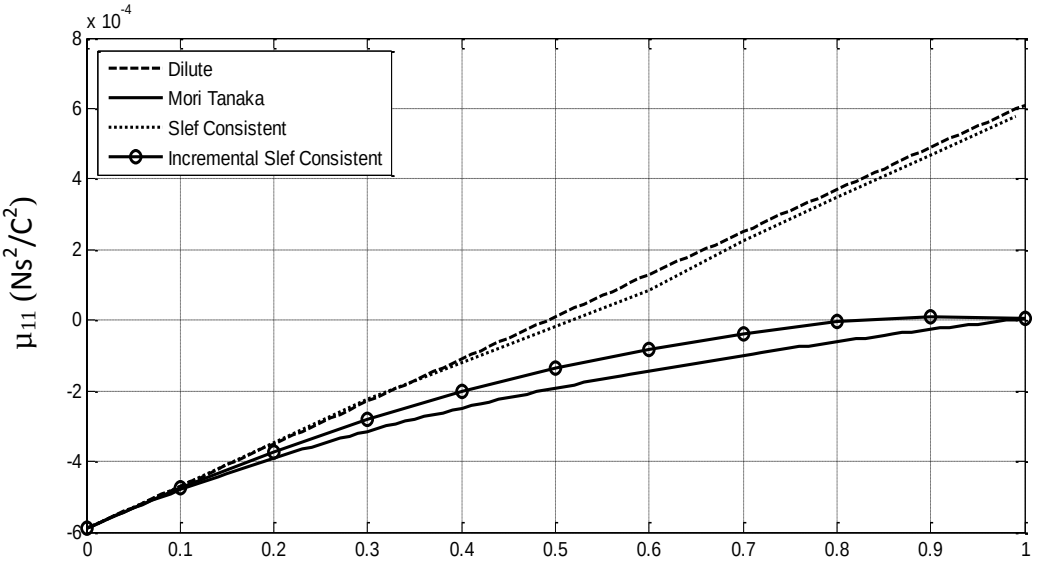

Figure 2.4: Effective magnetic modulus μ_{11} for fibrous composite $BaTiO_3$/ $CoFe_2O_4$ predicted by Mori-Tanaka, Dilute, Self Consistent and Incremental Self Consistent models.

In figures 2.3 and 2.4 the electromagnetic coefficient α_{11} and the permeability coefficient μ_{11} are presented respectively for fibrous composites (a=b, c/a=1000) based on Incremental Self Consistent, Self Consistent, Mori-Tanaka and Dilute models. It is clearly shown that the predictions given by these models are in good agreement for low volume fractions of inclusions. The figure 3 demonstrates that the Self Consistent model is not able to conduct the predictions for moderate and higher concentrations and it diverges beyond 40% concentration of inclusions. This is the main raison why the Incremental Self Consistent is developed here. This figure shows also that the Incremental Self Consistent model improves the prediction of the classical Self Consistent one and gives closer results to Mori-Tanaka's predictions.

Note also that the effective moduli of the composite predicted by the Dilute model does not take the property of the inclusion when the volume faction is close to 1. This is expected because the Dilute model is only applicable when the volume fraction of the inclusions is very small.

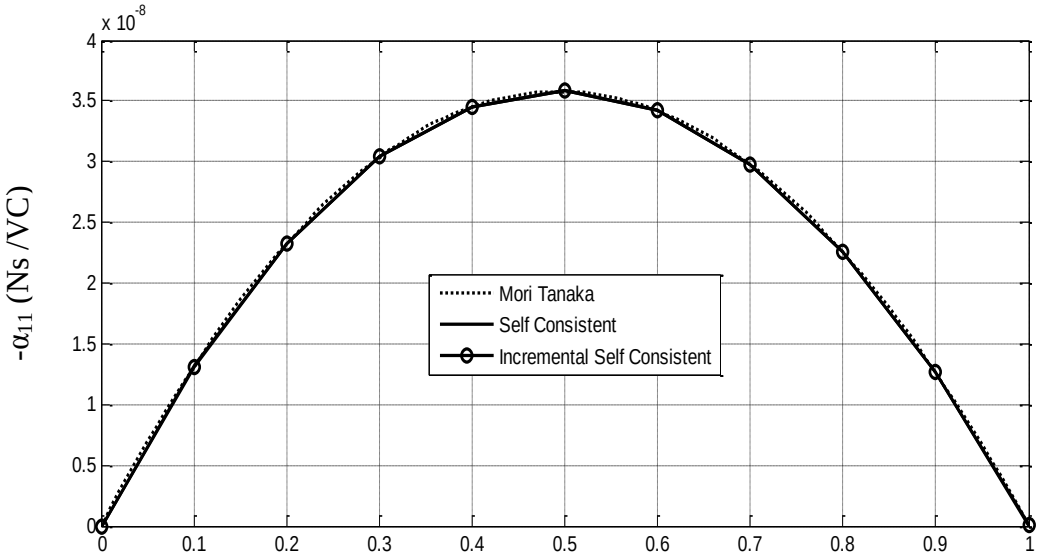

Figure 2.5: Effective electromagnetic modulus $-\alpha_{11}$ for laminated composite $BaTiO_3$/ $CoFe_2O_4$ predicted by Mori-Tanaka, Self Consistent and Incremental Self Consistent models.

In figure 2.5, the electromagnetic coefficient $-\alpha_{11}$ is presented for laminated magnetoelectroelastic composites (a=b and c/a=0.001). In this case the Mori-Tanaka, Self Consistent and ISC micromechanical models predict the same results. $-\alpha_{11}$ is maximized at 50% of inclusions concentration. These results are well compared with those obtained by [11, 12, 21].

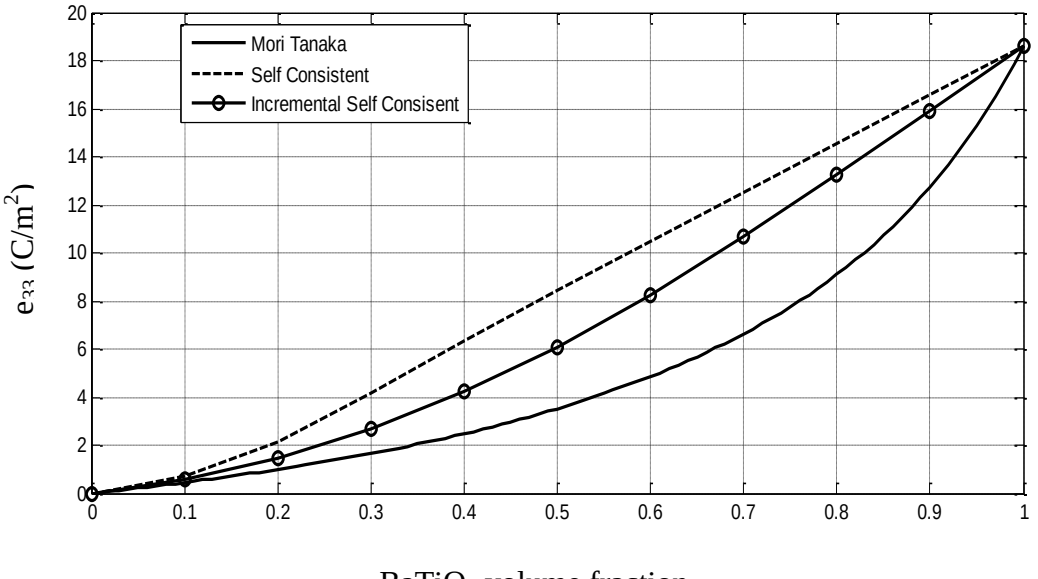

Figure 2.6: Effective piezoelectric modulus e_{33} for ellipsoidal composite (a=b, c/a=10) $BaTiO_3$/ $CoFe_2O_4$ predicted by Mori-Tanaka, Self Consistent and Incremental Self Consistent models.

The piezoelectric modulus e_{33} is presented in figure 2.6 for ellipsoidal inclusions. The results obtained by Self Consistent model and Mori-Tanaka and those obtained by ISC model are different and particularly in the vicinity of 50%. Experimental results are needed to test the accuracy of these predictions.

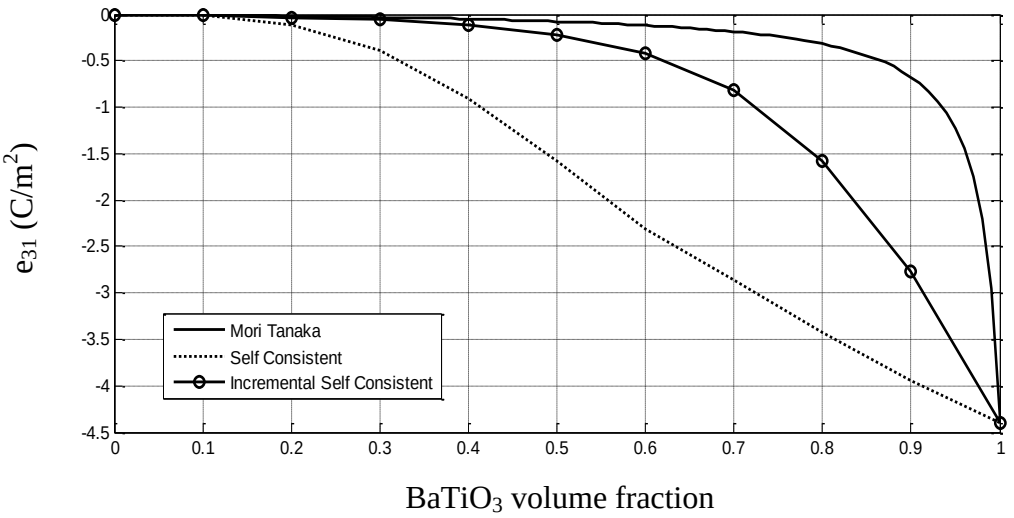

Figure 2.7: Effective piezoelectric modulus e_{31} for spherical composite $BaTiO_3$/ $CoFe_2O_4$ predicted by Mori-Tanaka, Self Consistent and Incremental Self Consistent models.

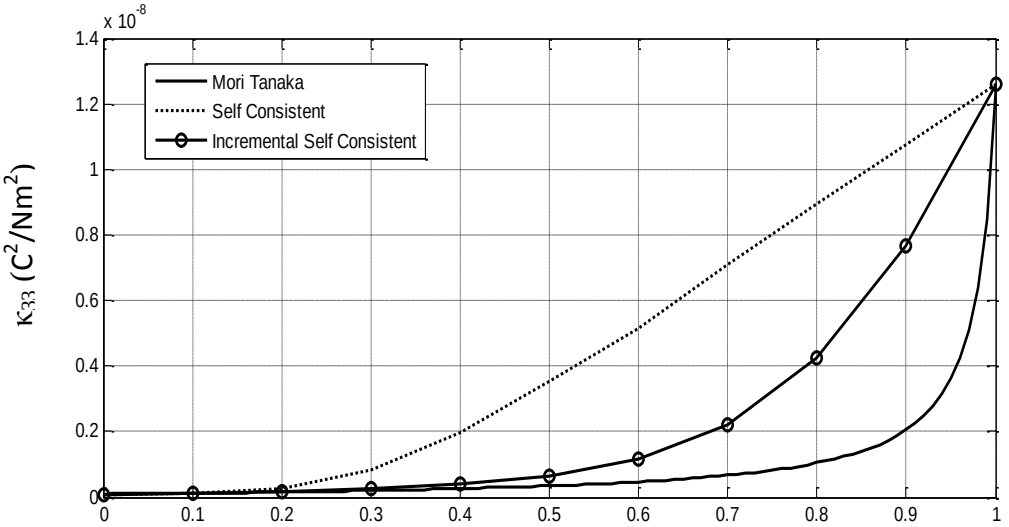

Figure 2.8: Effective dielectric modulus κ_{33} for spherical two- phase composite $BaTiO_3$/ $CoFe_2O_4$ predicted by Mori-Tanaka, Self Consistent and Incremental Self Consistent models.

In figures 2.7 and 2.8, the piezoelectric modulus e_{31} and the dielectric modulus κ_{33} are presented respectively for magnetoelectroelastic spherical composites (a=b=c). Again the Self Consistent model shows an over estimation especially over 20% volume fraction of inclusions. The ISC model improves the prediction of the classical Self Consistent model for high volume fraction of inclusions.

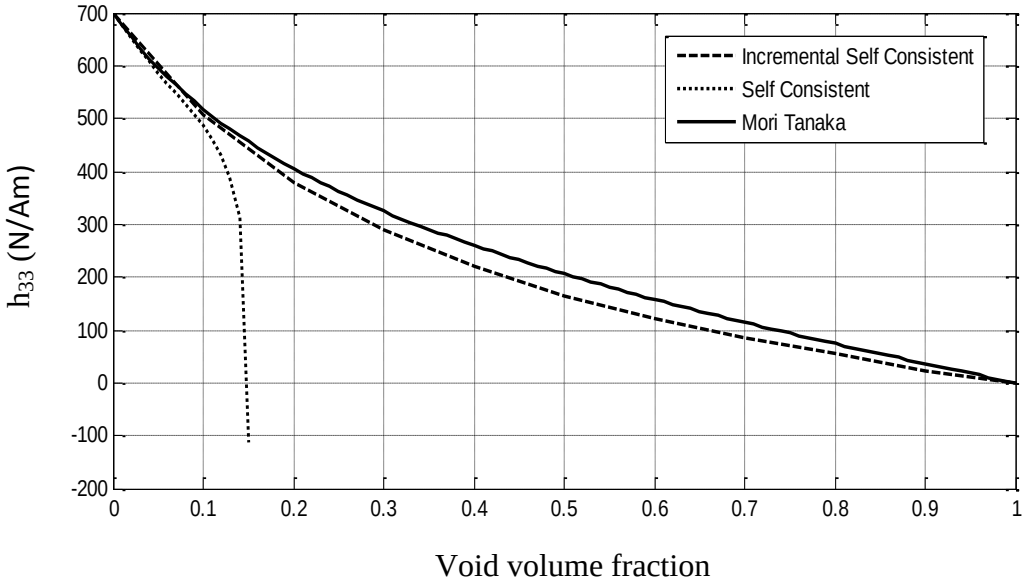

Figure 2.9: Effective piezomagnetic modulus h_{33} for fibrous composite $CoFe_2O_4$/ Void predicted by Mori-Tanaka, Self Consistent and Incremental Self Consistent models.

The effective piezomagnetic coefficients h_{33} is presented in figure 2.9 for $CoFe_2O_4$ matrix with fibrous voids (a=b, c/a=1000). It is clearly shown that the prediction given by the classical Self Consistent approach is limited for very low void concentration and the model diverges at 12% of voids inclusions. On the other hand, it is seen that the Incremental Self Consistent approach improves the prediction of the classical Self Consistent approach and conducted far the prediction.

2. 6.2 Three phase composites

In this subsection, the numerical results for three-phase composite materials are presented. Two kinds of three phase composites are investigated. One is consisting of a piezoelectric phase and a piezomagnetic phase surrounded by a matrix assumed to be Epoxy whose properties are listed in table 2.2. The other is consisting of piezoelectric phase and void phase surrounded by a piezomagnetic matrix. These voids are simulated as empty inclusions, which may have several

forms. Here, Mori-Tanaka, Self Consistent and Incremental Self Consistent micro mechanical models are used to predict the behavior of the considered three-phase magnetoelectroelastic composites. Numerical results are presented for various shapes and types of inclusions. In all presented results, the volume fraction of the matrix is fixed and the volume fractions of inclusions are varied.

Let us note that the Mori-Tanaka method has been already used by Lee, Boyd and Lagoudas [11] for three-phase magnetoelectroelastic composites materials. Thus, the numerical results presented in this section using the Mori-Tanaka method are the same as those of [11].

Table 2.2: Material properties of Epoxy

	C_{11}	C_{12}	C_{33}	C_{44}
Epoxy	5.53	2.97	5.53	1.28
	e_{15}	e_{31}	e_{33}	κ_{11}	κ_{33}
Epoxy	0	0	0	0.1×10^{-9}	0.1×10^{-9}
	h_{15}	h_{31}	h_{33}	μ_{11}	μ_{33}
Epoxy	0	0	0	1×10^{-6}	1×10^{-6}

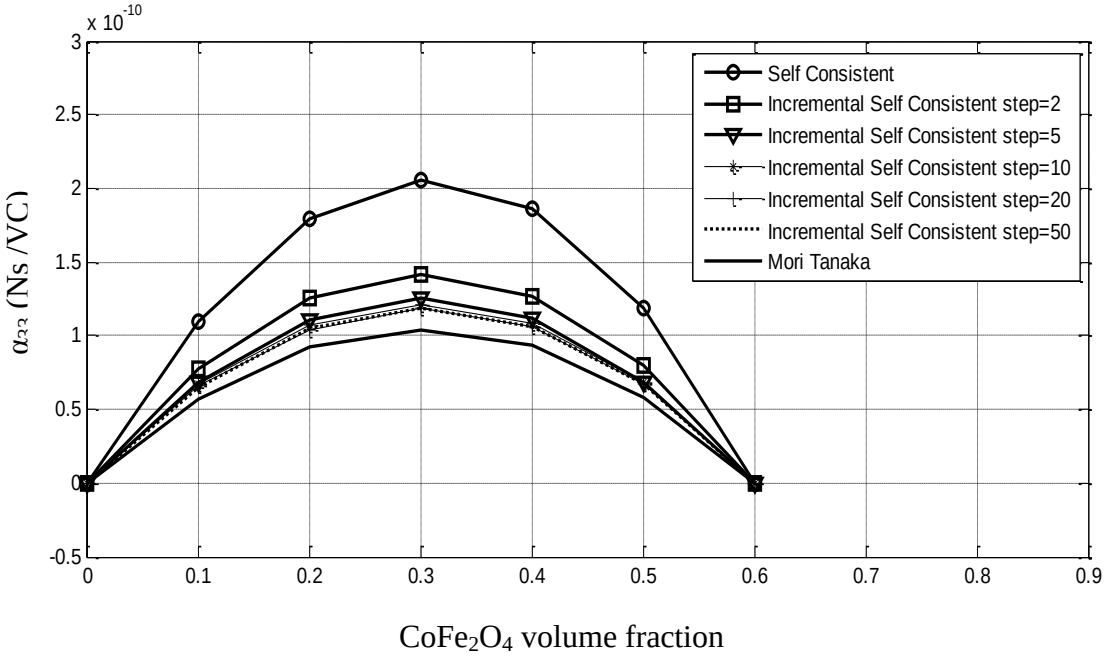

Figure 2.10: Effective electromagnetic modulus α_{33} for fibrous three- phase composite Epoxy/$BaTiO_3$/ $CoFe_2O_4$ predicted by Mori-Tanaka, Self Consistent, and Incremental Self Consistent models with the volume fraction of the matrix fixed at 40%.

In figure 2.10, the effective electromagnetic modulus α_{33} for fibrous three-phase magnetoelectroelastic composites (a=b; c/a=1000) is presented with respect to piezomagnetic inclusion by using Mori-Tanaka, Self Consistent and Incremental Self Consistent models. As in the two phase magnetoelectroelastic composites the convergence of the Incremental Self Consistent model is demonstrated. It is shown that the Incremental Self Consistent model with 10 steps of increments gives nearly the same results as with 20, 30, and 50 steps.

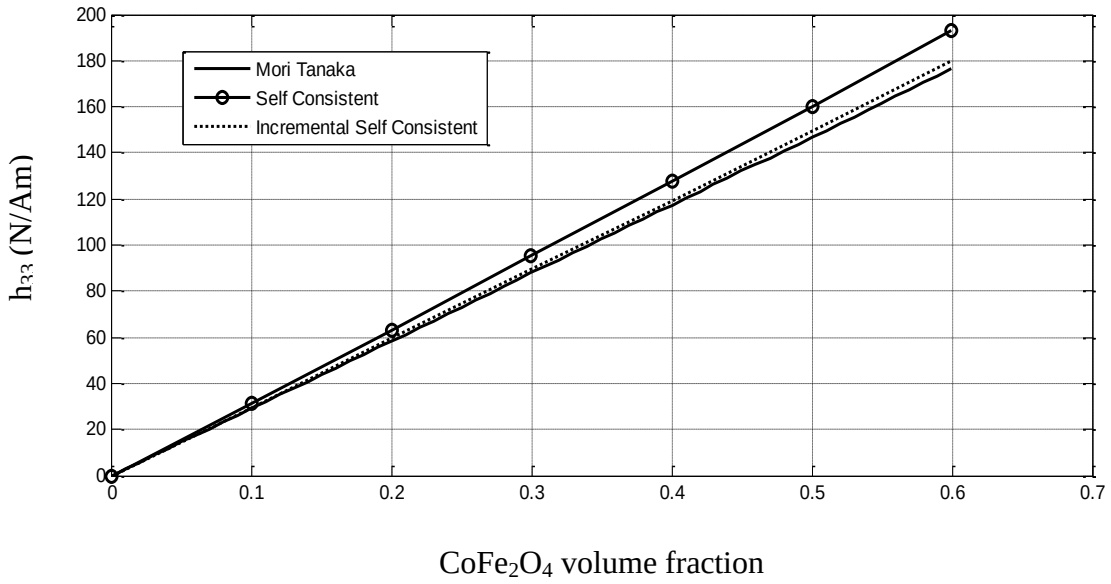

Figure 2.11: Effective piezomagnetic modulus h_{33} for fibrous three- phase composite Epoxy/$BaTiO_3$/ $CoFe_2O_4$ predicted by Mori-Tanaka, Self Consistent and Incremental Self Consistent models with the volume fraction of the matrix fixed at 40%.

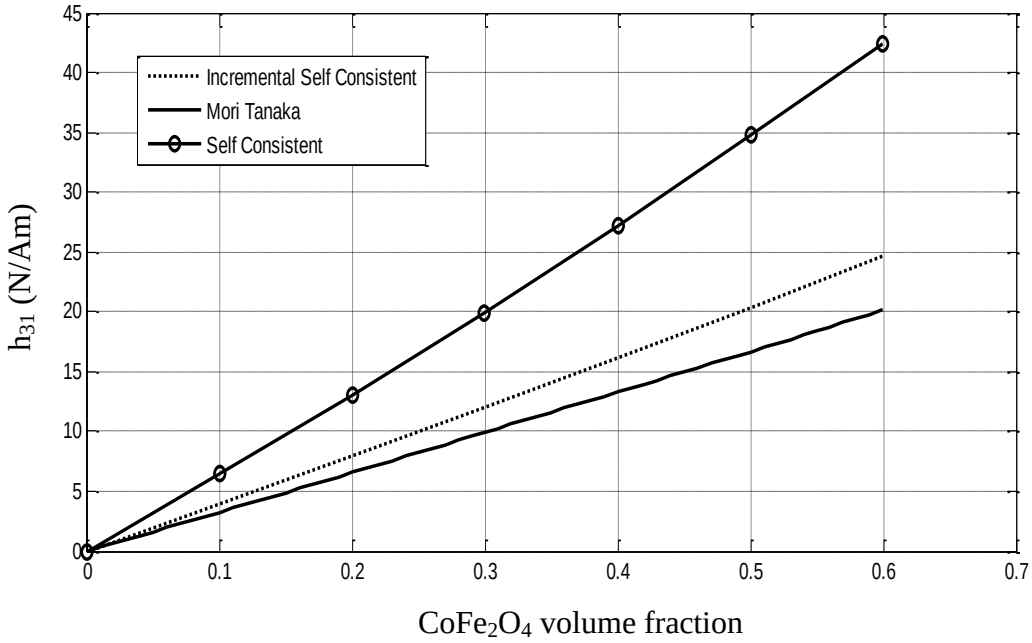

Figure 2.12: Effective piezomagnetic modulus h_{31} for fibrous three- phase composite Epoxy/$BaTiO_3$/ $CoFe_2O_4$ predicted by Mori-Tanaka, Self Consistent and Incremental Self Consistent models with the volume fraction of the matrix fixed at 40%.

In figures 2.11 and 2.12, piezomagnetic coefficients h_{33} and h_{31} are presented respectively for fibrous three-phase magnetoelectroelastic composite materials. The Incremental Self Consistent method improves the classical Self consistent method and gives closer results to Mori-Tanaka predictions.

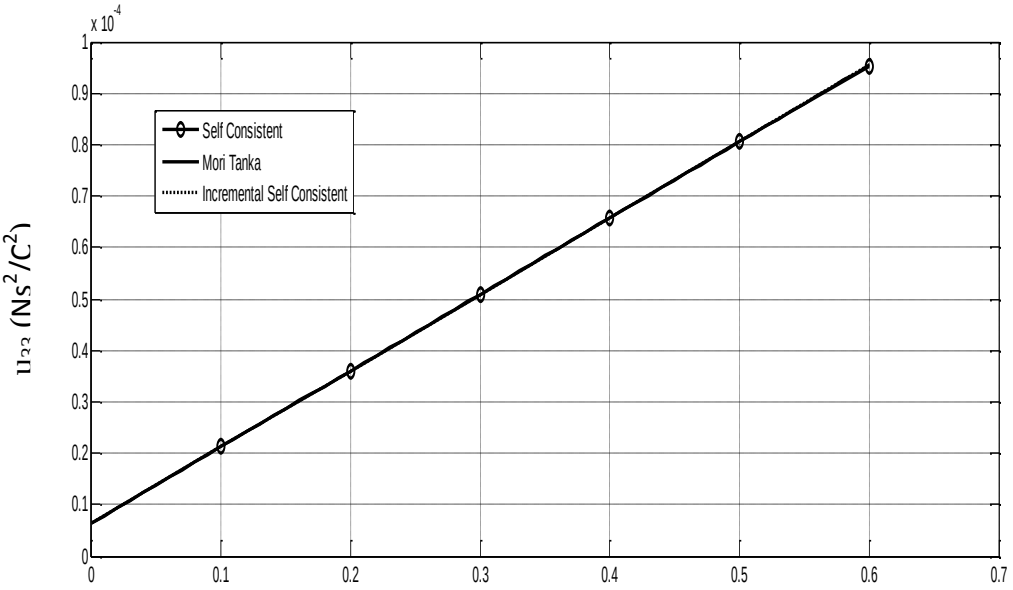

Figure 2.13: Effective magnetic modulus μ_{33} for fibrous three-phase composite Epoxy/$BaTiO_3$/ $CoFe_2O_4$ predicted by Mori-Tanaka, Self Consistent and Incremental Self Consistent models with the volume fraction of the matrix fixed at 40%.

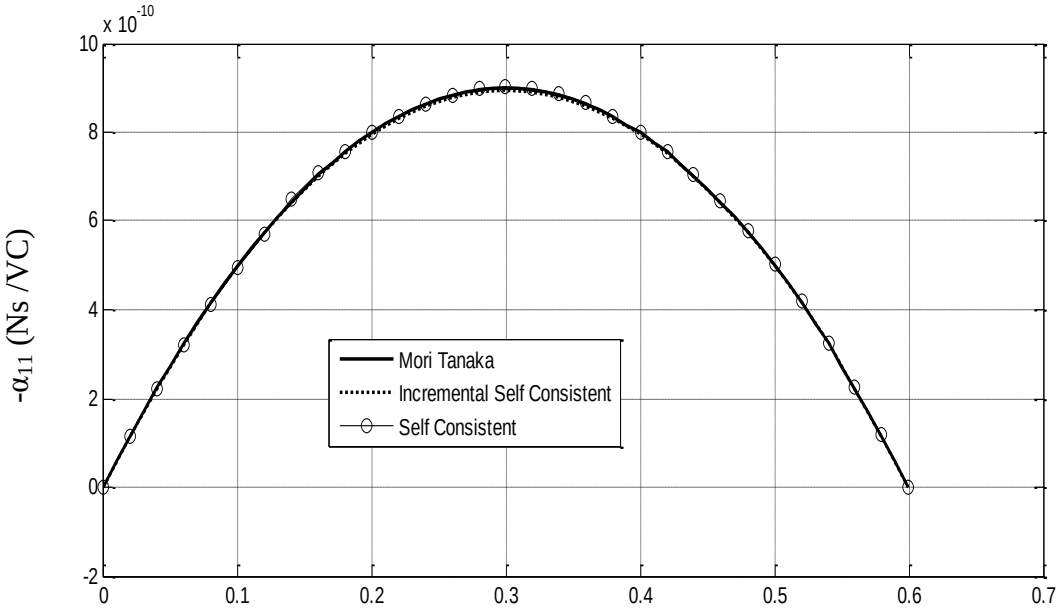

Figure 2.14: Effective electromagnetic modulus-$\alpha_{11}$for laminated three- phase composites Epoxy/$BaTiO_3$/ $CoFe_2O_4$ predicted by Mori-Tanaka, Self Consistent, and Incremental Self Consistent models with the volume fraction of the matrix fixed at 40%.

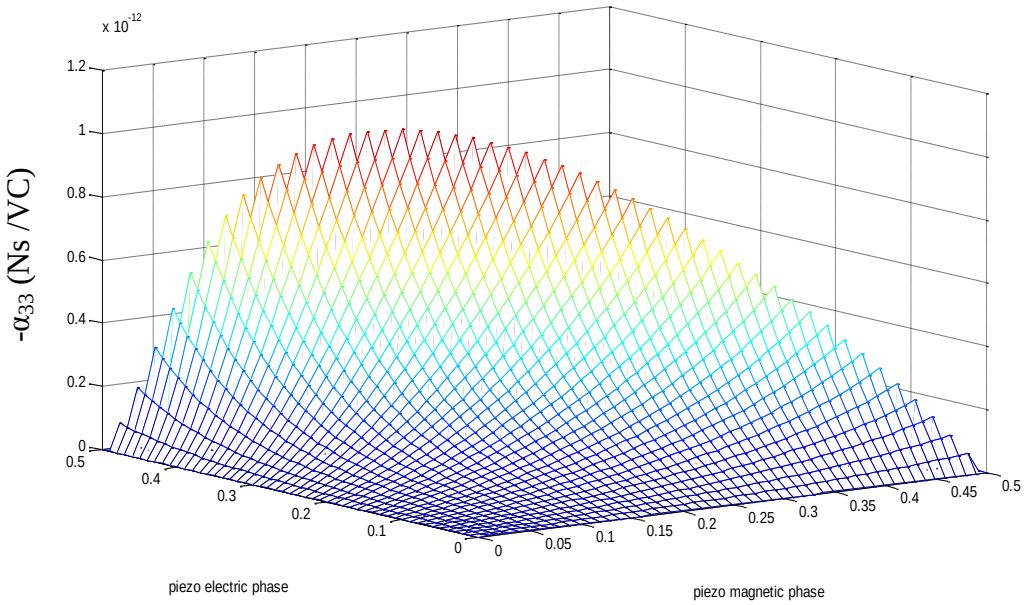

Figure 2.15: Effective electromagnetic modulus -α $_{33}$for spherical three- phase composites Epoxy/$BaTiO_3$/$CoFe_2O_4$ predicted by the Incremental Self Consistent model with the volume fraction of the matrix fixed at 50%.

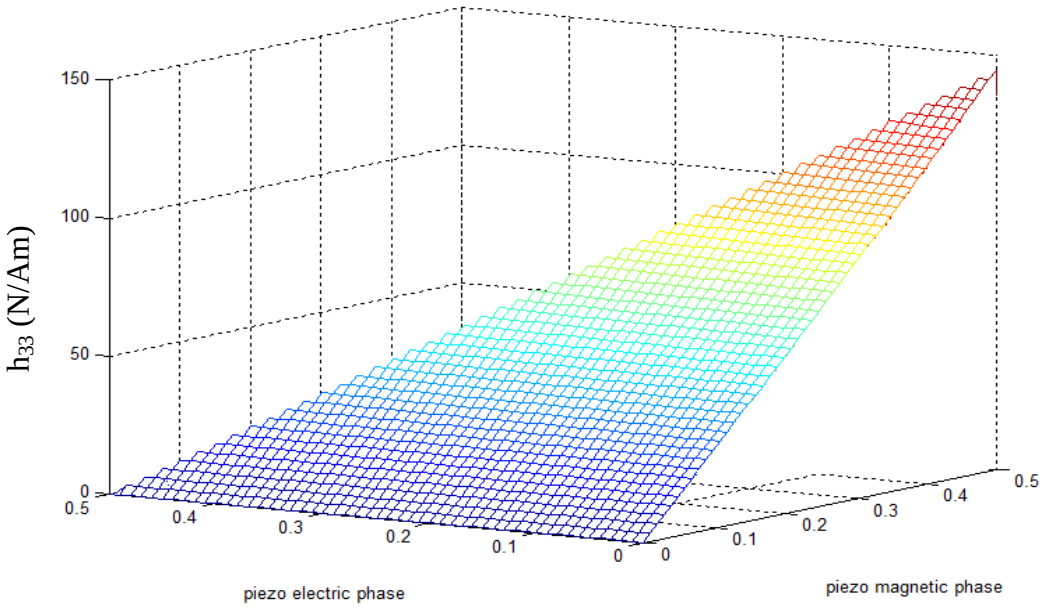

Figure 2.16: Effective electromagnetic modulus h $_{33}$for fibrous three-phase composites Epoxy/$BaTiO_3$/$CoFe_2O_4$ predicted by the Incremental Self Consistent model with the volume fraction of the matrix fixed at 50%.

In figures 2.13 and 2.14, the effective magnetic coefficient μ_{33} and the electromagnetic coefficient $-\alpha_{11}$ are presented respectively for fibrous (a=b; c/a=1000) and laminated (a=b; c/a=0.001) three-phase composite materials. For these coefficients it is shown that the three micromechanical models predict the same results. Also it is shown that the effective modulus $-\alpha_{11}$ takes a maximum value at 30% of the piezomagnetic phase and piezoelectric phase. By analyzing the numerical results presented above it is shown that the electromagnetic coefficients obtained in two phase composites are higher than the electromagnetic coefficients obtained in three-phase composites. This is due to the presence of the elastic matrix in three-phase composites. Also it can be explained that in two- phase composites there is more interaction between the piezoelectric phase and piezomagnetic phase than in three-phase composites.

In figures 2.15, 2.16 three dimension numerical results of a three phase composites Epoxy/$BaTiO_3$/ $CoFe_2O_4$ are presented to show the phases effects on the effective behavior of the composites by using the Incremental Self Consistent approach. Spherical (a=b=c) and fibrous (a=b; c/a=1000) inclusions are considered respectively in figures 2.15 and 2.16. The predictions are presented for 50% of the matrix and various concentrations of $BaTiO_3$ and $CoFe_2O_4$ inclusions. The variation of the effective magnetoelectric coefficient α_{33} with respect to the two spherical inclusions concentrations is clearly shown. This coefficient may be maximized with respect to concentrations of the piezoelectric and piezomagnetic phases. With the epoxy matrix, when the two phases, piezomagnetic and piezoelectric, do not coexist the magnetoelectric coupling effects are zeros. For the piezomagnetic effective coefficient h_{33} its variation is linear and its maximal value is obtained when the concentration of the piezomagnetic phase $CoFe_2O_4$ is maximal and vanishes when we have only the piezoelectric phase and the epoxy matrix.

In figure 2.17, the electromagnetic coefficient α_{33} is presented for fibrous (a=b; c/a=1000) magnetoelectroelastic three-phase composites containing voids ($CoFe_2O_4$/$BaTiO_3$/Void). This figure demonstrates clearly that the Self Consistent approach can not estimate the effective electromagnetic moduli α_{33} beyond 10% concentration of voids in contrast with the Incremental Self Consistent approach which can be used until 60% voids concentration. Also it can be seen that below 10% void concentrations the three micromechanical approaches almost give the same predictions.

In figures, 2.18 and 2.19 the piezomagnetic coefficient h_{33} and the dielectric coefficient κ_{33} are presented respectively for fibrous magnetoelectroelastic three-phase composites containing voids

as the third inclusion by using the Incremental Self Consistent and Mori-Tanaka approaches. It is seen that the Incremental Self Consistent approach conducted far the prediction until 60% void concentration. Also for the effective coefficient h_{33} the Incremental Self Consistent and the Mori-Tanaka approaches give different prediction and the prediction obtained by the Incremental Self Consistent approach is lower than that obtained by the Mori-Tanaka approach. On the other hand the numerical predictions obtained for the effective coefficient κ_{33} are almost the same.

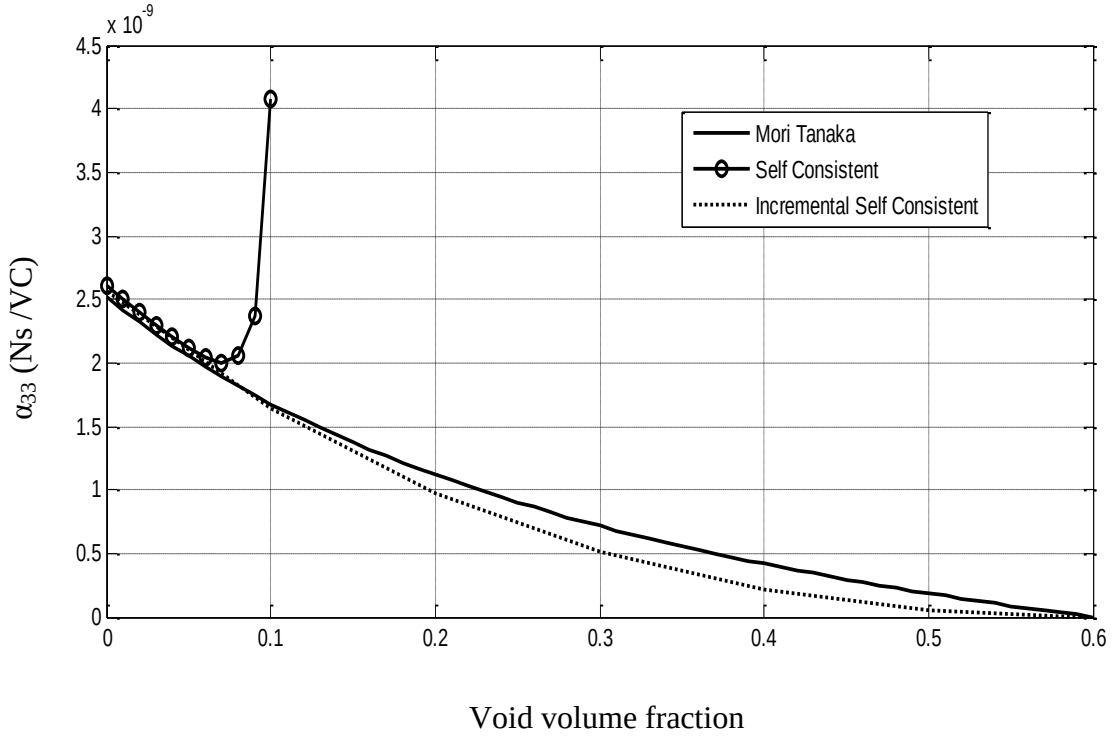

Figure 2.17: Effective electromagnetic modulus α_{33} for fibrous three- phase composites $CoFe_2O_4$ /$BaTiO_3$/Void predicted by Mori-Tanaka and Incremental Self Consistent models with the volume fraction of the matrix fixed at 40%.

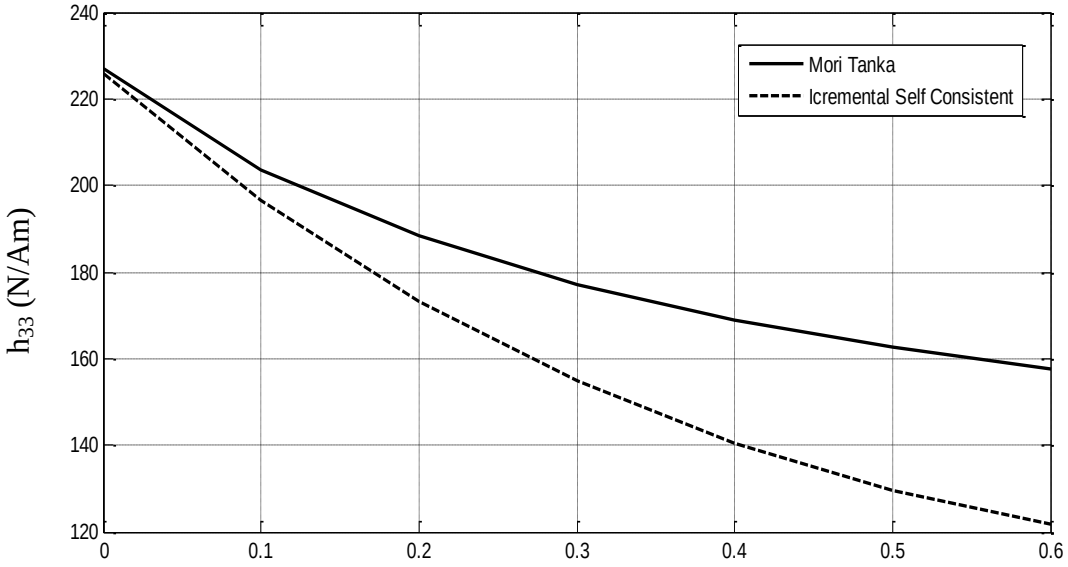

Figure 2.18: Effective piezomagnetic modulus $h_{33}$for fibrous three- phase composites $CoFe_2O_4$ /$BaTiO_3$/Void predicted by Mori-Tanaka and Incremental Self Consistent models with the volume fraction of the matrix fixed at 40%.

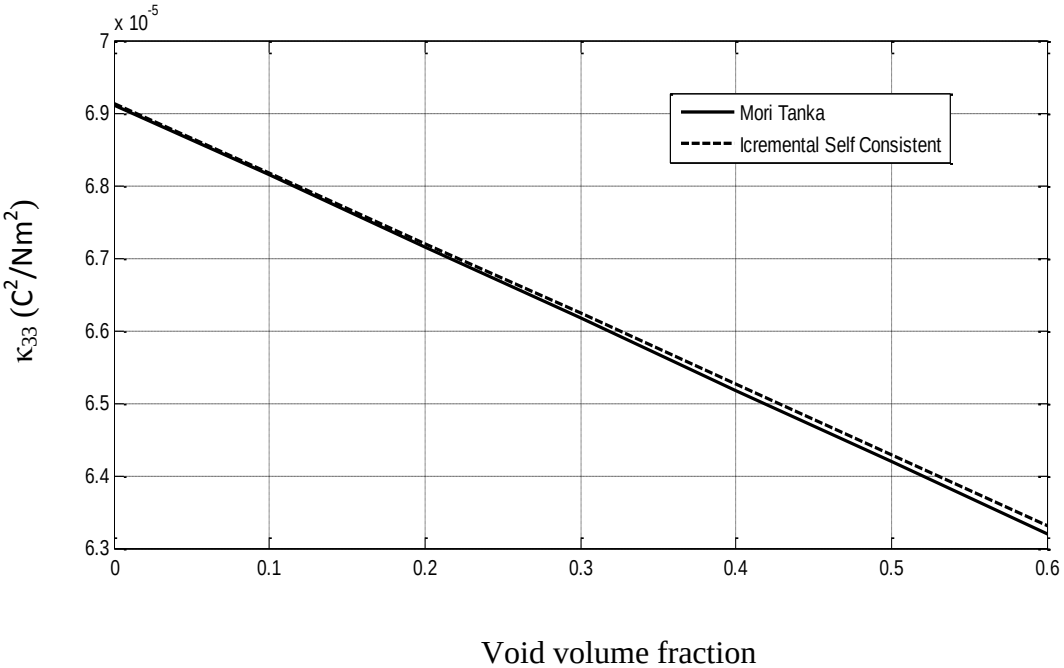

Figure 2.19: Effective electromagnetic modulus $\kappa_{33}$for fibrous three- phase composites $CoFe_2O_4$ /$BaTiO_3$/Void predicted by Mori-Tanaka and Incremental Self Consistent models with the volume fraction of the matrix fixed at 40%.

3.7 Conclusions

The Incremental Self Consistent, Self Consistent, Mori-Tanaka, and Dilute micromechanical models are elaborated to predict the effective moduli of multi-phase magnetoelectroelastic composite materials for different shapes, types and concentration of inclusions. The N-phase Incremental Self Consistent model is developed for magnetoelectroelastic effective properties. The expression of the effective behavior of the composite obtained by the micro mechanical models is written as function of the concentration tensors which are a function of the interaction tensors. The interaction tensor depends on the constituent properties and shape of ellipsoidal inclusions.

Numerical results have been presented for two phase composites and three phase composites with and without void by emphasizing the effect of shape and concentration inclusions. It is shown that the Self Consistent, Mori-Tanaka, and Dilute approaches lead to the same results for very low volume fraction of inclusions. However, for moderate and high volume fractions of inclusions the Self Consistent showed an over estimating especially over 20% inclusion concentration, and gives erroneous results for some coefficients. This drawback is corrected by the developed ISC model, which improves the prediction of the Self Consistent model for high volume fractions of the inclusions. In addition, it has been demonstrated from the above numerical results obtained for three-phase composites consisting of a piezoelectric phase and a void phase surrounded by a piezomagnetic matrix that the Incremental Self Consistent approach can estimate the properties of the composites for moderate volume fraction of voids. This model has been compared to the Mori-Tanaka one which is extensively used. This model will be next elaborated for predicting the behavior of disordered aggregates in nonlinear piezoelectric and magnetoelectroelastic heterogeneous media.

3.8 Perspectives

In this chapter, the effective properties of two-phase and multi-phase magnetoelectroelastic composites were investigated based on different micromechanical models. Various N-phase micromechanical models were elaborated to predict the effective N-phase magnetoelectroelastic moduli for different types, shapes and volume fractions of inclusions. Note that, the effective properties of the composite might be greatly affected by the presence of an interphase between the matrix and inclusions. Consequently, to enhance the prediction of the effective properties of

the composite the type and the structure of the interphase have to be taken into account in the modeling. In chapter 3, the multi-coated inclusion and functionally graded interphase concepts will be introduced. The multi-coating and functionally graded interphase effects will be taken into account by the generalization of the integral equation for N-phase composites and the introduction of the magnetoelectroelastic interfacial operators. The effective properties will be predicted with respect to the volume fractions, shapes of inclusions and the thickness of the coating.

References

[1] Deeg, W. F. (1980): The analysis of dislocation, Crack, and inclusion problems in piezoelectric solids. Ph.D. dissertation, Stanford University.

[2] Dunn, M. L.; Taya, M. (1993): Micromechanics predictions of the effective electroelastic moduli of piezoelectric composites. Int. J. Solids Structures, Vol.30, No. 2, pp. 161-175.

[3] Dunn, M. L.; Wienecke, H. A. (1996): Green's function for transversely isotropic piezoelectric solids. Int. J. Solids Structures, Vol. 33, No. 30, pp. 4571-4581.

[4] Dunn, M. L.; Wienecke, H. A. (1997): Inclusion and inhomogeneities in transversely isotropic solids. Int. J. Solids Structures, Vol. 34, No. 27, pp. 3571-3582.

[5] Eshelby, J. D. (1957): The determination of the elastic field of an ellipsoidal inclusion and related problems. Proc. R. Soc. Lond. A, Vol. 241, pp. 376-396.

[6] Fakri, N.; Azrar, L.; El Bakkali, L. (2003): Electoelastic behavior modeling of piezoelectric composite materials containing spatially oriented reinforcements. International Journal of Solids and Structures, Vol. 40, Issue 2, pp. 361-384.

[7] Fakri, N.; Azrar, L. (2010): Thermal and electro-elastic behaviour of piezo-composites and inhomogeneous piezoelectric materials with voids. Journal of Intelligent Materials Systems and Structures, Vol. 21, No. 2, pp. 161-174.

[8] Feng, X.; Fang, D.; Hwang, K. (2004): Closed-form solution for piezomagnetic inhomogeneities embedded in a non-piezomagnetic matrix. European Journal of Mechanics A/Solids, Vol. 23, pp. 1007-1019.

[9] Hershey, A. V. (1954): The elasticity of an isotropic aggregate of anisotropic cubic crystal. J. Appl. Mech., Vol. 21, pp. 236-241.

[10] Kroner, E. (1958): Berechnung der elastischen konstanten des vielkristalls aus den konstanten des einkristalls. Z. Phys., Vol. 151, pp. 504-518.

[11] Lee, J.; Boyd, J. G.; Lagoudas, D C. (2005): Effective properties of three-phase electro-magneto-elastic composites. Int. J. Engineering Science, Vol. 43, pp. 790-825.

[12] Li, J.Y.; Dunn, M. L. (1998): Micromechanics of magnetoelectroelastic composite materials: average fields and effective behavior. Journal of Intelligent Material and Structures, Vol. 9, pp.404-416.

[13] Li, J.Y. (2000): Magnetoelectroelastic multi-inclusion and inhomogeneity problems and their applications in composite materials. Int. J. of Engineering Science, Vol. 38, pp. 1993-2011.

[14] Li, J.Y (2004): The effective pyroelectric and thermal expansion coefficients of ferroelectric ceramics. Mechanics of Materials, Vol. 36, pp. 949–958.

[15] Mori T. Tanaka K. (1973): Average stress in matrix and average elastic energy of materials with misfitting Inclusions. Acta Metall., Vol. 21, pp. 571-574. [16] Odegard, G.M. (2004): Constitutive Modeling of Piezoelectric Polymer Composites. Acta Materialia, Vol. 52, No.18, pp.5315-5330.

[17] Srinivas, S.; Li, J. Y. (2005): The effective magnetoelectric coefficients of polycrystalline multiferroic composites. Acta Materialia. J., Vol. 53, pp. 4135–4142.

[18] Srinivas, S.; Li, J. Y.; Zhou, Y. C.; Soh, A. K. (2006): The effective magnetoelectroelastic moduli of matrix-based multiferroic composites. Journal of applied physics, Vol. 99, 043905.

[19] Wu, T.; Huang, J. H. (2000): Closed-form solution for the magnetoeletric coupling coefficients in fibrous composites with piezoelectric and piezomagnetic phases. International Journal of Solids and Structures, Vol. 37, pp. 2981-3009.

[20] Zhang, Z.K.; Soh, A.K. (2005): Micromechanics predictions of the effective moduli of magnetoelectroelastic composite materials. European. J. of Mechanics A/Solids, Vol. 24, pp.1054-1067.

Chapter 3

3. Micromechanical modeling of magnetoelectroelastic composite materials with multi-coated inclusions and functionally graded interphases

Abstract

In this paper micromechanical modelings of magnetoelectroelastic composites with multi-coated inclusions and functionally graded interphases are elaborated. The integral equation taking into account the continuously varying interphase properties as well as the multi-functional coating effects is introduced based on the Green's tensors and interfacial operators. Magnetoelectroelastic composites with functionally graded interphases are analyzed and the effective properties are derived. Based on the Mori-Tanaka, Self Consistent and Incremental Self Consistent models the numerically predicted effective properties of magnetoelectroelastic composites are presented with respect to the volume fractions, shapes of the multi-coated inclusions and the thickness of the coatings. The multi-coating and functionally graded interphase concepts can be used to optimize the effective properties of multi-functional composites. This can be used to design new multi-functional composite materials with higher coupling coefficients.

3.1 Introduction

Smart composites such piezoelectric, piezomagnetic and magnetoelectroelastic composites have been increasingly used in recent years due to their applications in actuators, sensors, ultrasonic imaging and transducers etc. (Konka, Wahab and Lian, 2012; Gururaja et al., 1985). These smart composites take the advantages of each phase and have better physical properties. For example, the most interesting behavior of smart composites consisting of piezoelectric and piezomagnetic constituents is that the magnetoeletric effect, which is only present in composites but absent in constituent phases, is created by the interaction between the constituent phases. Note that the overall effective properties of reinforced composite materials may be significantly influenced by the properties of the interface between the constituents. Therefore, for accurate predictions of the effective properties of composites, the behavior and structures of interfaces have to be considered in the modeling and numerical simulation. The local interaction between the matrix and the inclusion and then the overall performance of the whole composites can be influenced by the interphase and coating effects. The concept of functionally graded interphase and coated inclusions has been introduced to obtain composite materials with competent properties.

The effective properties of composite materials consisting of coated inclusions embedded in a matrix have been investigated by many researchers. Several works have been done to investigate the influence of the thin coating on the effective properties of coated composites. (Nemat-Nasser and Hori, 1993; Hori and Nemat-Nasser, 1994) proposed a double inclusion model to predict the effective behavior of multiphase composites and then applied by (Li, 2000a) to study the average magnetoelectroelastic field in a multi-inclusion or inhomogeneities embedded in an infinite matrix. (Cherkaoui et al., 1994, 1995, 1996) studied the effect of the thin coating on the local fields and on the effective properties of elastic composites and thermoelastic composites based on the Green's functions techniques and on the interfacial operators. (Li, 2000b) analyzed the thermoelastic behavior of composites with functionally graded interphase by the multi-inclusion model where the explicit expression of the effective thermoelastic moduli and thermoelastic field of the composites are obtained explicitly. (Vieville, Bonnet and Lipinski, 2006) developed some theoretical consideration concerning the modeling of effective properties of composite materials based on inclusion concept. (Dinzart and Sabar, 2009) predicted the effective properties of piezoelectric composites with thinly coated reinforcements by using the Mori-Tanaka's mean field approach. (Koutsawa et al., 2010) used a micromechanical model to investigate the

effective thermo-electro-elastic properties of piezoelectric composites materials containing multi-coated inhomogeneities as well as a finite element analysis for two phase piezoelectric composite materials. (Berbenri and cherkaoui, 2010) elaborated a micromechanical approach for arbitrary multi-coated ellipsoidal elastic inclusions with general eigenstrains.

The aim of this work is to elaborate micromechanical models for accurate prediction of multi-functional magnetoelectroelastic composites. Two kinds of composites are considered: one with multi-coated inclusions and the other with functionally graded interphases. Magnetoelectroelastic composite materials with functionally graded interphases refer to a kind of magnetoelectroelastic composite materials with continuously varying properties between the matrix and inclusions. However, magnetoelectroelastic composite materials with multi-coated inclusions may be seen as a special kind of functionally graded materials with discontinuously varying properties between the matrix and inclusions. This paper is an extension of the magnetoelectroelastic modeling recently developed by (Bakkali, Azar and Fakri, 2011) and is organized as follow. The concept of functionally graded continuously varying interphase properties is first introduced. The considered topology of multi-coated inclusions as well as the homogenization process and the localization tensors are derived. The concentration tensors of the adapted micromechanical models are explicitly given. Numerical results are presented for multi-functional composites with multi-coated inclusions and functionally graded interphases based on various micromechanical models. To take account of the defect that may exist in the interphase, a void layer is considered. Four-phase magnetoelectroelastic composites with various shapes and types of inclusions and coatings are analyzed. Various graded model parameters and thickness of the interphase are considered and their effects on the predicted effective properties are investigated.

3.2 Multi-phase considered topology

3.2.1 Composites with functionally graded continuously varying interphase properties

Three phase composites in which the interphase between the matrix and the reinforcements varies continuously are considered. As magnetoelectroelastic composites are considered the three phases matrix, reinforcement and interphase may be of different properties. A wide variety of interphase interactions can be considered and each phase may be elastic piezoelectric,

piezomagnetic or even magnetoelectroelastic. As shown in Figure 3.1, phase 1 is the reinforcement, phase 3 is the matrix having homogeneous material properties E^1 and E^3 respectively. Phase 2 is the interphase that is assumed to be of spatially varying properties. The reinforcements are perfectly bounded, aligned and have ellipsoidal shapes with the dimensions a_1, b_1, c_1 and a_2, b_2, c_2. The two ellipsoids are coaxial with $\frac{a_1}{a_2}=\frac{b_1}{b_2}=\frac{c_1}{c_2}=\gamma$. The volume fraction of the matrix is f_3 and of the inclusion and interphase are obtained by $f_1=(1-f_3)\gamma^3$ and $f_2=(1-f_3)(1-\gamma^3)$.

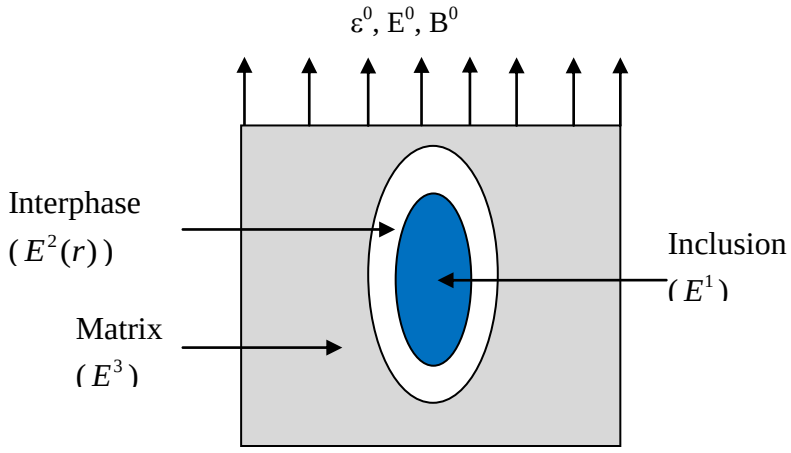

Figure 3.1: A representative volume element of a composite with functionally graded interphase between reinforcement 1 and matrix 3. The dimension of the reinforcement and interphase are a_1, b_1, c_1 and a_2, b_2, c_2 respectively. ε^0, E^0 and B^0 represent the macroscopically applied fields.

For structures with functionally graded materials, many models can be found in the open literature. But for inclusion problem, as it is our concern here, very few papers were focused on. The mathematical model, used by (Wacker et al., 1998) to describe the variation properties of Young's modulus in the interphase of a fibrous composite, is used here.

The magnetoelectroelastic moduli $E^2(r)$ of the interphase is taken as a radial function and its expression is given by the following relationship:

$$E^2(r)=(\alpha E^1-E^3)\left(\frac{1-r}{1-\gamma}\right)^n+E^3 \qquad (3.1)$$

with $0\le\alpha\le 1$, $n=2,3....$ and r represents the normalized radial distance from the inner surface of the interphase ranging from γ to 1 $0\le\gamma\le r\le 1$. Note that $E^2(1)=E^3$ and $E^2(\gamma)=\alpha E^1$. The

parameter α allows starting the graded effect from the inclusion (α =1), intermediate media $0<\alpha<1$ or even from a void coating (α =0). For the sake of clarity, the radial variation of a material modulus, say the elastic modulus $c^2_{1111}(r)$ of the interphase, for α =1, α =0.5 and various values of n, is presented in Figure 3.2 for magnetoelectroelastic composites consisting of piezoelectric inclusions ($BaTiO_3$) and piezomagnetic matrix ($CoFe_2O_4$).

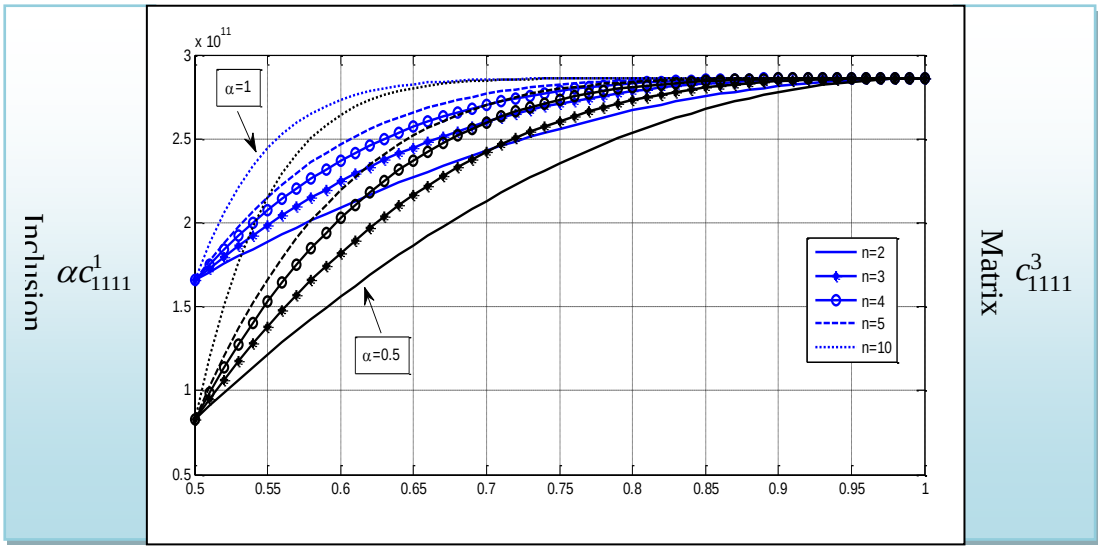

Figure 3.2: Variation of the elastic modulus $c^2_{1111}(r)$ of the functionally graded interphase, with fixed thickness (γ=0.5), in terms of normalized radial distance r and various values of n and α.

As shown in Figure 3.2, the variation of the elastic modulus of the functionally graded interphase starts with the elastic modulus αc^1_{1111} where c^1_{1111} is the elastic modulus of the inclusion and ends with the elastic modulus of the matrix c^3_{1111}.

The averaged magnetoelectroelastic moduli E^2 are given by:

$$< E^2 >= \frac{1}{\frac{4}{3}\pi(a_2b_2c_2 - a_1b_1c_1)} \int_{a_1}^{a_2}\int_{b_1}^{b_2}\int_{c_1}^{c_2} E^2(r)dxdydz = \frac{3}{1-\gamma^3}\int_{\gamma}^{1} r^2E^2(r)dr \qquad (3.2)$$

After integration, one obtains:

$$< E^2 >= \frac{3(\alpha E^1 - E^3)}{1+\gamma^2+\gamma}\left(\frac{(1-\gamma)^{n-2}}{n+1} - \frac{2(1-\gamma)^{n-1}}{n+2} + \frac{(1-\gamma)^n}{n+3}\right) + E^3 \qquad (3.3)$$

The micromechanical modeling, developed bellow, will be applied to predict the effective properties of the composite described in this section, with E^2 replaced by $< E^2 >$. It has to be noted that two limiting cases can also be considered. The first one is when γ approaches zero and then phase one disappears. The second one is when γ approaches 1 and then there is no interphase between the matrix and the inclusion.

3.2.2 Multi-Coated composites

For magnetoelectroelastic composites with multi-coated inclusions the matrix, inclusion and coatings may be elastic, piezoelectric, piezomagnetic or magnetoelectroelastic. The topology of the considered multi-coated inclusion problem, drawn in Figure 3.3, is described by an inclusion of a volume V_1 with magnetoelectroelastic moduli E^1 surrounded by (n-1) thin coatings of other materials whose behaviors are described by their respective magnetoelectroelastic moduli E^i and their volumes V_i with $i \in \{2,3,.....n\}$. The multi-coated inclusion is embedded in a homogenous media called the matrix whose behavior is described by the magnetoelectroelastic moduli E^M and the interphases are assumed perfectly bonded.

The used micromechanical modeling are based on two steps: (i) localization step, which gives the relationship between the microscopic field and macroscopic field through the localization tensors and (ii) homogenization step, which employs averaging techniques to estimates the effective properties of the composites. The derivation of the concentration tensors is based on the integral equation and the interfacial operators accounting for coatings effects.

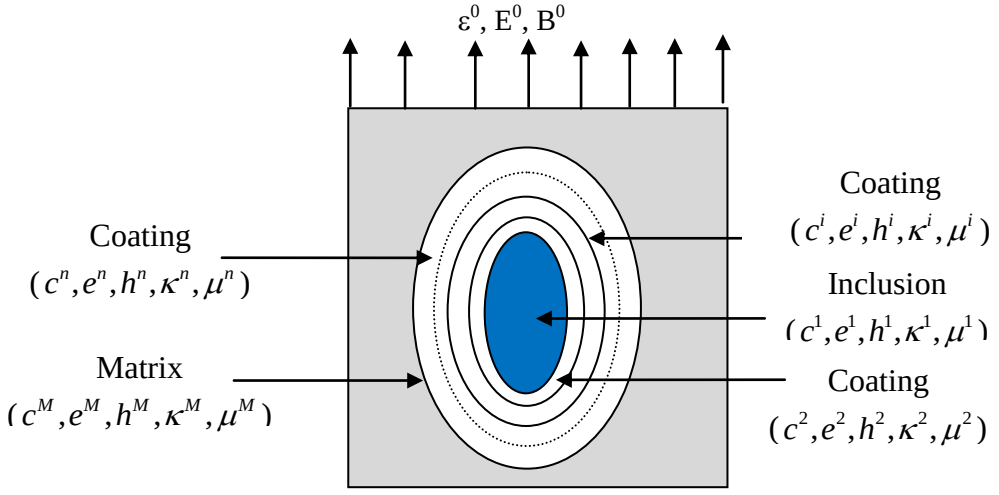

Figure 3.3: Topology of the multi-coated inclusion. ε^0, E^0 and B^0 represent the macroscopically applied fields.

3.3 Micromechanical modeling

3.3.1 Constitutive behavior and notations

The linear magnetoelectroelastic effect is considered, where the magnetic, electric and elastic fields are coupled through the following constitutive equations:

$$\begin{cases} \sigma_{ij} = c_{ijkl}\varepsilon_{kl} - e_{lij}E_l - h_{lij}H_l \\ D_i = e_{ikl}\varepsilon_{kl} + \kappa_{il}E_l + \alpha_{il}H_l \\ B_i = h_{ikl}\varepsilon_{kl} + \alpha_{il}E_l + \mu_{il}H_l \end{cases} \tag{3.4}$$

in which the elastic strain ε_{kl}, electric fields E_l and magnetic fields H_l are independent variables related to stresses σ_{ij}, electric displacements D_i and magnetic inductions B_i. The tensors c_{ijkl}, e_{lij}, h_{lij}, α_{il}, κ_{il} and μ_{il} are the elastic, piezoelectric, piezomagnetic, magnetoelectric, dielectric and magnetic permeability constants respectively. In the constitutive equations we use -E_l and -H_l rather than E_l and H_l as they will permit the construction of a symmetric matrix of constitutive moduli.

Using the condensed notations (Bakkali, Azrar and Fakri, 2011), the field variables take the following forms:

$$Z_{Mn} = \begin{cases} \varepsilon_{mn} & (M = 1,2,3) \\ -E_n & (M = 4) \\ -H_n & (M = 5) \end{cases} \qquad \sum_{iJ} = \begin{cases} \sigma_{ij} & (J = 1,2,3) \\ D_i & (J = 4) \\ B_i & (J = 5) \end{cases} \tag{3.5}$$

The magnetoelectroelastic constants can then be represented as follows:

$$E_{iJMn} = \begin{cases} c_{ijmn} & (J, M = 1,2,3) \\ e_{nij} & (J = 1,2,3; M = 4) \\ h_{nij} & (J = 1,2,3; M = 5) \\ e_{imn} & (J = 4; M = 1,2,3) \\ h_{imn} & (J = 5; M = 1,2,3) \\ -\kappa_{in} & (J = 4; M = 4) \\ -\alpha_{in} & (J = 4; M = 5 or J = 5; M = 4) \\ -\mu_{in} & (J = 5; M = 5) \end{cases} \tag{3.6}$$

With these notations the constitutive equations can be written as:

$$\Sigma_{iJ} = E_{iJMn} Z_{Mn} \tag{3.7}$$

The equilibrium equations, in the absence of body force, electric charge and electric current densities, are given by:

$$\sigma_{ij,i} = 0 \qquad D_{i,i} = 0 \qquad B_{i,i} = 0 \tag{3.8}$$

Using the above condensed notations, the equilibrium equations are written as follow:

$$\Sigma_{iJ,i} = 0 \tag{3.9}$$

Based on the symmetry of the tensors $c, e, h, \kappa, \mu, \alpha$ the following equilibrium partial differential equation is obtained:

$$(E_{iJKl} U_{K,l})_{,i} = 0 \tag{3.10}$$

3.3.2 Localizations and homogenization

V is considered as the representative volume of the composite. The average generalized strain field Z and generalized stress field Σ are related to the local generalized strain field $Z(r)$ and the local generalized stress field $\Sigma(r)$ by the following average relationships.

$$Z_{Kl} = \frac{1}{V} \int_V Z_{Kl}(r) dV \tag{3.11-a}$$

$$\Sigma_{iJ} = \frac{1}{V} \int_V \Sigma_{iJ}(r) dV \tag{3.11-b}$$

For an n phases' composite material, the volume average of the local generalized strain $Z(r)$ and generalized stress $\Sigma(r)$ are given by:

$$Z_{Kl} = \sum_{i=1}^{n} f_i Z_{Kl}^i \tag{3.12-a}$$

$$\Sigma_{lK} = \sum_{i=1}^{n} f_i \Sigma_{lK}^i \tag{3.12-b}$$

where the index 'i' denotes the ith phase and f_i is its corresponding volume fraction. Z^i and Σ^i are considered to be uniform in each phase. Additionally, the overall constitutive behavior of the composite and of phase p of the composite can be written as follow:

$$\Sigma_{iJ} = E^{eff}_{iJKl} Z_{Kl} \tag{3.13-a}$$

$$\Sigma^p_{iJ} = E^p_{iJKl} Z^p_{Kl} \tag{3.13-b}$$

in which E^{eff} is the effective magnetoelectroelastic moduli of the composites.

In order to make the transition between the local scale (phases) and the global scale (composite) the concentration tensors are used and the localization relationships are given as follow:

$$Z^p_{Kl} = A^p_{KlMn} Z_{Mn} \tag{3.14-a}$$

$$\Sigma^p_{iJ} = B^p_{iJnM} \Sigma_{nM} \tag{3.14-b}$$

where A and B are the fourth order concentration tensors that take into account the properties and the volume fraction of each phase as well as the shape of the multi-coated inclusion. Substituting (3.14) into (3.12) one gets:

$$\sum_{p=1}^{n} f_p A^p_{KlMn} = I_{KlMn} \tag{3.15-a}$$

$$\sum_{p=1}^{n} f_p B^p_{iJnM} = I_{iJnM} \tag{3.15-b}$$

where I is the shorthand notation of the identity tensors.

On the other hand, by substituting (3.14) into (3.13), the following concentration tensor B is obtained:

$$B^p_{iJmK} = E^p_{iJNl} A^P_{NlSv} (E^{eff}_{mKSv})^{-1} \tag{3.16}$$

The substitution of (3.13-b) into (3.12) and the consideration of equations (3.13) and (3.14), lead to the following expression of the effective moduli:

$$E_{kLSv}^{eff} = \sum_{p=1}^{n} f_p E_{kLIj}^{p} A_{IjSv}^{P} \tag{3.17-a}$$

$$(E_{kLSv}^{eff})^{-1} = \sum_{p=1}^{n} f_p (E_{nMSv}^{p})^{-1} B_{nMkL}^{P} \tag{3.17-b}$$

3.3.3 Derivation of the concentration tensors

A homogeneous fictitious media, called "reference media" which has the magnetoelectroelastic moduli E_{iJMn}^{0}, is considered. The expression of the local magnetoelectroelastic moduli is given by:

$$E_{iJMn}(r) = E_{iJMn}^{0} + \delta E_{iJMn}(r) \tag{3.18}$$

where ''r'' is the position vector in the media considered and δE is the deviation part. The introduction of this expression into (3.10) leads to

$$E_{iJMn}^{0} U_{M,ni}(r) + (\delta E_{iJMn}(r) U_{M,n}(r))_{,i} = 0 \tag{3.19}$$

Using the Green's function technique, this partial differential equation is transformed into an integral equation linking the local generalized strain field $Z_{Kl}(r)$ with the tensor $Z^{0}{}_{Kl}$.

$$Z_{Kl}(r) = Z_{Kl}^{0}(r) - \int_{V} \Gamma_{iJKl}(r - r') \delta E_{iJMn}(r') Z_{Mn}(r') dV' \tag{3.20}$$

where V is the volume of the infinite medium, Γ is the magnetoelectroelastic modified Green's tensor of the reference medium E^{0} whose components are related to those of the magnetoelectroelastic Green's tensor and given by (Bakkali, Azrar and Fakri, 2011):

$$\Gamma_{iJKl}(r - r') = -G_{JK,li}(r - r') \tag{3.21}$$

For the multicoated considered problem, represented in figure 3.3, the deviation part is expressed by:

$$\delta E_{iJMn} = \sum_{k=0}^{n} \Delta E_{iJMn}^{(k/0)} \theta^{k}(r) \quad ; \; k \in \{0,1,2,...n\} \tag{3.22}$$

where $\theta^{k}(r)$ is the characteristic function of the phase k, occupying the volume V_k, expressed by:

$$\theta^{k}(r) = \begin{cases} 1 & if \; r \in V_k \\ 0 & if \; r \notin V_k \end{cases}, \tag{3.23}$$

and $\Delta E_{iJMn}^{(k/0)} = E_{iJMn}^{k} - E_{iJMn}^{0}$

Substituting (3.22) into (3.20) and using the property (3.23), one gets:

$$Z_{Kl}(r) = Z^0_{Kl}(r) - \sum_{k=0}^{n} \int_{V_k} \Gamma_{iJKl}(r-r')\Delta E^{(k/0)}_{iJMn} Z_{Mn}(r')dV' \tag{3.24}$$

Using the fact that when k=0, $\Delta E^{(k/0)}_{iJMn} = 0$ leads to

$$Z_{Kl}(r) = Z^0_{Kl}(r) - \sum_{k=1}^{n} \int_{V_k} \Gamma_{iJKl}(r-r')\Delta E^{(k/0)}_{iJMn} Z_{Mn}(r')dV' \tag{3.25}$$

Let us denote by V_I the total volume of the composite inclusion, which consists of an inclusion surrounded by (n-1) coatings and f_k is the volume fraction of the phase k. Then one has:

$$V_I = \sum_{k=1}^{n} V_k \tag{3.26}$$

The average local generalized strain field can be written as:

$$Z_{Mn}(r) = \sum_{k=1}^{n} Z^k_{Mn}\theta^k(r) \tag{3.27}$$

The substituting (3.27) into (3.25) leads to

$$Z_{Kl}(r) = Z^0_{Kl}(r) - \sum_{k=1}^{n} \int_{V_k} \Gamma_{iJKl}(r-r')\Delta E^{(k/0)}_{iJMn} Z^k_{Mn} dV' \tag{3.28}$$

Averaging the generalized local field over the composite inclusion, one gets:

$$Z^I_{Kl} = Z^0_{Kl} - \sum_{k=1}^{n} \frac{1}{V_I} \int_{V_I}\int_{V_k} \Gamma_{iJKl}(r-r')\Delta E^{(k/0)}_{iJMn} Z^k_{Mn} dV'dV \tag{3.29}$$

This equation can be reformulated in the following form:

$$Z^I_{Kl} = Z^0_{Kl} - \frac{1}{V_I}\sum_{k=1}^{n} T^{Ik}_{iJKl}\Delta E^{(k/0)}_{iJMn} Z^k_{Mn} \tag{3.30}$$

in which $T^{Ik}_{iJKl} = \int_{V_I}\int_{V_k} \Gamma_{iJKl}(r-r')dV'dV$ represents the condensed notation of nine magnetoelectroelastic interaction tensors.

Using the fact that $Z^I_{Kl} = \sum_{k=1}^{n} \frac{V_k}{V_I} Z^k_{Kl}$ leads to:

$$\sum_{k=1}^{n} \frac{V_k}{V_I}(I_{KlMn} + \frac{1}{V_k} T^{Ik}_{iJKl}(E^0)\Delta E^{(k/0)}_{iJMn}) Z^k_{Mn} = Z^0_{Kl} \tag{3.31}$$

where I_{KlMn} is the shorthand notation of the fourth order and the second order identity tensors:

$$I_{KlMn}=\begin{cases}1/2(\delta_{km}\delta_{ln}+\delta_{kn}\delta_{lm}) & (K,M=1,2,3)\\ 0 & (K=1,2,3;M=4)\\ 0 & (K=1,2,3;M=5)\\ 0 & (K=4;M=1,2,3)\\ 0 & (K=5;M=1,2,3)\\ \delta_{ln} & (K=4;M=4)\\ 0 & (K=4;M=5 or K=5;M=4)\\ \delta_{ln} & (K=5;M=5)\end{cases} \tag{3.32}$$

Denoting by a^k the local concentration tensor relating the average generalized strain in each coating with the average generalized strain in the inclusion, one can put:

$$Z^k_{Mn}=a^k_{MnKl}Z^1_{Kl} \quad \text{with} \quad a^1_{MnKl}=I_{MnKl} \tag{3.33}$$

Based on equations (3.31) and (3.33) the following relationship is obtained:

$$Z^k_{Mn}=a^k_{MnPv}\left[\sum_{k=1}^{n}\left(\frac{f_k}{f_I}\left(I_{KlPv}+\frac{1}{V_k}T^{Ik}_{iJKl}(E^0)\Delta E^{(k/0)}_{iJRs}\right)a^k_{RsPv}\right)\right]^{-1}Z^0_{Kl} \tag{3.34}$$

The expression of the concentration tensor is then given by:

$$A^k_{MnKl}=a^k_{MnPv}\left[\sum_{k=1}^{n}\left(\frac{f_k}{f_I}\left(I_{KlRs}+\frac{1}{V_k}T^{Ik}_{iJKl}(E^0)\Delta E^{(k/0)}_{iJRs}\right)a^k_{RsPv}\right)\right]^{-1} \tag{3.35}$$

To complete the localization step, the local concentration tensor a^k must be expressed. It can be determined if the boundary conditions are taken into account through the interface in the composite inclusions. Note that the interfacial operators introduced by (Hill, 1983) constitute an efficient mathematical tool to determine the stress and the strain jump through an interface between two dissimilar materials. These operators are derived by writing the equations for the continuity of displacement and tension across the material interface (hypothesis of perfect interface). These interfacial operators are used by (Cherkaoui et al., 1994, 1995, 1996) for elastic composites with multi-coated inclusions.

A generalized case, of two solids whose magnetoelectroelastic moduli are noted E^k and E^{k+1} separated by an interface with a unit normal N, directed from phase k to phase k+1, is considered. The generalized strain jump ($Z^{k+1}-Z^k$) across the material interface is given as follow (see appendix 3.A for detail):

$$Z_{Mn}^{k+1}(r) - Z_{Mn}^{k}(r) = P_{iJMn}^{k+1}(E^{k+1}, N)(E_{iJRs}^{k} - E_{iJRs}^{k+1})Z_{Rs}^{k}(r) \tag{3.36}$$

where P_{iJMn}^{k+1} is the magnetoelectroelastic interfacial operators of the phase (k+1) which depends only on properties of the material phase and on the unit normal N. Equation (3.36) can be reformulated as follow:

$$Z_{Mn}^{k+1}(r) = (I_{MnRs} + P_{iJMn}^{k+1}(E^{k+1}, N)\Delta E_{iJRs}^{(k/k+1)})Z_{Rs}^{k}(r) \tag{3.37}$$

in which $\Delta E_{iJRs}^{(k/k+1)} = E_{iJRs}^{k} - E_{iJRs}^{k+1}$

Applying the last equation between phases 1 and 2 in the multi-coated inclusion problem, one obtains:

$$Z_{Mn}^{2}(r) = (I_{MnRs} + P_{iJMn}^{2}(E^{2}, N)\Delta E_{iJRs}^{(1/2)})Z_{Rs}^{1}(r) \tag{3.38}$$

Replacing the generalized strain field $Z^1(r)$ by its mean value Z^1 and then averaging over the coating volume V_2, the following relationship is obtained:

$$Z_{Mn}^{2} = (I_{MnRs} + T_{iJMn}^{2}(E^{2})\Delta E_{iJRs}^{(1/2)})Z_{Rs}^{1} \tag{3.39}$$

where $T_{iJMn}^{2}(E^{2}) = \dfrac{1}{V_2}\int_{V_2} P_{iJMn}^{2}(E^{2}, N)dV$

The following localization relationship is then resulted:

$$Z_{Mn}^{2} = W_{MnRS}^{(1/2)} Z_{Rs}^{1} \tag{3.40}$$

where $W_{MnRs}^{(1/2)} = (I_{MnRs} + T_{iJMn}^{2}(E^{2})\Delta E_{iJRs}^{(1/2)})$

Introducing a new volume notation:

$$\Omega_j = \bigcup_{i=1}^{j} V_i; \;\; j = 1,..n \tag{3.41}$$

Based on equation (3.38) for the second interface between the composite inclusion of volume ($\Omega_2 = V_1 \cup V_2$) and magnetoelectroelastic moduli E^{Ω_2} and the phase 3 of the volume V_3 and magnetoelectroelastic moduli E^3, then replacing $Z^{\Omega_2}(r)$ by its mean value Z^{Ω_2} and averaging all the equation over the coating volume V_3, one can obtain:

$$Z_{Mn}^{3} = (I_{MnRs} + T_{iJMn}^{3}(E^{3})\Delta E_{iJRs}^{(\Omega_2/3)})Z_{Rs}^{\Omega_2} \tag{3.42}$$

in which $T_{iJMn}^{3}(E^{3}) = \dfrac{1}{V_3}\int_{V_3} P_{iJMn}^{k}(E^{3}, N)dV$ and $\Delta E_{iJRs}^{(\Omega_2/3)} = E_{iJRs}^{\Omega_2} - E_{iJRs}^{3}$

The averaged generalized strain Z^{Ω_2} in the composite inclusion is given as a function of Z^1 and Z^2 as follow:

$$Z_{Rs}^{\Omega_2} = \frac{1}{\Omega_2}\int_{\Omega_2} Z_{Rs}(r)dV = \frac{f_1}{f_1+f_2}Z_{Rs}^1 + \frac{f_2}{f_1+f_2}Z_{Rs}^2 \tag{3.43}$$

Based on the Hooke's law the term $\Delta E_{iJRs}^{(\Omega_2/3)} Z_{Rs}^{\Omega_2}$ in equation (3.42) can be rewritten as follow:

$$\Delta E_{iJRs}^{(\Omega_2/3)} Z_{Rs}^{\Omega_2} = \frac{f_1}{f_1+f_2}\Delta E_{iJRs}^{(1/3)} Z_{Rs}^1 + \frac{f_2}{f_1+f_2}\Delta E_{iJRs}^{(2/3)} Z_{Rs}^2 \tag{3.44}$$

The substitution (3.44) into (3.42) leads to:

$$Z_{Mn}^3 = \frac{f_1}{f_1+f_2}(I_{MnRS} + T_{iJMn}^3(E^3)\Delta E_{iJRs}^{(1/3)})Z_{Rs}^1 + \frac{f_2}{f_1+f_2}(I_{MnRS} + T_{iJMn}^3(E^3)\Delta E_{iJRs}^{(2/3)})Z_{Rs}^2 \tag{3.45}$$

This equation can be rewritten as:

$$Z_{Mn}^3 = \frac{f_1}{f_1+f_2}W_{MnRS}^{(1/3)}Z_{Rs}^1 + \frac{f_2}{f_1+f_2}W_{MnRS}^{(2/3)}Z_{Rs}^2 \tag{3.46}$$

where $W_{MnRs}^{(1/3)} = (I_{MnRs} + T_{iJMn}^3(E^3)\Delta E_{iJRs}^{(1/3)})$

Using (3.40), this equation can be reformulated as:

$$Z_{Mn}^3 = (\frac{f_1}{f_1+f_2}W_{MnKl}^{(1/3)} + \frac{f_2}{f_1+f_2}W_{MnRS}^{(2/3)}W_{RsKl}^{(1/2)})Z_{Kl}^1 \tag{3.47}$$

Explicit expression of the localization tensor a^k can be then formulated as:

$$a_{MnKl}^1 = I_{MnKl}$$

$$a_{MnKl}^2 = W_{MnKl}^{(1/2)}$$

$$a_{MnKl}^3 = \frac{f_1}{f_1+f_2}W_{MnKl}^{(1/3)} + \frac{f_2}{f_1+f_2}W_{MnRS}^{(2/3)}W_{RsKl}^{(1/2)} = \frac{\sum_{i=1}^{2} f_i W_{MnRs}^{(i/3)} a_{RsKl}^i}{\sum_{i=1}^{2} f_i}$$

Using the same mathematical procedure, the expression of the localization tensor a^k could be explicitly given in general case of an interface between phases k and k+1 by:

$$a_{MnKl}^k = \frac{\sum_{i=1}^{k-1} f_i W_{MnRs}^{(i/k)} a_{RsKl}^i}{\sum_{i=1}^{k-1} f_i} \tag{3.48}$$

in which

$$W_{MnRs}^{(i/k)} = (I_{MnRs} + T_{iJMn}^{k}(E^{k})\Delta E_{iJRs}^{(i/k)}) \quad \text{and} \quad T_{iJMn}^{k}(E^{k}) = \frac{1}{V_k}\int_{V_k} P_{iJMn}^{k}(E^{k}, N)dV$$

The localization problem is now completely solved by giving explicit relationship of the local concentration tensor. The computation of these concentration tensors requires the determination of the interaction tensors T^{k} and T^{Ik}. The tensor T^{k} is given by (see appendix 3.B for detail):

$$T_{iJMn}^{k}(E^{k}) = T_{iJMn}^{\Omega_{k-1}}(E^{k}) - \frac{\sum_{j=1}^{k-1} f_j}{f_k}(T_{iJMn}^{\Omega_k}(E^{k}) - T_{iJMn}^{\Omega_{k-1}}(E^{k})) \tag{3.49}$$

where

$$T_{iJMn}^{\Omega_k}(E^{k}) = \frac{1}{\Omega_k}\int_{\Omega_k}\int_{\Omega_k} \Gamma_{iJMn}(E^{k})(r - r')dVdV'$$

Note that the tensor T^{Ω_k} is not affected by the size of the composites inclusion but depends on its shape. So, in the specific case of homothetic inhomogeneities, one can obtain:

$$T_{iJMn}^{k}(E^{k}) = T_{iJMn}^{\Omega_k}(E^{k}) = T_{iJMn}^{\Omega_{k-1}}(E^{k})$$

These tensors are evaluated numerically for various shapes of composite inclusion by using the Gaussian quadrature integration for the considered inclusion shape (Bakkali, Azrar and, Fakri, 2011). Based on these interaction and localization tensors various micromechanical models can be elaborated.

3.4 Micromechanical approach and effective properties

Based on the previous tensors and relationships various micromechanical approaches can be adapted. For multi-coated inclusions, the concentration tensors are explicitly given for Self Consistent, Mori-Tanaka and Dilute micromechanical approaches. Effective magnetoelectroelastic moduli corresponding to considered models can be numerically obtained. The expression of the effective moduli of magnetoelectroelastic composites with multi-coated reinforcements is given by:

$$E_{iJKl}^{eff} = E_{iJKl}^{m} + \sum_{k=1}^{n} f^{k}(E^{k}{}_{iJMn} - E^{m}{}_{iJMn})A_{MnKl}^{k} \tag{3.50}$$

where A^{k} is the magnetoelectroelastic localization tensors.

From (3.50) it is seen that the determination of the effective moduli of magnetoelectroelastic composites with multi-coated reinforcements requires only the evaluation of the localization tensors A^k .

3.4.1 Self Consistent approach

The Self Consistent approach takes into account the interaction between the matrix and the multi-coated reinforcements. In the Self Consistent approach the composite is considered as a multi-coated inclusion embedded in a matrix which takes the properties of the whole composite. For multi-coated inclusions the Self Consistent concentration tensors A^k is evaluated from (3.31) by replacing E^0 by E^{eff} and its expression is given by:

$$A^k_{MnKl} = a^k_{MnPv}\left[\sum_{k=1}^{n}\left(\frac{f_k}{f_I}\left(I_{KlRs} + \frac{1}{V_k}T^{Ik}_{iJKl}(E^{eff})\Delta E^{(k/eff)}_{iJRs}\right)a^k_{RsPv}\right)\right]^{-1} \tag{3.51}$$

in which $\Delta E^{(k/eff)}_{iJMn} = E^k_{iJMn} - E^{eff}_{iJMn}$

It has to be noted that A^k depends on the tensor E^{eff} which is not yet known. An iterative procedure is then necessary.

3.4.2 The Incremental Self Consistent approach

Note that, even if the Self Consistent model is well used in micromechanical analysis, it has some limitations. (Fakri, Azrar and Bakkali, 2003) investigated the effective properties of two-phase piezoelectric composites by using different micromechanical models and it is shown that the Self Consistent approach diverges for high volume fraction of inclusions and does not conduct far the prediction for piezoelectric composites with void inclusions. An improvement of the classical Self Consistent by incremental way was developed for two phase piezo composite materials by (Fakri and Azrar, 2010) and recently extended by (Bakkali, Azar and Fakri, 2011) for N-phase magnetoelectroelastic composite materials. In this paper, the Incremental Self Consistent method (ISCM) is extended to the case of magnetoelectroelastic composites with multi-coated inclusions. The ISCM constructed the effective behavior of composites by replacing a finite increment of the volume fraction of the homogeneities in a certain effective medium, and for each increment the SCM is applied to calculate the effective magnetoelectroelastic properties of the composite materials. The expression of the finite volume fraction to be injected in each step is given by (Bakkali, Azrar and Fakri, 2011):

$$\Delta f_{\mathrm{i}}^{\mathrm{k}} = \frac{\Delta f_k}{1-\sum_{k=1}^{n}(i-1)\Delta f_k} \tag{3.52}$$

in which $\Delta f_k = \frac{f_k}{S}$ is considered as the partial concentration of the considered phase and S is the number of steps. The overall properties of the composites, given by the ICSM, depend on the number of steps and it is written as follow:

$$E_{iJKl}^{eff\,(i)} = E_{iJKl}^{eff\,(i-1)} + \sum_{k=1}^{n} \Delta f_{\mathrm{i}}^{\mathrm{k}} (E_{iJMn}^{k} - E_{iJMn}^{eff\,(i-1)}) A_{MnKl}^{k} \tag{3.53}$$

with $E^{eff\,(0)} = E^{m}$

The ICSM does not affect the expression of the concentration tensors A^k given by the classical Self Consistent method. So, the formulations used in this method and in the classical Self Consistent method are the same. The only difference is in the manner of introducing the volume fraction of the reinforcements.

3.4.3 Mori-Tanaka mean field approach

The Mori-Tanaka mean field approach takes into account the effect of other multi-coated inhomogeneities by considering a finite concentration of a multi-coated inclusion embedded in an infinite matrix. Similarly to the Self Consistent approach, the expression of the effective magnetoelectroelastic composites is given by:

$$E_{iJKl}^{eff} = E_{iJKl}^{m} + \sum_{k=1}^{n} f^{k} (E^{k}{}_{iJMn} - E^{m}{}_{iJMn}) A_{MnKl}^{k} \tag{3.54}$$

where f^k denotes the volume fraction of the considered phase.

The Mori-Tanaka concentration tensors A^k is evaluated from (3.31) by replacing E^0 by E^m and Z^0 by Z^m. Its expression is given as follow:

$$A_{MnKl}^{k} = a_{MnPv}^{k} \left[\sum_{k=1}^{n} \left(\frac{f_k}{f_I} (I_{KlRs} + \frac{f_m}{V_k} T_{iJKl}^{Ik}(E^m) \Delta E_{iJRs}^{(k/m)}) a_{RsPv}^{k} \right) \right]^{-1} \tag{3.55}$$

in which $\Delta E_{iJMn}^{(k/m)} = E_{iJMn}^{k} - E_{iJMn}^{m}$ and $f_m = 1 - f_I$ the volume fraction of the matrix.

3.4.4 Dilute approach

The Dilute approach does not take any kind of interaction between the matrix and the multi-coated inhomogeneities. For multi-coated inclusions, the concentration tensor related to the Dilute approach is given by:

$$A^{k}_{MnKl} = a^{k}_{MnPv}\left[\sum_{k=1}^{n}\left(\frac{f_k}{f_I}\left(I_{KlRs} + \frac{1}{V_k}T^{Ik}_{iJKl}(E^m)\Delta E^{(k/m)}_{iJRs}\right)a^{k}_{RsPv}\right)\right]^{-1} \tag{3.56}$$

in which $\Delta E^{(k/m)}_{iJMn} = E^{k}_{iJMn} - E^{m}_{iJMn}$

The multi-coated concentration tensors, elaborated in this paper for magnetoelectroelastic composites, allow one to numerically predict the effective properties for a wide range of reinforcement types based on the presented micromechanical models. These micromechanical models will be used to predict the effective properties of multifunctional composite materials with multi-coated inclusions of various types and shapes as well as with functionally graded interphases.

3.5 Numerical results

Based on the presented micromechanical models wide varieties of numerical tests can be elaborated. The effective properties of magnetoelectroelastic composites can be predicted for various coating number and types as well as for various inclusion shapes and types. Two types of inclusion problems are considered and investigated in two subsections. In the first one, a four-phase composite consisting of glass inclusions surrounded by void and piezoelectric ($BaTiO_3$) interphase layers embedded in a piezomagnetic matrix ($CoFe_2O_4$). The consideration of a void layer is done in order to take into account the defect that might exist in the interphase and then in the composites. The effective properties obtained for magnetoelectroelastic composite with void are compared to those obtained for magnetoelectroelastic composite without the void layer. This four-phase composite is investigated as an application of multi-coated micromechanical modeling. The topology of a representative element of the four-phase composite is described in figure 3.4. The reinforcements are perfectly aligned and have ellipsoidal shape with the dimensions (a_1, b_1, c_1), (a_2, b_2, c_2) and (a_3, b_3, c_3). The three ellipsoids are coaxial with $\frac{a_1}{a_2} = \gamma_1; \frac{b_1}{b_2} = \gamma_2; \frac{c_1}{c_2} = \gamma_3$ and $\frac{a_2}{a_3} = \beta_1; \frac{b_2}{b_3} = \beta_2; \frac{c_2}{c_3} = \beta_3$. For the considered void coating, the

thickness in directions a_1 and b_1 is taken zeros $(\gamma_1 = 1; \gamma_2 = 1)$. The volume fraction of matrix is f_m and the volume fractions of inclusion and interphases are obtained by $f_1 = (1 - f_m)\gamma\beta$, $f_2 = (1 - f_m)(1 - \gamma)\beta$ and $f_3 = (1 - f_m)(1 - \beta)$ with $\gamma = \gamma_1\gamma_2\gamma_3$ and $\beta = \beta_1\beta_2\beta_3$. The effective properties of magnetoelectroelastic composites without the void layer are obtained by taking $(\gamma_1 = \gamma_2 = \gamma_3 = 1)$. In the second subsection, a functionally graded composite consisting of piezoelectric inclusions, piezomagnetic matrix and the properties of interphases varying continuously between the matrix and inclusion is considered. This composite material is described in the topology section. The parameters (n=2) and (α=1), in the mathematical model (1) describing the variation of the properties in the interphase, are chosen. The magnetoelectroelastic characteristics of the considered phases are listed in Table 3.1.

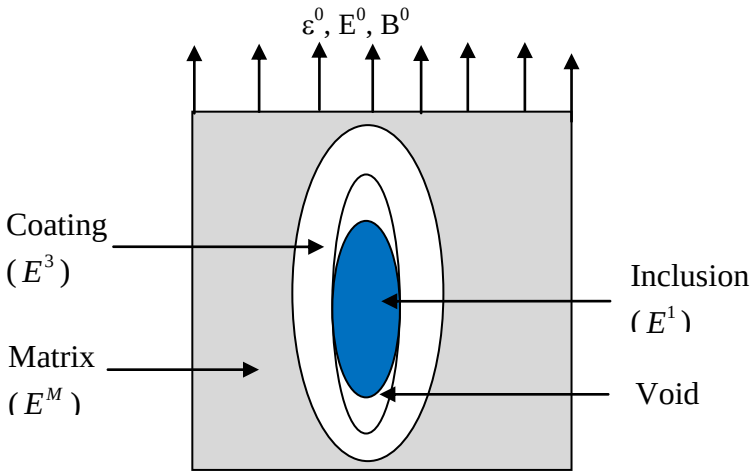

Figure 3.4: A representative volume element of a four-phase composite. The dimension of the reinforcement and interphases are (a_1, b_1, c_1), (a_2, b_2, c_2) and (a_3, b_3, c_3) respectively.

Table 3.1: Material properties

	C_{11}	C_{12}	C_{13}	C_{33}	C_{44}	e_{15}	e_{31}	e_{33}
$BaTiO_3$	166	77	78	162	43	11.5	-4.4	18.6
$CoFe_2O_4$	286	173	170	269.5	45.3	0	0	0
PZT-5H	126	55	53	117	35.3	17	-6.5	23.3
Glass	88.8	29.6	29.6	88.8	29.6	0	0	0

	κ_{11}	κ_{33}	h_{15}	h_{31}	h_{33}	μ_{11}	μ_{33}
$BaTiO_3$	11.2×10^{-9}	12.6×10^{-9}	0	0	0	5×10^{-6}	10×10^{-6}
$CoFe_2O_4$	0.08×10^{-9}	0.093×10^{-9}	550	580.3	699.7	-590×10^{-6}	157×10^{-6}
PZT-5H	15.1×10^{-9}	13.0×10^{-9}	0	0	0	5×10^{-6}	5×10^{-6}
Glass	0.056×10^{-9}	0.056×10^{-9}	0	0	0	1×10^{-6}	1×10^{-6}

Units: elastic constant GPa; dielectric constants C^2/Nm^2; magnetic constants Ns^2/C^2, piezoelectric constants C/m2; piezomagnetic constants N/Am; magnetoelectric coefficients Ns/VC.

3.5.1 Four-phase magnetoelectroelastic composites

In this subsection, magnetoelectroelastic composites with and without void interphase layers are investigated. The effective properties are predicted for different thicknesses and shapes of the void interphase layer.

In Figures 3.5, the magnetoelectric modulus $-\alpha_{33}$ is predicted for fibrous magnetoelectroelastic composites with and without void interphase layer, using the Mori-Tanaka, Self Consistent and Incremental Self Consistent micromechanical models with respect to the volume fraction of the multi-coated inclusion $(1-f_m = f_1 + f_2 + f_3)$. It can be seen that the presence of void interphase influences strongly the effective properties. Also, it is shown that the effective modulus $-\alpha_{33}$ decreases when the thickness of the void layer increases. Also, it is seen that the Self Consistent model diverges and can predict results only for very small volume fractions of the multi-inclusions. However, the Incremental Self Consistent model improves the prediction of the classical Self Consistent and gives almost the same results as the Mori-Tanaka model.

In Figure 3.6a, the effective piezoelectric modulus e_{33} is presented for fibrous magnetoelectroelastic composites with different thicknesses of the void layer using Mori-

Tanaka, Self Consistent and Incremental Self Consistent micromechanical models with respect to the volume fraction of the multi-coated inclusion. It is seen that the effective modulus e_{33} increases with respect to the total multi-inclusion volume fraction and increases when the thickness of the void layer increases. Again, it is shown that the Self Consistent approach diverges at high volume fraction of the multi-coated inclusion and the Incremental Self Consistent conducts far the prediction and gives the same results as the Mori-Tanaka approach.

In Figure 3.6b, the effective piezoelectric moduli e_{33} is presented for magnetoelectroelastic composites with fixed thicknesses of interphase layers and different shape of inclusions (spheroidal inclusions ($a_1=b_1=c_1=1$), ellipsoidal inclusions ($a_1=b_1=1$; $c_1=10$), fibrous inclusions ($a_1=b_1=1$; $c_1=10$) and laminated inclusions ($a_1=b_1=1000$; $c_1=1$)) by using the Mori-Tanaka micromechanical model. The effect of the shape on e_{33} is shown. It is seen that the shape of inclusion affects significantly the effective piezoelectric moduli e_{33}.

In Figure 3.7a, the effective magnetoelectric modulus α_{11} is predicted for laminated magnetoelectroelastic composites with different thicknesses of the void interphase layer with respect to the volume fraction of the multi-coated inclusion. The effective modulus α_{11} slowly decreases with respect to the thickness of the void layer. It is also seen that for α_{11} with the thickness of the void layer $(\gamma_1=\gamma_2=1;\ \gamma_3=0.8)$, the Self Consistent, Incremental Self Consistent and Mori-Tanaka models predict almost the same results. However, when the thickness of the void layer increases, the Self Consistent approach diverges and leads for erroneous results for high volume fraction of the multi-coated inclusion.

In Figure 3.7b, the effective magnetoelectric moduli α_{11} is presented for magnetoelectroelastic composites with fixed thicknesses of interphase layers and different shape of inclusions by using the Mori-Tanaka micromechanical model. The effect of the shape on α_{11} is shown. It is seen that the shape of inclusion affects significantly the effective magnetoelectric moduli α_{11}. It is also seen that α_{11} is maximized for laminated composites which is explained by the fact that in laminated composites the interaction is more prominent in x_1 direction.

The prediction of the effective elastic modulus c_{11} for ellipsoidal magnetoelectroelastic composites with different thicknesses of the void interphase layer is given in figure 3.8. It seen that the presence of the void layer affects the elastic modulus c_{11}. The elastic modulus decreases with respect to the thickness of the void layer as well as with the volume fraction of the multi-

coated inclusion. Again the divergence of the Self Consistent model is observed as well as the erroneous prediction of the considered Dilute approach for large volume fractions.

Three dimension numerical results, for fibrous magnetoelectroelastic composites, predicted by Mori-Tanaka model, are presented in figure 3.9. The evolution of the magnetoelectric modulus -α_{33} with respect to the thickness of the void interphase layer and to the volume fraction of the composite inclusion is presented. It is clearly seen that α_{33} is strongly affected by the thickness of the void interphase layer as well as by the composite inclusions volume fraction. α_{33} can be maximized or minimized with respect to these values. Its maximum is reached when the void interphase layer disappears (γ_3=1) and fm=0.6 and minimized when the inclusion disappears and the void interphase layer takes its place and fm=0.7.

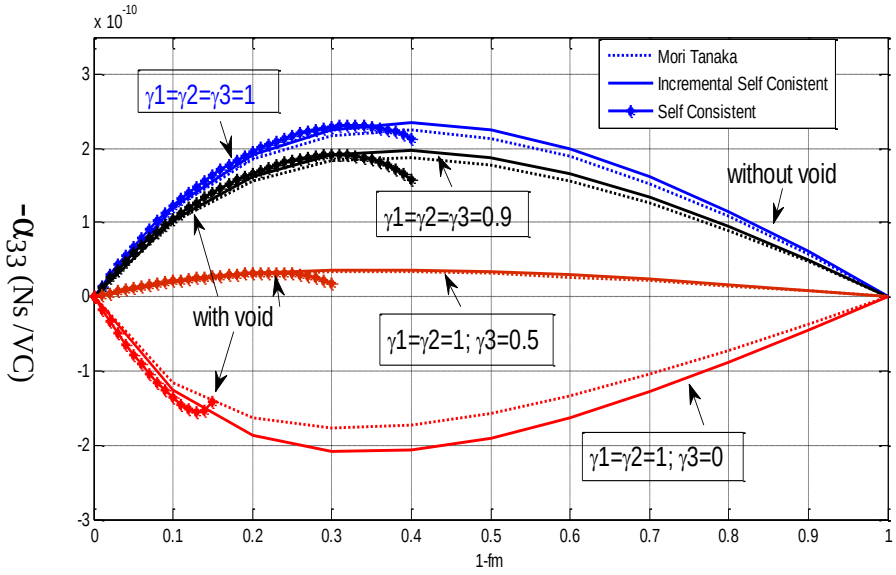

Volume fraction of the multi-coated inclusion

Figure 3.5: Effective magnetoelectric modulus -α_{33} of fibrous magnetoelectroelastic composites (a_1=b_1=1; c_1=1000) consisting of Glass inclusions surrounded by a piezoelectric ($BaTiO_3$) coating and with or without void interphase layer embedded in a piezomagnetic matrix ($CoFe_2O_4$); β_1= β_2= β_3=0.95.

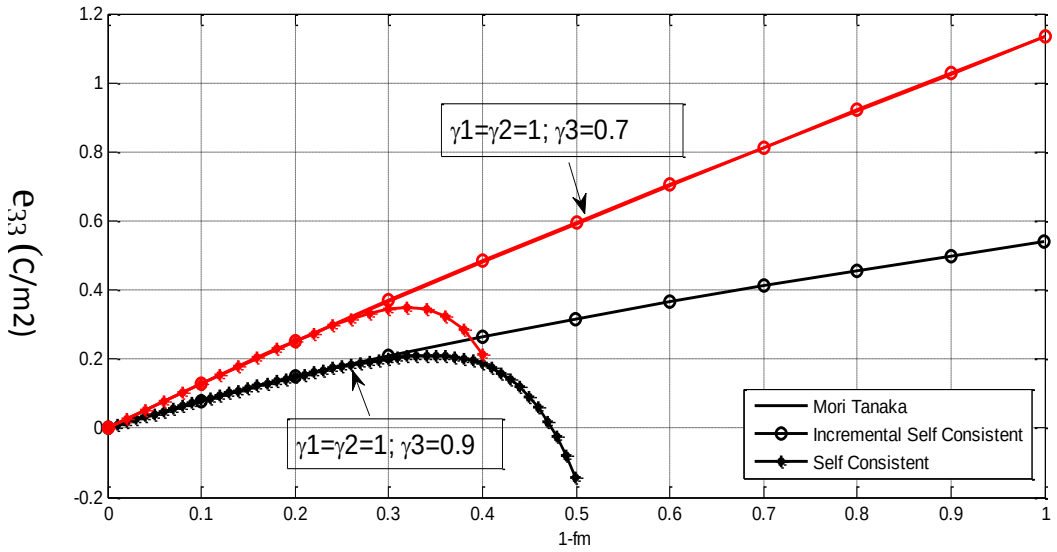

Volume fraction of the multi-coated inclusion

Figure 3.6a: Effective piezoelectric modulus e_{33} of fibrous magnetoelectroelastic composites consisting of Glass inclusions surrounded by Void and piezoelectric ($BaTiO_3$) coatings embedded in a piezomagnetic matrix ($CoFe_2O_4$); $\beta_1= \beta_2= \beta_3=0.95$.

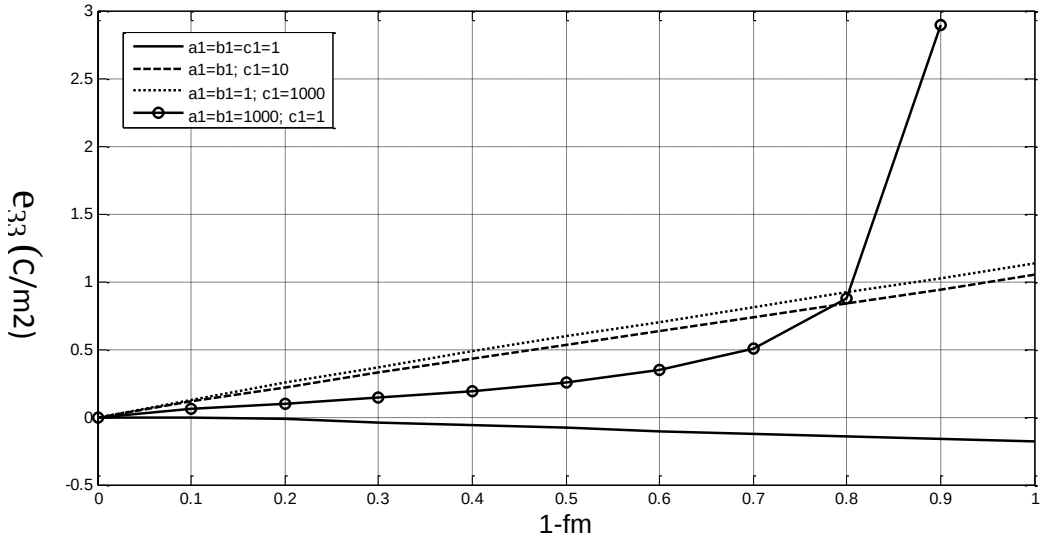

Volume fraction of the multi-coated inclusion

Figure 3.6b: Effective piezoelectric modulus e_{33} of magnetoelectroelastic composites consisting of Glass inclusions surrounded by Void and piezoelectric ($BaTiO_3$) coatings embedded in a piezomagnetic matrix ($CoFe_2O_4$); $\beta_1= \beta_2= \beta_3=0.95$; $\gamma_1 = \gamma_2 = 1$; $\gamma_3 = 0.7$.

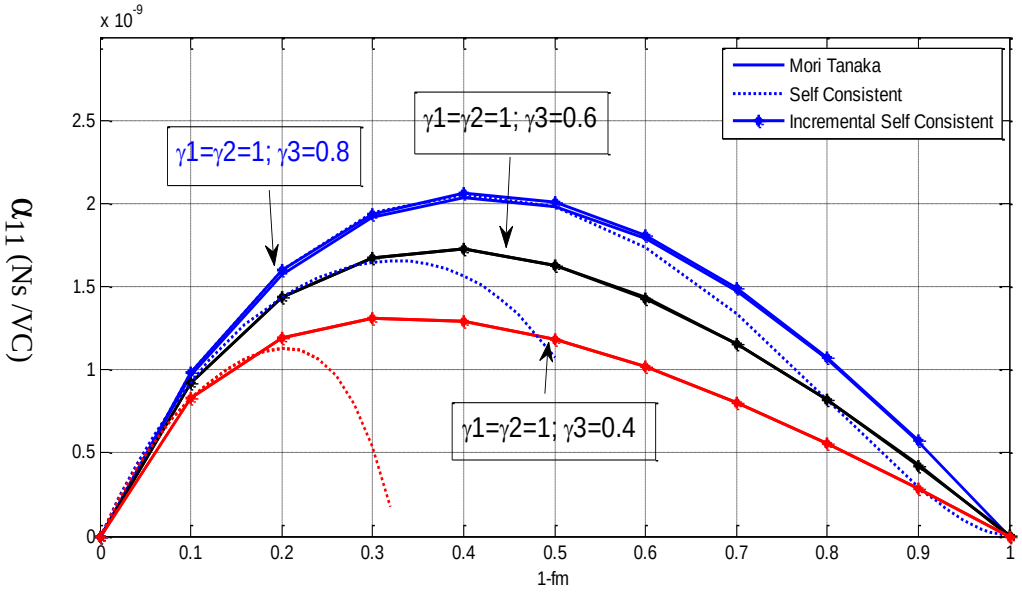

Figure 3.7a: Effective magnetoelectric modulus α_{11} of laminated magnetoelectroelastic composites ($a_1=b_1=1000$; $c_1=1$) consisting of Glass inclusions surrounded by void and piezoelectric ($BaTiO_3$) coatings embedded in a piezomagnetic ($CoFe_2O_4$) matrix; $\beta_1= \beta_2= \beta_3=0.95$.

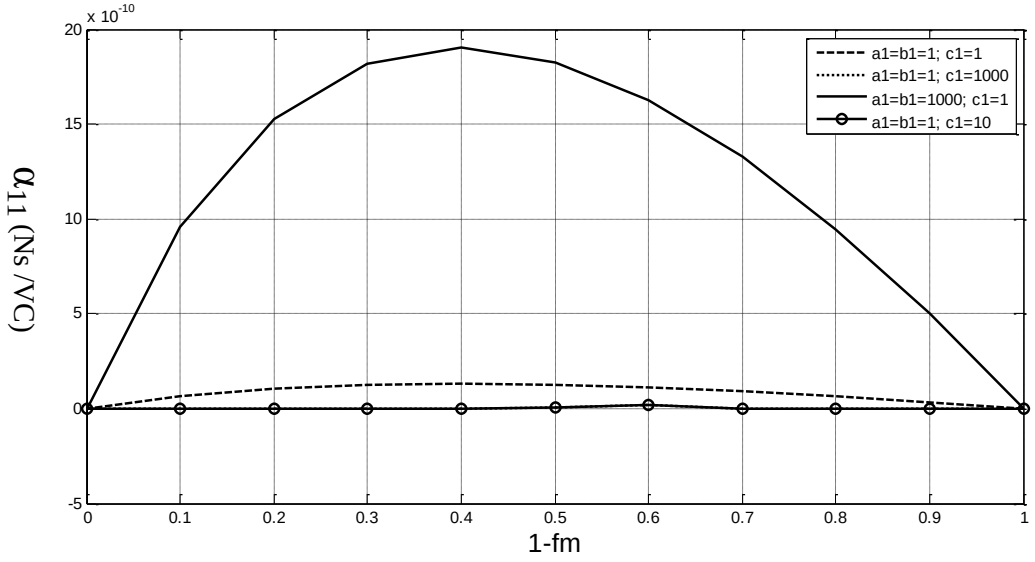

Figure 3.7b: Effective magnetoelectric modulus α_{11} of magnetoelectroelastic composites consisting of Glass inclusions surrounded by Void and piezoelectric ($BaTiO_3$) coatings embedded in a piezomagnetic matrix ($CoFe_2O_4$); $\beta_1= \beta_2= \beta_3=0.95$; $\gamma_1 = \gamma_2 = 1$; $\gamma_3 = 0.7$.

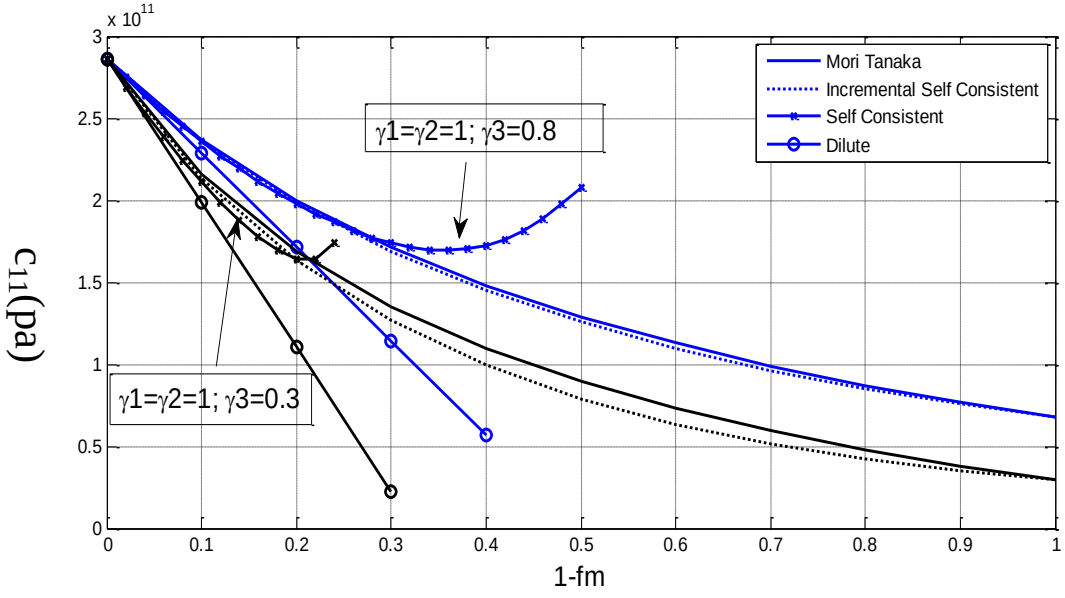

Figure 3.8: Effective elastic modulus c_{11} of ellipsoidal magnetoelectroelastic composites (a1=b1=1; c1=10) consisting of Glass inclusions surrounded by void and piezoelectric ($BaTiO_3$) coatings embedded in piezomagnetic ($CoFe_2O_4$) matrix; $\beta_1= \beta_2= \beta_3=0.95$.

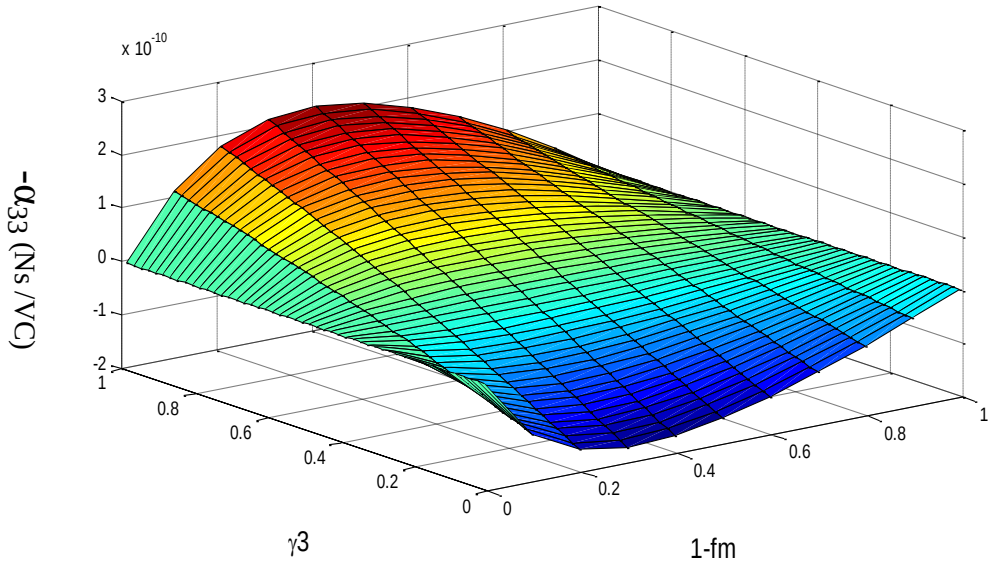

Figure 3.9: Effective magnetoelectric modulus $-\alpha_{33}$ of fibrous magnetoelectroelastic composites consisting of Glass inclusions surrounded by void and piezoelectric ($BaTiO_3$) coatings embedded in a piezomagnetic ($CoFe_2O_4$) matrix.

3.5.2 Functionally graded magnetoelectroelastic composite

In this subsection, functionally graded interphase will be considered. Based on the relationship (3.1), various graded model parameters and thickness of the interphase can be easily considered. The case n=2 and α=1 is considered in this analysis.

The magnetoelectric coefficient α_{33} is predicted, for magnetoelectroelastic fibrous composites consisting of piezomagnetic matrix $CoFe_2O_4$ and piezoelectric inclusions $BaTiO_3$ with functionally graded interphase using the Mori-Tanaka model with respect to the volume fraction of the coated inclusion and the thickness of the interphase (1-γ) is presented in figure 3.10. The thickness of the interphase (1-γ) effects on α_{33} is clearly shown and this coefficient is optimized around 1-fm=0.4. Also, it is seen that without the interphase (γ=1) the same results predicted by Zhang and Soh (2005) and Bakkali et al. (2011) for two phases magnetoelectroelastic composites are obtained. The evolution of the effective modulus α_{33} starts with the effective properties of the piezomagnetic matrix $CoFe_2O_4$ and finishes with the effective properties of the piezoelectric inclusion surrounded by the functionally graded interphase layer.

In Figures 3.11 and 3.12, the evolution of the effective modulus α_{33} with respect to the interphase thickness (1-γ) is predicted for laminated and ellipsoidal composites, with fixed volume fraction of the matrix f_m=0.6, consisting of piezomagnetic matrix $CoFe_2O_4$, piezoelectric inclusion $BaTiO_3$ and functionally graded interphase. The prediction of α_{33} is done using the presented Self Consistent, Incremental Self Consistent, Mori-Tanka and Dilute micromechanical models. The evolution is bounded between two limiting cases. The first one is γ=0 which corresponds to the case where the interphase becomes the inclusion and the second one when γ=1 (r=1) in which the interphase disappears. It is shown that α_{33} varies significantly with respect to γ. α_{33} increases with γ because with matrix volume fraction fixed increasing γ means increasing the inclusion volume fraction. As the volume fraction of the inclusion increases the interaction between the matrix and the inclusion becomes more significant which increases the effective modulus α_{33}. For fibrous inclusion and interphase the evolution of the effective modulus α_{33} with respect to the interphase thickness (1-γ), with fixed volume fraction of the matrix (f_m=0.6; 0.2), consisting of piezomagnetic matrix $CoFe_2O_4$, piezoelectric inclusions $BaTiO_3$ and functionally graded interphases is presented in figure 3.13. It is shown that in this case the Self Consistent, Incremental Self Consistent predict the same results and α_{33} increases with γ.

In Figure 3.14, the coefficient α_{11} is presented, for magnetoelectroelastic fibrous composites with fixed coating thickness γ=0.93 consisting of piezomagnetic matrix $CoFe_2O_4$ and piezoelectric inclusions $BaTiO_3$ with functionally graded interphase as function of the volume fraction of the coated inclusions. The divergence of the Self Consistent and Dilute is again observed. However, the Incremental Self Consistent improves the prediction of the classical Self Consistent model and gives almost the same results than the Mori-Tanaka model. This coefficient can be optimized with respect to γ and 1-fm.

In figure 3.15, three dimension numerical results are presented for magnetoelectroelastic fibrous composites based on the Mori-Tanaka model. The evolution of magnetoelectric modulus α_{33} with respect to the thickness of the interphase and to the volume fraction of the composites inclusion is presented. It is seen that α_{33} varies significantly with the interphase thickness (1-γ) and the volume faction of the composites inclusion (1-fm) and this coefficient can be optimized with respect to γ and fm.

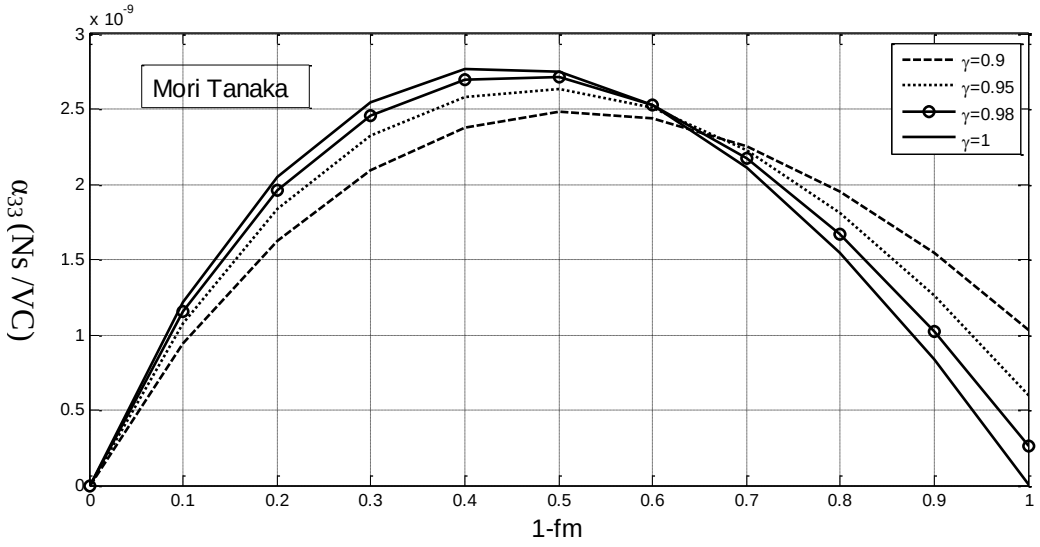

Volume fraction of the coated inclusion

Figure 3.10: Effective magnetoelectric modulus α_{33}, of magnetoelectroelastic fibrous composites consisting of piezomagnetic matrix $CoFe_2O_4$ and piezoelectric inclusions $BaTiO_3$ with functionally graded interphase, with respect to volume fraction of the coated inclusion and the thickness of the interphases; (n=2, α=1).

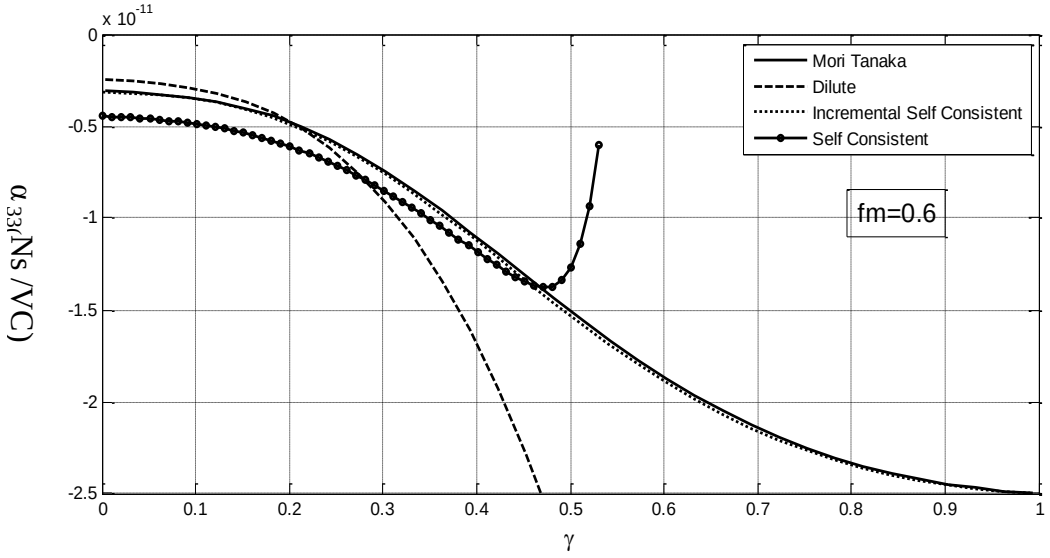

Figure 3.11: Effective magnetoelectric modulus α_{33}, of magnetoelectroelastic laminated composites with fixed volume fraction of the matrix (f_m=0.6) consisting of piezomagnetic matrix $CoFe_2O_4$ and piezoelectric inclusions $BaTiO_3$ with functionally graded interphases, predicted by Mori-Tanaka, Self Consistent, incremental Self Consistent and Dilute models, as a function of the normalized coating thickness (1- γ); (n=2, α=1).

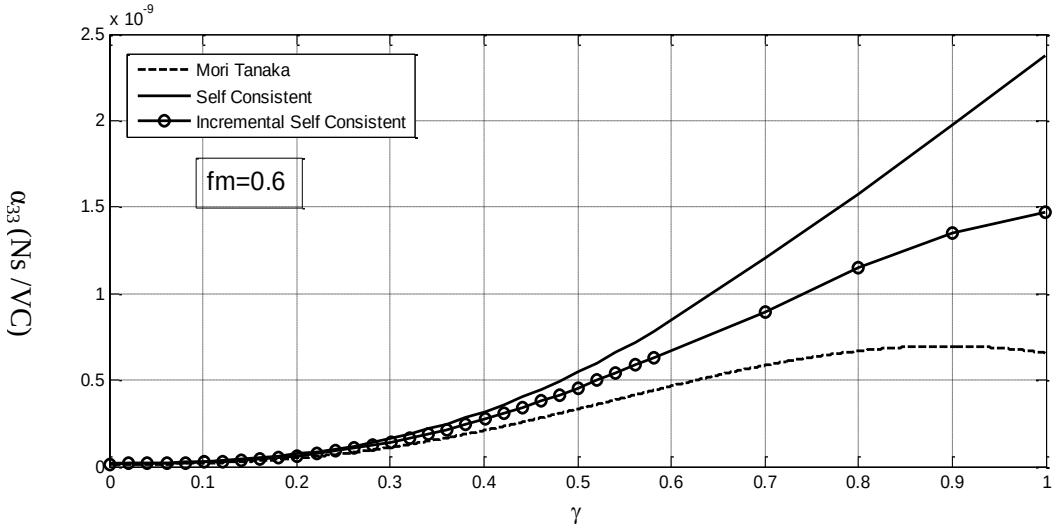

Figure 3.12: Effective magnetoelectric modulus α_{33}, of magnetoelectroelastic ellipsoidal composites with fixed volume fraction of the matrix (f_m=0.6) consisting of piezomagnetic matrix $CoFe_2O_4$ and piezoelectric inclusions $BaTiO_3$ with functionally graded interphases, predicted by Mori-Tanaka, Self Consistent and Incremental Self Consistent models, as a function of the normalized coating thickness (1- γ).

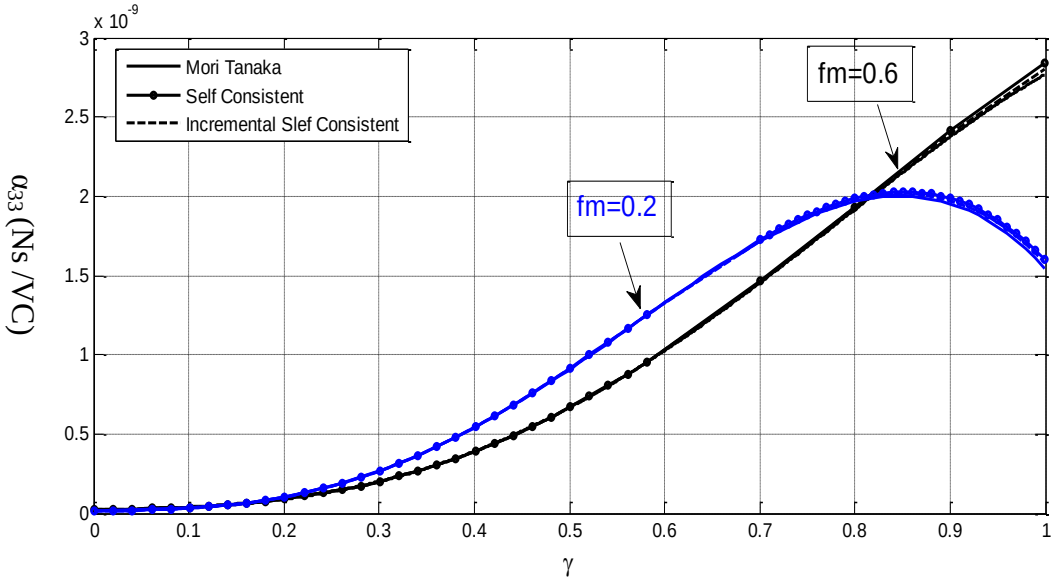

Figure 3.13: Effective magnetoelectric modulus α_{33}, of magnetoelectroelastic fibrous composites with fixed volume fraction of the matrix (f_m=0.6; 0.2) consisting of piezomagnetic matrix $CoFe_2O_4$ and piezoelectric inclusions $BaTiO_3$ with functionally graded interphases, predicted by Mori-Tanaka, Self Consistent and Incremental Self Consistent models, as a function of the normalized coating thickness (1- γ).

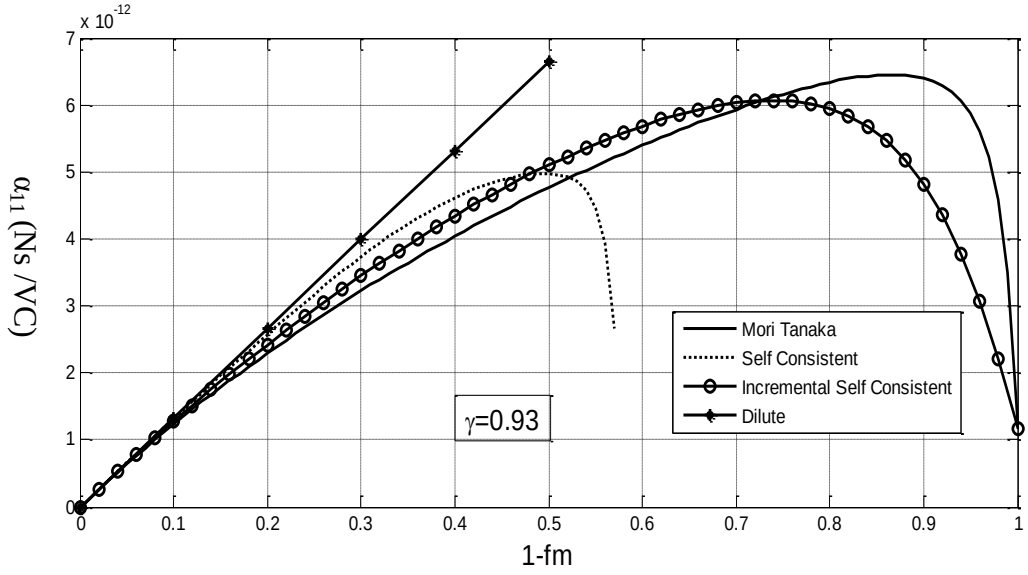

Figure 3.14: Effective magnetoelectric modulus α_{11}, of magnetoelectroelastic fibrous composites consisting of piezomagnetic matrix $CoFe_2O_4$ and piezoelectric inclusions $BaTiO_3$ with functionally graded interphases of thickness γ=0.93, predicted by Mori-Tanaka, Self Consistent, incremental Self Consistent and Dilute models, as a function of the volume fraction of the coated inclusion; (n=2, α=1).

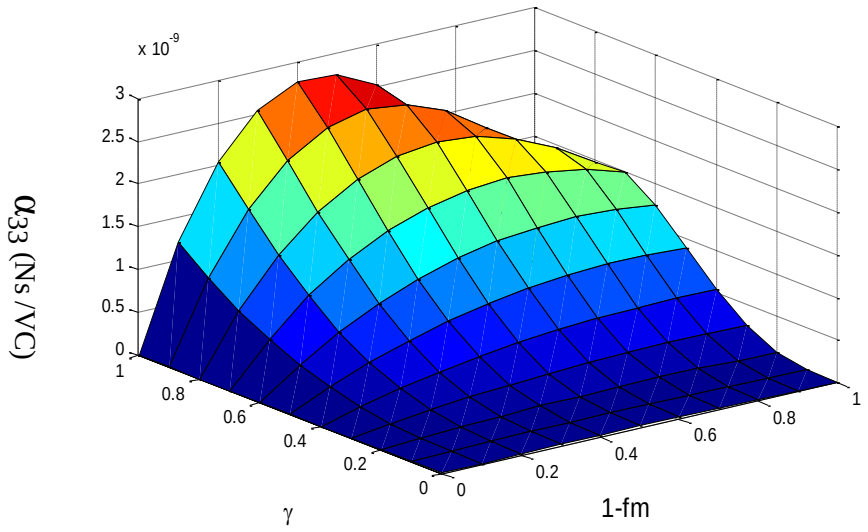

Figure 3.15: Effective magnetoelectric modulus α_{33}, of magnetoelectroelastic fibrous composites consisting of piezomagnetic matrix $CoFe_2O_4$ and piezoelectric inclusions $BaTiO_3$ with functionally graded interphase, with respect to volume fraction of the coated inclusion (inclusion+interphase) and the thickness of the interphases; (n=2, α=1).

3.6 Conclusions

Various micromechanical models with multi-coated inclusions and functionally graded interphases of magnetoelectroelastic composites are elaborated. Numerical predictions of the effective properties of magnetoelectroelastic composites with multi-coated reinforcements and functionally graded interphases are presented based on Self Consistent, Incremental Self Consistent, Mori-Tanaka and Dilute models. Mathematical formulations are given in the general case of anisotropic materials and ellipsoidal inclusions with nonhomothetic coatings. Effective properties are presented in terms of the volume fraction and shape of the coated inclusions as well as of the thickness of the coating. Two kinds of magnetoelectroelastic composite materials are analyzed. The effective properties of magnetoelectroelastic composite consisting of Glass inclusions surrounded by void and piezoelectric ($BaTiO_3$) interphase layer embedded in piezomagnetic matrix ($CoFe_2O_4$) are predicted and then compared to the effective properties of the same composite without void phase. Secondly, the effective properties of magnetoelectroelastic composite consisting of piezoelectric inclusions ($BaTiO_3$), piezomagnetic matrix ($CoFe_2O_4$) where the properties of interphases vary continuously between the matrix and

inclusions are predicted. The effective properties are presented with respect to the volume fraction, shape, thickness and the functionally graded interphase parameters. It is shown that the presence of the void interphase layer influences strongly the effective properties which are well predicted by Mori-Tanaka and Incremental Self Consistent models. The interphase thickness and shape have also strong effects on the effective properties of the multi-functional composites. The multi-coating and functionally graded interphase concepts can be used to optimize the coupling multi-functional effective properties. This is of big interest to design new multi-functional materials with higher coupling coefficients.

3.7 Perspectives

So far, the studied composite materials are considered to have time independent properties. Piezoelectric and magnetoelectroelastic composites with polymer matrix show significant time dependent properties and particularly at high elevated temperature. This kind of composites, besides of their actuation and sensing effect, show a damping effect that could be useful in many industrial applications. In chapter 4, micromechanical modelings will be developed to predict the viscopiezoelectric behavior of piezoelectric heterogeneous materials. Two kinds of composites are going to be investigated: two-phase viscoelectroelastic composites and multi-coated viscoelectroelastic composites. The modeling well be based on the correspondence principle of linear viscoelectroelasticity combined with Mori-Tanaka micromechanical model. The use of the Carson transformation will allow the extension of the micromechanical model to the Carson domain. . The conversion from the Carson domain to the time domain of the effective properties is going to be made numerically by using the inverse of the Laplace transform.

References

[1]Bakkali, A., Azrar, L. and Fakri, N. 2011. "Modeling of effective properties of multiphase magnetoelectroelastic heterogeneous materials," Journal Computers, Materials & Continua, 23: 201-231.

[2]Berbenni, S. and Cherkaoui, M. 2010. "Homogenization of multicoated inclusion-reinforced linear elastic composites with eigenstrains," Philosophical Magazine, 90: 3003-3026.

[3]Cherkaoui, M., Sabar, H. and Berveiller, M. 1994. "Micromechanical approach of the coated inclusion problem and applications to composites materials," J. Eng. Mater. Technol., 116: 247-278.

[4]Cherkaoui, M., Sabar, H. and Berveiller, M. 1995. "Elastic composites with coated reinforcement: A micromechanical approach for nonhomothetic topology" Int. J. Engng Sci., 33: 829-843, No. 6.

[5]Cherkaoui, M., Sabar, H., and Berveiller, M. 1996. "Elastic behavior of composites with coated inclusions: micromechanical approach and applications," Compos. Sci. Technol., 56: 877-882.

[6]Dinzart, F. and Sabar, H. 2009. "Electroelastic behavior of piezoelectric composites with coated reinforcements: Micromechanical approach and applications," International Journal of Solids and Structures, 46: 3556–3564.

[7]Fakri, N., Azrar, L.and El Bakkali, L. 2003. "Electoelastic behavior modeling of piezoelectric composite materials containing spatially oriented reinforcements," International Journal of Solids and Structures, 40: 361-384, Issue 2.

[8]Fakri, N. and Azrar, L. 2010. "Thermal and electro-elastic behaviour of piezo-composites and inhomogeneous piezoelectric materials with voids," Journal of Intelligent Materials Systems and Structures, 21:161-174, N°2.

[9]Gururaja, T. R., Walter, A., Schulze, Cross, L. E. and Newnham, R. E. 1985 "Piezoelectric composite materials for ultrasonic transducer applications. Part II: Evaluation of Ultrasonic Medical Applications," IEEE Transactions on Sonics and Ultrasonics, Vol. SU-32: 499-513, N°4.

[10]Hill, R. 1983. "Interfacial operators in the mechanics of composite media," J. Mech. Phys. Solids, 31: 347.

[11]Hori, M. and Nemat-Nasser, S. 1994. “Double-inclusion model and overall moduli of multi-phase composites,” Journal of Engineering Materials and Technology, 116: 305-309.

[12]Koutsawa, Y., Biscani, F., Belouettar, S., Belouettar, H. and Carrera, E. 2010. “ Multi-coating inhomogeneities approach for the effective thermo-electro-elastic properties of piezoelectric composite materials,” Composite structures, 92: 964–972.

[13]Konka, H. P., Wahab, M. A. and Lian, K. 2012. “The effects of embedded piezoelectric fiber composite sensors on the structural integrity of glass-fiber–epoxy composite laminate," Smart Materials and Structures, 21 (015016).

[14]Li, J.Y. 2000a. “Magnetoelectroelastic multi-inclusion and inhomogeneity problems and their applications in composite materials,’’ Int. J. of Engineering Science, 38: 1993-2011.

[15]Li, J.Y. 2000b. “Thermoelastic behavior of composites with functionally graded interphase: a multi-inclusion model,”International Journal of solid and structures, 37: 5579-5597.

[16]Nemmat-Nasser, S. and Hori, M. 1993. “Micromechanics: Overall properties of the heterogeneous materials,” Elsiever, New York.

[17]Vieville, P., Bonnet, A. S. and Lipinski, P. 2006. “Modeling effective properties of composite materials using the inclusion concept. General considerations,” Arch. Mech., 58: 207–239.

[18]Wacker, G., Bledzki, A. K. and Chate, A., 1998. "Effect of interphase on the transverse young's modulus of glass/epoxy composites," Composites, 29A, pp. 619-626.

[19]Zhang, Z.K. and Soh, A.K. 2005, “Micromechanics predictions of the effective moduli of magnetoelectroelastic composite materials,” European. J. of Mechanics A/Solids, 24: 1054-1067.

Chapter 4

4. Viscoelectroelastic effective properties of heterogeneous and multi-coated piezoelectric materials

Abstract

In this paper, the effective behavior of viscoelectroelastic composites is investigated. By using the correspondence principle of linear viscoelectroelasticity, the Mori-Tanaka micromechanical mean field approach is extended to the Carson domain. Based on the integral equation and on viscoelectroelastic interfacial operators the concentration tensors for viscoelectroelastic composites are derived. The effective properties are derived in the Carson domain and then inverted numerically to the time domain by using the inverse of the Laplace transform. The effective properties are presented in frequency and time domain. The effect of shape and volume fraction of reinforcements as well as the thickness of the coating is shown on the effective properties.

4.1 Introduction

The effective behavior of piezoelectric composites has been investigated by many researchers due to their applications in many industrial fields such as aerospace, aeronautics and automobiles etc. through sensors and actuators. Piezoelectric composites with polymer matrix show a significant time dependent properties and particularly at elevated temperature. This kind of composites, besides of their actuation and sensing effect, shows a damping effect that could be useful in many industrial applications. The investigation of the effective properties of viscoelastic composites has been done by many researchers. Brinson and Lin (1998) examined the use of different micromechanics method for the determination of the effective composite properties when all the phases are viscoelastic. Fisher and Brinson (2001) predicted the effective properties of a three-phase viscoelastic composite using the original Mori-Tanaka micromechanical model and the extended one that takes the interphase regions between the matrix and fibers. The obtained results are compared to the ones obtained by finite element analysis. Haberman et al. (2002) used the Self Consistent micromechanical model to predict the effective properties of viscoelastic composites consisting of spherical coated inclusion. Matzenmiller and Gerlach (2004) used the micromechanical method of cells to investigate the effective properties of viscoelastic composites. The micromechanical model equations was established and solved based on two approaches: the first one based on the Laplace-transformation of the time-dependent material functions and the application of the correspondence principle of linear viscoelasticity to the governing equations of the micromechanical model. In the second approach a numerical time integration scheme is developed to compute the convolution integrals. Fei et al. (2004) investigated the influence of the gradual interphase on the effective elastic and viscoelastic properties of particulate composites. Levesque et al. (2004) developed a theoretical model to predict the nonlinear behavior of viscoelastic composites where the matrix is nonlinear viscoelastic.

The electromechanical behavior of piezoelectric composites has been investigated in several works. Dunn and Taya (1993) predicted the effective properties based on different micromechanical models. Fakri et al. (2003, 2010) predicted the piezoelectric and the thermal-piezoelectric behavior of composite materials and presented the numerical results for the effective properties in term of phase properties, orientation angles, volume fraction and shapes of inclusions. Odegard (2004) proposed a new modeling approach to predict the bulk

electromechanical properties of piezoelectric composites and compared the obtained results with those obtained by the Mori-Tanaka approach and the finite element method. Li (2004) applied the Self Consistent approach to predict the effective pyroelectric and thermal expansion coefficients of ferroelectric ceramics taking into account the texture change due to domain switching during poling. Our interest in this work is to investigate the coupled effective behavior of viscoelectroelastic composites. Only restricted works have been done on this area. Jiang and Batra (2001) investigate the effective properties of viscoelectroelastic composites based of the Mori-Tanaka mean field micromechanical. Closed form expressions of the effective moduli were given for viscoelectroelastic composites consisting of parallel PZT cylinder of elliptic cross section embedded in a viscoelastic matrix. Aldelrahem et al. (2007) proposed an analytical model to investigate viscoelastic properties of hybrid composites with shunted piezoelectric particles. Muliana and Li (2010) developed a micromechanical modeling and a finite element model to investigate the effective time dependent properties of piezoelectric composites consisting of PZT fiber and a polymer matrix.

In this paper, a micromechanical modeling is developed to predict the time and frequency dependent effective properties of viscoelectroelastic composites. Two kinds of composites are investigated: two-phase viscoelectroelastic composites and multi-coated viscoelectroelastic composites. The modeling is based on the correspondence principle of linear viscoelectroelasticity combined with Mori-Tanaka micromechanical model. The use of the Carson transformation allows the extension of the micromechanical model to the Carson domain. To derive the effective properties we have gone through two steps: the derivation of the concentration tensor step which is based on the solution of the integral equation for two-phase viscoelectroelastic composites and on the solution of the integral equation that takes into account the multi-coating effects and viscoelectroelastic interfacial operators for multi-coated viscoelectroelastic composites, the homogenization step which is based on averaging techniques to investigate the macroscopic behavior of the composites. The conversion from the Carson domain to the time domain of the effective properties is made numerically by using the inverse of the Laplace transform. Parametrical studies are done by presenting the effective properties in term of shape, volume fraction of the reinforcements and thickness of the coating.

4.2 Constitutive equations for linear electroviscoelastic materials

For linear homogeneous piezoelectric materials, the constitutive equations that relate the electric and elastic fields are given by:

$$\begin{aligned} \sigma_{ij} &= c_{ijkl}\varepsilon_{kl} - e_{lij}E_l \\ D_i &= e_{ikl}\varepsilon_{kl} + \kappa_{il}E_l \end{aligned} \tag{4.1}$$

where σ, ε, E, and D are the stress tensor, strain tensor, electric filed and the electric displacement vector, respectively. c, e and κ are the elastic stiffness tensor, piezoelectric tensor and the dielectric tensor, respectively.

Using the condensed notation (Fakri et al. 2003) [9] the variable field takes the following form:

$$Z_{Mn} = \begin{cases} \varepsilon_{mn} & (M = 1,2,3) \\ -E_n & (M = 4) \end{cases} \qquad \sum_{iJ} = \begin{cases} \sigma_{ij} & (J = 1,2,3) \\ D_i & (J = 4) \end{cases} \tag{4.2}$$

The above equations were used for linear independent time properties of homogeneous piezoelectric materials. This work deals with the viscoelectroelastic behavior of polymer piezoelectric composites. This kind of composites shows time dependent properties. One of the most widely used models for viscoelasticity in materials is the Baltzman convolution low. The time dependent constitutive model of piezoelectric homogeneous material is obtained by generalizing the Blotzmann principle for linear viscoelastic materials, one can write:

$$\begin{aligned} \sigma_{ij}(t) &= \int_0^t c_{ijkl}(t-\tau)\frac{d\varepsilon_{kl}(\tau)}{d\tau}d\tau + \int_0^t e_{lij}(t-\tau)\frac{dE_l(\tau)}{d\tau}d\tau \\ D_i(t) &= \int_0^t e_{ikl}(t-\tau)\frac{d\varepsilon_{kl}(\tau)}{d\tau}d\tau + \int_0^t \kappa_{il}(t-\tau)\frac{dE_l(\tau)}{d\tau}d\tau \end{aligned} \tag{4.3}$$

Where c, e and κ are the associated relaxation tensors.

Using the condensed notation the time dependent constitutive model takes the following form:

$$\Sigma_{iJ}(t) = \int_0^t E_{iJKl}(t-\tau)\frac{dZ_{Kl}(\tau)}{d\tau}d\tau \tag{4.4}$$

where $E_{iJKl}(t) = \begin{cases} c_{ijkl}(t) & (J,K = 1,2,3) \\ e_{lij}(t) & (J = 1,2,3; K = 4) \\ e_{ikl}(t) & (J = 4; K = 1,2,3) \\ -\kappa_{il}(t) & (J = 4; K = 4) \end{cases}$

is the time dependent viscoelectroelastic relaxation tensor, Σ and Z are the generalized stress and strain respectively.

The convolution integral (4) gives a mathematical equation that relates the generalized stress Σ to the generalized strain Z through the viscoelectroelastic generalized relaxation tensor $E(t)$.

The constitutive equation (3) is given in the time domain. To convert its form the time domain to the frequency domain the following harmonic deformation and electrical field are considered:

$$\varepsilon_{mn}(t) = \bar{\varepsilon}_{mn}(\omega)e^{i\omega t}; \quad E_m(t) = \bar{E}_m(\omega)e^{i\omega t} \tag{4.5}$$

Replacing (4.5) into (4.3) and using the following changing variable, $u = t - \tau$, one can find

$$\begin{aligned} \sigma_{ij}(t) &= \bar{\varepsilon}_{kl}(\omega)i\omega e^{i\omega t}\int_0^t c_{ijkl}(u)e^{-i\omega u}du + \bar{E}_l(\omega)i\omega e^{i\omega t}\int_0^t e_{lij}(u)e^{-i\omega u}du \\ D_i(t) &= \bar{\varepsilon}_{kl}(\omega)i\omega e^{i\omega t}\int_0^t e_{ikl}(u)e^{-i\omega u}du + \bar{E}_l(\omega)i\omega e^{i\omega t}\int_0^t \kappa_{il}(u)e^{-i\omega u}du \end{aligned} \tag{4.6}$$

Considering $\sigma_{ij}(t) = \bar{\sigma}_{ij}(\omega)e^{i\omega t}; \quad D_i(t) = \bar{D}_i(\omega)e^{i\omega t}$ and using (4.6), the following frequency integral equations are obtained:

$$\begin{aligned} \bar{\sigma}_{ij}(\omega) &= i\omega\int_0^t c_{ijkl}(u)e^{-i\omega u}du\,\bar{\varepsilon}_{kl}(\omega) + i\omega\int_0^t e_{lij}(u)e^{-i\omega u}du\,\bar{E}_l(\omega) \\ \bar{D}_i(\omega) &= i\omega\int_0^t e_{ikl}(u)e^{-i\omega u}du\,\bar{\varepsilon}_{kl}(\omega) + i\omega\int_0^t \kappa_{il}(u)e^{-i\omega u}du\,\bar{E}_l(\omega) \end{aligned} \tag{4.7}$$

Like in viscoelasticity, viscoelectroelastic problem can be formally reduced to electroelastic one by using Carson transform. The Carson transform of a time dependent function is given by:

$$\bar{f}(s) = s\int_0^t f(t)e^{-ts}dt \tag{4,8}$$

where s is the Carson variable.

Taking $s = i\omega$, equation (4.7) could be written as follow

$$\begin{aligned} \bar{\sigma}_{ij}(s) &= \bar{c}_{ijkl}(s)\bar{\varepsilon}_{kl}(s) + \bar{e}_{lij}(s)\bar{E}_l(s) \\ \bar{D}_i(s) &= \bar{e}_{ikl}(s)\bar{\varepsilon}_{kl}(s) + \bar{\kappa}_{il}(s)\bar{E}_l(s) \end{aligned} \tag{4.9}$$

where

$\bar{\sigma}(s) = s\,\bar{\sigma}(\omega)$, $\bar{c}(s) = s\int_0^t c(u)e^{-su}du$, $\bar{e}(s) = s\int_0^t e(u)e^{-su}du$, $\bar{E}_l(s) = s\bar{E}(\omega)$, $\bar{\varepsilon}(s) = s\bar{\varepsilon}(\omega)$ and

$\bar{D}(s) = s\bar{D}(\omega)$.

Using the condensed notation, the constitutive equation in Carson domain is given by

$$\bar{\Sigma}_{iJ}(s) = \bar{E}_{iJKl}(s)\bar{Z}_{Kl}(s) \tag{4.10}$$

in which

$$\bar{E}_{iJKl}(s) = \begin{bmatrix} \bar{c}_{ijkl}(s) & \bar{e}_{lij}(s) \\ \bar{e}_{ikl}(s) & -\bar{\kappa}_{il}(s) \end{bmatrix}$$

Equation (4.10) shows the analogy between the linear viscoelectroelasticity problem and linear electroelastic problem. The role played by $\bar{E}(s)$ in linear viscoelectroelasticity is the same role played by the electroelastic moduli E in linear electroelasticity.

The equilibrium equations, in the absence of body force, electric charge, are given in the frequency domain by:

$$\bar{\sigma}_{ij,i}(s) = 0 \qquad \bar{D}_{i,i}(s) = 0 \tag{4.11}$$

Using the above condensed notations, the equilibrium equations are written as follow:

$$\bar{\Sigma}_{iJ,i}(s) = 0 \tag{4.12}$$

Based on the symmetry of the tensors c, e, κ the following equilibrium partial differential equation is obtained:

$$(\bar{E}_{iJKl}(s)\bar{U}_{K,l}(s))_{,i} = 0 \tag{4.13}$$

4.3 Localization and effective electroviscoelastic properties

Considering V as the representative volume element of an N-phase composite. The averaged stress and strain over the composite are given by:

$$\bar{Z}_{Kl}(s) = \sum_{i=1}^{n} f_i \bar{Z}^i_{Kl}(s) \tag{4.14-a}$$

$$\bar{\Sigma}_{lK}(s) = \sum_{i=1}^{n} f_i \bar{\Sigma}^i_{lK}(s) \tag{4.14-b}$$

where the index 'i' denotes the ith phase and f_i is its corresponding volume fraction. $\bar{Z}^i(s)$ and $\bar{\Sigma}^i(s)$ are considered to be uniform in each phase.

Based on the same mathematical development presented in Fakri et al. (2003, 2010) and Bakkali et al (2011, 2012 and 2013), the local field variables $\bar{Z}^i(s)$ and $\bar{\Sigma}^i(s)$ in the ith-phase are related

to global fields $\bar{Z}(s)$ and $\bar{\Sigma}(s)$ applied to the composite through the concentration tensors A and B respectively by:

$$\bar{Z}_{Kl}^{p}(s) = \bar{A}_{KlMn}^{p}(s)\bar{Z}_{Mn}(s) \tag{4.15-a}$$

$$\bar{\Sigma}_{iJ}^{p}(s) = \bar{B}_{iJnM}^{p}(s)\bar{\Sigma}_{nM}(s) \tag{4.15-b}$$

The overall constitutive viscoelectroelastic behavior of the composite and of the phase p can be written as follow:

$$\bar{\Sigma}_{iJ}(s) = \bar{E}_{iJKl}^{eff}(s)\bar{Z}_{Kl}(s) \tag{4.16-a}$$

$$\bar{\Sigma}_{iJ}^{p}(s) = \bar{E}_{iJKl}^{p}(s)\bar{Z}_{Kl}^{p}(s) \tag{4.16-b}$$

The introduction of (4.16-b) into (4.14-b) and the use of (4.15-a) lead to the expression of the effective viscoelectroelastic moduli in the transformed domain:

$$\bar{E}_{kLSv}^{eff}(s) = \sum_{p=1}^{n} f_p \bar{E}_{kLIj}^{p}(s)\bar{A}_{IjSv}^{P}(s) \tag{4.17}$$

From (4.17) it is clearly seen that the prediction of the effective moduli relies on the calculation of the concentration tensor A which could be approximated by using different micromechanical models. Based on this relationship, various micromechanical models can be applied to two-phase and multi-coated viscoelectroelastic materials. This condensed relationship gives the effective properties of the considered heterogeneous and multi-coated materials in the Carson or frequency domain. The effective viscoelectroelastic moduli in time domain can be obtained by using the inverse of Laplace transform, given by:

$$E_{iJKl}^{eff}(t) = \frac{1}{2\pi i}\int_{\delta+i\infty}^{\delta+i\infty} \frac{\bar{E}_{iJKl}^{eff}(s)}{s} \mathrm{e}^{st}\, ds \tag{4.18}$$

Let us note that the tensor $\bar{E}_{kLSv}^{eff}(s)$ depends implicitly on s and then it is impossible to evaluate the integral (4.18) analytically. Various studies focus on the investigating of the viscoelastic response of composites in Lapace or Carson domain instead of time domain due to the difficulties in accurately and efficiently evaluating the integral (4.18). In this paper, the inversion of the viscoelectroelastic moduli from the Carson domain to the physical domain (time domain) is done numerically by using the mutli-precision algorithm developed in [2]. This multi precision algorithm is already used by [15] to invert the effective properties of carbon Nanotube-Reinforced Polymer Composites from the Carson domain to the time domain.

Once $E_{iJKl}^{eff}(t)$ is calculated then the overall viscoelectroelastic behavior of the composite in time domain can be given as follow:

$$\Sigma_{iJ}(t) = \int_0^t E_{iJKl}^{eff}(t-\tau)\frac{dZ_{Kl}(\tau)}{d\tau}d\tau \tag{4.19}$$

Where Σ and Z are the generalized averaged viscoelectroelastic strain and stress over the composite.

4.4 Two-phase viscoelectroelastic composites

This section deals with two-phase viscoelectroelastic composites consisting with a viscoelastic matrix and piezoelectric inclusions. The derivation of the localization equation goes through the solution of the viscoelectroelastic integral equation and then the Mori-Tanaka mean field approach is used to derive the concentration tensor.

4.4.1 Localization equation and The Mori-Tanaka mean field approach

Considering a homogeneous fictitious media called "reference media" which has the viscoelectroelastic moduli $\bar{E}_{iJMn}^{0}(s)$. The expression of the local viscoelectroelastic moduli is given as follow:

$$\bar{E}_{iJMn}(r,s) = \bar{E}_{iJMn}^{0}(s) + \delta\bar{E}_{iJMn}(r,s) \tag{4.20}$$

where "r'' is the position vector in the media considered and $\delta\bar{E}$ is the deviation part. The introduction of this expression into (4.13) leads to

$$\bar{E}_{iJMn}^{0}(s)\bar{U}_{M,ni}(r,s) + (\delta\bar{E}_{iJMn}(r,s)\bar{U}_{M,n}(r,s))_{,i} = 0 \tag{4.21}$$

The viscoelectroelastic Green tensor of the reference media is related to the reference medium by the following equation:

$$\bar{E}_{iJMn}^{0}(s)\bar{G}_{MK,in}(r-r',s) + \delta_{JK}\delta(r-r') = 0 \tag{4.22}$$

Using (4.21), (4.22) and after some mathematical manipulations, the same integral equation derived by Fakri et al. (2003)[10] for linear piezoelectric composite materials, is obtained here in Carson domain for viscoelectroelastic composite materials:

$$\bar{Z}_{Kl}(r,s) = \bar{Z}_{Kl}^{0}(r,s) - \int_V \bar{\Gamma}_{iJKl}(r-r',s)(\delta\bar{E}_{iJMn}(r',s)\bar{Z}_{Mn}(r',s))dV' \tag{4.23}$$

where $\bar{\Gamma}_{iJKl}(r-r',s) = -\bar{G}_{JK,li}(r-r',s)$ is a condensed notation of four tensors.

To solve this integral equation, the same procedure used by Fakri et al. (2003)[10] is followed which leads to the following localization equation:

$$\bar{Z}^{I}_{Kl}(s) = \bar{Z}^{0}_{Kl}(s) - \frac{1}{V^{I}} \bar{T}^{II}_{iJKl}(\bar{E}^{0}(s)) \Delta \bar{E}^{I}_{iJMn}(s) \bar{Z}^{I}_{Mn}(s) \tag{4.24}$$

where $\bar{T}^{II}_{iJKl}(\bar{E}^{0}(s)) = \int_{V^{I}} \int_{V^{I}} \bar{\Gamma}_{iJKl}(r - r', s) dV' dV$ represents the condensed notation of the viscoelectroelastic interaction tensors. These tensors are computed numerically [3, 10 and 11] for various shapes of inclusions using the Gaussian quadrature integration for the considered inclusion shape.

The Mori-Tanaka mean field approach, besides of its ease of implementation, is well known to be the best in precision. The main assumption of the Mori-Tanaka Mean field approach is the consideration that the infinite reference medium has the properties of the matrix. So, to have the expression of the Mori-Tanaka concentration tensor, the generalized strain field $\bar{Z}^{0}(s)$ and the viscoelectroelastic moduli $\bar{E}^{0}(s)$ of the reference medium in equation (4.24) are replaced respectively by the generalized strain field $\bar{Z}^{m}(s)$ and the viscoelectroelastic moduli $\bar{E}^{m}(s)$ of the matrix. So, one can write the expression of the s-dependent concentration tensor as follow:

$$\bar{A}^{MT}_{MnKl}(s) = (I_{KlMn} + \frac{f_m}{V^{I}} \bar{T}^{II}_{iJKl}(\bar{E}^{m}(s) \Delta \bar{E}^{I}_{iJMn}(s))^{-1} \tag{4.25}$$

in which $\Delta \bar{E}^{I}_{iJMn}(s) = \bar{E}^{I}_{iJMn}(s) - \bar{E}^{m}_{iJMn}(s)$

4.5 Multi-coated viscoelectroelastic composites

The aim of this section is to generalize the previous mathematical developments to the case of multi-coated viscoelectroelastic composites. The derivation of the localization equation goes through the solution of the multi-coated viscoelectroelastic integral equation and the use of the viscoelectroelastic interfacial operator. The concentration tensors are derived based on the Mori-Tanaka mean field approach.

4.5.1 Localization equation and the Mori-Tanaka mean field approach

In this subsection the integral equation (4.23) is extended for multi-coated viscoelectroelastic composites by expressing the deviation part as follow:

$$\delta\bar{E}_{iJMn}(s)=\sum_{k=0}^{n}\Delta\bar{E}_{iJMn}^{(k/0)}(s)\theta^{k}(r)\quad ;\ k\in\{0,1,2,...n\} \tag{4.26}$$

where $\theta^{k}(r)$ is the characteristic function of the phase k, occupying the volume V_k , expressed by:

$$\theta^{k}(r)=\begin{cases}1 & if\ \ r\in V_k\\ 0 & if\ \ r\notin V_k\end{cases}, \tag{4.27}$$

and $\Delta\bar{E}_{iJMn}^{(k/0)}(s)=\bar{E}_{iJMn}^{k}(s)-\bar{E}_{iJMn}^{0}(s)$

Using (4.26) the following integral equation is obtained:

$$\bar{Z}_{Kl}(r,s)=\bar{Z}_{Kl}^{0}(r,s)-\sum_{k=1}^{n}\int_{V_k}\bar{\Gamma}_{iJKl}(r-r',s)\Delta\bar{E}_{iJMn}^{(k/0)}(s)\bar{Z}_{Mn}(r',s)dV' \tag{4.28}$$

Considering V_I the total volume of the composite inclusion, which consists of an inclusion surrounded by (n-1) coatings and f_k is the volume fraction of the phase k. One can write:

$$V_I=\sum_{k=1}^{n}V_k \tag{4.29}$$

The average local generalized strain field can be written as:

$$\bar{Z}_{Mn}(r,s)=\sum_{k=1}^{n}\bar{Z}_{Mn}^{k}(s)\theta^{k}(r) \tag{4.30}$$

Substituting (4.30) into (4.28) and averaging over the volume of the composite inclusion, one can find the following localization equation:

$$\bar{Z}_{Kl}^{I}(s)=\bar{Z}_{Kl}^{0}(s)-\frac{1}{V_I}\sum_{k=1}^{n}\bar{T}_{iJKl}^{Ik}(\bar{E}^{0}(s))\bar{E}_{iJMn}^{(k/0)}(s)\bar{Z}_{Mn}^{k}(s) \tag{4.31}$$

where $\bar{T}_{iJKl}^{Ik}(\bar{E}^{0}(s))=\int_{V_I}\int_{V_k}\bar{\Gamma}_{iJKl}(r-r',s)dV'dV$ represents the condensed notation of the viscoelectroelastic interaction tensor.

Using the fact that $\bar{Z}_{Kl}^{I}(s)=\sum_{k=1}^{n}\frac{V_k}{V_I}\bar{Z}_{Kl}^{k}(s)$ leads to:

$$\sum_{k=1}^{n}\frac{V_k}{V_I}(I_{KlMp}+\frac{1}{V_k}\bar{T}_{iJKl}^{Ik}(\bar{E}^{0}(s))\Delta\bar{E}_{iJMp}^{(k/0)})\bar{Z}_{Mp}^{k}(s)=\bar{Z}_{Kl}^{0}(s) \tag{4.32}$$

where I_{KlMn} is the shorthand notation of the fourth order and the second order identity tensors:

$$I_{KlMp}=\begin{cases}1/2(\delta_{km}\delta_{lp}+\delta_{kp}\delta_{lm}) & (K,M=1,2,3)\\ 0 & (K=1,2,3;M=4)\\ 0 & (K=4;M=1,2,3)\\ \delta_{lp} & (K=4;M=4)\end{cases} \tag{4.33}$$

To complete the localization step, the viscoelectroelastic interfacial operators are introduced which give the generalized strain jump field across an interface between two different phases by the following equation:

$$\bar{Z}^{k+1}_{Mn}(r,s)-\bar{Z}^{k}_{Mn}(r,s)=\bar{P}^{k+1}_{iJMn}(\bar{E}^{K+1}(s),N)(\bar{E}^{k}_{iJRs}(s)-\bar{E}^{k+1}_{iJRs}(s))\bar{Z}^{k}_{Rs}(r,s) \tag{4.34}$$

The concentration tensors were derived for multi-coated magnetoelectroelastic composites by Bakkali et al. (2012) based on the solution of the integral equation and the magnetoelectroelastic interfacial operators. Here, the same procedure is followed and the expression of the concentration tensors in Carson domain is given by the following generalized relationship:

$$\bar{A}^{k}_{MnKl}(s)=\bar{a}^{k}_{MnPv}(s)\left[\sum_{k=1}^{n}\left(\frac{f_k}{f_I}\left(I_{KlRs}+\frac{1}{V_k}\bar{T}^{Ik}_{iJKl}(\bar{E}^{0}(s))\Delta\bar{E}^{(k/0)}_{iJRs}(s)\right)\bar{a}^{k}_{RsPv}(s)\right)\right]^{-1} \tag{4.35}$$

where $\bar{a}^{k}$ is the local localization tensor and its expression is given by :

$$\bar{a}^{k}_{MnKl}(s)=\sum_{i=1}^{k-1}f_i\bar{W}^{(i/k)}_{MnRs}(s)\bar{a}^{i}_{RsKl}(s)/\left(\sum_{i=1}^{k-1}f_i\right) \tag{4.36-a}$$

$$\text{And } \bar{W}^{(i/k)}_{MnRs}(s)=(I_{MnRs}+\bar{T}^{k}_{pJMn}(\bar{E}^{k}(s))\Delta\bar{E}^{(i/k)}_{pJRs}(s)) \text{ and } \bar{a}^{1}_{MnKl}(s)=I_{MnKl} \tag{4.36-b}$$

Note that various micromechanical approaches can be obtained based on the presented concentration tensors (4.35) in the Carson domain. In this paper we restrict ourselves to Mori-Tanaka mean field and Dilute approaches.

To obtain the expression of the Mori-Tanaka mean field approach localization tensors, the generalized strain field $\bar{Z}^{0}(s)$ and the viscoelectroelastic moduli $\bar{E}^{0}(s)$ of the reference medium in (4.32) are replaced respectively by the generalized strain field $\bar{Z}^{m}(s)$ and the viscoelectroelastic moduli $\bar{E}^{m}(s)$ in the matrix. The following frequency dependent localization tensor is then obtained:

$$\bar{A}^{k(MT)}_{MnKl}(s)=\bar{a}^{k}_{MnPv}(s)\left[\sum_{k=1}^{n}\left(\frac{f_k}{f_I}\left(I_{KlRs}+\frac{f_m}{V_k}\bar{T}^{Ik}_{iJKl}(\bar{E}^{M}(s))\Delta\bar{E}^{(k/m)}_{iJRs}(s)\right)\bar{a}^{k}_{RsPv}(s)\right)\right]^{-1} \tag{4.37}$$

in which $\Delta\bar{E}^{(k/m)}_{iJRs}(s)=\bar{E}^{k}_{iJRs}(s)-\bar{E}^{m}_{iJRs}(s)$ and $f_m=1-f_I$ is the volume fraction of the matrix.

For the Dilute approach, one has to replace, the generalized strain field $\bar{Z}^0(s)$ and the viscoelectroelastic moduli $\bar{E}^0(s)$ of the reference medium in (4.32) are replaced respectively by the average generalized strain field $\bar{Z}(s)$ applied over the composite and the viscoelectroelastic moduli $\bar{E}^m(s)$ in the matrix. The following frequency dependent localization tensor is then obtained:

$$\bar{A}^{k(Dil)}_{MnKl}(s) = \bar{a}^{k}_{MnPv}(s)\left[\sum_{k=1}^{n}\left(\frac{f_k}{f_I}\left(I_{KlRs} + \frac{1}{V_k}\bar{T}^{Ik}_{iJKl}(\bar{E}^0(s))\Delta\bar{E}^{(k/m)}_{iJRs}(s)\right)\bar{a}^{k}_{RsPv}(s)\right)\right]^{-1} \tag{4.38}$$

in which $\Delta\bar{E}^{(k/m)}_{iJRs}(s) = \bar{E}^{k}_{iJRs}(s) - \bar{E}^{m}_{iJRs}(s)$.

Based on the developed methodological approach the frequency dependent effective coefficients are given by:

$$\bar{E}^{eff}_{kLSv}(s) = \bar{E}^{m}_{kLSv}(s) + \sum_{p=1}^{n} f_p(\bar{E}^{p}_{kLIj}(s) - \bar{E}^{m}_{kLIj}(s))\bar{A}^{P(MT)}_{IjSv}(s) \tag{4.39}$$

This relationship allows one to investigate the viscoelectroelastic frequency dependent behavior of the newly created viscoelectroelastic composite. This hybrid behavior can be numerically analyzed with respect to the shape, volume fractions inclusions. For the time dependent effective coefficients the inverse of Laplace transform is applied to $\bar{E}^{eff}(s)$. The used numerical inversion procedure is given by [2]:

$$E^{eff}_{kLSv}(t,M) = \frac{r}{M}\left[\frac{1}{2}\bar{E}^{eff}_{kLSv}(r)\exp(rt) + \sum_{k=1}^{M-1}\mathrm{Re}\left[\exp(ts(\theta_k))\bar{E}^{eff}_{kLSv}(s(\theta_k))(1+i\sigma(\theta_k))\right]\right] \tag{4.40}$$

with $r = \frac{2M}{5t}$, $\theta_k = \frac{k\pi}{M}$ and $\sigma(\theta_k) = \theta_k + (\theta_k\cot(\theta_k) - 1)\cot(\theta_k)$

$E^{eff}_{kLSv}(t,M)$ is approximated by (4.40). It is has only a free parameter M, which is the number of terms to be summed. By this way the frequency and time dependent viscoelectroelastic coefficients are obtained for two-phase and multi-coated composites.

4.6Numerical results

Based on the previous mathematical modelings, the effective properties of two kinds of viscoelectroelastic composites are investigated. The first one is a two-phase composite consisting of piezoelectric inclusions (PZT-7A) embedded in a viscoelastic matrix (LaRC-SI). The second one is a three-phase viscoelectroelastic composite consisting of Glass inclusions surrounded by

(PZT-7A) coating embedded in a viscoelastic matrix (LaRC-SI). The topology of a representative volume element of the three-phase composite is described in figure 1. As shown in Figure 1, phase 1 is the Glass inclusion, phase 2 is the piezoelectric coating and phase three is the viscoelastic matrix having homogeneous material properties E^1, E^2 and E^3 respectively. The reinforcements are perfectly aligned and have ellipsoidal shapes with the dimensions (a_1, b_1, c_1) and (a_2, b_2, c_2). The two ellipsoids are coaxial with $\frac{a_1}{a_2} = \frac{b_1}{b_2} = \frac{c_1}{c_2} = \gamma$.

The variation of the volume fraction of the inclusion f_1 and the coating f_2 are given as function of the volume fraction of the matrix and the thickness of the piezoelectric coating 'γ' as follow.

$$f_1 = (1 - f_3)\gamma^3,\ f_2 = (1 - f_3)(1 - \gamma^3) \tag{4.41}$$

Note that, there are two limiting cases. When $\gamma = 0$, Glass inclusions disappear and the effective properties of a viscoelectroelastic composites consisting of (PZT-7A) inclusions embedded in viscoelastic matrix (LaRC-SI) are obtained and when $\gamma = 1$ the coatings disappear and the effective properties of a viscoelastic composites consisting of Glass inclusions embedded in viscoelastic matrix (LaRC-SI) are obtained.

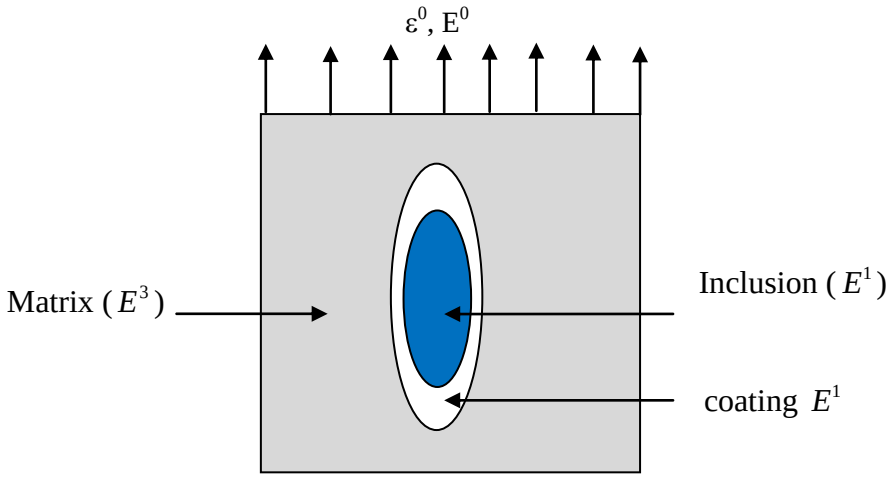

Figure 4.1: A representative volume element of a three-phase composite. The dimension of the inclusion and the coating are (a_1, b_1, c_1), (a_2, b_2, c_2) respectively.

4.6.1 Two-phase composites

In this subsection, effective properties of the considered two-phase composite are presented in the frequency and in time domain. (PZT-7A) is considered to have independent time properties. Also, its properties are considered to remain constant with variation of temperature. At elevated

temperature (LaRC-SI) shows a significant viscoelastic response. The creep compliance of the matrix in time domain $M_0(t)$ may be represented by the power low model [15]

$$M_0(t) = D_0 + D_1 t^n \tag{4.42}$$

where D_0 is the initial elastic compliance, and D_1 and n are experimentally determined parameters. For simplicity, the Poisson's ratio of the matrix is assumed unchanged. The Carson transform of Eq. (4.42) gives

$$\bar{M}_0(s) = D_0 + \frac{D_1 n!}{s^n} \tag{4.43}$$

The Young modulus $\bar{E}(s)$ is taken as the inverse of $\bar{M}_0(s)$. Variables values of D_0, D_1 and n at T= 213°c are given in table 2 [15]. The dielectric constant of (LaRC-SI) [18] are considered to be constant ($\kappa_{11}/\kappa_0 = \kappa_{22}/\kappa_0 = \kappa_{33}/\kappa_0 = 2.8$) with $\kappa_0 = 8.854187816 \times 10^{-12}$ (C^2/Nm^2). The properties of PZT-7A and Glass materials are given in table 4.1.

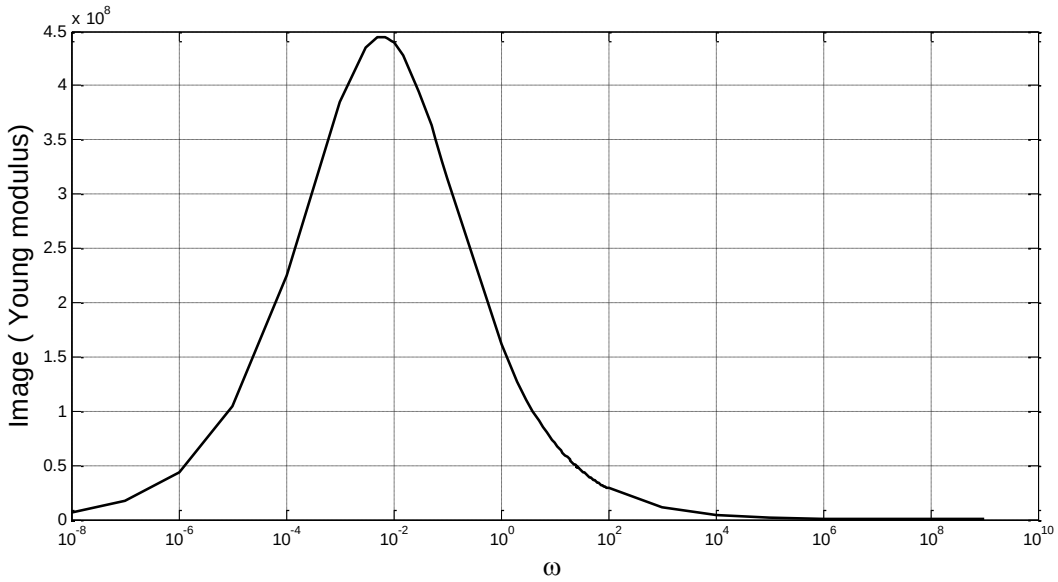

(a)

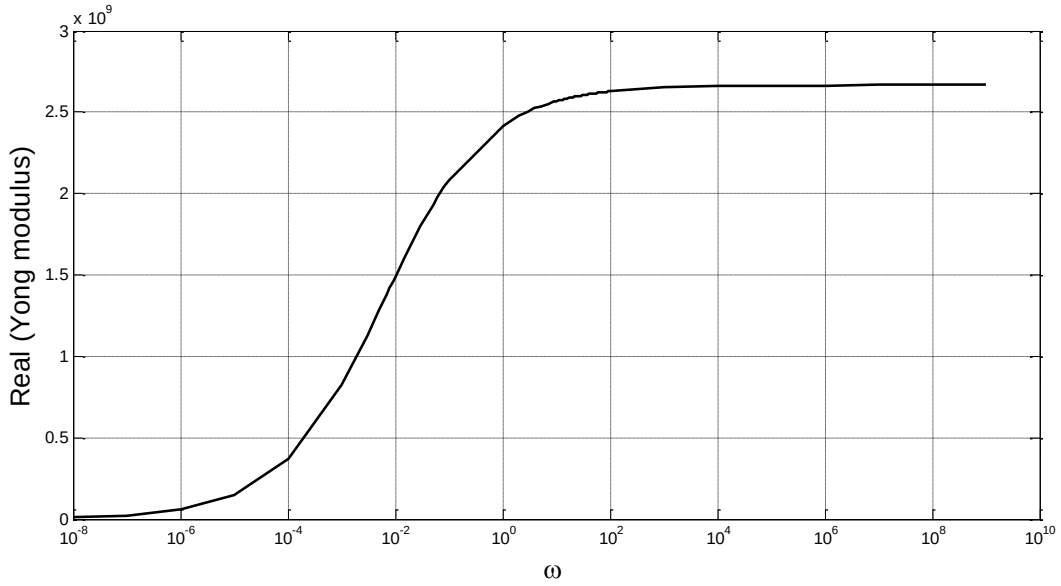

(b)

Figure 4.2: Storage (b) and loss (a) part of the Yong moduli of LaRC-SI

Table 4.1: PZT. 7A properties

	C_{11}	C_{12}	C_{13}	C_{33}	C_{44}	e_{15}	e_{31}	e_{33}	κ_{11}	κ_{33}
PZT-7A	148	6.2	4.2	131	25.4	9.2	-2.1	9.5	4.071×10^{-9}	2.0798×10^{-9}
Glass	88.8	29.6	29.6	88.8	29.6	0	0	0	0.056×10^{-9}	0.056×10^{-9}

Units: elastic constant GPa; dielectric constants C^2/Nm^2; piezoelectric constants C/m^2.

Table 4.2: Viscoelastic properties of LaRC-SI (power low model (T=231°c))

$D_0(Gpa^{-1})$	$D_1(Gpa^{-1}hour^{-1})$	n	γ_0
0.375	0.051606	0.4103	0.367

4.6.1.1 Frequency domain

In this study, PZT-7A in considered as inclusions embedded in a viscoelastic matrix LaRC-SI. The resulting new composite will have a viscopiezoelectric behavior. The associated coefficients are frequency or time dependent and their behavior will be investigated.

In figures 4.3 and 4.4, the storage and loss part of the elastic modulus c_{11} are presented respectively for a viscoelectroelastic composite with respect to the shape of inclusions and the frequency $\omega(1/hour)$. The volume fraction 40% of inclusions is considered. The inclusion shape effects on the storage and loss part of the elastic modulus c_{11} of the composite are presented.

In figures 4.5 and 4.6, the storage and loss part of the piezoelectric modulus e_{31} are presented respectively for a viscoelectroelastic composite with respect to the shape of inclusions and the frequency. Although the piezoelectric inclusions are assumed to have independent time properties, it is shown that the effective piezoelectric modulus e_{31} varies with the frequency and particularly for fibrous inclusion. This modulus is strongly affected by the viscoelastic behavior of the matrix. Also it is shown that the storage and the loss part of e_{31} are strongly affected by the shape of inclusions and there is a frequency range in which the loss part can be optimized.

The storage and loss part of the dielectric modulus κ_{33} are presented in figures 4.7 and 4.8 for a viscoelectroelastic composite with respect to the shape of inclusions and the frequency. The viscoelectroelastic frequency dependence effects are presented.

In figures 4.9 and 4.10, storage and loss map of elastic and piezoelectric effective properties are presented for a fibrous viscoelastic composite with respect to the volume fraction of the inclusions and fixed value of frequency. It is seen that the loss part of the effective moduli is maximized at some fiber volume fraction regions.

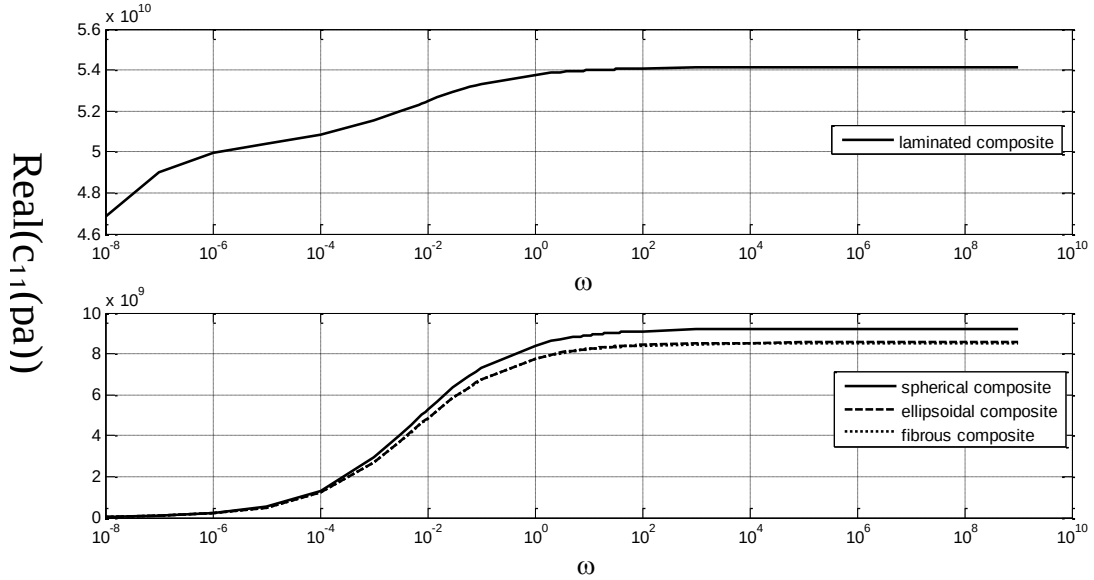

Figure 4.3: Effective storage elastic modulus Real(c_{11}) for a viscoelectroelastic composite, with various shapes of inclusions, consisting of piezoelectric inclusions (PZT-7A) embedded in a viscoelastic matrix (LaRC-SI) with fixed volume fraction of the matrix (fm=0.6).

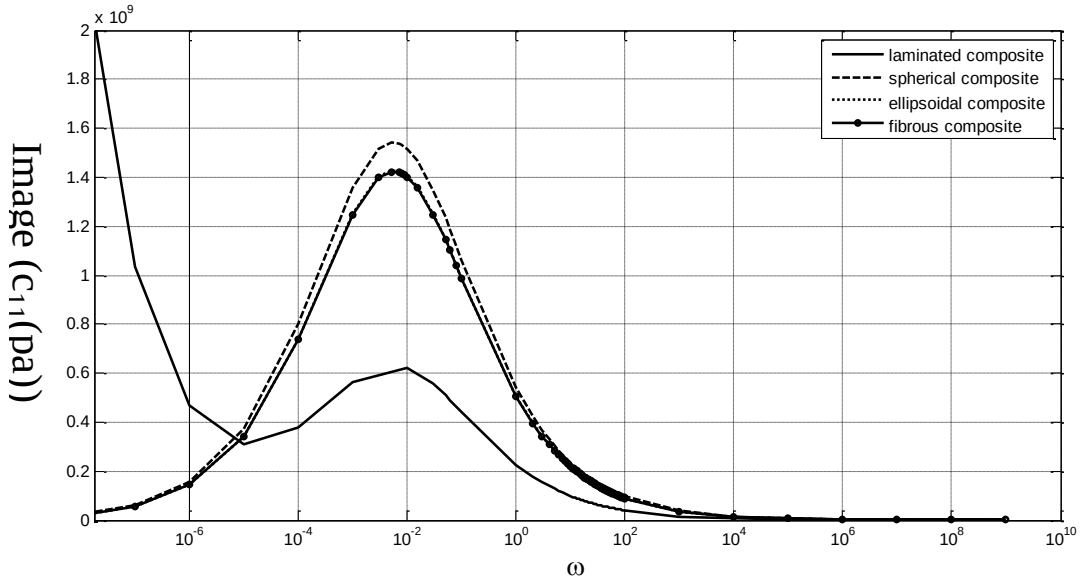

Figure 4.4: Effective loss elastic modulus Image(c_{11}) for a viscoelectroelastic composite, with various shapes of inclusions, consisting of piezoelectric inclusions (PZT-7A) embedded in viscoelastic matrix (LaRC-SI) with fixed volume fraction of the matrix (fm=0.6).

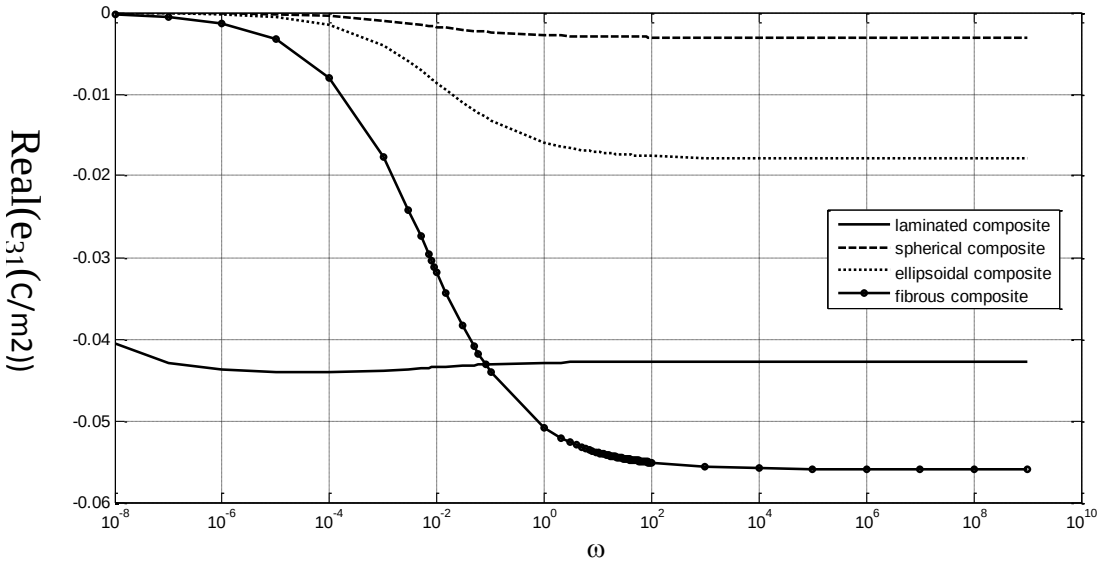

Figure 4.5: Effective storage piezoelectric modulus Real(e_{31}) for a viscoelectroelastic composite, with various shapes of inclusions, consisting of piezoelectric inclusions (PZT-7A) embedded in viscoelastic matrix (LaRC-SI) with fixed volume fraction of the matrix (fm=0.6).

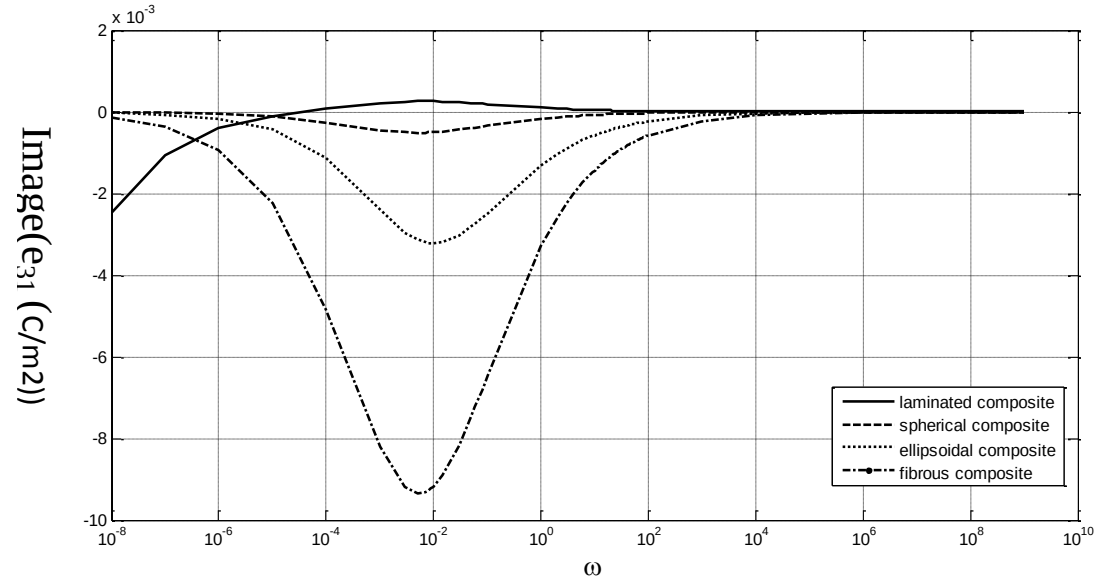

Figure 4.6: Effective loss piezoelectric modulus Image(e_{31}) for a viscoelectroelastic composite, with various shapes of inclusions, consisting of piezoelectric inclusions (PZT-7A) embedded in viscoelastic matrix (LaRC-SI) with fixed volume fraction of the matrix (fm=0.6).

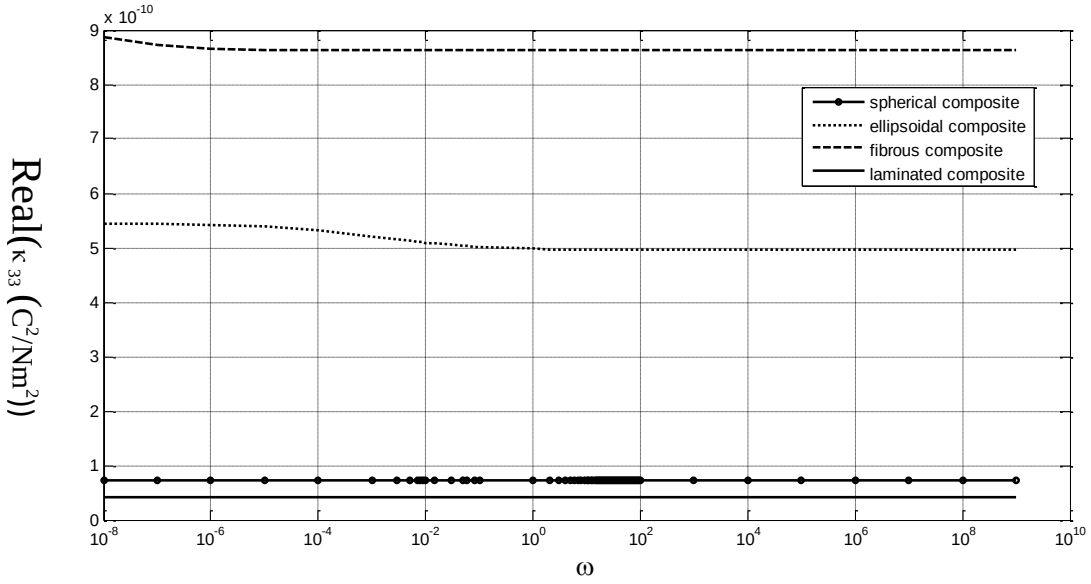

Figure 4.7: Effective storage dielectric modulus Real(κ_{33}) for a viscoelectroelastic composite, with various shaps of inclusions, consisting of piezoelectric inclusions (PZT-7A) embedded in viscoelastic matrix (LaRC-SI) with fixed volume fraction of the matrix (fm=0.6).

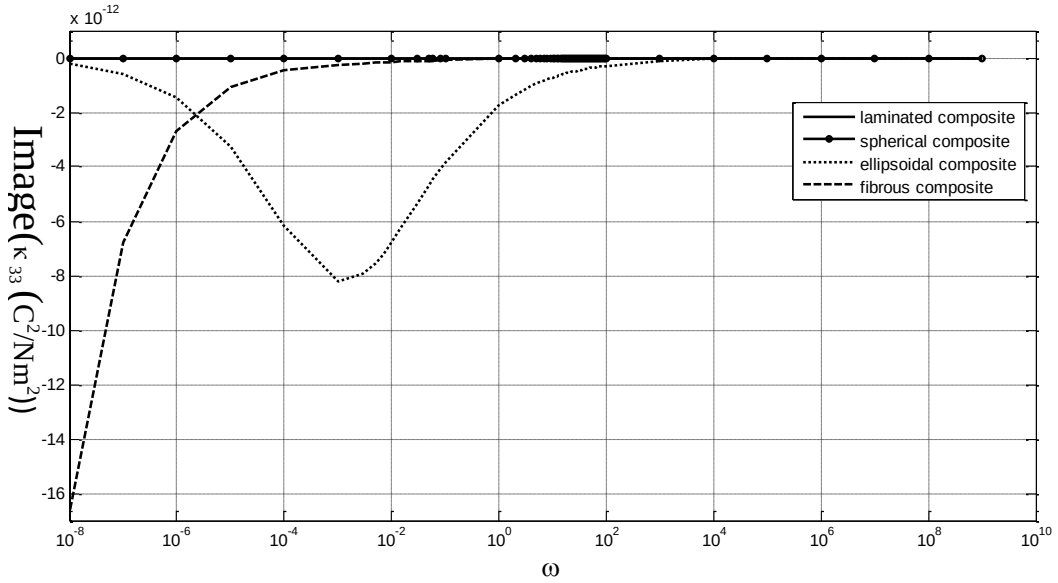

Figure 4.8: Effective loss dielectric modulus Image(κ_{33}) for a viscoelectroelastic composite, with various shapes of inclusions, consisting of piezoelectric inclusions (PZT-7A) embedded in viscoelastic matrix (LaRC-SI) with fixed volume fraction of the matrix (fm=0.6).

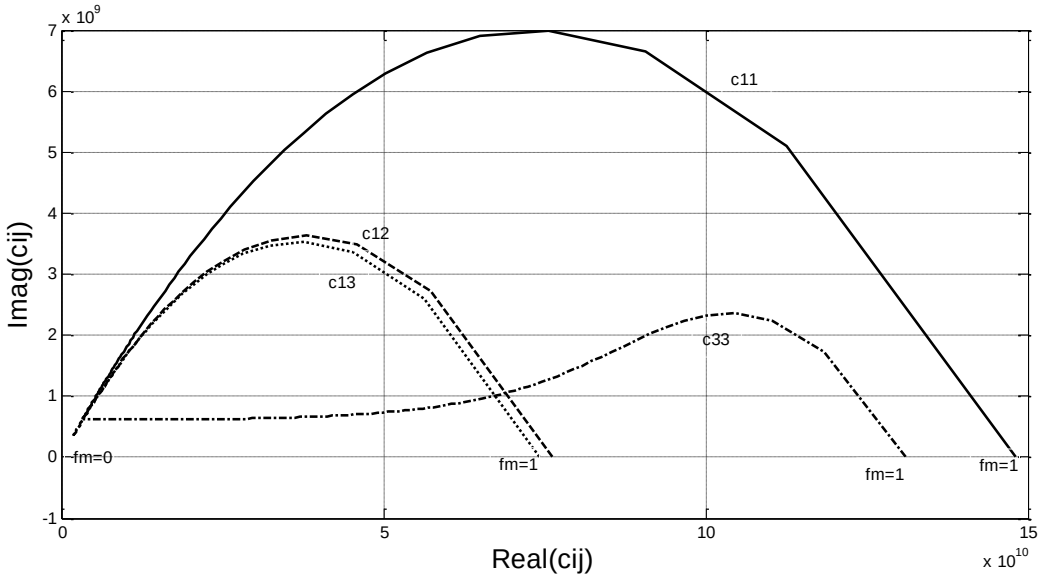

Figure 4.9: Storage and loss map of elastic moduli of a fibrous viscoelectroelastic composite with respect to the volume faction of the inclusion and with fixed value of frequency $\omega = 0.05(1/hour)$.

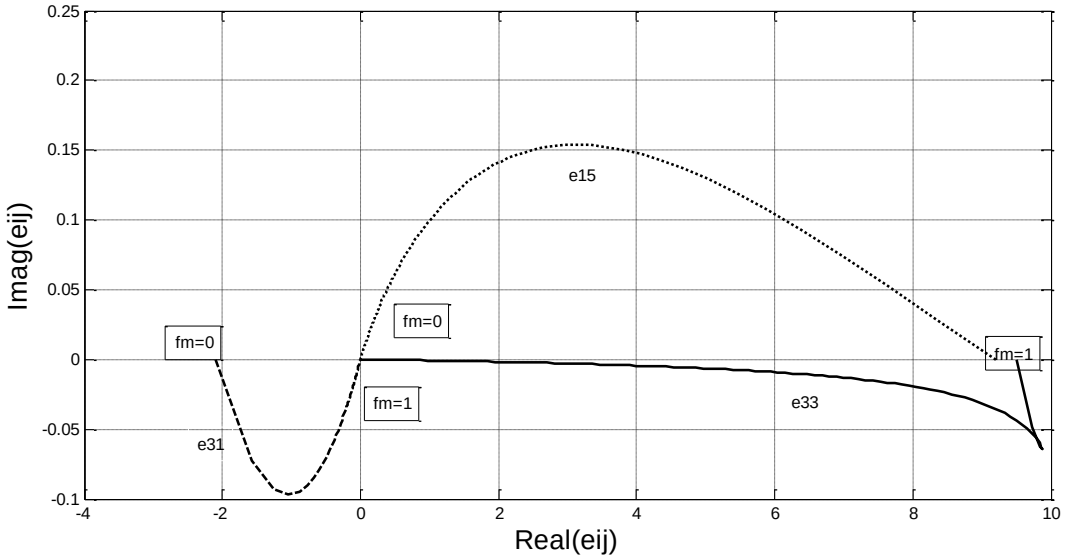

Figure 4.10: Storage and loss map of piezoelectric moduli of a fibrous viscoelectroelastic composite with respect to the volume faction of the inclusion and with fixed value of frequency $\omega = 0.05(1/hour)$.

4.6.1.2 Time domain

Based on the inverse Laplace transform the effective time dependent coefficients are obtained for various inclusion shapes and types.

Effective relaxation time dependent moduli c_{11} and c_{22} are presented in figure 4.11 for a fibrous viscoelectroelastic composite consisting of piezoelectric inclusion (PZT-7A) embedded in a (60%) viscoelastic matrix (LaRC-SI). c_{11} and c_{22} of the composite are compared to those of the matrix. The effect of the composite on the effective relaxation moduli is shown.

In figures 4.12, 4.13 and 4.14, effective piezoelectric moduli e_{15}, e_{33} and e_{31} are predicted, for a fibrous viscoelectroelastic composite consisting of piezoelectric inclusions (PZT-7A) embedded a viscoelastic matrix (LaRC-SI). Various volume factions of inclusions are considered. It is seen that e_{15} decreases with time but e_{33} and e_{31} increase with time. Also the effect of the variation of the volume fraction is shown on the effective properties. Even the piezoelectric moduli of inclusions are considered to be time independent it is shows that the effective piezoelectric moduli of the composites are time dependent. That means, these coefficients are affected by the time dependent behavior of the viscoelastic matrix. Also one can see from the figures that e_{15} and e_{31} are more affected by the viscoelastic behavior of the matrix than e_{33}. e_{33} varies very slightly with time.

In figure 4.15, three dimension numerical results are presented for a fibrous viscoelectroelastic composite. The evolution of e_{31} with respect to time and the shape of inclusion (c/a) is presented. It is seen that e_{31} varies significantly as the shape of the inclusion varies. Also it is seen that e_{31} always increases with time for different shapes of inclusion.

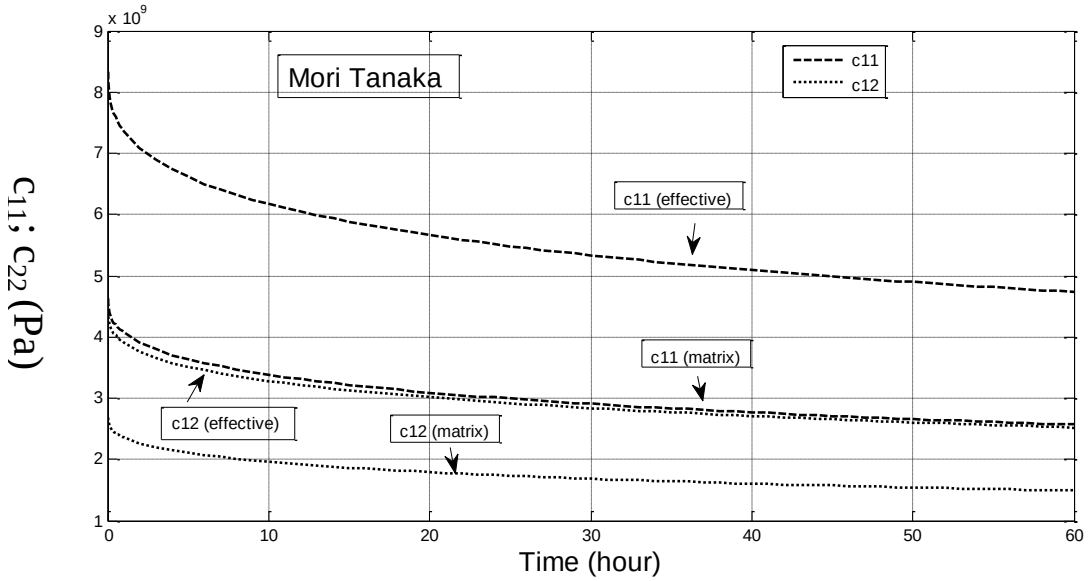

Figure 4.11: Elastic relaxation moduli c_{11} and c_{12} of the matrix and effective elastic relaxation moduli c_{11} and c_{12} for a fibrous viscoelectroelastic composite consisting of piezoelectric inclusions (PZT-7A) embedded a viscoelastic matrix (LaRC-SI) with fixed volume fraction of the matrix fm=0.6.

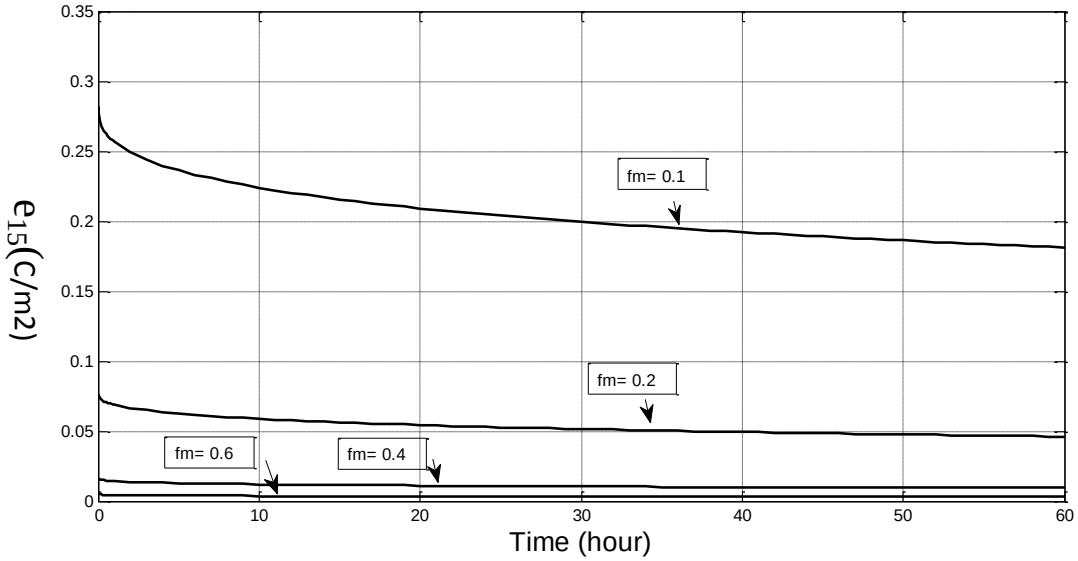

Figure 4.12: Effective piezoelectric modulus e_{15} for a fibrous viscoelectroelastic composite consisting of piezoelectric inclusions (PZT-7A) embedded in a viscoelastic matrix (LaRC-SI) with fixed volume fraction of the matrix fm=0.6.

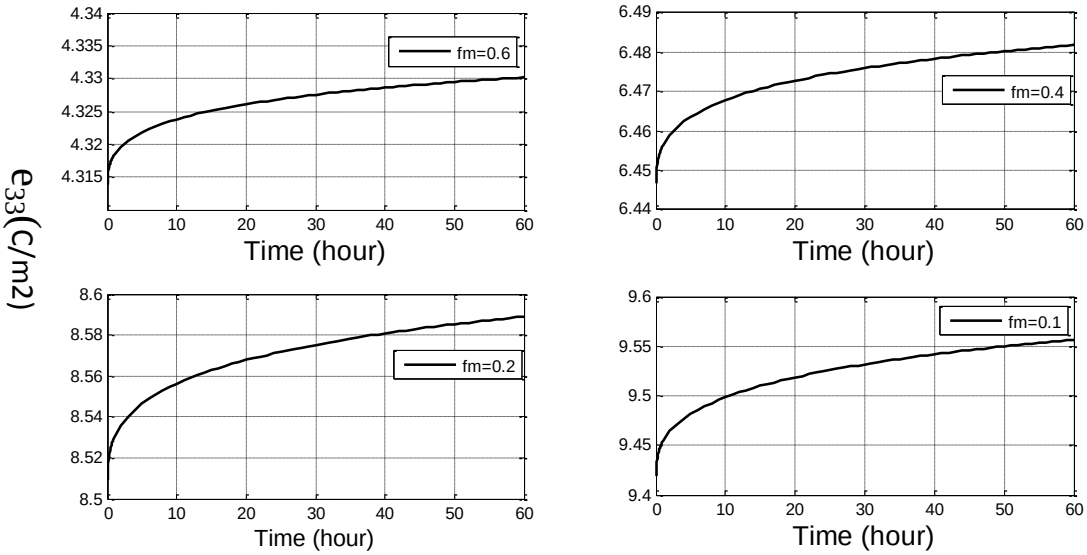

Figure 4.13: Effective piezoelectric modulus e_{33} for a fibrous viscoelectroelastic composite consisting of piezoelectric inclusions (PZT-7A) embedded in a viscoelastic matrix (LaRC-SI) with fixed volume fraction of the matrix fm=0.6.

.

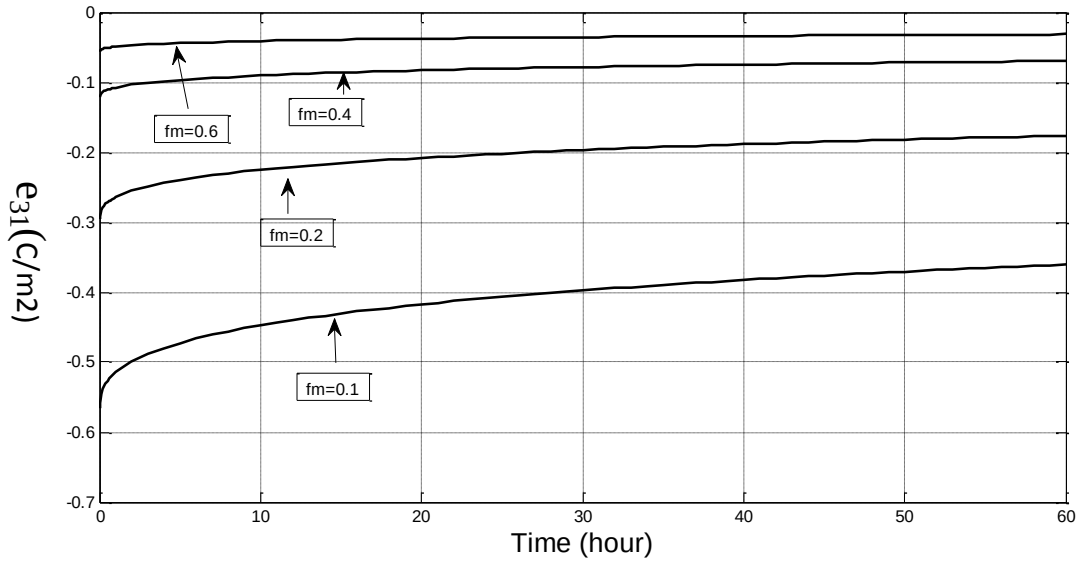

Figure 4.14: Effective piezoelectric modulus e_{31} for a fibrous viscoelectroelastic composite consisting of piezoelectric inclusions (PZT-7A) embedded in a viscoelastic matrix (LaRC-SI) with fixed volume fraction of the matrix fm=0.6.

.

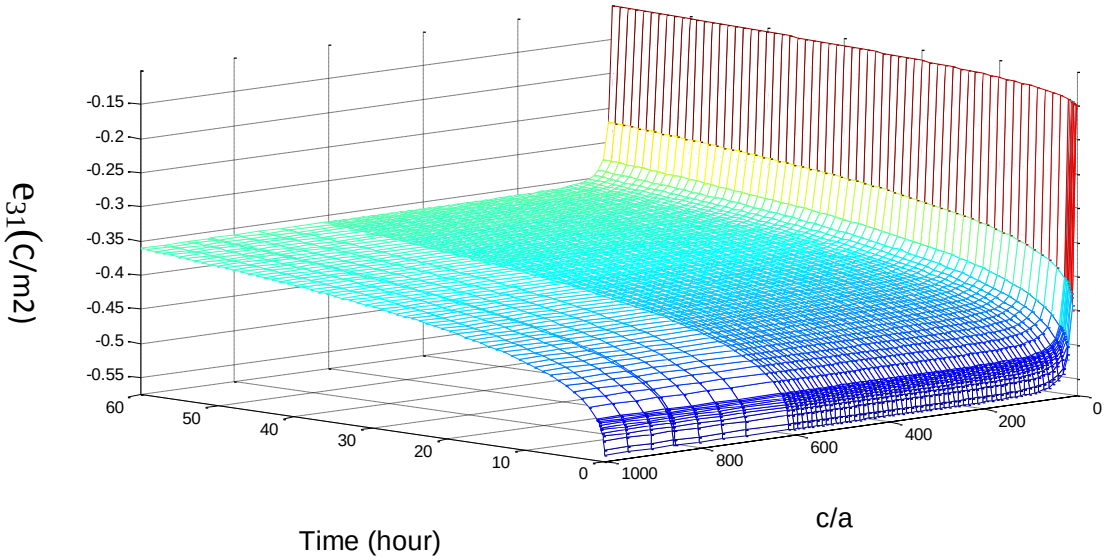

Figure 4.15: Effective piezoelectric modulus e_{31} for a viscoelectroelastic composite consisting of piezoelectric inclusions (PZT-7A) embedded a viscoelastic matrix (LaRC-SI) with fixed volume fraction of the matrix fm=0.6.

4.6.2 Three-phase composites

In this subsection, the effective properties of a three-phase composite consisting of glass inclusion surrounded by piezoelectric PZT-7A layer embedded in a LaRC-SI viscoelastic matrix are obtained in frequency and in time domain. The shape and coating thickness effects on the effective properties are investigated.

4.6.2.1 Frequency domain

The frequency dependence storage and loss part of the effective piezoelectric modulus e_{31} are presented in figures 4.16 and 4.17 for a fibrous viscoelectroelastic composites consisting of Glass inclusions surrounded by piezoelectric coating layer embedded in viscoelastic matrix for various thicknesses of the piezoelectric coating layer. It is seen that e_{31} is strongly affected by the frequency as well as by the thickness of the coating layer.

In figures 4.18 and 4.19, the storage and loss part of e_{33} are presented for a fibrous viscoelectroelastic composites consisting of Glass inclusions surrounded by piezoelectric coating layer embedded in viscoelastic matrix with respect to frequencies and the thickness of the piezoelectric coating layer. It is seen that e_{33} is strongly affected by the thickness of the coating as well as by the viscoelastic behavior of the matrix.

In figures 4.20 and 4.21, storage and loss map of elastic and piezoelectric effective properties are presented for the three-phase composite with respect to the volume fraction of the inclusion and fixed value of frequency and thickness of the coating layer. It is seen that the loss part of the effective moduli is maximized at some fiber volume fraction regions.

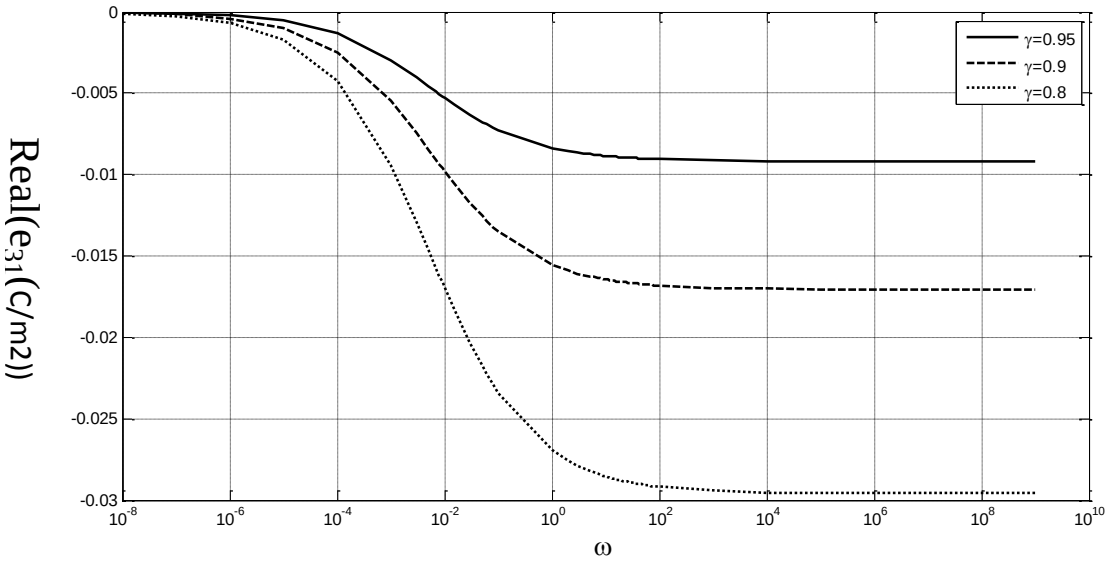

Figure 4.16: Effective piezoelectric modulus Real(e_{31}) for a fibrous viscoelectroelastic composites consisting of Glass inclusions surrounded by piezoelectric coating layer (PZT-7A) embedded in a viscoelastic matrix (LaRC-SI) with fixed volume fraction of the matrix (fm=0.6).

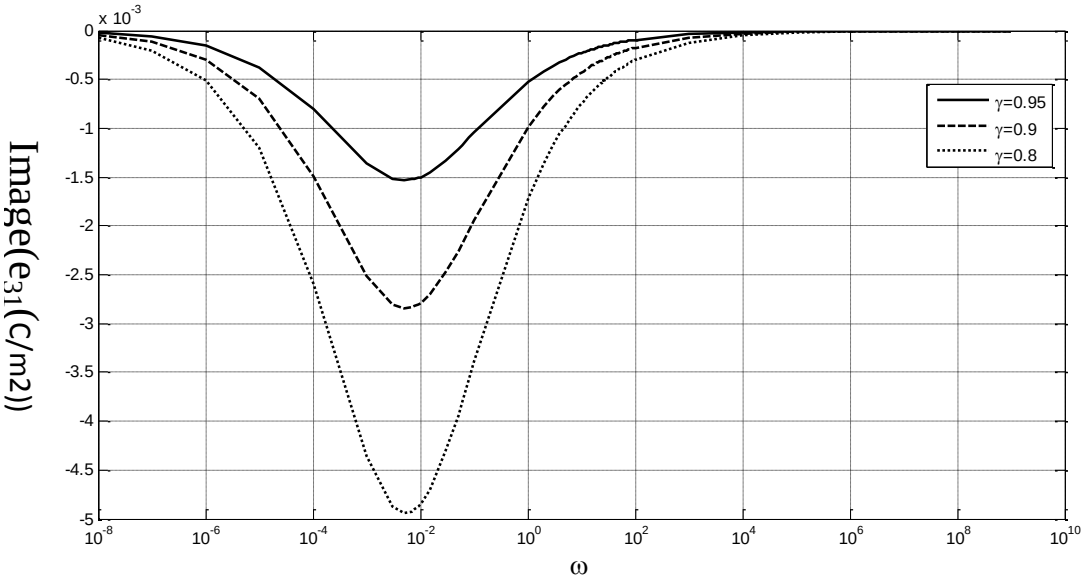

Figure 4.17: Effective piezoelectric modulus Image(e_{31}) for a fibrous viscoelectroelastic composites consisting of Glass inclusions surrounded by piezoelectric coating layer (PZT-7A) embedded in a viscoelastic matrix (LaRC-SI) with fixed volume fraction of the matrix (fm=0.6).

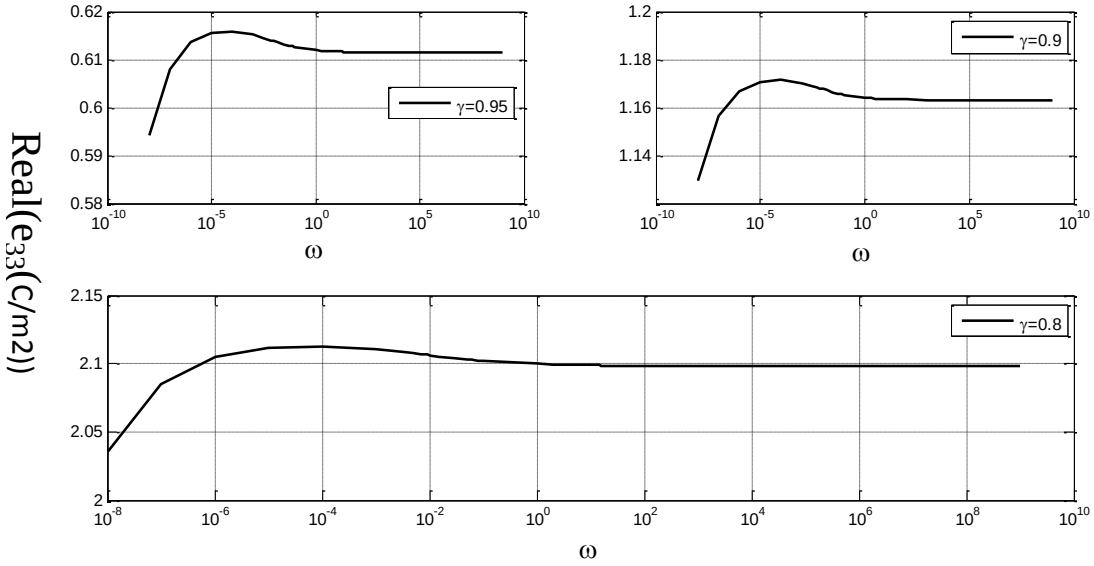

Figure 4.18: Effective piezoelectric modulus Real(e_{33}) for a fibrous viscoelectroelastic composites consisting of Glass inclusions surrounded by piezoelectric coating layer (PZT-7A) embedded in a viscoelastic matrix (LaRC-SI) with fixed volume fraction of the matrix (fm=0.6).

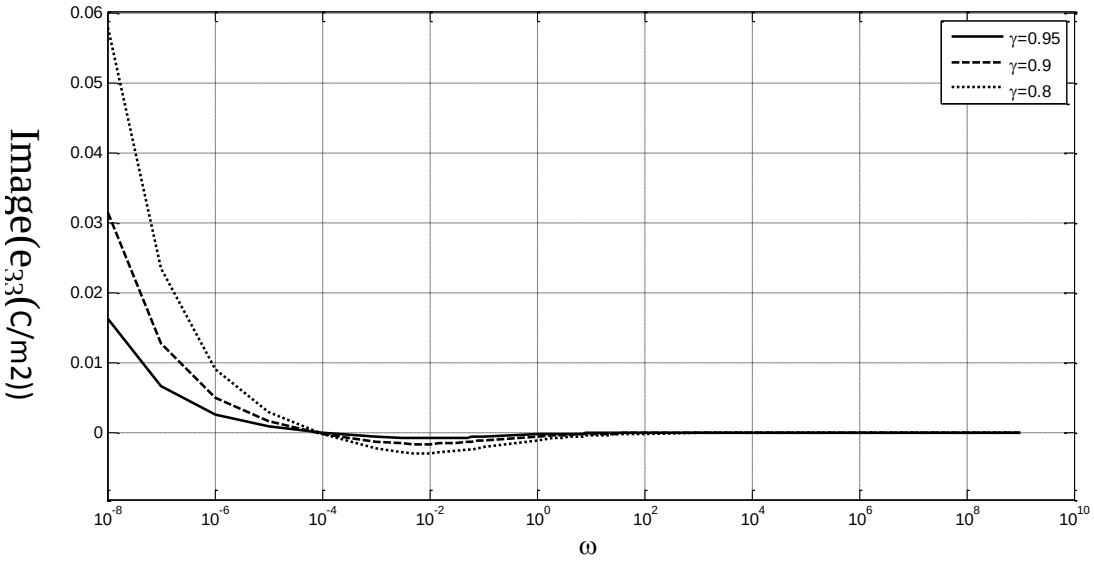

Figure 4.19: Effective piezoelectric modulus Image(e_{33}) for a fibrous viscoelectroelastic composites consisting of Glass inclusions surrounded by piezoelectric coating layer (PZT-7A) embedded in a viscoelastic matrix (LaRC-SI) with fixed volume fraction of the matrix (fm=0.6).

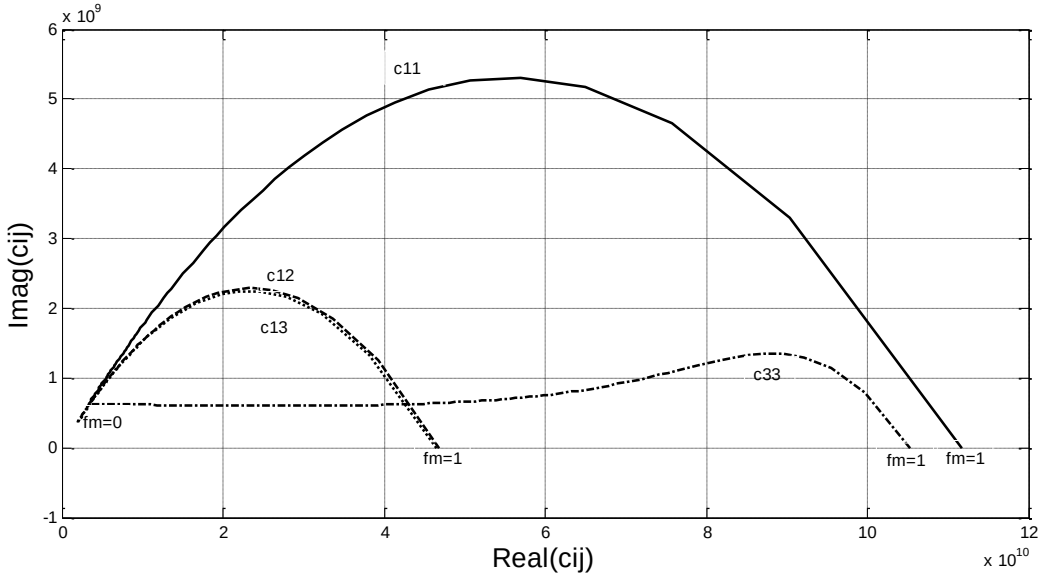

Figure 4.20: Storage and loss map of elastic moduli, of a fibrous viscoelectroelastic composite consisting of Glass inclusions surrounded by piezoelectric coating layer (PZT-7A) embedded in a viscoelastic matrix (LaRC-SI), with respect to the volume faction of reinforcements and with fixed value of frequency $\omega = 0.05(1/hour)$ and fixed thickness of the coating $\gamma = 0.8$.

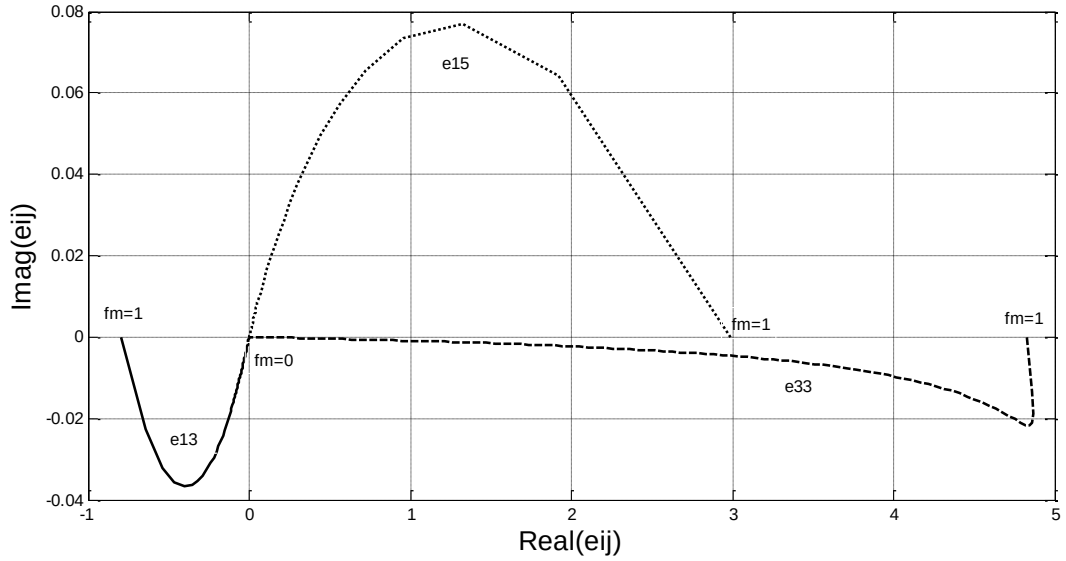

Figure 21: Storage and loss map of piezoelectric moduli, of a fibrous viscoelectroelastic composite consisting of Glass inclusions surrounded by piezoelectric coating layer (PZT-7A) embedded in a viscoelastic matrix (LaRC-SI), with respect to the volume faction of reinforcements and with fixed value of frequency $\omega = 0.05(1/hour)$ and fixed thickness of the coating $\gamma = 0.8$.

4.6.2.2 Time domain

The time dependent effective piezoelectric moduli e_{31} and e_{33} are presented in figures 4.22 and 4.23 for a fibrous viscoelectroelastic composites consisting of Glass inclusions surrounded by piezoelectric coating layer embedded in a viscoelastic matrix with respect to time and thickness of the piezoelectric coating layer. It is shown that e_{31} and e_{33} are affected by the viscoelastic behavior of the matrix and increases with time. One can deduce from figure that e_{31} is more affected by the viscoelastic behavior of the matrix than e_{33}. e_{33} seems to vary slightly with time.

The evolution e_{31} is shown with respect to the shape of inclusion (c_1/a_1) and time for a fibrous viscoelectroelastic composite consisting of Glass inclusions surrounded by piezoelectric coating layer embedded in viscoelastic matrix is shown in figure 4.24 for fixed thickness of the coating layer and fixed volume fraction of the matrix. The inclusion shape effect on e_{31} with respect to time is shown.

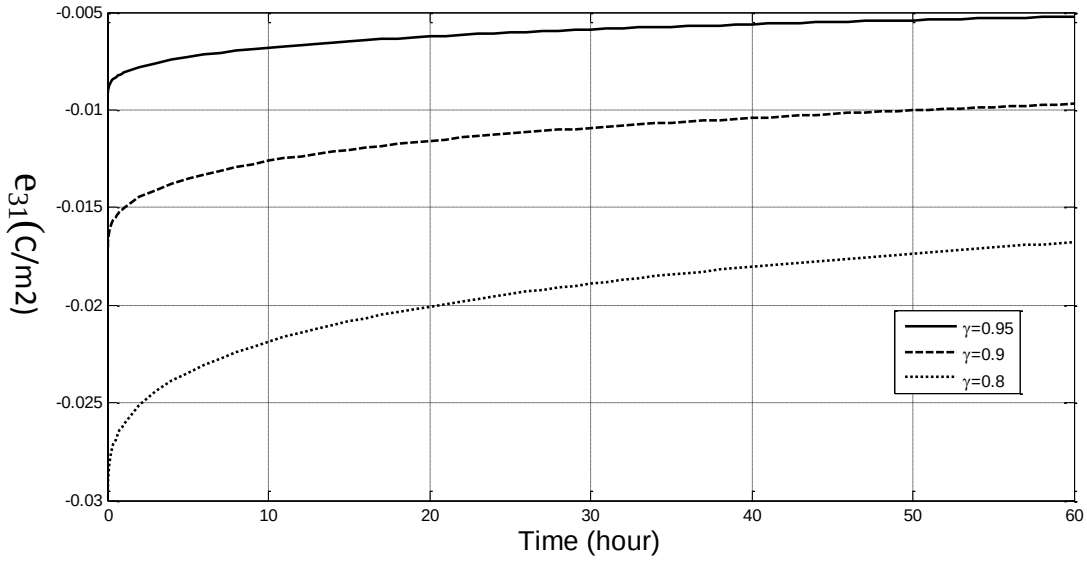

Figure 4.22: Effective piezoelectric modulus e_{31} for a fibrous viscoelectroelastic composite consisting of Glass inclusions surrounded by piezoelectric layer (PZT-7A) embedded in a viscoelastic matrix (LaRC-SI) with fixed volume fraction of the matrix (fm=0.6).

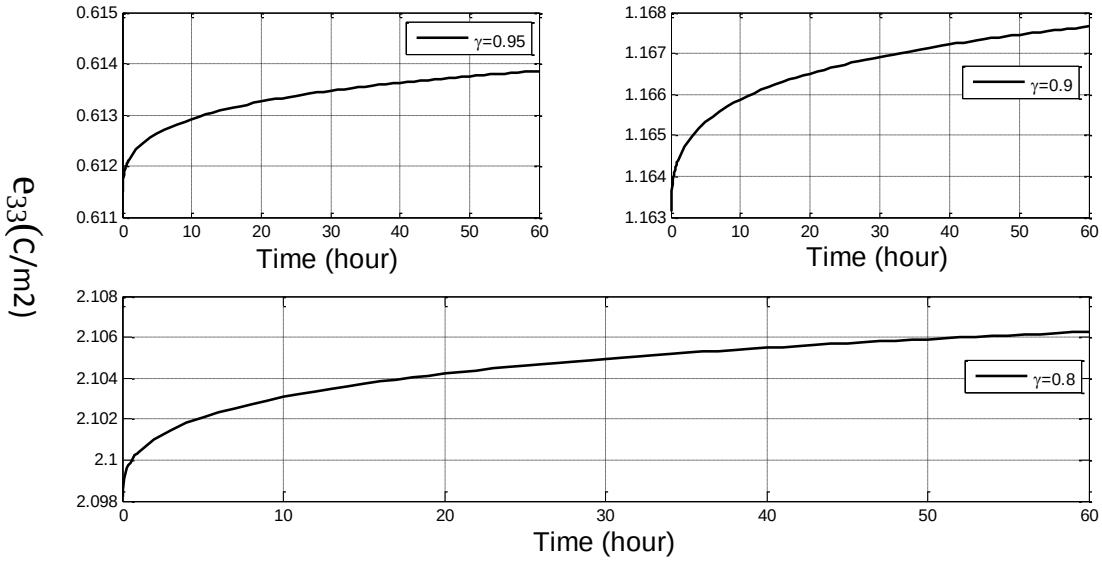

Figure 4.23: Effective piezoelectric modulus e_{33} for a fibrous viscoelectroelastic composite consisting of Glass inclusions surrounded by piezoelectric layer (PZT-7A) embedded in a viscoelastic matrix (LaRC-SI) with fixed volume fraction of the matrix (fm=0.6).

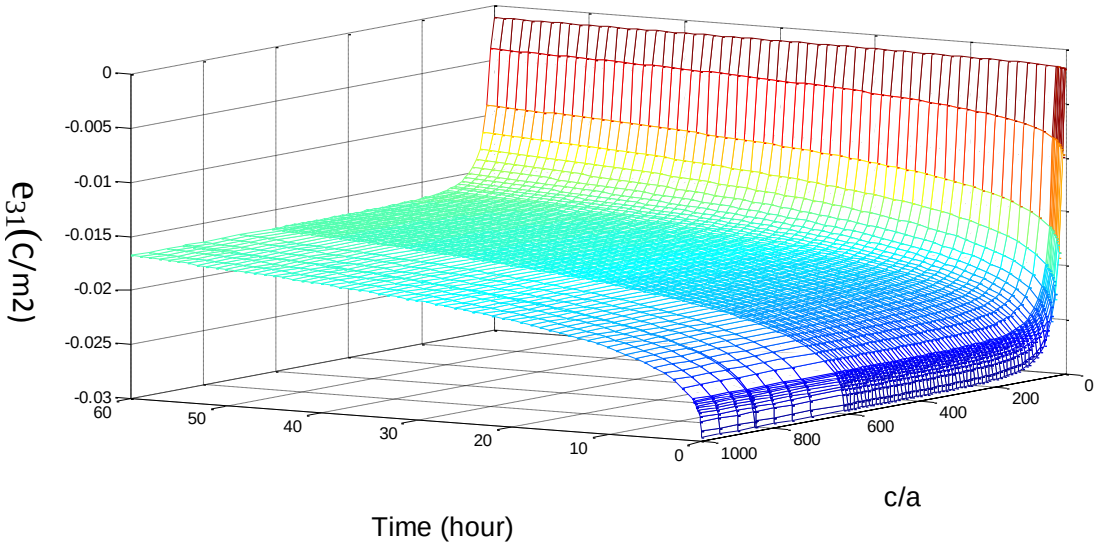

Figure 4.24: Effective piezoelectric modulus e_{31} of a fibrous viscoelectroelastic composite consisting of Glass inclusions surrounded by piezoelectric layer (PZT-7A) embedded in a viscoelastic matrix (LaRC-SI) with fixed volume fraction of the matrix (fm=0.6) and fixed thickenss of the coating layer ($\gamma = 0.8$).

4.7 Conclusion

In this work, a micromechanical modeling is developed to predict viscoelectroelastic effective properties of piezoelectric composites. Two kinds of composites are investigated. One is consisting of piezoelectric inclusions embedded in a viscoelastic matrix. The other one is consisting of Glass inclusions surrounded with a piezoelectric coating layer embedded in a viscoelastic matrix. The piezoelectric and Glass material properties are considered to be time independent. The modeling is based on the correspondence principle and the Mori-Tanka mean field approach. The effective properties are first derived in Carson frequency domain and then inverted numerically to time domain by using the inverse of Laplace transform. The numerical results are presented both in frequency and time domain. The effect of volume fraction and shape of inclusions as well as the thickness of the coating layer is shown on the effective properties. It is shown from the numerical results that even if the piezoelectric coefficients of the piezoelectric material are assumed to be time independent, the effective piezoelectric moduli of composites shows time dependence. This is explained by the fact that the viscoelastic behavior of the matrix affects the whole behavior of the composite.

4.8 Perspectives

The mathematical methodology developed for viscoelectroelastic composites will be generalized in chapter 5 to investigate the behavior of materials with fourth functionality visco-magneto-electro-elastic. The aim will be to predict new materials with optimized active and damping properties. The modeling is going to be developed for two kinds of viscomagnetoelectroelastic composites: multi-phase and multi-coated viscomagnetoelectroelastic composites. Applying the Carson transform to the constitutive equation allows the extension of the classical Mori-Tanaka model to the Carson domain. The effective properties will first be derived in the Frequency domain and the converted numerically the time domain based on Laplace transform. The numerical results will be presented with respect to time, frequency, shape, volume fraction of reinforcements as well as to the coated thickness.

References

[1]Aldraihem, O. J.;Baz, A.; Al-Saud, T. S. (2007)**:** Hybrid Composites with Shunted Piezoelectric Particles for Vibration Damping. Mechanics of Advanced Materials and Structures, Vol. 14, pp. 413–426.

[2]Abate, J.; Valko, P. P. (2004): Multi-precision Laplace transform inversion. Int. J. Numer. Meth. Engng. Vol. 60, pp. 979–993.

[3]Bakkali, A.; Azrar, L.; Fakri, N. (2011): Modeling of effective properties of multiphase magnetoelectroelastic heterogeneous materials" Journal Computers, Materials & Continua, Vol. 23, N°3, pp 201-231.

[4]Bakkli, A.; Azrar, L.; Aljinaidi, A. A. (2012): Multi-coated magnetoelectroelastic composites with functionally graded interphases. MATEC Web of Conferences 1, 09001.

[5]Brinson, L. C.; Lin, W. S. (1998): Comparison of micromechanics methods for effective properties of multiphase viscoelastic composites. Composites Structures, Vol. 41, pp. 353-367.

[6]Dunn, M. L.; Taya, M. (1993): Micromechanics predictions of the effective electroelastic moduli of piezoelectric composites. Int. J. Solids Structures, Vol.30, No. 2, pp. 161-175.

[7]Fei, X.; Gengkai, H.; Zhuping, H. (2004): Influence of Gradual Interphase on Overall Elastic and Viscoelastic Properties of Particulate Composites. International Journal of Thermoplastic Composites Materials, Vol. 17, pp.411-425.

[8]Fisher, F. T.; Brinson, L.C. (2001): Viscoelastic interphases in polymer-matrix composites: theoretical models and finite-element analysis. Composites Science and Technology, Vol. 61, pp. 731-748.

[9]Fakri, N.; Azrar, L.; El Bakkali, L. (2003): Electoelastic behavior modeling of piezoelectric composite materials containing spatially oriented reinforcements. International Journal of Solids and Structures, Vol. 40, Issue 2, pp. 361-384.

[10]Fakri, N.; Azrar, L. (2010): Thermal and electro-elastic behavior of piezo-composites and inhomogeneous piezoelectric materials with voids. Journal of Intelligent Materials Systems and Structures, Vol. 21, N°2, pp. 161-174.

[11]Jiang, B.; Batra, R. C. (2001): Effective electroelastic properties of a piezocomposite with viscoelastic and dielectric relaxing matrix. Journal of Intelligent Materials Systems and Structures, Vol. 12, pp. 847-866.

[12]Haberman, M. R.; Berthelot, Y. H.; Jarzynski, J.; Cherkaoui, M. (2002): Micromechanical modeling of viscoelastic voided composites in the low-frequency approximation. Acoustical Society of America, Vol. 112, N°5, pp. 1937-1943.

[13]Lévesque, M.; Derrien, K.; Mishnaevski Jr., L.; Baptiste, D.; Gilchrist, M. D. (2004): A micromechanical model for nonlinear viscoelastic particle reinforced polymeric composite materials-undamaged state. Composites: Part A, Vol. 35, pp. 905-913.

[14]Li, J.Y (2004): The effective pyroelectric and thermal expansion coefficients of ferroelectric ceramics. Mechanics of Materials, Vol. 36, pp. 949–958.

[15]Li, K.; Gaw, X.-L.; Roy, A. K. (2006): Micromechanical Modeling of Viscoelastic Properties of Carbon Nanotube-Reinforced Polymer Composites. Mechanics of Advanced Materials and Structures, Vol. 13, pp. 317-328.

[16]Matzenmiller, A.; Gerlach, S. (2004): Micromechanical modeling of viscoelastic composites with compliant fiber–matrix bonding. Computational Material Science, Vol. 29, pp. 283-300.

[17] Muliana, A.; Li, K. (2010): Time-dependent response of active composites with thermal, electrical, and mechanical coupling effect. International Journal of Engineering Science, Vol. 48, pp. 1481–1497.

[18]Odegard, G.M. (2004): Constitutive Modeling of Piezoelectric Polymer Composites. Acta Materialia, Vol. 52, No.18, pp.5315-5330.

Chapter 5

5. Modeling and prediction of viscomagnetoelectroelastic effective properties of heterogeneous materials

Abstract

In this paper, the effective properties of new active-passive multifunctional viscomagnetoelectroelastic composite materials are modeled and numerically predicted. The use of the correspondence principle of linear viscomagnetoelectroelasticity and the Carson transform allow the extension of the Mori-Tanaka micromechanical model to the Carson domain. Based on the viscomagnetoelectroelastic integral equations and the interfacial operators the concentration tensors are derived for multi-phase and multi-coated viscomagnetoelectroelastic composites. The effective properties are derived in the Carson domain and then inverted numerically to the time domain using the inverse of the Laplace transform. The effective properties are obtained in both frequency and time domains. The obtained hybrid coupling coefficients can be used for active and passive properties. The multifunctional effect can be enhanced by a proper choice of the shape and volume fraction of reinforcements as well as by coating thickness.

5.1 Introduction

Smart composites have attracted the attention of many researchers due to their unique properties obtained by combining two different active materials. The magnetoelectric effect has attracted attention due its several application broadband magnetic field probes, electronic packaging, acoustic devices, hydrophones, medical ultrasonic imaging, sensors, and actuators [1-5]. Piezoelectric and piezomagnetic materials are usually brittle and they are susceptible to fracture. The addition of a polymer phase to the magnetoelectroelastic composites will give to the composite ductility and formability [6]. At elevated temperature these kinds of composites have a time dependent behavior due to the polymer phase that has a strong viscoelastic behavior at elevated temperature. The viscoelastic and viscoelectroelastic behaviors of composite materials have been investigated by many researchers.

For viscoelastic composites, [7] examined the use of different micromechanics method to determine the effective composite properties when all the phases are viscoelastic. The effective properties of a three-phase viscoelastic composite predicted by [8] using the original Mori-Tanaka micromechanical model and the extended one that takes into account the interphase regions between the matrix and fibers. The Self Consistent micromechanical model was used by [9] to predict the effective properties of viscoelastic composites consisting of spherical coated inclusions. The effective properties of viscoelastic composites was investigated based on the micromechanical method of cells in [10]. The effect of the gradual interphase on the effective elastic and viscoelastic properties of particulate composites was investigated in [11]. A theoretical model was developed in [12] to investigate the nonlinear behavior of nonlinear viscoelastic composites. [13] investigated the effective properties of a carbon nanotube-reinforced polymer composites by using the Mori-Tanaka micromechanical model combined with correspondence principle.

For viscoelectroelastic composites, the effective properties of viscoelectroelastic composites were investigated in [14] based on the Mori-Tanaka mean field micromechanical approach coupled with the correspondence principle. Closed form expressions of the effective moduli were given for viscoelectroelastic composites consisting of parallel PZT cylinder of elliptic cross section embedded in a viscoelastic matrix. An analytical model was proposed in [15] to investigate viscoelastic properties of hybrid composites with shunted piezoelectric particles. [16] developed a micromechanical modeling and a finite element model to investigate the effective

time dependent properties of piezoelectric composites consisting of PZT fiber and a polymer matrix. The viscopiezoelectric effective properties of piezoelectric heterogeneous materials are predicted in both time and frequency domains in [17] based on the correspondence principle combined with the Mori-Tanaka micromechanical model.

The aim of this work is to generalize the methodological approach presented in [17] for the prediction of the effective viscomagnetoelectroelastic behavior of heterogeneous magnetoelectroelastic composites. The modeling is developed for two kinds of viscomagnetoelectroelastic composites: multi-phase and multi-coated viscomagnetoelectroelastic composites. Applying the Carson transform to the constitutive equation allows the extension of the classical Mori-Tanaka model to the Carson domain. The derivation of the concentration tensors of multi-phase viscomagnetoelectroelastic composites is based on the solution of the integral equation. For multi-coated viscomagnetoelectroelastic composites the multi-coated inclusion effect and the viscomagnetoelectroelastic interfacial operators are accounted for. Once the concentration tensors are derived, the homogenization process is used to express the effective behavior of composites. The obtained effective properties are in the Carson domain and the conversion to the time domain is done numerically based on the Laplace transform inversion. The numerical results are presented with respect to time, frequency, shape, volume fraction of reinforcements as well as to the coated thickness.

5.2 Constitutive equations for linear viscomagnetoelectroelastic materials

For linear magnetoelectroelastic materials, the magnetic, electric and elastic fields are coupled through the following constitutive equations:

$$\begin{aligned} \sigma_{ij} &= c_{ijkl}\varepsilon_{kl} - e_{lij}E_l - h_{lij}H_l \\ D_i &= e_{ikl}\varepsilon_{kl} + \kappa_{il}E_l + \alpha_{il}H_l \\ B_i &= h_{ikl}\varepsilon_{kl} + \alpha_{il}E_l + \mu_{il}H_l \end{aligned} \tag{5.1}$$

where the elastic strain ε_{kl}, electric fields E_l and magnetic fields H_l are independent variables related to stresses σ_{ij}, electric displacements D_i and magnetic inductions B_i. The tensors c_{ijkl}, e_{lij}, h_{lij}, α_{il}, κ_{il} and μ_{il} are the elastic, piezoelectric, piezomagnetic, magnetoelectric, dielectric and magnetic permeability constants respectively. In the constitutive equations we use $-E_l$ and -

H_l rather than E_l and H_l as they will permit the construction of a symmetric matrix of constitutive moduli.

This work deals with the viscomagnetoelectroelastic behavior of polymer magnetoelectroelastic composites at fixed temperature. These kinds of composites show time dependent properties due to polymer phase that have a strong time-dependent behavior at elevated temperature. The time dependent constitutive model of magnetoelectroelastic homogeneous material is obtained by generalizing the Blotzmann principle for linear viscoelastic materials. One can write:

$$\begin{aligned}
\sigma_{ij}(t) &= \int_0^t c_{ijkl}(t-\tau)\frac{d\varepsilon_{kl}(\tau)}{d\tau}d\tau + \int_0^t e_{lij}(t-\tau)\frac{dE_l(\tau)}{d\tau}d\tau + \int_0^t h_{lij}(t-\tau)\frac{dH_l(\tau)}{d\tau}d\tau \\
D_i(t) &= \int_0^t e_{ikl}(t-\tau)\frac{d\varepsilon_{kl}(\tau)}{d\tau}d\tau + \int_0^t \kappa_{il}(t-\tau)\frac{dE_l(\tau)}{d\tau}d\tau + \int_0^t \alpha_{il}(t-\tau)\frac{dH_l(\tau)}{d\tau}d\tau \\
B_i(t) &= \int_0^t h_{ikl}(t-\tau)\frac{d\varepsilon_{kl}(\tau)}{d\tau}d\tau + \int_0^t \alpha_{il}(t-\tau)\frac{dE_l(\tau)}{d\tau}d\tau + \int_0^t \mu_{il}(t-\tau)\frac{dH_l(\tau)}{d\tau}d\tau
\end{aligned} \tag{5.2}$$

Using the condensed notation [18, 21], one can write the time constitutive model in the following form

$$\Sigma_{iJ}(t) = \int_0^t E_{iJKl}(t-\tau)\frac{dZ_{Kl}(\tau)}{d\tau}d\tau \tag{5.3}$$

where

$$E_{iJKl}(t) = \begin{cases} c_{ijkl}(t) & (J,K=1,2,3) \\ e_{lij}(t) & (J=1,2,3;K=4) \\ h_{lij}(t) & (J=1,2,3;K=5) \\ e_{ikl}(t) & (J=4;K=1,2,3) \\ h_{ikl}(t) & (J=5;K=1,2,3) \\ -\kappa_{il}(t) & (J=4;K=4) \\ -\alpha_{il}(t) & (J=4;K=5 or J=5;K=4) \\ -\mu_{il}(t) & (J=5;K=5) \end{cases} ; Z_{Kl}(t) = \begin{cases} \varepsilon_{kl}(t) & (K=1,2,3) \\ -E_l(t) & (K=4) \\ -H_l(t) & (K=5) \end{cases} \text{ and } \Sigma_{iJ}(t) = \begin{cases} \sigma_{ij}(t) & (J=1,2,3) \\ D_i(t) & (J=4) \\ B_i(t) & (J=5) \end{cases} \tag{5.4}$$

are the time dependent viscomagnetoelectroelastic relaxation tensor, Z and Σ are the generalized stress and strain respectively.

The convolution integral (5.3) gives a mathematical equation that relates the generalized stress Σ to the generalized strain Z through the viscomagnetoelectroelastic relaxation function $E(t)$.

For frequency analysis, let us consider the following time harmonic generalized strain

$$Z_{Kl}(t) = \bar{Z}_{Kl}(\omega)e^{i\omega t} \tag{5.5}$$

Substituting (5.5) into (5.3) and using the following changing variable $u = t - \tau$, one can find

$$\Sigma_{iJ}(t) = i\omega e^{i\omega t}\int_0^t E_{iJKl}(u)e^{-i\omega u}du\bar{Z}_{Kl}(\omega) \tag{5.6}$$

This leads to the following harmonic generalized stress tensor

$$\Sigma_{iJ}(t) = \bar{\Sigma}_{iJ}(\omega)e^{i\omega t} \tag{5-7-a}$$

$$\bar{\Sigma}_{iJ}(\omega) = i\omega\int_0^t E_{iJKl}(u)e^{-i\omega u}du\bar{Z}_{Kl}(\omega) \tag{5.7-b}$$

Viscomagnetoelectroelastic problem can be formally reduced to a magnetoelectroelastic one by using the Carson transform. The Carson transform of a time dependent function is given by:

$$\bar{f}(s) = s\int_0^t f(t)e^{-ts}dt \tag{5.8}$$

in which s is the Carson variable.

By taking $s = i\omega$, equation (5.7) could be written as following

$$\bar{\Sigma}_{iJ}(s) = s\bar{E}_{iJKl}(s)\bar{Z}_{Kl}(s) \tag{5.9}$$

where $\bar{\Sigma}(s) = s\bar{\Sigma}(\omega)$, $\bar{E}(s) = s\int_0^t E(u)e^{-su}du$ and $\bar{Z}(s) = s\bar{Z}(\omega)$

Equation (5.9) shows the analogy between the linear viscomagnetoelectroelastic problem and linear magnetoelectroelastic problem. The role played by $E(s)$ in linear viscomagnetoelectroelasticity is the same role played by the magnetoelectroelastic moduli E in linear magnetoelectroelasticity.

The equilibrium equations, in the absence of body force, electric charge and electric current densities, are given in the frequency domain by:

$$\bar{\sigma}_{ij,i}(s) = 0 \qquad \bar{D}_{i,i}(s) = 0 \qquad \bar{B}_{i,i}(s) = 0 \tag{5.10}$$

Using the above condensed notations, the equilibrium equations are written as follow:

$$\bar{\Sigma}_{iJ,i}(s) = 0 \tag{5.11}$$

Based on the symmetry of the tensors $c, e, h, \kappa, \mu, \alpha$ the following equilibrium partial differential equation is obtained:

$$(\bar{E}_{iJKl}(s)\bar{U}_{K,l}(s))_{,i} = 0 \tag{5.12}$$

5.3 Multi-phase viscomagnetoelectroelastic composites

This section deals with N-phase viscomagnetoelectroelastic composites. The Mori-Tanaka mean field concentration tensors are derived based on the solution of the viscomagnetoelectroelastic integral equation.

5.3.1 Localization equation

Considering a homogeneous fictitious media called "reference media" which has the viscomagnetoelectroelastic moduli $\bar{E}^0_{iJMn}(s)$. The expression of the local viscomagnetoelectroelastic moduli is given as follow:

$$\bar{E}_{iJMn}(r,s) = \bar{E}^0_{iJMn}(s) + \delta\bar{E}_{iJMn}(r,s) \tag{5.13}$$

where "r'' is the position vector in the considered media and δE is the deviation part. The introduction of this expression into (5.12) leads to

$$\bar{E}^0_{iJMn}(s)\bar{U}_{M,ni}(r,s) + (\delta\bar{E}_{iJMn}(r,s)\bar{U}_{M,n}(r,s))_{,i} = 0 \tag{5.14}$$

The viscomagnetoelectroelastic Green tensor of the reference media is related to the reference medium by the following equation:

$$\bar{E}^0_{iJMn}(s)\bar{G}_{MK,in}(r-r',s) + \delta_{JK}\delta(r-r') = 0 \tag{5.15}$$

Using (5.14), (5.15) and after some mathematical manipulations, the same integral equation derived by [18] for linear magnetoelectroelastic composite materials, is obtained here in the Carson domain for viscomagnetoelectroelastic composite materials.

$$\bar{Z}_{Kl}(r,s) = \bar{Z}^0_{Kl}(r,s) - \int_V \bar{\Gamma}_{iJKl}(r-r',s)(\delta\bar{E}_{iJMn}(r',s)\bar{Z}_{Mn}(r',s))dV' \tag{5.16}$$

where $\bar{\Gamma}_{iJKl}(r-r',s) = -\bar{G}_{JK,li}(r-r',s)$ is a condensed notation of nine tensors.

To solve this integral equation, the same procedure used by [18] is flowed. An infinite medium is considered with viscomagnetoelectroelastic moduli $\bar{E}^0_{iJMn}(s)$ which contains a single inclusion ''I" of volume V^I and viscomagnetoelectroelastic moduli $\bar{E}^I_{iJMn}(s)$ assumed to be constant

inside the volume V^I. Based on these assumptions, the derivation part in (5.16) is expressed as follow:

$$\delta\bar{E}_{iJMn}(r,s) = \Delta\bar{E}^I_{iJMn}(s)\theta^I(r) \tag{5.17}$$

in which $\Delta\bar{E}^I_{iJMn}(s) = \bar{E}^I_{iJMn}(s) - \bar{E}^0_{iJMn}(s)$ and $\theta^I(r)$ is the characteristic function of V^I.

Using (5.17) and averaging (5.16) over the inclusion volume lead to the expression of the local generalized viscomagnetoelectroelastic strain in the inclusion.

$$\bar{Z}^I_{Kl}(s) = \bar{Z}^0_{Kl}(s) - \frac{1}{V^I}\int_{V^I}\int_V \bar{\Gamma}_{iJKl}(r-r',s)\Delta\bar{E}^I_{iJMn}(s)\theta^I(r')\bar{Z}_{Mn}(r',s)dV'dV \tag{5.18}$$

Replacing $\bar{Z}_{Mn}(r',s)$ by its average value $\bar{Z}^I_{Kl}(s)$ in the considered inclusion leads to the following localization equation:

$$\bar{Z}^I_{Kl}(s) = \bar{Z}^0_{Kl}(s) - \frac{1}{V^I}\bar{T}^{II}_{iJKl}(\bar{E}^0(s))\Delta\bar{E}^I_{iJMn}(s)\bar{Z}^I_{Mn}(s) \tag{5.19}$$

where $\bar{T}^{II}_{iJKl}(\bar{E}^0(s)) = \int_{V^I}\int_{V^I}\bar{\Gamma}_{iJKl}(r-r',s)dV'dV$ represents the condensed notation of the nine viscomagnetoelectroelastic interaction tensors. These tensors are computed numerically [18] for various shapes of inclusions using the Gaussian quadrature integration for the considered inclusion shape. After the derivation of the localization equation (5.19) many micro mechanical models could be used to derive the concentration tensors. In this work the Mori-Tanaka micromechanical model is used to derive the viscomagnetoelectroelastic concentration tensor for multi-phase viscomagnetoelectroelastic composites.

5.3.2 N-phase Mori-Tanaka model

The main assumption of the Mori-Tanaka Mean field approach is the consideration that the infinite reference medium has the properties of the matrix and the generalized strain $\bar{Z}^0(s)$ in the infinite medium equal the average generalized strain in the matrix $\bar{Z}^m(s)$. So, to have the expression of the Mori-Tanaka concentration tensor, the generalized strain field $\bar{Z}^0(s)$ and the viscomagnetoelectroelastic moduli $\bar{E}^0(s)$ of the reference medium in equation (5.19) are replaced respectively by the generalized strain field $\bar{Z}^m(s)$ and the viscomagnetoelectroelastic moduli $E^m(s)$ of the matrix. Using these assumptions one can write.

$$\bar{Z}^I_{Mn}(s) = \bar{A}^I_{MnKl}(s)\bar{Z}^m_{Kl}(s) \tag{5.20}$$

in which $\bar{A}^{I}_{MnKl} = (I_{KlMn} + \frac{1}{V^{I}} \bar{T}^{II}_{iJKl}(\bar{E}^{m}(s))\Delta\bar{E}^{I}_{iJMn}(s))^{-1}$ and $\Delta\bar{E}^{I}_{iJMn}(s) = \bar{E}^{I}_{iJMn}(s) - \bar{E}^{m}_{iJMn}(s)$

The expression of the averaged generalized strain applied over the composite is given by

$$\bar{Z}(s) = f_m \bar{Z}^{m}(s) + \sum_{I=2}^{n} f_I \bar{Z}^{I}(s) \tag{5.21}$$

Using (5.20) and (5.21), one can derive the expression that relates the local generalized strain in the inclusion with the applied generalized strain over the composite.

$$\bar{Z}^{I}_{Sj}(s) = \bar{A}^{I}_{KlSj}(s)(f_m I_{KlMn} + \sum_{I=2}^{N} f_I \bar{A}^{I}_{MnKl}(s))^{-1} \bar{Z}_{Mn}(s) \tag{5.22}$$

Form (5.22), one can write the expression of the Mori-Tanaka concentration tensor for multi-phase viscomagnetoelectroelastic composites.

$$\bar{A}^{MT}_{SjMn}(s) = \bar{A}^{I}_{KlSj}(s)(f_m I_{KlMn} + \sum_{I=2}^{N} f_I \bar{A}^{I}_{MnKl}(s))^{-1} \tag{5.23}$$

Using the homogenization processes, the effective properties for multi-phase viscomagnetoelectroelastic composites is given

$$\bar{E}^{eff}_{iJKl}(s) = \bar{E}^{m}_{iJKl}(s) + \sum_{I=2}^{N} f^{I}(\bar{E}^{I}_{iJMn}(s) - \bar{E}^{m}_{iJMn}(s))\bar{A}^{MT}_{MnKl}(s) \tag{5.24}$$

5.4 Multi-coated viscomagnetoelectroelastic composites

This section deals with multi-coated viscomagnetoelectroelastic composites. The derivation of the localization equation goes through the solution of the multi-coated viscomagnetoelectroelastic integral equation and the use of the viscomagnetoelectroelastic interfacial operators. The Mori-Tanaka mean field approach is used to derive the concentration tensors.

5.4.1 Localization equation

Here, Equation (5.16) is extended for multi-coated viscomagnetoelectroelastic composites by expressing the deviation part as follow:

$$\delta\bar{E}_{iJMn}(s) = \sum_{k=0}^{n} \Delta\bar{E}^{(k/0)}_{iJMn}(s)\theta^{k}(r) \quad ; \; k \in \{0,1,2,...n\} \tag{5.25}$$

where $\theta^{k}(r)$ is the characteristic function and $\Delta\bar{E}^{(k/0)}_{iJMn}(s) = \bar{E}^{k}_{iJMn}(s) - \bar{E}^{0}_{iJMn}(s)$

Using (5.25) the following integral equation is obtained:

$$\bar{Z}_{Kl}(r,s)=\bar{Z}^{0}_{Kl}(r,s)-\sum_{k=1}^{n}\int_{V_k}\bar{\Gamma}_{iJKl}(r-r',s)\Delta\bar{E}^{(k/0)}_{iJMn}(s)\bar{Z}_{Mn}(r',s)dV' \tag{5.26}$$

Considering V_I the total volume of the composite inclusion, which consists of an inclusion surrounded by (n-1) coatings and f_k is the volume fraction of the phase k. One can write:

$$V_I=\sum_{k=1}^{n}V_k \tag{5.27}$$

The average local generalized strain field can be written as:

$$\bar{Z}_{Mn}(r,s)=\sum_{k=1}^{n}\bar{Z}^{k}_{Mn}(s)\theta^{k}(r) \tag{5.28}$$

Substituting (5.28) into (5.26) and averaging (5.26) over the volume of the composite inclusion, one can find the following localization equation:

$$\bar{Z}^{I}_{Kl}(s)=\bar{Z}^{0}_{Kl}(s)-\frac{1}{V_I}\sum_{k=1}^{n}\bar{T}^{Ik}_{iJKl}(E^{0}(s))\bar{E}^{(k/0)}_{iJMn}(s)\bar{Z}^{k}_{Mn}(s) \tag{5.29}$$

where $\bar{T}^{Ik}_{iJKl}(\bar{E}^{0}(s))=\int_{V_I}\int_{V_k}\bar{\Gamma}_{iJKl}(r-r',s)dV'dV$ represents the condensed notation of the viscomagnetoelectroelastic interaction tensor.

Using the fact that $\bar{Z}^{I}_{Kl}(s)=\sum_{k=1}^{n}\frac{V_k}{V_I}\bar{Z}^{k}_{Kl}(s)$ leads to:

$$\sum_{k=1}^{n}\frac{V_k}{V_I}(I_{KlMp}+\frac{1}{V_k}\bar{T}^{Ik}_{iJKl}(\bar{E}^{0}(s))\Delta\bar{E}^{(k/0)}_{iJMp})\bar{Z}^{k}_{Mp}(s)=\bar{Z}^{0}_{Kl}(s) \tag{5.30}$$

where I_{KlMn} is the shorthand notation of the fourth order and the second order identity tensors:

$$I_{KlMp}=\begin{cases}1/2(\delta_{km}\delta_{lp}+\delta_{kp}\delta_{lm}) & (K,M=1,2,3)\\ 0 & (K=1,2,3;M=4)\\ 0 & (K=1,2,3;M=5)\\ 0 & (K=4;M=1,2,3)\\ 0 & (K=5;M=1,2,3)\\ \delta_{lp} & (K=4;M=4)\\ 0 & (K=4;M=5 or K=5;M=4)\\ \delta_{lp} & (K=5;M=5)\end{cases} \tag{5.31}$$

Denoting by $\bar{a}^{k}$ the local concentration tensor relating the average generalized strain in each coating with the average generalized strain in the inclusion, one can put:

$$\bar{Z}^k_{Mn}(s) = \bar{a}^k_{MnKl}(s)\bar{Z}^1_{Kl}(s) \quad \text{with} \quad \bar{a}^1_{MnKl} = I_{MnKl} \tag{5.32}$$

Using (5.32) and (5.30), the following relationship is obtained

$$\bar{Z}^k_{Mn}(s) = \bar{a}^k_{MnPv}(s)\left[\sum_{k=1}^{n}\left(\frac{f_k}{f_I}\left(I_{KlPv} + \frac{1}{V_k}\bar{T}^{Ik}_{iJKl}(E^0(s))\Delta\bar{E}^{(k/0)}_{iJRs}\right)\bar{a}^k_{RsPv}(s)\right)\right]^{-1}\bar{Z}^0_{Kl}(s) \tag{5.33}$$

To derive the expression of the local concentration tensor $\bar{a}^k$ the viscomagnetoelectroelastic interfacial operators are introduced which give the generalized strain jump field across an interface between two different phases by the following equation [18, 19, 20]:

$$\bar{Z}^{k+1}_{Mn}(r,s) - \bar{Z}^k_{Mn}(r,s) = \bar{P}^{k+1}_{iJMn}(E^{K+1}(s), N)(\bar{E}^k_{iJRs}(s) - \bar{E}^{k+1}_{iJRs}(s))\bar{Z}^k_{Rs}(r,s) \tag{5.34}$$

Using (5.34) and following the same procedure done by Bakkali et al. (2013)[19, 20, 21] to derive the concentration tensors for multi-coated magnetoelectroelastic composites, the expression of the local localization tensor is obtained as follow:

$$\bar{a}^k_{MnKl}(s) = \sum_{i=1}^{k-1} f_i \bar{W}^{(i/k)}_{MnRs}(s)\bar{a}^i_{RsKl}(s) / (\sum_{i=1}^{k-1} f_i) \quad \text{and} \quad W^{(i/k)}_{MnRs}(s) = (I_{MnRs} + \bar{T}^k_{pJMn}(\bar{E}^k(s))\Delta\bar{E}^{(i/k)}_{pJRs}(s)) \tag{5.35}$$

5.4.2 Multi-coated Mori-Tanaka model

To obtain the expression of the Mori-Tanaka mean field approach localization tensors, the generalized strain field $\bar{Z}^0(s)$ and the viscomagnetoelectroelastic moduli $\bar{E}^0(s)$ of the reference medium in (5.30) are replaced respectively by the generalized strain field $\bar{Z}^M(s)$ and the viscomagnetoelectroelastic $\bar{E}^m(s)$ in the matrix. The following relationship is obtained:

$$\bar{A}^{MT}_{MnKl}(s) = \bar{a}^k_{MnPv}(s)\left[\sum_{k=1}^{n}\left(\frac{f_k}{f_I}\left(I_{KlRs} + \frac{f_m}{V_k}T^{Ik}_{iJKl}(\bar{E}^M(s))\Delta\bar{E}^{(k/m)}_{iJRs}(s)\right)\bar{a}^k_{RsPv}(s)\right)\right]^{-1} \tag{5.36}$$

in which $\Delta\bar{E}^{(k/m)}_{iJRs}(s) = \bar{E}^k_{iJRs}(s) - \bar{E}^m_{iJRs}(s)$ and $f_m = 1 - f_I$ is the volume fraction of the matrix.

Similarly to the N-phase Mori-Tanaka model, the effective behavior of multi-coated viscomagnetoelectroelastic composites can be obtained by

$$\bar{E}^{eff}_{iJKl}(s) = \bar{E}^m_{iJKl}(s) + \sum_{I=2}^{N} f^I(\bar{E}^I_{iJMn}(s) - \bar{E}^m_{iJMn}(s))\bar{A}^{MT}_{MnKl}(s) \tag{5.37}$$

(5.24) and (5.37) give the effective behavior of N-phase and multi-coated viscomagnetoelectroelastic in Carson domain. The effective behavior could be inverted to the time domain based on the numerical inversion of Laplace transform.

$$E_{iJKl}^{eff}(t)=\frac{1}{2\pi i}\int_{\delta+i\infty}^{\delta+i\infty}\frac{\bar{E}_{iJKl}^{eff}(s)}{s}\mathrm{e}^{st}\,ds \tag{5.38}$$

As the expression of $\bar{E}_{kLSv}^{eff}(s)$ is of complicated form, it is difficult to evaluate the integral in (4.38) analytically. A numerical algorithm in this case is needed. In this paper, the inversion of the viscomagnetoelectroelastic moduli from the Carson domain to the physical domain (time domain) is done numerically by using the mutli-precision algorithm developed in [22].

The effective constitutive viscomagnetoelectroelastic behavior of the composite in the time domain is then given by:

$$\Sigma_{iJ}(t)=\int_{0}^{t}E_{iJKl}^{eff}(t-\tau)\frac{dZ_{Kl}(\tau)}{d\tau}d\tau \tag{5.39}$$

where Σ and Z are the generalized averaged viscomagnetoelectroelastic strain and stress over the composite.

5.5 Numerical results

5.5.1 Three-phase viscomagnetoelectroelastic composites

This subsection deals with three-phase viscoelectroelastic composites consisting of viscoelastic matrix (LaRC-SI) in which piezoelectric ($BaTiO_3$) and piezomagnetic inclusions ($CoFe_2O_4$) are embedded. The creep compliance of the matrix in time domain $M_0(t)$ may be represented by the power low model [13]

$$M_0(t)=D_0+D_1t^n \tag{5.40}$$

where D_0 is the initial elastic compliance, and D_1 and n are experimentally determined parameters. For simplicity, the Poisson's ratio of the matrix is assumed unchanged. The Carson transform of Eq. (40) gives

$$\bar{M}_0(s)=D_0+\frac{D_1n!}{s^n} \tag{5.41}$$

The Young modulus $\bar{E}(s)$ is taken as the inverse of $\bar{M}_0(s)$. Variables values of D_0, D_1 and n at T= 213°c are given in table 4.1 [13]. The dielectric and magnetic permeability coefficients of (LaRC-SI) are considered to be constant ($\kappa_{11}/\kappa_0=\kappa_{22}/\kappa_0=\kappa_{33}/\kappa_0=2.8$)

with $\kappa_0 = 8.854187816 \times 10^{-12}$ (C^2/Nm^2) and (μ_{11}= μ_{22}= μ_{33}=.1×10^{-6}). The properties of $BaTiO_3$ and $CoFe_2O_4$ (table 4.2) are assumed to be time independent and remain constant with variation of temperature.

Table 5. 1: Piezoelectric and piezomagnetic material properties

	C_{11}	C_{12}	C_{13}	C_{33}	C_{44}	e_{15}	e_{31}	e_{33}
$BaTiO_3$	166	77	78	162	43	11.5	-4.4	18.6
$CoFe_2O_4$	286	173	170	269.5	45.3	0	0	0
	κ_{11}	**κ_{33}**	**h_{15}**	**h_{31}**	**h_{33}**	**μ_{11}**	**μ_{33}**	
$BaTiO_3$	11.2×10^{-9}	12.6×10^{-9}	0	0	0	5×10^{-6}	10×10^{-6}	
$CoFe_2O_4$	0.08×10^{-9}	0.093×10^{-9}	550	580.3	699.7	-590×10^{-6}	157×10^{-6}	

Units: Elastic constant GPa; dielectric constants C^2/Nm^2; magnetic constants Ns^2/C^2, piezoelectric constants C/m2; piezomagnetic constants N/Am; magnetoelectric coefficients Ns/VC.

Table 5. 2: Viscoelastic properties of LaRC-SI

$D_0(Gpa^{-1})$	$D_1(Gpa^{-1}hour^{-1})$	n	γ_0
0.375	0.051606	0.4103	0.367

5.5.1.1 Frequency domain

In figures 5.1, 5.2, 5.3 and 5.4 the storage and loss part of effective piezomagnetic moduli $h_{33}(\omega)$ and $h_{31}(\omega)$ are presented for a three-phase magnetoelectroelastic composite with respect to the shape of inclusions and frequency $\omega(1/hour)$. It is shown that even the piezoelectric and piezomagnetic phases are supposed time independent, the effective piezomagnetic moduli varies with frequency. This means that they are affected by the viscoelastic behavior of the matrix. The fiber inclusions have a strong affect for these coefficients than the laminated, spherical and ellipsoidal inclusions. Also it is seen that the piezomagnetic moduli are strongly affected by the shape of inclusions and their storage part have a maximum value at some frequencies.

The storage and loss part of the effective magnetoelectric modulus $\alpha_{11}(\omega)$ are presented in figures 5.5 and 5.6 for a three-phase magnetoelectroelastic composite with respect to the shape

of inclusions and frequency $\omega(1/hour)$. Note that the magnetoelectric moduli are absent in all the phase and it is created by the interaction between the piezomagnetic and piezoelectric phases. It seen that $\alpha_{11}(\omega)$ is affected by the viscoelastic behavior of the matrix. Also, it is shown that the magnetoelectric moduli are strongly affected by the shape of the inclusion. α_{11} is prominent for laminated composites.

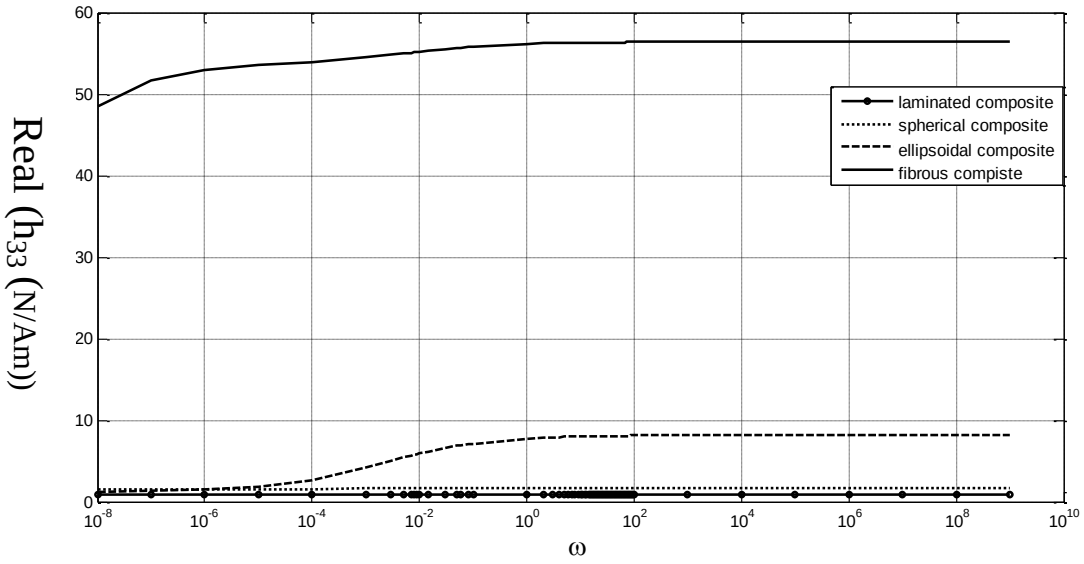

Figure 5.1: Effective storage piezomagnetic modulus Real ($h_{33}(\omega)$) for a viscomagnetoelectroelastic composite consisting of piezoelectric inclusions ($BaTiO_3$) and piezomagnetic inclusions ($CoFe_2O_4$) embedded in a viscoelastic matrix (LaRC-SI) with fixed volume fractions: 60% of the matrix, 20% of the piezoelectric phase and 20% of the piezomagnetic phase.

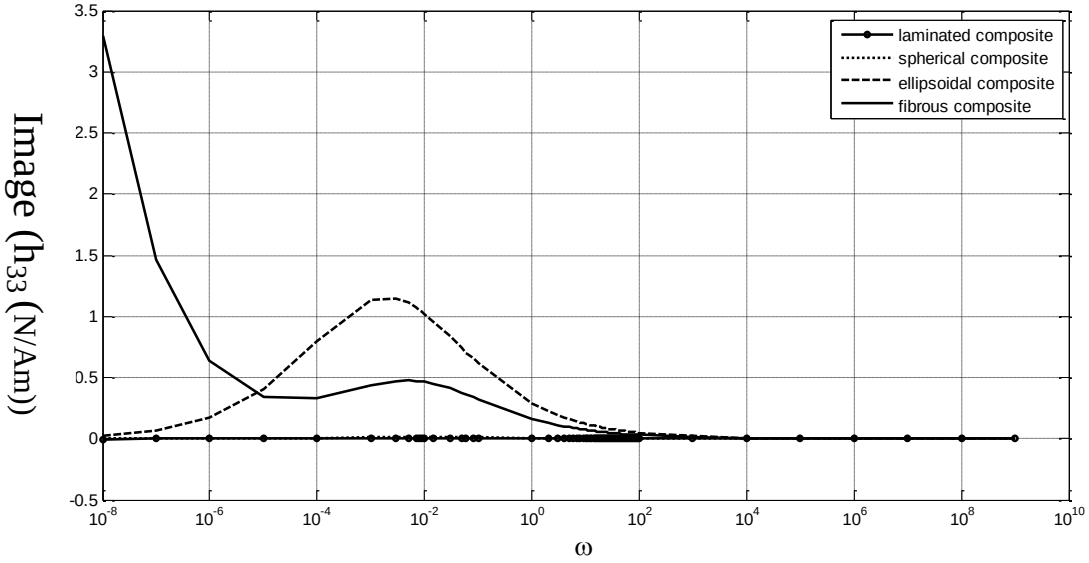

Figure 5.2: Effective loss piezomagnetic modulus Image ($h_{33}(\omega)$) for a viscomagnetoelectroelastic composite consisting of piezoelectric inclusions ($BaTiO_3$) and piezomagnetic inclusions ($CoFe_2O_4$) embedded in a viscoelastic matrix (LaRC-SI) with fixed volume fractions: 60% of the matrix, 20% of the piezoelectric phase and 20% of the piezomagnetic phase.

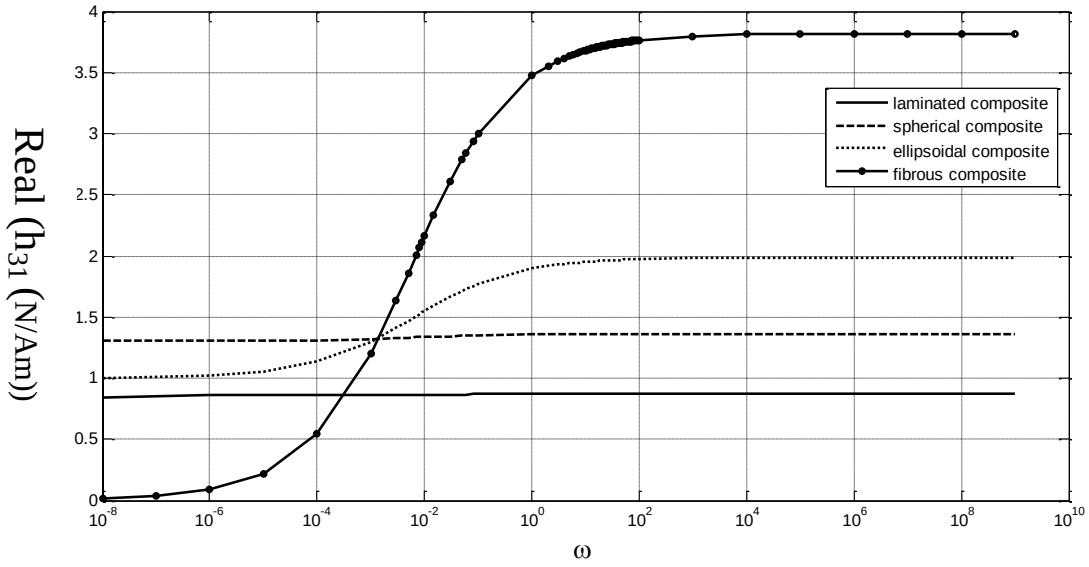

Figure 5.3: Effective storage piezomagnetic modulus Real ($h_{31}(\omega)$) for a viscomagnetoelectroelastic composite consisting of piezoelectric inclusions ($BaTiO_3$) and piezomagnetic inclusions ($CoFe_2O_4$) embedded in a viscoelastic matrix (LaRC-SI) with fixed volume fractions: 60% of the matrix, 20% of the piezoelectric phase and 20% of the piezomagnetic phase.

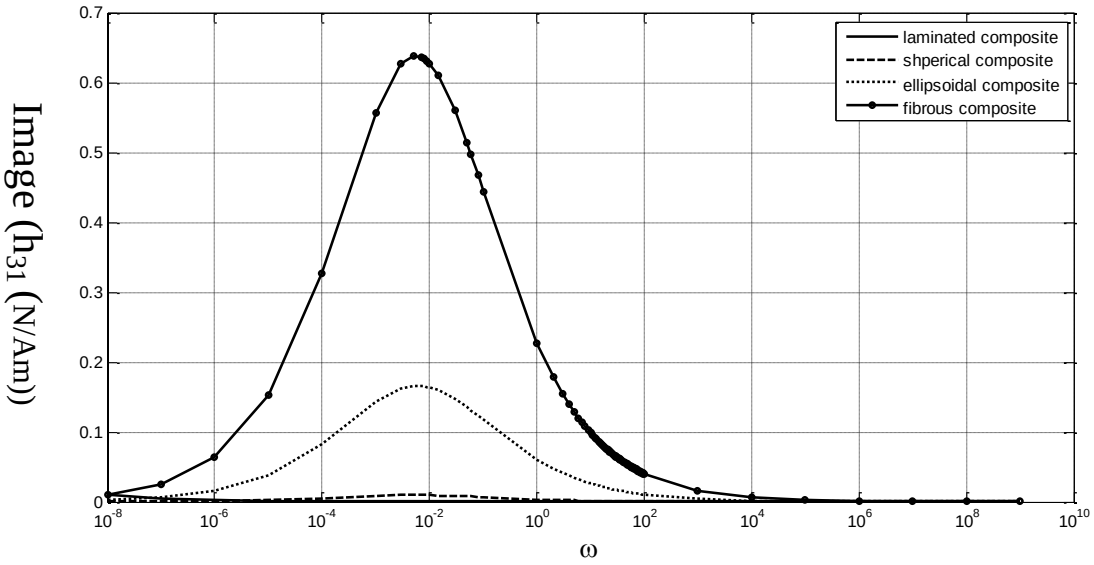

Figure 5.4: Effective loss piezomagnetic modulus Image ($h_{31}(\omega)$) for a viscomagnetoelectroelastic composite consisting of piezoelectric inclusions ($BaTiO_3$) and piezomagnetic inclusions ($CoFe_2O_4$) embedded in a viscoelastic matrix (LaRC-SI) with fixed volume fractions: 60% of the matrix, 20% of the piezoelectric phase and 20% of the piezomagnetic phase.

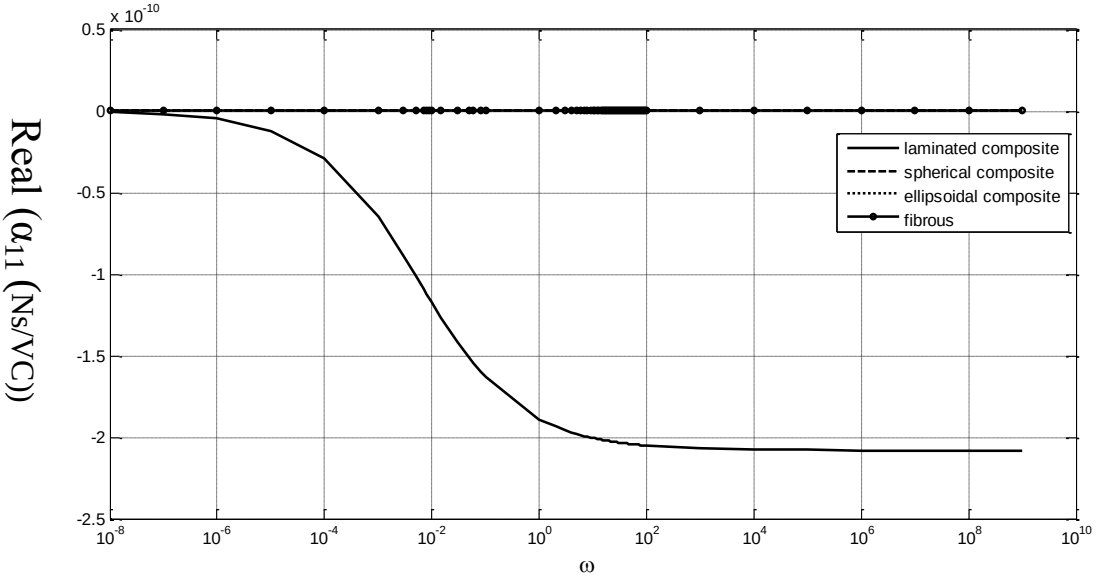

Figure 5.5: Effective storage magnetoelectric modulus Real ($\alpha_{11}(\omega)$) for a viscomagnetoelectroelastic composite consisting of piezoelectric inclusions ($BaTiO_3$) and piezomagnetic inclusions ($CoFe_2O_4$) embedded in a viscoelastic matrix (LaRC-SI) with fixed volume fractions: 60% of the matrix, 20% of the piezoelectric phase and 20% of the piezomagnetic phase.

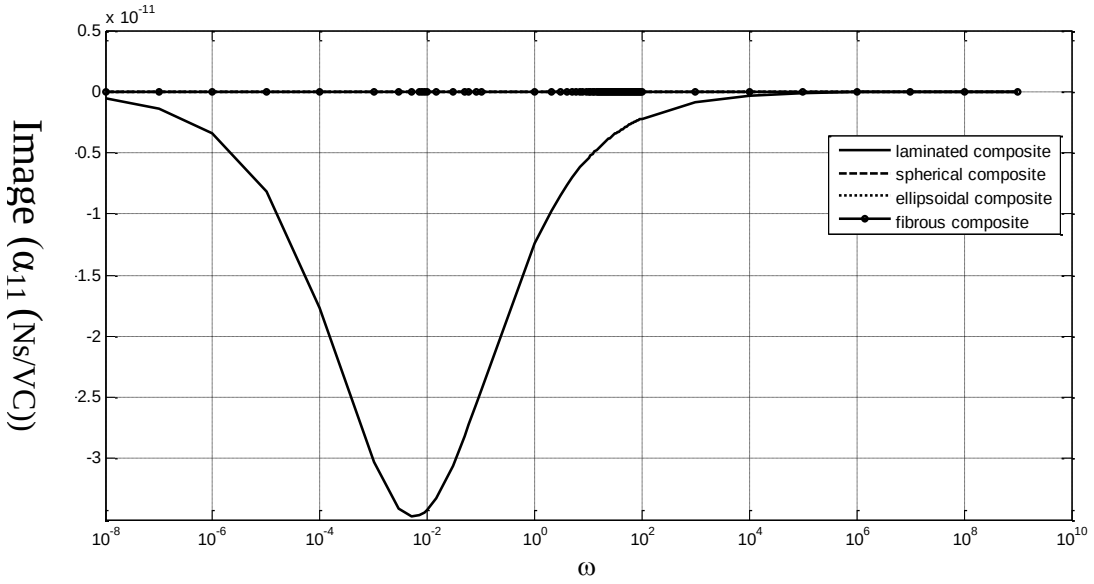

Figure 5.6: Effective loss magnetoelectric modulus Image ($\alpha_{11}(\omega)$) for a viscomagnetoelectroelastic composite consisting of piezoelectric inclusions ($BaTiO_3$) and piezomagnetic inclusions ($CoFe_2O_4$) embedded in a viscoelastic matrix (LaRC-SI) with fixed volume fractions: 60% of the matrix, 20% of the piezoelectric phase and 20% of the piezomagnetic phase.

5.5.1.2 Time domain

In figures 5.7, 5.8 and 5.9 the effective moduli $h_{31}(t)$ and $\alpha_{33}(t)$ and $\alpha_{11}(t)$ are presented respectively for a three-phase fibrous viscomagnetoelectroelastic composite. The presented effective properties show a time dependent behavior. Also, it is shown that the piezomagnetic modulus h_{31} and the magnetoelectric moduli α_{33} and α_{11} decrease with time. The effect of phase constituent volume fractions on the effective properties is shown.

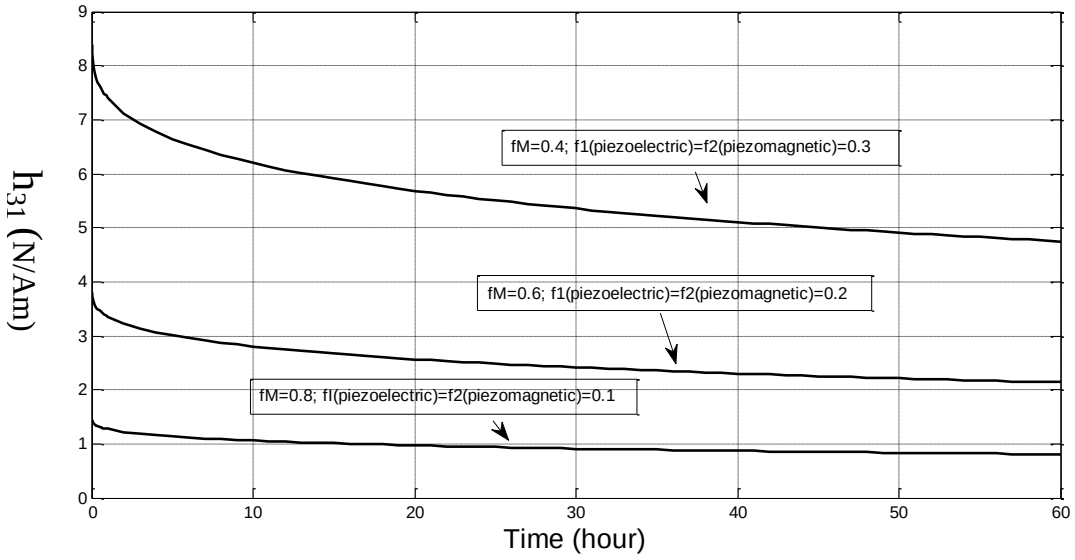

Figure 5.7: Effective piezomagnetic modulus $h_{31}(t)$ for a fibrous viscomagnetoelectroelastic composite consisting of piezoelectric inclusions ($BaTiO_3$) and piezomagnetic inclusions ($CoFe_2O_4$) embedded in a viscoelastic matrix (LaRC-SI) with different volume fractions of phase constituents.

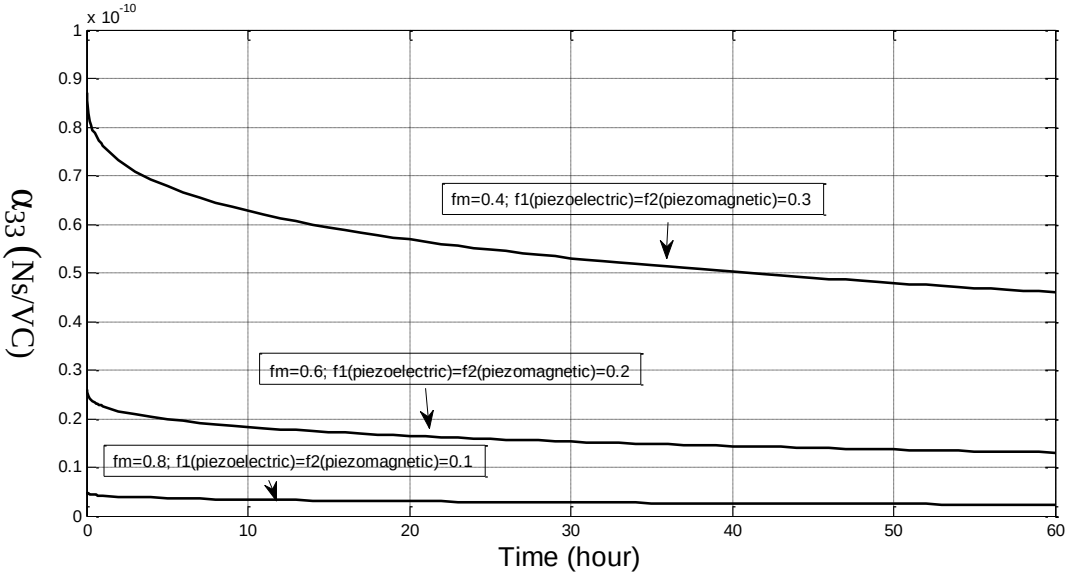

Figure 5.8: Effective magnetoelectric modulus $\alpha_{33}(t)$ for a fibrous viscomagnetoelectroelastic composite consisting of piezoelectric inclusions ($BaTiO_3$) and piezomagnetic inclusions ($CoFe_2O_4$) embedded in a viscoelastic matrix (LaRC-SI) with different volume fractions of phase constituents.

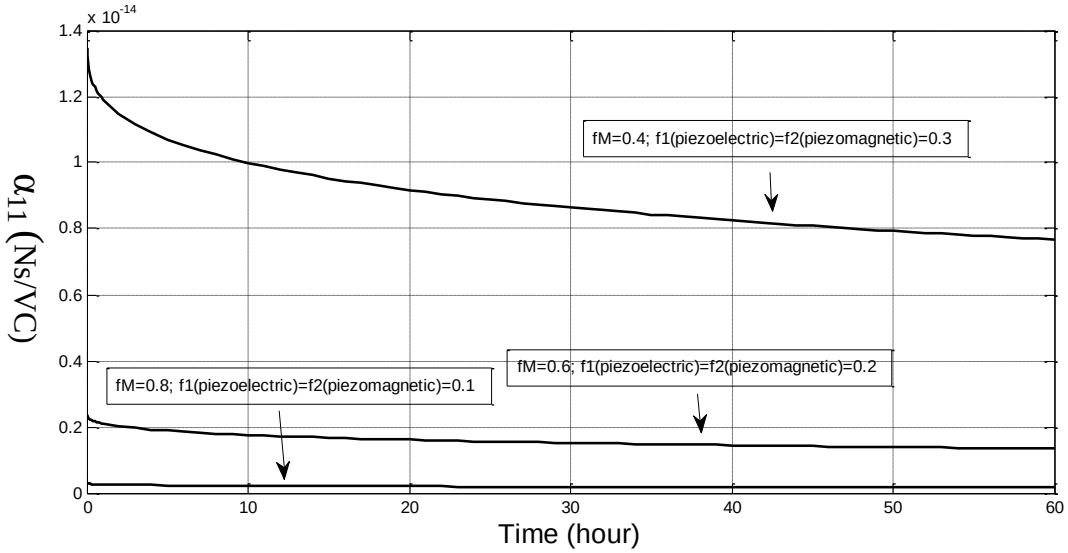

Figure 5.9: Effective magnetoelectric modulus $\alpha_{11}(t)$ for a fibrous viscomagnetoelectroelastic composite consisting of piezoelectric inclusions ($BaTiO_3$) and piezomagnetic inclusions ($CoFe_2O_4$) embedded in a viscoelastic matrix (LaRC-SI) with different volume fractions of phase constituents.

5.5.2 Coated viscomagnetoelectroelastic composites

This subsection deals with coated viscomagnetoelectroelastic composites consisting with piezoelectric ($BaTiO_3$) inclusion surrounded by piezomagnetic matrix ($CoFe_2O_4$) embedded in a viscoelastic matrix (LaRC-SI). The Topology of a representative volume element of the coated composite is described in figure 5.1.

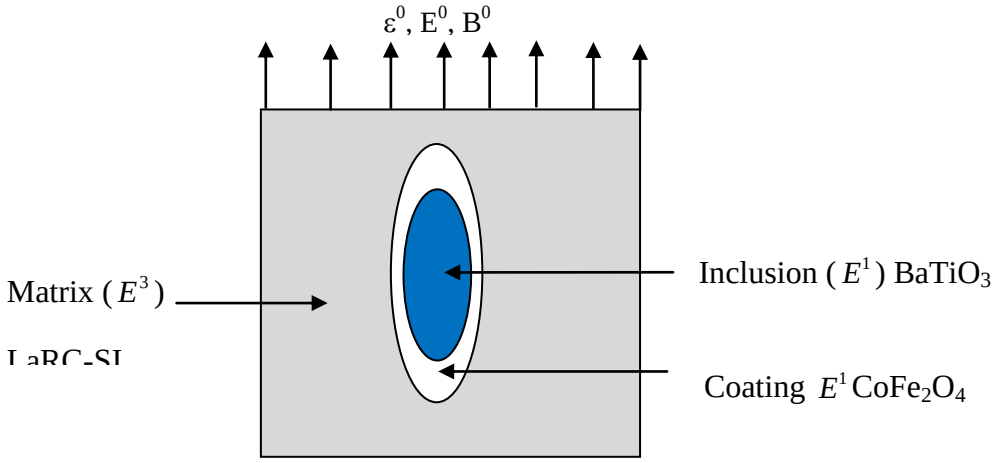

Figure 5.11: A representative volume element of a coated composite. The dimension of the inclusion and the coating are (a_1, b_1, c_1), (a_2, b_2, c_2) respectively.

As shown in Figure 5.1, phase 1 is the piezoelectric inclusion, phase 2 is the piezomagnetic coating and phase three is the viscoelastic matrix having homogeneous material properties E^1, E^2 and E^3 respectively. The reinforcements are perfectly aligned and have ellipsoidal shapes with the dimensions (a_1, b_1, c_1) and (a_2, b_2, c_2). The two ellipsoids are coaxial with $\frac{a_1}{a_2} = \frac{b_1}{b_2} = \frac{c_1}{c_2} = \gamma$. The variation of the volume fraction of the inclusion and the coating is given as function of the volume fraction of the matrix and the thickness of the piezomagnetic coating γ as follow.

$f_1 = (1 - f_3)\gamma^3$, $f_2 = (1 - f_3)(1 - \gamma^3)$.

5.5.2.1 Frequency domain

In figures 5.12 and 5.13, the storage and loss part of the effective piezomagnetic modulus $h_{31}(\omega)$ is presented for a fibrous viscomagnetoelectroelastic composite consisting of piezoelectric inclusion surrounded by piezomagnetic coating embedded in a viscoelastic matrix with respect to the frequencies and the coating thickness. It is shown that $h_{31}(\omega)$ is affected by the viscoelastic behavior of the matrix. Also, $h_{31}(\omega)$ is strongly affected by the thickness of the coating. The loss part of $h_{31}(\omega)$ can be maximized at certain frequency values.

In figures 5.14, 5.15, 5.16 and 5.17, the storage and loss part of magnetoelectric moduli are presented a fibrous viscomagnetoelectroelastic composite consisting of piezoelectric inclusion surrounded by piezomagnetic coating embedded in a viscoelastic matrix with respect to the frequencies and the coating thickness. It is shown that the magnetoelectric moduli are strongly affected by the thickness of the coating. Also, it is shown that α_{11} and α_{33} are affected by the viscoelastic behavior of the matrix. The loss part of the magnetoelectric modulus α_{11} is maximized at certain frequency values.

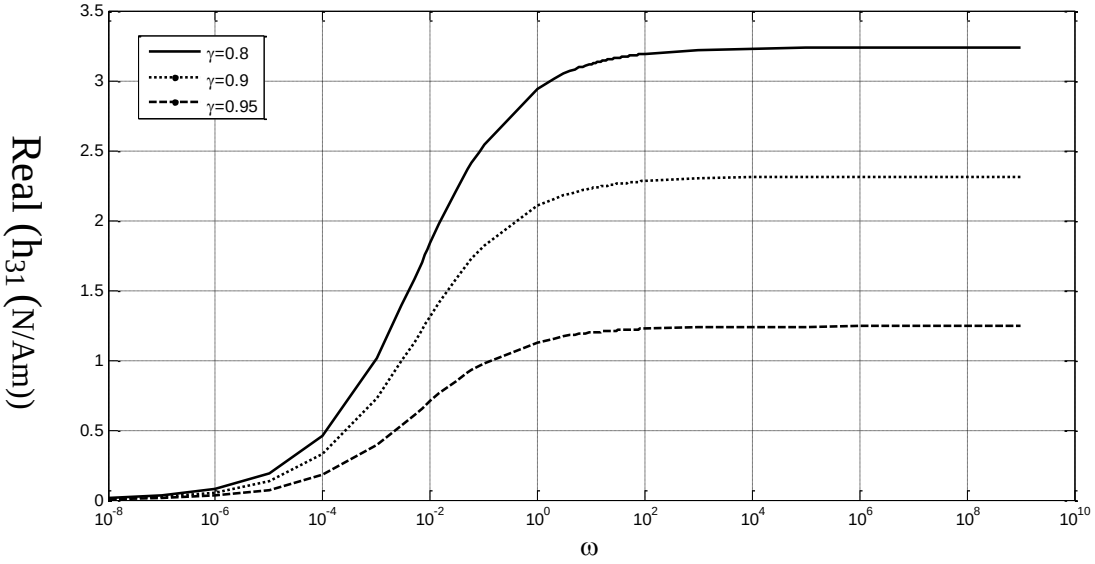

Figure 5.12: Effective storage piezomagnetic modulus Real ($h_{31}(\omega)$) for a fibrous viscomagnetoelectroelastic composite consisting of piezoelectric inclusions ($BaTiO_3$) surrounded by piezomagnetic coating layer ($CoFe_2O_4$) embedded in a viscoelastic matrix (LaRC-SI) with fixed volume fraction of the matrix (fm=0.6).

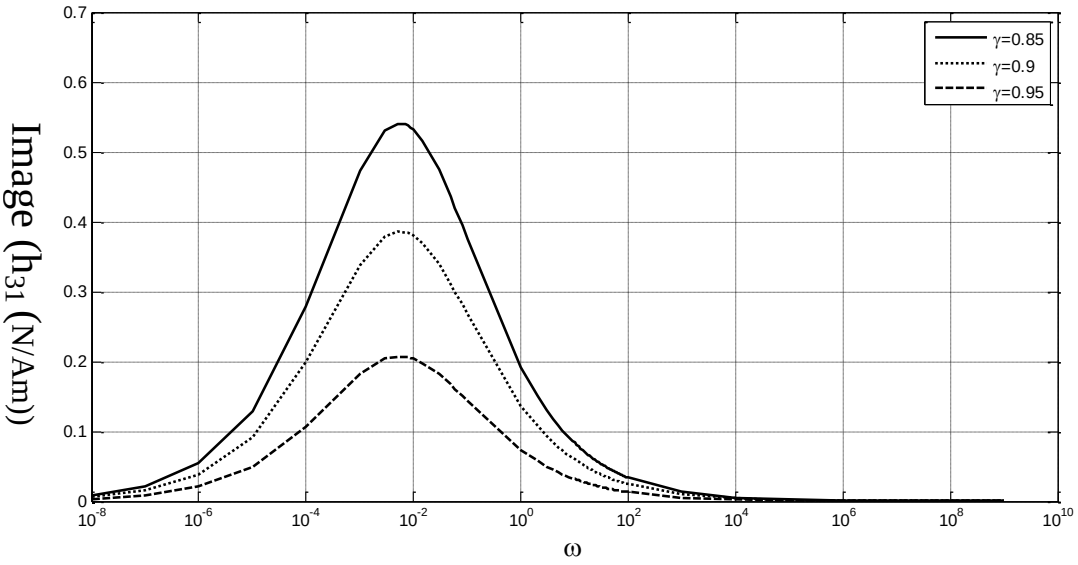

Figure 5.13: Effective loss piezomagnetic modulus Image ($h_{31}(\omega)$) for a fibrous viscomagnetoelectroelastic composite consisting of piezoelectric inclusions ($BaTiO_3$) surrounded by piezomagnetic coating layer ($CoFe_2O_4$) embedded in a viscoelastic matrix (LaRC-SI) with fixed volume fraction of the matrix (fm=0.6).

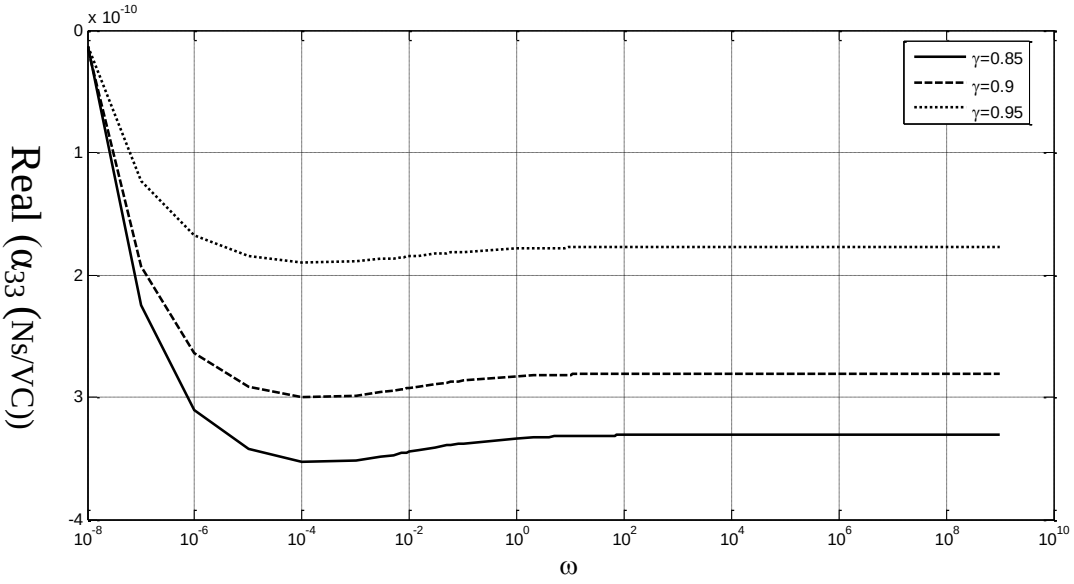

Figure 5.14: Effective storage magnetoelectric modulus Real ($\alpha_{33}(\omega)$) for a fibrous viscomagnetoelectroelastic composite consisting of piezoelectric inclusions ($BaTiO_3$) surrounded by piezomagnetic coating layer ($CoFe_2O_4$) embedded in a viscoelastic matrix (LaRC-SI) with fixed volume fraction of the matrix (fm=0.6).

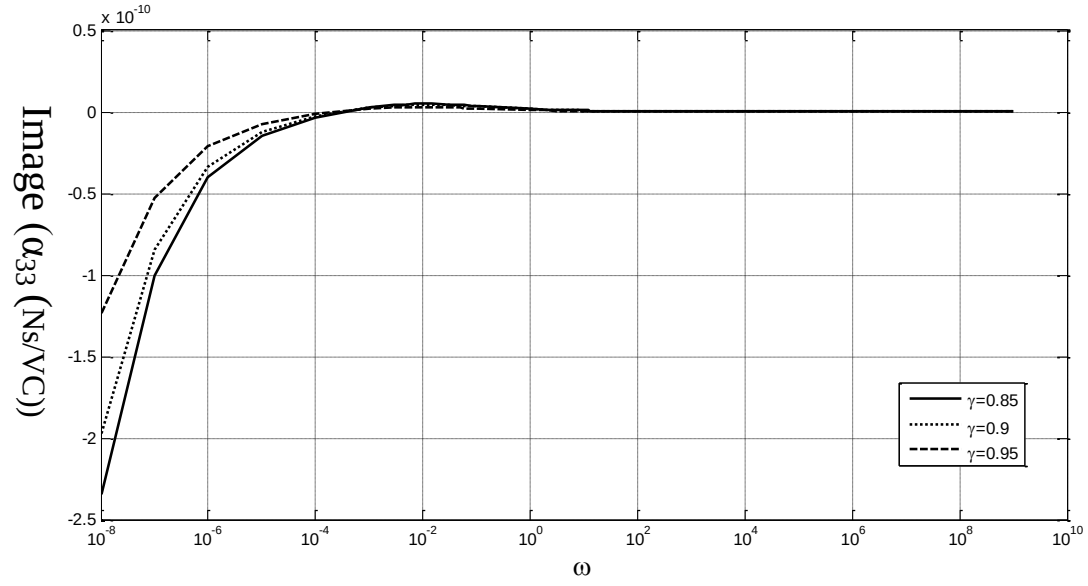

Figure 5.15: Effective loss magnetoelectric modulus Image ($\alpha_{33}(\omega)$) for a fibrous viscomagnetoelectroelastic composite consisting of piezoelectric inclusions ($BaTiO_3$) surrounded by piezomagnetic coating layer ($CoFe_2O_4$) embedded in a viscoelastic matrix (LaRC-SI) with fixed volume fraction of the matrix (fm=0.6).

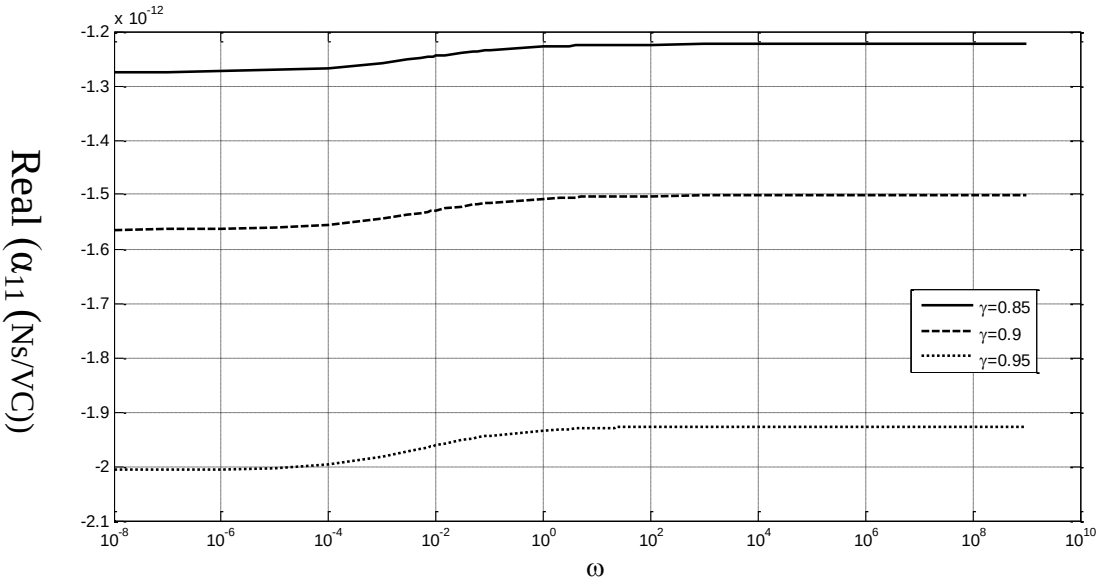

Figure 5.16: Effective storage magnetoelectric modulus Real ($\alpha_{11}(\omega)$) for a fibrous viscomagnetoelectroelastic composite consisting of piezoelectric inclusions ($BaTiO_3$) surrounded by piezomagnetic coating layer ($CoFe_2O_4$) embedded in a viscoelastic matrix (LaRC-SI) with fixed volume fraction of the matrix (fm=0.6).

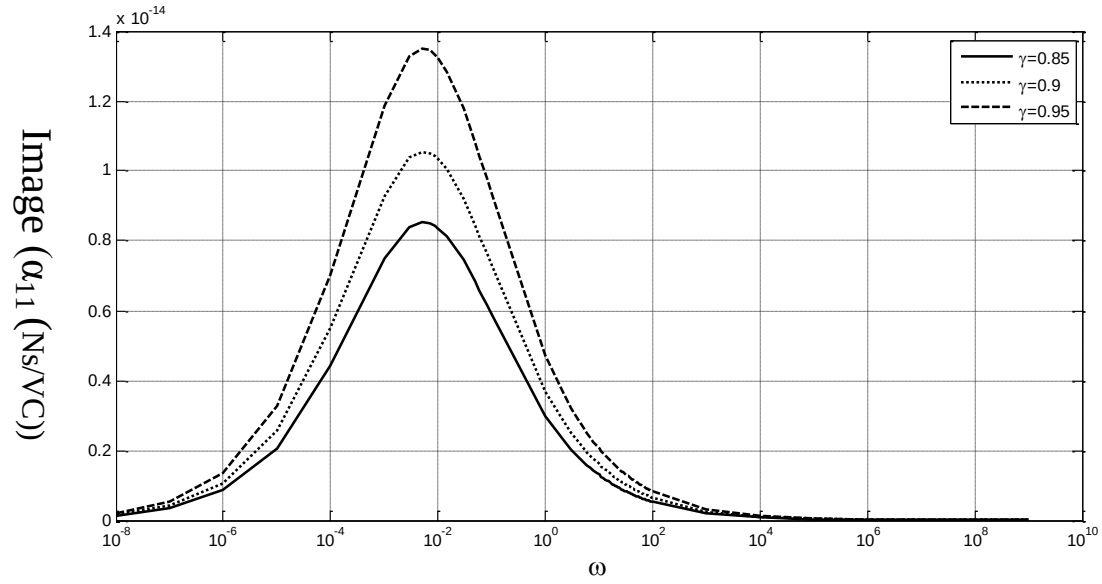

Figure 5.17: Effective loss magnetoelectric modulus Image ($\alpha_{11}(\omega)$) for a fibrous viscomagnetoelectroelastic composite consisting of piezoelectric inclusions ($BaTiO_3$) surrounded by piezomagnetic coating layer ($CoFe_2O_4$) embedded in a viscoelastic matrix (LaRC-SI) with fixed volume fraction of the matrix (fm=0.6).

5.5.2.2 Time domain

In figures 5.18, 5.19, 5.20 and 5.21, the effective moduli $h_{31}(t)$, $h_{33}(t)$, $\alpha_{33}(t)$ and $\alpha_{11}(t)$ are presented for a fibrous viscomagnetoelectroelastic consisting of piezoelectric inclusions surrounded by piezomagnetic coating embedded in viscoelastic matrix with respect to time and the coating thickness. It is shown that the effective moduli are affected by the viscoelastic behavior of the matrix.

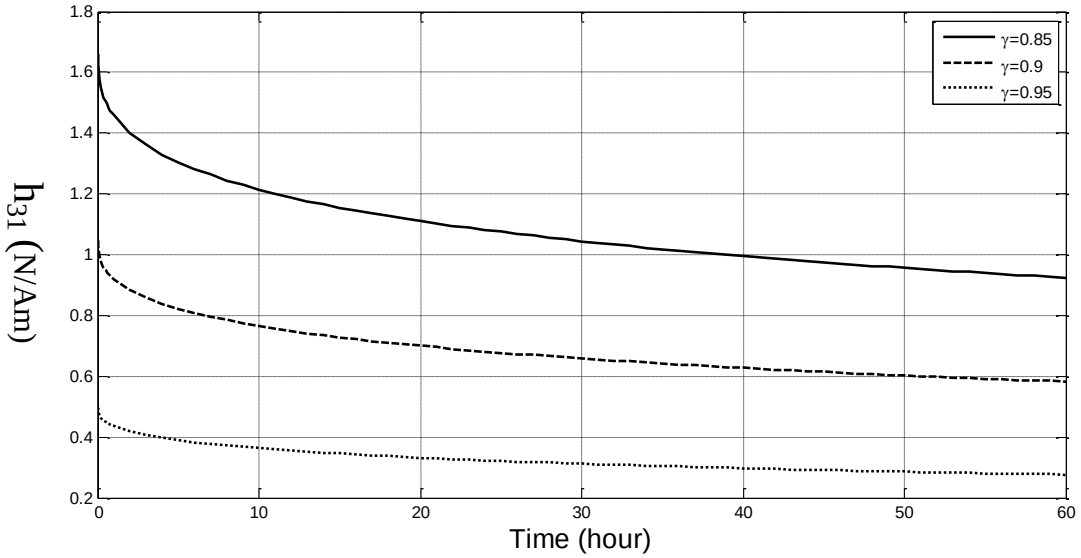

Figure 5.18: Effective piezomagnetic modulus $h_{31}(t)$ for a fibrous viscomagnetoelectroelastic composite consisting of piezoelectric inclusions ($BaTiO_3$) surrounded by piezomagnetic coating layer ($CoFe_2O_4$) embedded in a viscoelastic matrix (LaRC-SI) with fixed volume fraction of the matrix (fm=0.6).

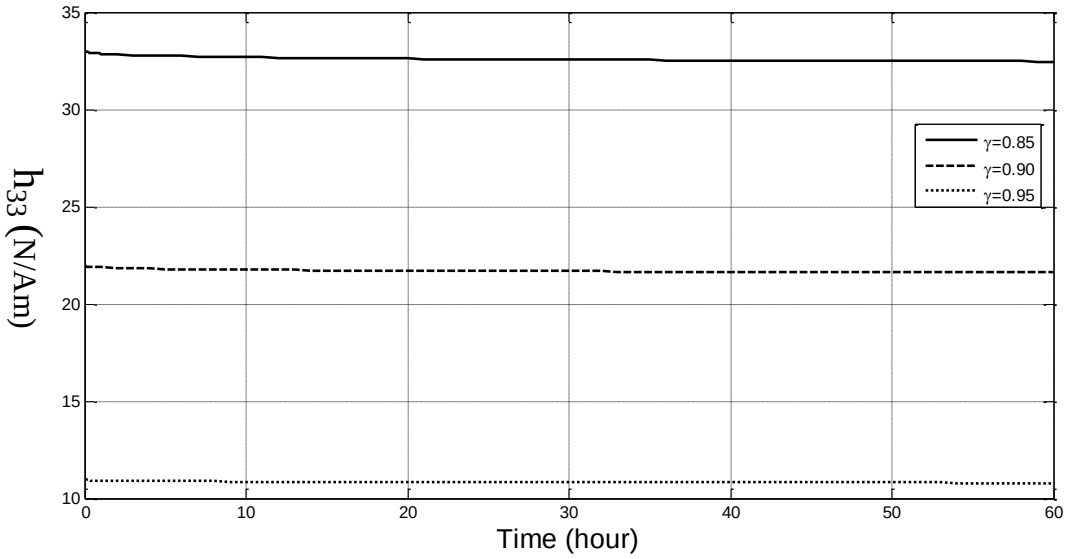

Figure 5.19: Effective piezomagnetic modulus $h_{33}(t)$ for a fibrous viscomagnetoelectroelastic composite consisting of piezoelectric inclusions ($BaTiO_3$) surrounded by piezomagnetic coating layer ($CoFe_2O_4$) embedded in a viscoelastic matrix (LaRC-SI) with fixed volume fraction of the matrix (fm=0.6).

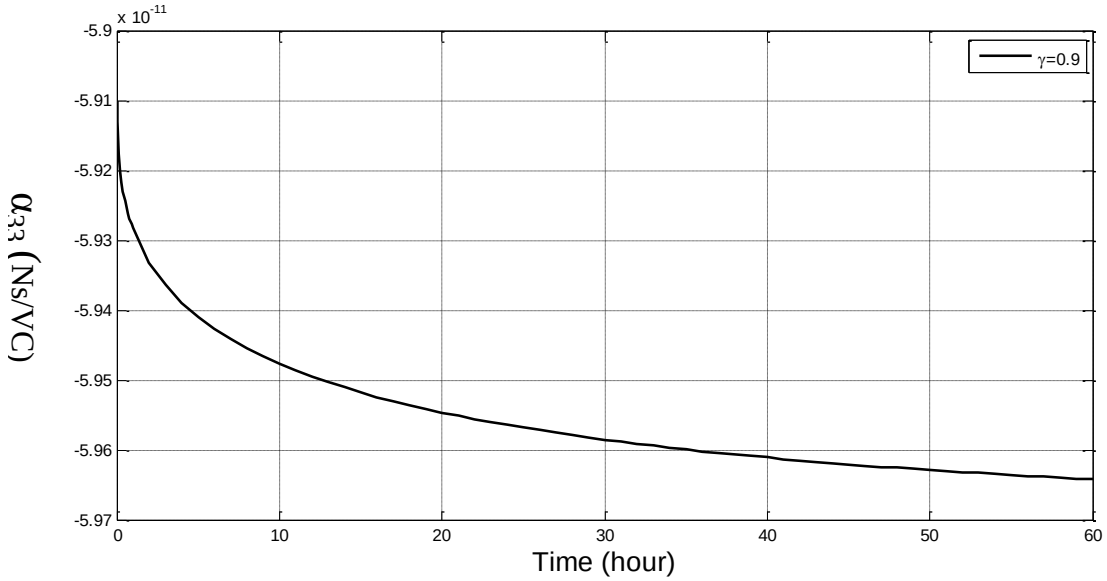

Figure 5.20: Effective piezomagnetic modulus $\alpha_{33}(t)$ for a fibrous viscomagnetoelectroelastic composite consisting of piezoelectric inclusions ($BaTiO_3$) surrounded by piezomagnetic coating layer ($CoFe_2O_4$) embedded in a viscoelastic matrix (LaRC-SI) with fixed volume fraction of the matrix (fm=0.6).

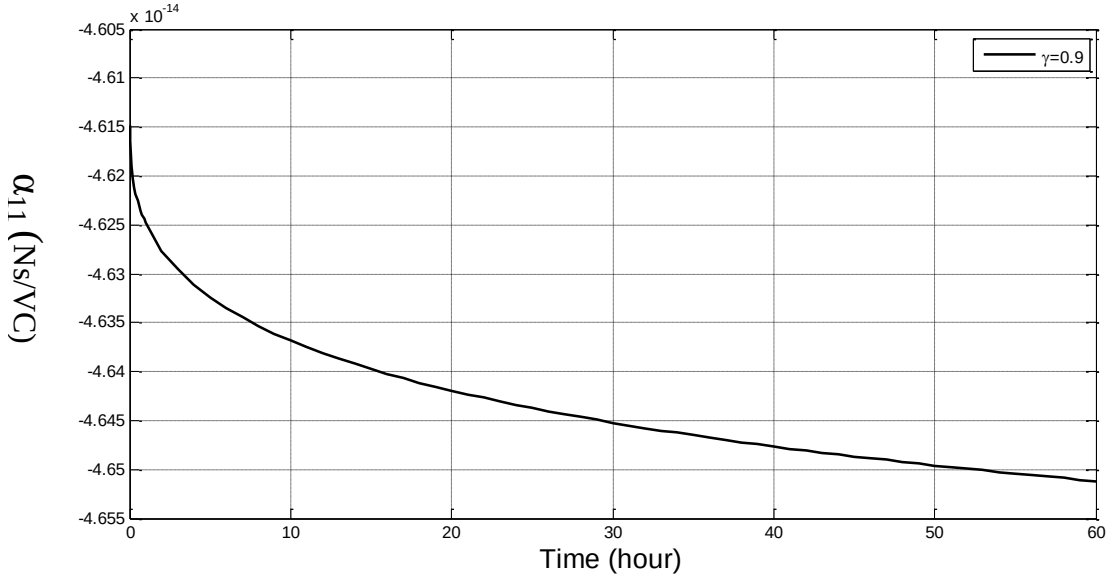

Figure 5.21: Effective piezomagnetic modulus $\alpha_{11}(t)$ for a fibrous viscomagnetoelectroelastic composite consisting of piezoelectric inclusions ($BaTiO_3$) surrounded by piezomagnetic coating layer ($CoFe_2O_4$) embedded in a viscoelastic matrix (LaRC-SI) with fixed volume fraction of the matrix (fm=0.6).

5.6 Conclusion

In this work, the effective properties of viscomagnetoelectroelastic composites are modeled and numerically investigated. The modeling is developed for multi-phase and multi-coated viscomagnetoelectroelastic composites. The effective properties are first derived in the Carson domain and then inverted numerically to the time domain. For multi-phase composites a composite consisting with piezoelectric and piezomagnetic inclusion separated by a viscoelastic matrix is considered and for multi-coated composites a composite consisting with piezoelectric inclusions surrounded by piezomagnetic coatings embedded in viscoelastic matrix is considered. The effective properties of the considered composites are presented both in time and frequency domain with respect to the shape, volume fraction of reinforcement and thickness of the coating. It is shown, even the piezoelectric and piezomagnetic phase properties are assumed to be time independent, the effective piezomagnetic and magnetoelectric moduli are time dependent. The obtained active-passive multifunctional properties can be optimized with respect to the shape, type and the volume fraction of the reinforcements as well as with the coating concept.

5.7 Perspectives

Form chapter 2 to 5 the linear behavior of the magnetoelectroelastic, viscopiezoelectric and viscomagnetoelectroelastic composites was investigated. In chapter 6, the nonlinear behavior of shape memory alloy composites will be investigated. The aim will be to extend the previous methodological approach to the case of the nonlinear behavior of shape memory alloy composites. The modeling will be based on the combination of the Mori-Tanaka model and the coating concept with the constitutive equations describing the transformation behavior of shape memory alloy materials.

References

[1]Li, J.Y.; Dunn, M.L. (1998): Micromechanics of magnetoelectroelastic composite materials: Average fields and effective behavior. J. Intell. Mater. Syst. Struct.Vol. 9, pp. 404–416.

[2]Aboudi, J. (2001): Micromechanical analysis of fully coupled electro-magneto-thermo-elastic multiphase composites. Smart Mater. Struct., Vol. 10, pp.867–877.

[3]Huang, J.H.; Kuo, W.S. (1998): The analysis of piezoelectric/piezomagnetic composite materials containing ellipsoidal inclusions. J. Appl. Phys., Vol. 81, pp. 1378–1386.

[4]Li, J.Y.; Dunn, M.L. (1998): Anisotropic coupled-field inclusion and inhomogeneity problems. Philos. Mag., Vol. A 77, pp. 1341–1350.

[5]Li, J.Y.; Dunn, M.L. (1999): Analysis of microstructural fields in heterogeneous piezoelectric solids, Int. J. Eng. Sci., Vol. 37, pp. 665–685.

[6]Lee, J.; Boyd, J. G.; Lagoudas, D C. (2005): Effective properties of three-phase electro-magneto-elastic composites. Int. J. Engineering Science, Vol. 43, pp. 790-825.

[7]Brinson, L. C.; Lin, W. S. (1998): Comparison of micromechanics methods for effective properties of multiphase viscoelastic composites. Composites Structures, Vol. 41, pp. 353-367.

[8]Fisher, F. T.; Brinson, L.C. (2001): Viscoelastic interphases in polymer-matrix composites: Theoretical models and finite-element analysis. Composites Science and Technology, Vol. 61, pp. 731-748.

[9]Haberman, M. R.; Berthelot, Y. H.; Jarzynski, J.; Cherkaoui, M. (2002): Micromechanical modeling of viscoelastic voided composites in the low-frequency approximation. Acoustical Society of America, Vol. 112, N°5, pp. 1937-1943.

[10]Matzenmiller, A.; Gerlach, S. (2004): Micromechanical modeling of viscoelastic composites with compliant fiber–matrix bonding. Computational Material Science, Vol. 29, pp. 283-300.

[11]Fei, X.; Gengkai, H.; Zhuping, H. (2004): Influence of Gradual Interphase on Overall Elastic and Viscoelastic Properties of Particulate Composites. International Journal of Thermoplastic Composites Materials, Vol. 17, pp.411-425.

[12]Lévesque, M.; Derrien, K.; Mishnaevski Jr., L.; Baptiste, D.; Gilchrist, M. D. (2004): A micromechanical model for nonlinear viscoelastic particle reinforced polymeric composite materials-undamaged state. Composites: Part A, Vol. 35, pp. 905-913.

[13]Li, K.; Gaw, X.-L.; Roy, A. K. (2006): Micromechanical Modeling of Viscoelastic Properties of Carbon Nanotube-Reinforced Polymer Composites. Mechanics of Advanced Materials and Structures, Vol. 13, pp. 317-328.

[14]Jiang, B.; Batra, R. C. (2001): Effective electroelastic properties of a piezocomposite with viscoelastic and dielectric relaxing matrix. Journal of Intelligent Materials Systems and Structures, Vol. 12, pp. 847-866.

[15]Aldraihem, O. J.;Baz, A.; Al-Saud, T. S. (2007)**:** Hybrid Composites with Shunted Piezoelectric Particles for Vibration Damping. Mechanics of Advanced Materials and Structures, Vol. 14, pp. 413–426.

[16]Muliana, A.; Li, K. (2010): Time-dependent response of active composites with thermal, electrical, and mechanical coupling effect. International Journal of Engineering Science, Vol. 48, pp. 1481–1497.

[18]Bakkali, A.; Azrar, L.; Fakri, N. (2011): Modeling of effective properties of multiphase magnetoelectroelastic heterogeneous materials" Journal of Computers, Materials & Continua, Vol. 23, N°3, pp 201-231.

[17] Azrar, L.; Bakkali, A.; Aljinaidi, A. A. (2013): Viscoelectroelastic effective properties of heterogeneous and multi-coated piezoelectric materials. Submitted to the International Journal of Solids and Structures.

[19]Bakkali, A.; Azrar, L.; Aljinaidi, A. A. (2012): Multi-coated magnetoelectroelastic composites with functionally graded interphases. MATEC Web of Conferences, Vol. 1, 09001.

[20]Bakkali, A.; Azrar, L.; Aljinaidi, A. A. (2013): Micromechanical modeling of magnetoelectroelastic composite materials with multi-coated inclusions and functionally graded interphases. Journal of Intelligent Materials Systems and Structures, in press.

[21]Bakkali, A.; Azrar, L.; Aljinaidi, A. (2013): Effective properties of heterogeneous magnetoelectroelastic materials with multi-Coated inclusions. Key Engineering Materials, Vol. 550, pp 25-32.

[22]Abate, J.; Valko, P. P. (2004): Multi-precision Laplace transform inversion. Int. J. Numer. Meth. Engng. Vol. 60, pp. 979–993.

Chapter 6

6. Micromechanical modeling of SMA composite materials

Abstract

The aim of this work is the extension of the previous methodological approaches to multifunctional materials with a nonlinear behavior. The shape memory alloys have been selected. The Mori-Tanaka model and coating concept will be used for phase transformation modeling.

6.1 Introduction

SMA materials have been taking the attention of many researchers and engineers due to their application from aerospace and naval to surgical instrument and medical implants and fixtures. This kind of composites may have the desired properties and sometimes a unique overall response under a thermo-mechanical loading. Many researchers have studied the effective transformation behavior of composites made by the addition of shape memory alloy inclusions to an elastic or an elasto-plastic matrix. Some micro mechanical models have been used to investigate the thermo-mechanical behavior of shape memory alloy materials.

A study on the numerical implementation of SMA constitutive thermomechanical response based on the return mapping algorithm is presented in [1]. [2] developed A micromechanical modeling to predict the effective behavior of composite with ductile matrix and shape memory alloy reinforcement. The thermoelectroelastic behavior of a four phase composite consisting of PZT, SMA, NPZT inclusions embedded in a polymer matrix is investigated in [3] based on the equivalence energy principle and the Mori-Tanaka micromechanical model. [4-5] predicted the transformation behavior of porous shape memory alloy materials based on micromechanical averaging techniques. A micromechanical modeling for polycrystalline shape memory alloys is developed in [6].

In this work the effective transformation behavior of SMA composite materials in which elastic inclusions are embedded in SMA matrix will be investigated. Note that the SMA matrix in the beginning is fully austenitic but after loading the matrix undergoes a phase transformation which results in the apparition of the martensitic phase. After sufficient loading the matrix becomes fully martensitic. To take into account this phase transformation the Mori–Tanaka coated micromechanical model developed in [7-8] is used. The modeling of SMA composites is splitted into two parts: The micro mechanical modeling is used to calculate the effective properties of the SMA composite and then the constitutive model that describes the transformation behavior of the SMA matrix is presented. To describe the effective transformation behavior the two models are combined.

6.2 Micromechanical modeling

The micromechanical modeling developed in this section is for three-phase composites made by inclusions surrounded by a coating layer embedded in a matrix. The properties of the matrix, inclusion and the coating layer are different. The Mori-Tanaka micro mechanical model is used in this paper to investigate the effective moduli of the composites. Generally, micromechanics are based on two steps: (i) localization step, which gives the relationship between the microscopic filed and macroscopic field through the localization tensors and (ii) homogenization step which employs averaging techniques to estimates the effective properties of the composite. The derivation of the concentration tensors is based on the integral equation that takes into account the coating effect and on the interfacial operators.

The topology of the coated inclusion embedded in a matrix is described below in figure 6.1 by an inclusion occupying the volume V_I with elastic moduli L^I . Surrounding this elastic inclusion by a coating layer with a volume V_C and whose property described by the tangent moduli L^C . The whole coated inclusion is embedded in an infinite matrix whose property described by the tangent moduli L^M . The interface between the inclusion- coating and coating-matrix are assumed to be perfect.

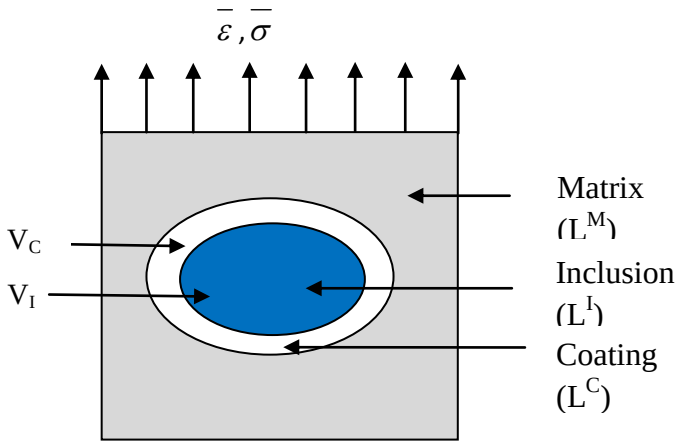

Figure 6.1: The topology of the coated inclusion. $\bar{\varepsilon}$ and $\bar{\sigma}$ represent the macroscopic applied field.

6.2.1 Constitutive behavior

The local constitutive behavior that represents the SMA composites is given as follow:

$$\dot{\sigma}_{ij} = l_{ijkl}\,(\dot{\varepsilon}_{kl} - \dot{\varepsilon}^{tr}_{kl}) \tag{6.1-a}$$

or

$$\dot{\sigma}_{ij} = S_{ijkl}\,(\dot{\varepsilon}_{kl} - \alpha_{kl}\dot{T} - \dot{\varepsilon}^{tr}_{kl}) \tag{6.1-b}$$

where

l_{ijkl} : is the tangent moduli; S_{ijkl} : is the elastic moduli; α_{kl} : is the thermal expansion.

$\dot{\varepsilon}_{kl} = \dot{\varepsilon}^{e}_{kl} + \dot{\varepsilon}^{tr}_{kl}$ is the total rate strain in which $\dot{\varepsilon}^{e}_{kl}$, $\dot{\varepsilon}^{tr}_{kl}$ represents respectively the rate elastic strain and the rate transformation strain.

For the elastic inclusions the tangent moduli $l_{ijkl}(r)$ becomes the elastic moduli and the rate transformation is equal to zero.

The total strain rate $\dot{\varepsilon}_{kl}(r)$ and the particle velocity v_i are related through the kinematic relations:

$$\dot{\varepsilon}_{kl} = \frac{1}{2}(v_{k,l} + v_{l,k}) \tag{6.2}$$

The quasi static equilibrium equation with no body forces is written as follow:

$$\dot{\sigma}_{ij,j} = 0 \tag{6.3}$$

Form (6.1), (6.3) can be written as follow:

$$(l_{ijkl}(\dot{\varepsilon}_{kl} - \dot{\varepsilon}^{tr}_{kl}))_{,j} = 0 \tag{6.4}$$

The symmetry properties of l_{ijkl} leads to this expression

$$(l_{ijkl}(\dot{v}_{k,l} - \dot{\varepsilon}^{tr}_{kl})_{,j} = 0 \tag{6.5}$$

The transformation strain is given as function of state variables.

6.2.2 Localization and homogenization

Let us consider V as the representative volume element of the composite. The average strain rate $\dot{E}$ and stress rate $\dot{\Sigma}$ are related to the local strain rate and stress rate by the average relations of Hill- Mandel (Hill, 1963).

$$\dot{E}_{kl} = \frac{1}{V}\int_V \dot{\varepsilon}_{kl}(r)dV \tag{6.6-a}$$

$$\dot{\Sigma}_{kl} = \frac{1}{V}\int_V \dot{\sigma}_{kl}(r)dV \tag{6.6-b}$$

For composite materials the volume average of $\dot{\varepsilon}_{kl}(r)$ and $\dot{\sigma}_{kl}(r)$ can be written as follow:

$$\dot{E}_{kl} = \sum_{i=1}^{n} f_i \dot{\varepsilon}^i_{kl} \tag{6.7-a}$$

$$\dot{\Sigma}_{kl} = \sum_{i=1}^{n} f_i \dot{\sigma}^i_{kl} \tag{6.7-b}$$

where the subscript 'i' denotes the i-th phase and f_i is the corresponding volume fraction. $\dot{\varepsilon}^i$ and $\dot{\sigma}^i$ are uniform in each phase.

Additionally, the overall constitutive behavior of the composite can be written as follow:

$$\dot{\Sigma}_{kl} = L^{eff}_{klij}(\dot{E}_{ij} - \dot{E}^{tr}_{ij}) \tag{6.8}$$

In which L^{eff} is the effective tangent moduli of the composite and $\dot{E}^t_{ij}$ the macroscopic transformation strain rate that the composite undergoes.

In order to make the transition between the local scale (phases) and the global scale (composite) the concentration tensors are introduced. The localization relationships are given as follow:

$$\dot{\varepsilon}^p_{kl} = A^p_{klij}\dot{E}_{ij} + a^p_{kl} \tag{6.9-a}$$

$$\dot{\sigma}^p_{kl} = B^p_{klij}\dot{\Sigma}_{ij} + b^p_{kl} \tag{6.9-b}$$

where A and B are the fourth order concentration tensors that take into account heterogeneity of the tangent moduli while a and b are the corresponding second order tensors to take into account the heterogeneity of the transformation strain rate inside the material. Substituting (6.9-a) and (6.9-b) respectively into (6.7-a) and (6.7-b) lead to

$$\sum_{p=1}^{n} A_{klij}^{p} = I_{klij} \quad \text{and} \quad \sum_{p=1}^{n} a_{kl}^{p} = 0 \tag{6.10-a}$$

$$\sum_{p=1}^{n} B_{klij}^{p} = I_{klij} \quad \text{and} \quad \sum_{p=1}^{n} b_{kl}^{p} = 0 \tag{6.10-b}$$

where I is the fourth order identity tensor.

On the other hand, by substituting (6.9-a) and (6.9-b) into (6.1) and then using (6.8), the concentration tensor B can be easily obtained as:

$$B_{ijmk}^{p} = l_{ijkl}^{p} A_{klsv}^{P} L_{svmk}^{eff} \tag{6.11-a}$$

$$b_{ij}^{p} = l_{ijmn}^{p} A_{mnpq}^{P} \dot{E}_{pq}^{tr} + l_{ijmn}^{p} a_{mn}^{p} - l_{ijmn}^{p} \dot{\varepsilon}_{mn}^{tr(p)} \tag{6.11-b}$$

Substituting (6.1) into (6.7) and considering of equations (6.8) and (6.9), lead to the expression of the effective moduli as:

$$l_{klsv}^{eff} = \sum_{p=1}^{n} f_p l_{klij}^{p} A_{ijsv}^{P} \tag{6.12-a}$$

$$(l_{klsv}^{eff})^{-1} = \sum_{p=1}^{n} f_p (l_{klij}^{p})^{-1} B_{ijsv}^{P} \tag{6.12-b}$$

6.3 The effective transformation behavior of an SMA composite

The SMA composites investigated in this work are composites in which elastic inclusions are embedded in SMA matrix. The matrix in the beginning is fully austenitic and after a loading is applied on the composite a new phase which is martensitic appears. After sufficient loading the matrix becomes fully martensitic. The complexity of this work comes from how to develop a micro mechanical modeling combined with SMA constitutive model that take into account the localization of the new phase that appears when the matrix undergoes transformation. To investigate the effective transformation behavior of the considered composite the cutting plane algorithm developed by Qidwai and Lagoudas (2000) is combined with the Mori-Tanaka micromechanical model that takes into account the coating effect around the inclusion.

6.3.1 SMA transformation behavior

In this subsection, the transformation strain is given as function of state variables [1]. The evolution of the transformation strain is related to the martensitic volume fraction by the following relationship:

$$\dot{\varepsilon}^{tr} = \dot{\xi}\Lambda^{t} \tag{6.15}$$

where ξ is the martensitic volume fraction and Λ^{t} is the direction tensor defined as

$$\Lambda^{t} = \begin{cases} H\dfrac{3}{2}\dfrac{\sigma'}{\bar{\sigma}} & if \quad \dot{\xi} > 0 \\ H\dfrac{\varepsilon^{t-r}}{\bar{\varepsilon}^{t-r}} & if \quad \dot{\xi} < 0 \end{cases} \tag{6.16}$$

in which, H is the maximum uniaxial transformation, ε^{t-r} is the transformation strain at the reversal of phase transformation, σ'represents the deviatoric part of the stress tensor and

$$\sigma' = \sigma - \frac{1}{3}\boldsymbol{tr(\sigma)I}\ ,\ \bar{\sigma} = \sqrt{\frac{3}{2}}\left\|\sigma'\right\|,\ \ \bar{\varepsilon}^{\boldsymbol{t-r}} = \sqrt{\frac{3}{2}}\left\|\varepsilon^{\boldsymbol{t-r}}\right\| \tag{6.17}$$

Constraints on the evolution of the martensitic volume fraction are given by

$$\begin{aligned} &\dot{\xi} \geq 0,\ \Phi(\sigma, T, \xi) \leq 0,\ \Phi\dot{\xi} = 0 \\ &\dot{\xi} \leq 0,\ \Phi(\sigma, T, \xi) \leq 0,\ \Phi\dot{\xi} = 0 \end{aligned} \tag{6.18}$$

Where $\Phi(\sigma, T, \xi)$ is the transformation function. T is temperature. The inequalities (6.18) are called the transformation condition. For $\Phi < 0$, then $\dot{\xi} = 0$ and elastic response is obtained. On the other hand, the forward-phase transformation (austenite to martensite) is characterized by $\Phi = 0$ and $\dot{\xi} > 0$ while reverse-phase transformation is characterized by $\Phi = 0$ and $\dot{\xi} < 0$.

6.3.2 Numerical implementation of the constitutive transformation behavior

The cutting plane algorithm for SMA constitutive models given in [8] is presented here.

1. Let k=0, $\xi_{n+1}^{(0)} = \xi_n$, $\varepsilon_{n+1}^{t(0)} = \varepsilon_n^t$, $S_{n+1}^{(0)} = S_n$, $\alpha_{n+1}^{(0)} = \alpha_n$
2. Calculate the elastic prediction and evaluate the transformation condition

   $\sigma_{n+1}^{(k)} = S_{n+1}^{(k)}(\varepsilon_{n+1} - \alpha_{n+1}^{k}(T_{n+1} - T_0) - \varepsilon_{n+1}^{t(k)})$

$$\Phi_{n+1}^{(k)} = \Phi\left[\sigma_{n+1}^{k}, T, \xi_{n+1}^{k}\right]$$

$$If \left|\Phi_{n+1}^{(k)} \le 0\right|$$

Exit

Else

Forward or reverse transformation.

3. Compute the increment of the martensitic volume fraction and transformation strain.

$$\Delta\xi_{n+1}^{(k)} = \frac{\Phi_{n+1}^{(k)}}{\pm\partial_{\sigma}\Phi_{n+1}^{(k)} : S_{n+1}^{(k)} : \partial_{\sigma}\Phi_{n+1}^{(k)} - \partial_{\xi}\Phi_{n+1}^{(k)}}$$

$$\Delta\varepsilon_{n+1}^{t(k)} = \Delta\xi_{n+1}^{(k)}\Lambda_{n+1}^{(k)}$$

4. Update martensitic volume fraction and transformation strain

$$\xi_{n+1}^{(k+1)} = \Delta\xi_{n+1}^{(k)} + \xi_{n+1}^{(k)}$$

$$\varepsilon_{n+1}^{t(k+1)} = \Delta\varepsilon_{n+1}^{t(k)} + \varepsilon_{n+1}^{t(k)}$$

Let k=k+1 and go to 2

6.3.3 Numerical implementation of the micromechanical transformation behavior

In this subsection, the cutting plane algorithm is combined with the Mori-Tanaka model that takes into account the coating layer around the inclusion.

5. Let k=0, $\xi_{n+1}^{(0)} = \xi_n$, $\varepsilon_{n+1}^{t(0)} = \varepsilon_n^t$, $S_{n+1}^{(0)} = S_n$, $\alpha_{n+1}^{(0)} = \alpha_n$
6. Calculate the elastic prediction and evaluate the transformation condition

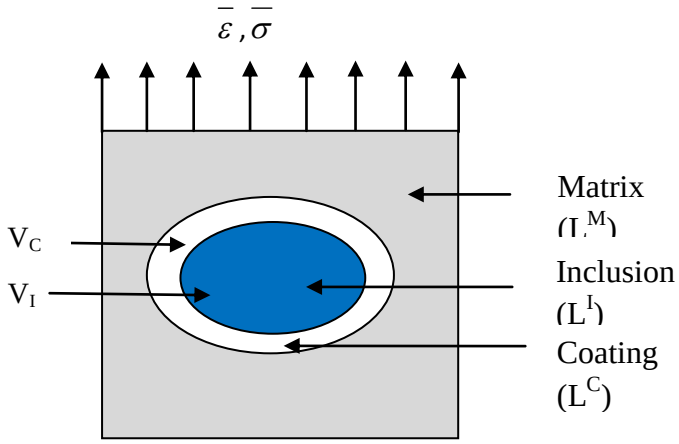

$$\varepsilon_{n+1}^{M} = A_{n+1}^{M(k)} E_{n+1} + a_{n+1}^{M(k)}$$

$$\sigma_{n+1}^{M(k)} = S_{n+1}^{M(k)} (\varepsilon_{n+1}^{M} - \alpha_{n+1}^{M(k)} (T_{n+1} - T_0) - \varepsilon_{n+1}^{t(k)})$$

$$\Phi_{n+1}^{(k)} = \Phi\left[\sigma_{n+1}^{M(k)}, T, \xi_{n+1}^{k}\right]$$

$$If \left|\Phi_{n+1}^{(k)} \le 0\right|$$

Exit

Else

Forward or reverse transformation.

7. Compute the increment of the martensitic volume fraction and transformation strain.

$$\Delta\xi_{n+1}^{(k)} = \frac{\Phi_{n+1}^{(k)}}{\pm\partial_\sigma \Phi_{n+1}^{(k)} : S_{n+1}^{M(k)} : \partial_\sigma \Phi_{n+1}^{(k)} - \partial_\xi \Phi_{n+1}^{(k)}}$$

$$\Delta\varepsilon_{n+1}^{t(k)} = \Delta\xi_{n+1}^{(k)} \Lambda_{n+1}^{(k)}$$

8. Update martensitic volume fraction and transformation strain

$$\xi_{n+1}^{(k+1)} = \Delta\xi_{n+1}^{(k)} + \xi_{n+1}^{(k)}$$

$$\varepsilon_{n+1}^{t(k+1)} = \Delta\varepsilon_{n+1}^{t(k)} + \varepsilon_{n+1}^{t(k)}$$

9. Update of the volume fractions of constituents

$f_c = (1 - f_I)\xi_{n+1}^{k+1}$ the volume fraction of the coating layer

$f_M = (1 - f_I)(1 - \xi_{n+1}^{k+1})$ the volume fraction of the matrix.

Let k=k+1 and go to 2

6.4 Numerical results

Below the numerical results obtained by the Mori-Tanaka that takes the coating layer into account combined with the constitutive model that describes the transformation behavior of the matrix are presented. The obtained results are compared to the results obtained by using the two-phase Mori-Tanaka model that does not take the coating layer into account and those obtained the finite element method.

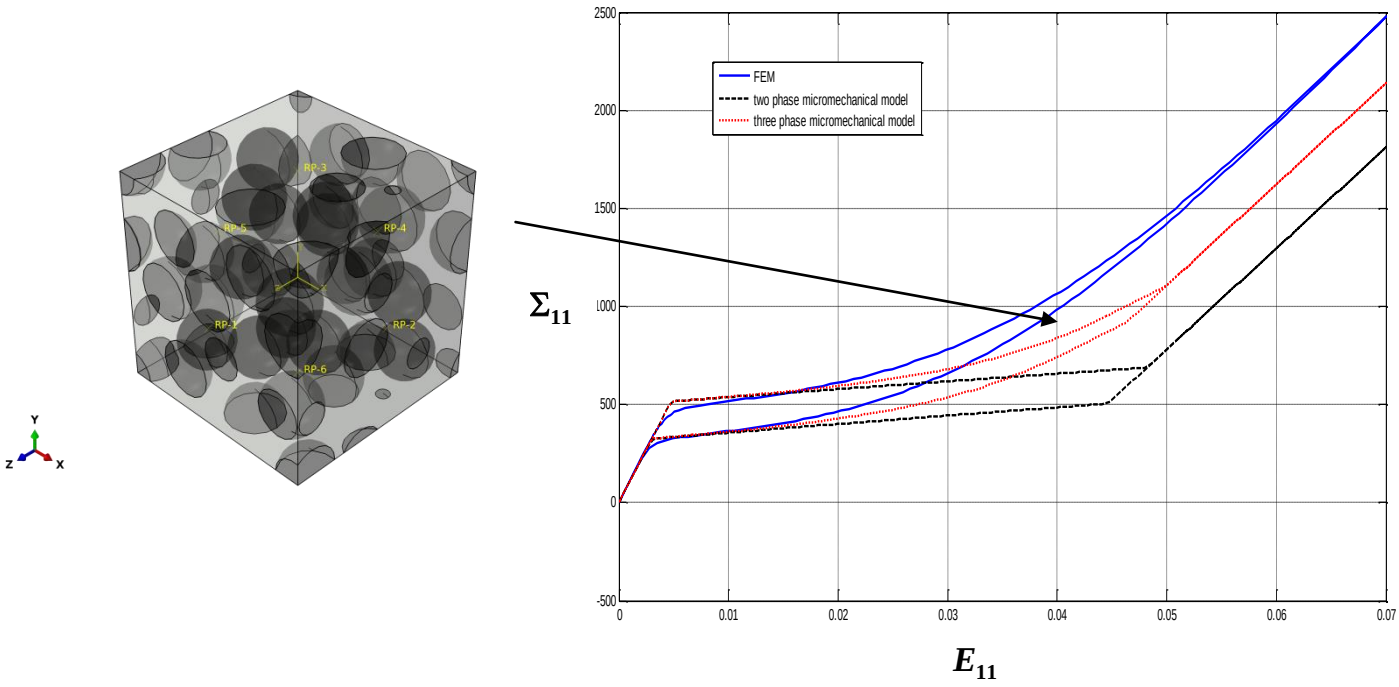

Figure 6.2: Effective stress strain of the considered shape memory alloy composite.

It is shown that the three-phase Mori-Tanaka model that takes into account the coating layer around the inclusion captures the effective transformation behavior of the SMA composite better than the two phase Mori-Tanka model. The obtained results based on the developed model still need more mathematical and numerical developments for agreement with the ones obtained based on the finite element method.

6.4 Conclusion

In this work, the effective transformation behavior of shape memory alloy composites has been investigated. The considered composite is consisting of a shape memory alloys matrix reinforced by elastic inclusions. The transformation behavior of the composite is predicted based on the Mori-Tanaka model and the concept of the coated inclusions combined with the constitutive equations describing the transformation behavior of shape memory alloy materials. The obtained results are compared with those obtained based on the finite element method.

References

[1]Qidwai, M. A.; Lagoudas, D. C. (2000): Numerical implementation of a shape memory alloy thermomechanical constitutive model using return mapping algorithms. International Journal for Numaerical Methods in Engineering, 47, 1123-1168.

[2]Cherkaoui, M.; Sun, Q. P.; Song, G. Q. (2000): Micromechanics modeling of composites with ductile matrix and shape memory allow reinforcement. International Journal of solids and Structures, 37, 1577-1594.

[3]Jiang, B.; Barta, R. C. (2001): Micro mechanical modeling of a composites Containing Piezoelectric and Shape Memory Alloy Inclusions. Journal of Intelligent Material System And Structures, 12, 1045-389X.

[4]Entchev, B. P.; Lagoudas, D. C. (2002): Modeling porous shape memory allows using Micro mechanical Averaging Techeniques. Journal of Mechanics of Materials, 34, 1-24.

[5]Entchev, B. P.; Lagoudas, D. C. (2004): Modeling of transformation-induced plasticity and it effect on the behavior of porous shape memory alloys. Mechanics of Materials, 36, 893-913.

[6]Lagoudas, D. C.; Entchev, B. P; Popov, P.; Patoor, E.; Catherine Brinson, L.; Gao, X. (2006): Shape memory alloys, Part II: Modeling of plycrystals. Mechanics of Materials, 38 , 430-462.

[7]Bakkali, A.; Azrar, L.; Aljinaidi, A. (2013): Effective properties of heterogeneous magnetoelectroelastic materials with multi-Coated inclusions. Key Engineering Materials, Vol. 550, pp 25-32.

[8]Bakkali, A.; Azrar, L.; Aljinaidi, A. A. (2013): Micromechanical modeling of magnetoelectroelastic composite materials with multi-coated inclusions and functionally graded interphases. Journal of Intelligent Materials Systems and Structures, in press.

Chapter 7

7. Summary and conclusion

The use of smart composite materials such as piezoelectric, piezomagnetic, magnetoelectroelastic and shape memory alloy composites etc. continue to grow in many industrial fields: biomedical, automotive, aerospace, civil engineering and many other industries. Because of the potential of smart composite materials for novel application, it is of great interest to develop efficient models predicting accurately the effective behavior of these kinds of composites with respect to shape and types of reinforcements. These models will be helpful to design new multifunctional materials with optimized properties. Contributions have been made in this dissertation toward these goals.

7.1 Summary of the results

Micromechanical models were developed to predict the effective behavior of different kinds of smart composite materials such as: magnetoelectroelastic composites, piezoelectric composites, shape memory alloy composites.

In chapter 2, the effective behavior of magnetoelectroelastic composites is investigated based on various micromechanical models. The modeling is developed for N-phase magnetoelectroelastic composites and the numerical results are presented for two-phase and three-phase magnetoelectroelastic composites. It is shown that Self Consistent micromechanical model underestimates the prediction of the effective moduli at high volume fraction of inclusions. Also, for magnetoelectroelastic composites with void inclusion the prediction of the Self Consistent model is limited for small volume fraction of inclusions. To overcome the underestimation and anomalies presented by the classical Self Consistent an N-phase Incremental Self Consistent is developed. This model has shown its efficiency for high volume fraction of inclusions and also for magnetoelectroelastic composites with void inclusions. An N-phase Mori-Tanaka and Dilute model have been developed to predict the effective properties for two-phase and three-phase magnetoelectroelastic composite with and without voids.

Note that the effective properties of composite materials may be influenced by the presence of an interphase between the matrix and inclusions. For efficient prediction of the effective properties

the type and the structure of the interphase have to be taken into account in the modeling. Chapter 3 investigates the effective properties of magnetoelectroelastic composites with multi-coated and functionally graded interphases based on different micromechanical models: Incremental Self Consistent, Self Consistent, Mori-Tanaka and Dilute. The modeling has been developed for the general case of anisotropic materials and ellipsoidal inclusions with nonhomothetic coatings. For the case of functionally graded interphase the formulation is given for the case of anisotropic materials and ellipsoidal inclusions with homothetic growing. The developed micromechanical modeling consists of two steps: the localization step which is based on the solution of the integral equation and on the interfacial operators, and the homogenization step which is based on the averaging techniques. Two kinds of magnetoelectroelastic composite materials are analyzed. The effective properties of magnetoelectroelastic composite consisting of glass inclusions surrounded by void and piezoelectric interphase layer embedded in piezomagnetic matrix are predicted and then compared to the effective properties of the same composite without void phase. Secondly, the effective properties of magnetoelectroelastic composite consisting of piezoelectric inclusions, piezomagnetic matrix where the properties of interphases vary continuously between the matrix and inclusions are predicted. The effect of shape of reinforcements, thickness of the interphase and functionally graded interphase parameters are shown on the effective properties.

The effective viscoelectroelastic behavior of piezoelectric composites is investigated in chapter 4. The modeling is developed for two-phase piezoelectric composite consisting of piezoelectric inclusions embedded in a viscoelastic matrix and for multi-coated piezoelectric composite consisting of multi-coated piezoelectric inclusions embedded in a viscoelastic matrix. Based on the linear correspondence principle of piezoelectricity the Mori-Tanaka micromechanical model is extended to the Carson domain. The effective properties are first derived in Carson domain and then inverted numerically to the time domain. For numerical results, two kinds of composites are investigated. One is consisting of piezoelectric inclusions embedded in a viscoelastic matrix. The other one is consisting of glass inclusions surrounded with a piezoelectric coating layer embedded in a viscoelastic matrix. The piezoelectric and glass material properties are considered to be time independent. The numerical results are presented both in frequency and time domain. The effects of volume fraction and shape of inclusions as well as of the thickness of the coating layer are shown on the effective properties. It is clearly shown from the numerical results that

even if the piezoelectric coefficients of the piezoelectric material are assumed to be time independent, the effective piezoelectric moduli of composites show time dependence. This is explained by the fact that the viscoelastic behavior of the matrix affects the whole behavior of the composite.

In chapter 5, the effective viscomagnetoelectroelastic behavior of magnetoelectroelastic composites is investigated. The modeling is developed for multi-phase magnetoelectroelastic composites consisting with piezoelectric and piezomagnetic inclusions embedded in a viscoelastic matrix and for multi-coated magnetoelectroelastic composites consisting of multicoated magnetoelectroelastic inclusions embedded in a viscoelastic matrix. Based on the correspondence principle of linear magnetoelectroelasticity, the Mori-Tanaka model is extended to the Carson domain. For multi-phase composites, a composite consisting of piezoelectric and piezomagnetic inclusions embedded in a viscoelastic matrix is considered. For multi-coated composites a composite consisting of piezoelectric inclusions surrounded by piezomagnetic coatings embedded in viscoelastic matrix is considered. The effective properties of the considered composites are presented with respect to time, frequency as well as shape and volume fraction of the reinforcement. It is shown that even the piezoelectric and piezomagnetic phase properties are assumed to be time independent, the effective piezomagnetic and magnetoelectric moduli of the composite are time dependent.

From the work done in chapters 4 and 5 one can see that the time dependent behavior could be introduced to piezoelectric and magnetoelectroelastic composites by adding viscoelastic phases to the composite materials. This leads to new hybrid multifunctional materials that will be of great interest for active and passive controls as well as to sensing and actuating multifunctional materials.

The nonlinear behavior of shape memory alloy composite materials is investigated in chapter 6. The effective properties of shape memory alloy composites consisting of elastic inclusions embedded in a shape memory alloy matrix. The transformation behavior of the matrix is taken into account by using the Mori-Tanaka coated micromechanical model. The martensitic phase that appears after sufficient loading on the composite is considered as a coating layer around the inclusion. This martensitic coating layer grows until the matrix which is initially austenitic disappears and takes its place. The transformation effective behavior of the considered composite

is predicted by combining the constitutive equations of shape memory alloy materials with the coated Mori-Tanaka model. The results obtained by the coated Mori-Tanaka model is compared with the ones obtained by the Mori-Tanaka model that does not consider the martensitic phase as a coating layer around the inclusion. It is shown that the coated Mori-Tanaka model captures the effective behavior of the composite better than the simple Mori-Tanka model. However by comparing the obtained results with the ones obtained based on the finite element method it is seen that the results obtained by the coated Mori-Tanaka model still does not coincide with the ones obtained by the finite element method.

7.2 Directions for future works

- **Multi-site approach**

The micromechanical models developed in this dissertation are called mono-site micromechanical models which do not take into account the interactions between inclusions but the reinforcement are supposed to be far from each other so that the interaction between them is neglected. An alternative micromechanical formulation cloud be developed based on the multi-site formulation of the micromechanical models. The multi-site formulation allows taking into account the morphology and the topology of reinforcements.

- **Improved interface effects**

The developed multi-coated micromechanical models in this thesis are based on the solution of the integral equation and the on the interfacial operators. This developed micromechanical models give good results only for thin coatings. To overcome this limitation an alternative approach could be used based on the Green functions techniques and the concept of the interior and exterior-point Eshelby tensors for an ellipsoidal inclusion embedded in an infinite matrix.

- **Nonlinear effective properties**

In chapter 6, the Mori-Tanaka micromechanical model is combined with the constitutive behavior of shape memory alloys materials. It is shown that the obtained results based on the Mori-Tanaka model still do not coincide with the ones obtained based on the finite element method. It is known that the Incremental Self Consistent is more adapted for nonlinear behavior of composite materials. For future work the Incremental Self Consistent will be combined with

the constitutive behavior of shape memory alloy materials to predict the effective transformation behavior of the considered shape memory alloy composites.

- **Nonlinear time dependent behaviors**

In chapter 4 and 5, the linear viscoelastic behavior of the polymer phase is considered. For future work the nonlinear behavior of the viscoelastic polymer will be considered and micromechanical modelings will be developed to investigate the nonlinear time dependent behavior of various composites materials.

- **Nano composite effective properties**

In the work of this thesis, the micromechanical modelings are developed for composite materials where the reinforcements are considered to be at a micro level. In a future work we intend to investigate the effective properties of composite materials reinforced with nano inclusions. For nano composites the inclusions are separated in two regions: the core inclusions and the interphase layer that separates the core inclusions from the matrix. The interphase properties have to be determined at atomistic scale. Once the interphase properties are determined then the developed micromechanical models in this these cloud be used to investigate the effective properties of nano composites.

Appendix 3.A

Consider an interface between two homogenous magnetoelectroelastic medium made of two different phases whose magnetoelectroelastic moduli are denoted by E^{k+1} and E^{k}. In the context of continuum mechanics, the interface is assumed to be mathematical surface across whish material properties change discontinuously. With the perfect bounding assumption, the continuity of the generalized potential field U_M, the interfacial tension, electric displacement and magnetic induction are expressed as:

$$\left[U_M\right] = U_M^+ - U_M^- = 0 \tag{3A.1}$$

$$\left[\Sigma_{iJ}\right] N_J = (\Sigma_{iJ}^+ - \Sigma_{iJ}^-) N_J = 0 \tag{3A.2}$$

where the normal unit vector is given by:

$$N_J = \begin{cases} n_j & (J = 1,2,3) \\ 1 & (J = 4) \\ 1 & (J = 5) \end{cases} \tag{3A.3}$$

in which n_j is the outward unit normal of the interface.

At an arbitrary point $r(x_i)$ of the interface, the compatibility condition $du_i = u_{i,j} dx_j$, $d\varphi^e = \varphi^e_{,j} dx_j$ and $d\varphi^m = \varphi^m_{,j} dx_j$ added to the continuity of the displacement, electric and magnetic potential field along the boundary impose the relations: $\left[u_{i,j}\right] dx_j = 0$, $\left[\varphi^e{}_{,j}\right] dx_j = 0$ and $\left[\varphi^m{}_{,j}\right] dx_j = 0$. Since $n_j dx_j = 0$, the displacement, electric and magnetic potential gradient are proportional to the unit normal $\left[u_{i,j}\right] = \lambda_i n_j$, $\left[\varphi^e{}_{,j}\right] = \lambda^e n_j$ and $\left[\varphi^m{}_{,j}\right] = \lambda^m n_j$ where λ_i, λ^e and λ^m are the proportionality vector and scalars.

The generalized strain field jump is expressed as:

$$\left[Z_{Mn}\right] = \lambda_M N_N \tag{3A.4}$$

The magnitude of the jump λ_M is defined by:

$$\lambda_M = \begin{cases} \lambda_m & (M = 1,2,3) \\ -\lambda^e & (M = 4) \\ -\lambda^m & (M = 5) \end{cases} \tag{3A.5}$$

The continuity equation (3A.2) leads to

$$(E^{k+1}_{iJMn} Z^{k+1}_{Mn} - E^{k}_{iJMn} Z^{k}_{Mn}) N_J = 0 \tag{3A.6}$$

Which is equivalent to $E^{k+1}_{iJMn}\left[Z_{Mn}\right]N_J = -\Delta E^{(k+1/k)}_{iJMn} Z^{k}_{Mn} N_J$ where $\Delta E^{(k+1/k)}_{iJMn} = E^{k+1}_{iJMn} - E^{k}_{iJMn}$. By introducing the Christoffel's matrix K^{*}_{iM} (*=k+1 or k) defined by:

$$K^{*}_{iM} = E^{*}_{iJMn} N_J N_N \tag{3A.7}$$

The magnitude of the jump λ_M is given by:

$$\lambda_M = -K^{k+1^{-1}}_{iM} \Delta E^{(k+1/k)}_{iJRs} Z^{k}_{Rs} N_J = -K^{k^{-1}}_{iM} \Delta E^{(k/k+1)}_{iJRs} Z^{k+1}_{Rs} N_J \tag{3A.8}$$

The generalized strain field jump is evaluated in terms of the generalized strain field on both sides of the interface via a pair of equivalent formulae expressed as:

$$\begin{aligned} Z^{k+1}_{Mn} - Z^{k}_{Mn} &= P^{k+1}_{iJMn}(E^{k+1}, N) \Delta E^{(k/k+1)}_{iJRs} Z^{k}_{Rs} \\ Z^{k+1}_{Mn} - Z^{k}_{Mn} &= P^{k}_{iJMn}(E^{k}, N) \Delta E^{(k/k+1)}_{iJRs} Z^{k+1}_{Rs} \end{aligned} \tag{3A.9}$$

Appendix 3.B

Consider an infinite media with magnetoelectroelastic moduli E^0_{iJMn} which contains a single composite inclusion of volume Ω_{k-1} and magnetoelectroelastic moduli $E^{\Omega_{k-1}}_{iJMn}$ assumed to be constant inside the volume Ω_{k-1}.

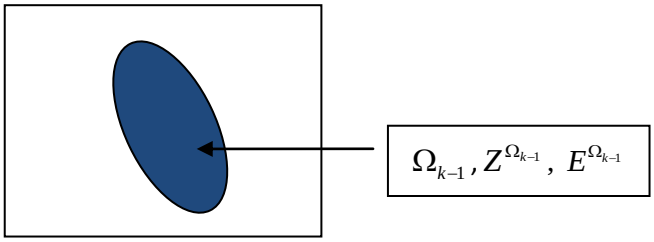

Figure 3.B.1: representative volume element of the infinite magnetoelectroelastic media containing a single composite inclusion.

The generalized strain field is given, as follow:

$$Z_{Kl}(r) = Z^0_{Kl} - \int_{\Omega_{k-1}} \Gamma_{iJKl}(r - r')\Delta E^{(\Omega_{k-1}/0)}_{iJMn} Z^{\Omega_{k-1}}_{Mn} dV' \qquad (3.B.1)$$

where $Z^{\Omega_{k-1}}$ is the uniform generalized strain inside the composite inclusion, Γ is the modified magnetoelectroelastic Green's tensor of the reference media of magnetoelectroelastic moduli E^0_{iJMn}.

The generalized strain field $Z_{Kl}(r)$ by $Z(r^k)$ where r approaches the interface from the outside of the composite inclusion is defined by:

$$Z_{Kl}(r^k) = Z^0_{Kl} - \int_{\Omega_{k-1}} \Gamma_{iJKl}(r^k - r')\Delta E^{(\Omega_{k-1}/0)}_{iJMn} Z^{\Omega_{k-1}}_{Mn} dV' \qquad (3.B.2)$$

Similarly, the generalized strain field inside the composite inclusion is defined by:

$$Z_{Kl}(r^{k-1}) = Z^0_{Kl} - \int_{\Omega_{k-1}} \Gamma_{iJKl}(r^{k-1} - r')\Delta E^{(\Omega_{k-1}/0)}_{iJMn} Z^{\Omega_{k-1}}_{\Omega_{k-1}} dV' \qquad (3.B.3)$$

Since $r^{k-1} \in \Omega_{k-1}$, $\int_{\Omega_{k-1}} \Gamma_{iJKl}(r^{k-1} - r')dV' = T^{\Omega_{k-1}}_{iJKl}$ is uniform, so that:

$$Z_{Kl}(r^{k-1}) = Z^{\Omega_{k-1}}_{Kl} = Z^0_{Kl} - T^{\Omega_{k-1}}_{iJKl}(E^0)\Delta E^{(\Omega_{k-1}/0)}_{iJMn} Z^{\Omega_{k-1}}_{Mn} \qquad (3.B.4)$$

Form (3.B.2) and (3.B.4) one obtains:

$$Z_{Kl}(r^k) - Z^{\Omega_{k-1}}_{Kl} = \left[T^{\Omega_{k-1}}_{iJKl}(E^0) - \int_{\Omega_{k-1}} \Gamma_{iJKl}(r^k - r')dV' \right] \Delta E^{(\Omega_{k-1}/0)}_{iJMn} Z^{\Omega_{k-1}}_{Mn} \qquad (3.B.5)$$

On the other hand, the generalized strain $Z(r^k)$ and $Z(r^{k-1})$ can be linked using the magnetoelectroelastic interfacial operators see Eq. (3.36), so that:

$$Z_{Mn}(r^k) - Z_{Mn}(r^{k-1}) = P^0_{iJMn}(E^0, N)\Delta E^{(\Omega_{k-1}/0)}_{iJRs} Z^{\Omega_{k-1}}_{Rs} \tag{3.B.6}$$

From (3.B.5) and (3.B.6) one can write:

$$P^0_{iJKl}(E^0, N) = T^{\Omega_{k-1}}_{iJKl}(E^0) - \int_{\Omega_{k-1}} \Gamma_{iJKl}(r^k - r')dV' \tag{3.B.7}$$

By integrating (3.B.7) over the volume V_k, one obtains:

$$\int_{V_k} P^0_{iJKl}(E^0, N)dV = V_k T^{\Omega_{k-1}}_{iJKl}(E^0) - \int_{V_k}\int_{\Omega_{k-1}} \Gamma_{iJKl}(r^k - r')dV'dV \tag{3.B.8}$$

Using the fact that $\Omega_k = \Omega_{k-1} + V_k$, we can write:

$$\int_{V_k}\int_{\Omega_{k-1}} \Gamma_{iJKl}(r^k - r')dV'dV = \int_{\Omega_k}\int_{\Omega_{k-1}} \Gamma_{iJKl}(r^k - r')dV'dV - \int_{\Omega_{k-1}}\int_{\Omega_{k-1}} \Gamma_{iJKl}(r^k - r')dV'dV \tag{3.B.9}$$

Due to the uniformity of the tensors

$$\int_{\Omega_{k-1}} \Gamma_{iJKl}(r^k - r')dV' = T^{\Omega_{k-1}}_{iJKl}(E^0) \text{ and } \int_{\Omega_k} \Gamma_{iJKl}(r^k - r')dV' = T^{\Omega_k}_{iJKl}(E^0)$$

We obtain:

$$\int_{V_k}\int_{\Omega_{k-1}} \Gamma_{iJKl}(r^k - r')dV'dV = \Omega_{k-1}(T^{\Omega_k}_{ilJK}(E^0) - T^{\Omega_{k-1}}_{ilJK}(E^0)) \tag{3.B.10}$$

By substituting (3.B.10) into (3.B.8), one gets:

$$\int_{V_k} P^0_{iJKl}(E^0, N)dV = V_k T^{\Omega_{k-1}}_{iJKl}(E^0) - \Omega_{k-1}(T^{\Omega_k}_{ilJK}(E^0) - T^{\Omega_{k-1}}_{ilJK}(E^0)) \tag{3.B.11}$$

Finally, according to the definition of the tensor T^{k+1} the following relationship is obtained:

$$T^k_{iJKl}(E^k) = T^{\Omega_{k-1}}_{iJKl}(E^k) - \frac{\Omega_{k-1}}{V_k}(T^{\Omega_k}_{ilJK}(E^k) - T^{\Omega_{k-1}}_{ilJK}(E^k)) \tag{3.B.12}$$